

**TOWARDS THE DEVELOPMENT OF AN INTEGRATED  
SCALABLE BIOPROCESS FOR THE PRODUCTION OF  
hiPSC-DERIVED NPC**

FRITZ ANTHONY DE LA RAGA

Doctor of Philosophy

Aston University

March 2022

©Fritz Anthony de la Raga, 2022

Fritz Anthony de la Raga  
asserts their moral right to be identified as the author of  
this thesis

This copy of the thesis has been supplied on condition that anyone who consults it is understood to recognise that its copyright belongs to its author and that no quotation from the thesis and no information derived from it may be published without appropriate permission or acknowledgement.

Towards the development of an integrated scalable bioprocess for the production of hiPSC-derived NPC

Fritz Anthony de la Raga

PhD

2022

## **Abstract**

Neural precursor cells (NPCs) can be used as a cell source for disease modelling, tissue engineering and cell-based regenerative therapies for neurological disorders. However, due to the limited availability of NPCs sourced from foetal tissues, ethical concerns and invasive methods, their use in late-stage clinical trials and commercial availability is hindered. Human induced pluripotent stem cells (hiPSCs) have the potential to differentiate towards NPCs, thus providing an alternative unlimited source for generating NPCs which bypasses the current sourcing limitations. hiPSC-derived NPCs have been successfully produced using direct or indirect methods. However, those methods have predominantly been carried out using traditional planar culture systems. To achieve the high cell numbers required for therapeutic treatments, translation of these protocols to scalable production methods is necessary.

In this thesis, we have developed an integrated bioprocess for production of hiPSC-derived NPCs. This would enable the development of a process using dynamic 3D suspended culture systems and stirred tank bioreactors (STBs), which are scalable and relevant for clinical productions of hiPSC-derived NPCs. We have identified a suitable microcarrier for hiPSC expansion by performing systematic screenings of 8 commercially available microcarriers. We have also assessed the potential of microcarriers as a platform for the neural induction of hiPSC. We have deployed these microcarriers to develop towards a scalable integrated bioprocess in spinner flasks. Overall, we demonstrated the translation of the baseline and microcarrier integrated bioprocesses towards a scalable bioprocess utilising scalable spinner flasks. However, although spinner flasks have been successfully employed for the expansion of

mammalian cells such as Chinese hamster ovary (CHO) or human embryonic kidney (HEK) cell lines, results here show that the expansion and neuralisation of hiPSCs on tissue culture plastic planar platforms remained superior in terms of maintaining pluripotency, growth kinetics and differentiation potential.

**Keywords:** pluripotent stem cells (PSCs), neural precursor cells (NPCs), bioprocessing, scaled-up production, microcarriers

## **Acknowledgements**

I would like to sincerely thank Dr. Eric Hill for his wise mentorship and continuous support throughout my entire journey at Aston University. From undergraduate, you opened doors for me towards the field of stem cells, and I owe it to you for inspiring me to walk through each one of them. I would not be where I am now without your guidance. Thank you to Dr. Patricia Perez-Esteban for inspiring me to always do better and for kindly accepting my burdens amidst starting a beautiful family. I would also like to thank Dr. Petra Hanga for giving me the opportunity to explore science. Your help and guidance towards this thesis will always be appreciated.

Thank you Dr. Shibani Ratnayake for teaching me the technical skills during your time in the lab and for your continuing support. Thank you, Dr. Junaid Ali, for bringing so much life into the lab. It was a great pleasure working with everyone in Lab 343. I want to thank all my friends at Aston University for the many wonderful memories.

Shelley Ramirez and Tricia Perez, thank you for being my rock. I am constantly reminded that I can never be as good to my friends as you are to me. You both are the best. I want to thank my friends outside of Aston University for bringing so much joy and sharing your wise advice. To Precious Salazar, I want to thank you for everything you do especially all the happiness you bring.

Finally, I want to thank my talented sister, Kirsten de la Raga, for all the joy she has brought to the family. To my beautiful mama, Gloria de la Raga, thank you for your unconditional love, understanding and endless support. To my brilliant papa, Jeffrey de la Raga, thank you for being an inspiration, and for showing me how to love a family.

# Table of contents

## Table of Contents

<b>1, Introduction.....</b>	<b>12</b>
<b>1.1. General introduction.....</b>	<b>12</b>
<b>1.2. Neurodegenerative diseases .....</b>	<b>13</b>
<b>1.3. Current therapies for neurodegenerative diseases .....</b>	<b>14</b>
<b>1.4. Cell-based therapies as an alternative for treating neurodegenerative diseases.....</b>	<b>17</b>
<b>1.5. General stem cell terminology.....</b>	<b>18</b>
<b>1.6. Adult stem cells (ASCs) .....</b>	<b>19</b>
1.6.1. Neural stem, Neural progenitor, and Neural precursor terminology.....	21
1.6.2. Role of adult NPCs <i>in vivo</i> .....	23
1.6.3. Clinical applications of NPCs.....	25
1.6.4. Challenges with NPC-based cells as a cell therapy .....	30
<b>1.7. Pluripotent stem cells.....</b>	<b>33</b>
1.7.1. Naïve vs primed PSCs .....	34
1.7.2. Limitations and safety concerns surrounding PSCs in cell-based therapies.....	37
1.7.3. Towards clinical grade hiPSC-based therapies .....	40
1.7.4. Workflow of allogeneic and autologous hiPSCs based therapy .....	44
1.7.5. hiPSCs culture systems .....	51
<b>1.8. NPCs: neural induction and maintenance .....</b>	<b>66</b>
1.8.1. The molecular mechanisms that drive neural induction.....	68
1.8.2. Consideration of the culture substrate during neural induction.....	72
1.8.3. Neural induction using suspension culture systems .....	73
1.8.4. Neural induction using adherent culture systems.....	76
<b>1.9. Scalable strategies to produce clinical-grade hiPSC-derived NPCs .....</b>	<b>77</b>
1.9.1. Scale-out and scale-up strategies .....	80
1.9.2. Bioreactor platforms .....	81
1.9.3. Microcarrier technologies .....	84
1.9.4. Scalable culture systems .....	87
1.9.5. Scalable neural induction and NPC culture strategies.....	94
<b>1.10. Other bioprocessing considerations using STBs .....</b>	<b>96</b>
1.10.1. Operation mode .....	96
1.10.2. Mixing speed .....	97
1.10.3. Overall literature summary .....	99
<b>1.11. Aims and objectives .....</b>	<b>100</b>
<b>2. General materials and methods.....</b>	<b>101</b>
<b>2.1. Chemical reagents, consumables, and equipment .....</b>	<b>101</b>
<b>2.2. Cell lines.....</b>	<b>101</b>
<b>2.3. Preparation of cell culture media .....</b>	<b>102</b>

2.3.1. hiPSC maintenance media .....	102
2.3.2. Preparation of neural induction media .....	103
<b>2.4. Preparation of cell culture substrates .....</b>	<b>103</b>
2.4.1. Vitronectin.....	103
2.4.2. Matrigel .....	104
2.4.3. Poly-L-Ornithine and Laminin .....	104
<b>2.5. Preparation of cell culture platforms .....</b>	<b>105</b>
2.5.1. TCP planar platforms .....	105
2.5.2. Microcarrier platforms .....	105
2.5.3. Spinner flask platforms.....	106
<b>2.6. General cell culture procedures.....</b>	<b>107</b>
2.6.1. Monolayer cultures of hiPSC on planar platforms .....	107
2.6.2. Suspended aggregate cultures of hiPSCs on planar platforms.....	108
2.6.3. Monolayer cultures of hiPSC on microcarrier platforms in static conditions.....	108
2.6.4. Monolayer cultures of hiPSC on microcarrier platforms in dynamic conditions.....	109
2.6.5. Microcarrier culture in agitated conditions in spinner flasks.....	110
2.6.6. Cell harvest from microcarriers in ULA well plates platforms.....	111
2.6.7. Cell harvest from microcarriers in spinner flask platforms .....	112
2.6.8. Cell storage and thawing .....	113
<b>2.7. Analytical techniques .....</b>	<b>113</b>
2.7.1. Cell counting.....	113
2.7.2. Live/dead staining for viability assessment.....	114
2.7.3. Metabolic analysis .....	115
2.7.4. Immunocytochemistry staining for marker assessment .....	115
2.7.5. Trilineage differentiation of hiPSCs.....	119
2.7.6. Scanning electron microscope imaging.....	119
2.7.7. Quantification by Image J analysis .....	119
<b>2.8. Engineering characterisation of bioreactors .....</b>	<b>120</b>
2.8.1. Mixing studies .....	120
<b>2.9. Statistical analysis .....</b>	<b>122</b>
<b>2.10. Other equations used .....</b>	<b>123</b>
<b>3. Establishing a baseline integrated bioprocess for the production of hiPSC-derived NPCs on planar platform .....</b>	<b>124</b>
<b>3.1. Introduction .....</b>	<b>124</b>
3.1.1. Establishing the baseline bioprocess.....	125
3.1.2. Chapter aims and objectives .....	128
<b>3.2. Results .....</b>	<b>129</b>
3.2.1. Quality assessment of hiPSC lines in TeSR™-E8™ / VTN culture systems .....	129
3.2.2. Growth characteristics of kiPSC and piPSC in TeSR™-E8™ / VTN culture system.....	140
3.2.3. Comparison of TeSR™-E8™ with a newly developed mTeSR™ Plus medium composition .....	150
3.2.4. Optimisation of mTeSR™ Plus / VTN culture system by feeding regime .....	154
3.2.5. Neural induction of hiPSCs towards NPCs following their expansion in mTeSR™ / VTN culture system .....	166
<b>3.3. Discussion .....</b>	<b>171</b>
3.3.1. kiPSCs was chosen as the model cell line for further bioprocess development.....	172
3.3.2. Establishing the baseline expansion process for kiPSC .....	176

3.3.3. Cost optimisation of the baseline bioprocess .....	177
3.3.4. kiPSC expanded by the optimised expansion process could differentiate towards NPCs in an integrated bioprocess on planar platforms.....	179
<b>4. Expansion and neural induction of hiPSC on microcarrier platforms .....</b>	<b>181</b>
<b>4.1. Introduction .....</b>	<b>181</b>
4.1.1. Microcarriers – an enabling technology for scalable culture systems .....	181
4.1.2. Choosing a suitable microcarrier .....	182
4.1.3. Chapter aims and objectives .....	183
<b>4.2. Results .....</b>	<b>185</b>
4.2.1. Screening of commercially available non-modified microcarriers in static conditions .....	185
4.2.2. Screening of VTN coated microcarriers under static conditions .....	189
4.2.3. Determining the efficiency of the harvest process of kiPSCs from VTN-coated microcarriers in static conditions.....	202
4.2.4. Screening of VTN coated microcarriers in dynamic conditions.....	205
4.2.5. Determining the efficiency of the harvest process of kiPSCs from VTN-coated microcarriers in dynamic conditions .....	212
4.2.6. Selection of VTN coated Plastic microcarrier .....	216
4.2.7. Quality assessment of kiPSC on VTN coated Plastic microcarriers.....	218
4.2.8. Neural induction of kiPSCs on VTN coated Plastic microcarriers .....	221
<b>4.3. Discussion .....</b>	<b>225</b>
4.3.1. The process of selecting VTN-coated microcarrier.....	225
4.3.2. VTN coated Plastic microcarriers supported the expansion and neural induction of kiPSCs.....	234
<b>5. Expansion and neural induction of hiPSC on microcarrier platforms in STBs .....</b>	<b>236</b>
<b>5.1. Introduction .....</b>	<b>236</b>
5.1.1. Designing the baseline scalable bioprocess .....	236
5.1.2. Neural induction in scalable bioprocesses .....	238
5.1.3. Chapter aims and objectives .....	239
<b>5.2. Results .....</b>	<b>240</b>
5.2.1. Determining the mixing speed required to suspend the microcarriers .....	240
5.2.2. Characterising the expansion of kiPSC in the baseline scalable bioprocess.....	243
Optimisation of the baseline scalable bioprocess .....	250
5.2.3. Optimisation of the baseline scalable bioprocess .....	250
<b>5.3. Discussion .....</b>	<b>254</b>
5.3.1. Cell-microcarrier aggregation slows down kiPSC growth in spinner flasks .....	254
5.3.2. Influence of shear stress on cell growth.....	257
5.3.3. Inefficient seeding protocol may lead to reduced cell growth.....	258
5.3.4. Dynamic cultures negatively affected the differentiation potential of kiPSCs.....	260
5.3.5. Process parameter optimisation .....	261
<b>6. Final remarks and Future work .....</b>	<b>263</b>
<b>6.1. Future work .....</b>	<b>263</b>
6.1.1. Future work towards optimising a microcarrier dependent bioprocess.....	263
6.1.2. Future work towards developing a microcarrier independent process .....	267
<b>6.2. Experimental improvements .....</b>	<b>268</b>
<b>6.3. Concluding remarks.....</b>	<b>270</b>

## List of Figures

Figure 1.1. Diagram showing the factors involved in the differentiation steps from neuroepithelial cells to RG cells and their differentiation towards the neuronal and glial lineages.....	25
Figure 1.2. Schematic diagram of hPSC CAMs (E-cadherin and integrin) and their intracellular pathways leading to maintenance of pluripotency and cell survival.....	58
Figure 1.3. Schematic diagram of key signalling pathways during neural induction. Diagram is adopted from Pownall and Isaacs, (2010).....	72
Figure 1.4. The different methods of neural induction. Methods (1) and (2) mediate the neural induction process through EB formation and neural rosettes.....	76
Figure 2.1. Photograph of 50 mL spinner flask (Wheaton). Spinner flask features are labelled.....	107
Figure 2.2. Illustrative example of control for secondary antibodies to assess for non-specific binding.	119
Figure 3.1. Representative phase contrast images of hiPSC colonies in TeSR™-E8™ / VTN culture systems.....	133
Figure 3.2. Assessment of piPSCs and kiPSCs for the presence of SOX2 and TRA-1-60 markers when cultured on VTN and TeSR™- E8™ culture system.....	135
Figure 3.3. Assessment of piPSCs and kiPSCs for the presence of SSEA4 and OCT4 markers when cultured on VTN and TeSR™- E8™ culture system.....	136
Figure 3.4. Trilineage assessment of kiPSC after culturing in TeSR™-E8™ / VTN culture systems.....	139
Figure 3.5. Trilineage assessment of piPSC after culturing in TeSR™-E8™ / VTN culture systems.....	140
Figure 3.6. Representative images of kiPSC cells passaged with different techniques.....	142
Figure 3.7. Measured cell viability of kiPSC and piPSC cell lines when seeded at different seeding densities and cultured over 120 h.....	144
Figure 3.8. Measured VCN, SPGR, DT and FI of hiPSCs when seeded at different seeding densities over 120 h incubation in TeSR™-E8™/ VTN culture system.....	147
Figure 3.9. Glucose and lactate profiles of kiPSCs and piPSCs over 120 h of culture, when seeded at different seeding densities.....	150
Figure 3.10. Viability, VCN and growth kinetics of hiPSCs in different media.....	152
Figure 3.11. Pluripotency assessment of kiPSCs in mTeSR™ Plus / VTN culture system using fluorescent imaging. kiPSCs were grown in 48 well plates and cultured for 96 h.....	154
Figure 3.12. Viability, VCN and growth kinetics of kiPSCs under different feeding strategies.....	157
Figure 3.13. Glucose and lactate profiles of kiPSC cultures in different feeding regimes.....	159
Figure 3.14. Cost analysis of the different feeding strategies.....	162
Figure 3.15. Viability and growth kinetics of kiPSC over 8 consecutive passages.....	165
Figure 3.16. Pluripotency assessment of kiPSCs after multiple serial passaging. ....	166
Figure 3.17. Representative images of cell and colony morphologies of kiPSC cultures after passage 14 in mTeSR™ Plus / VTN culture system up to passage 19.....	167
Figure 3.18. Process workflow of the integrated bioprocess for deriving NPCs from kiPSCs.....	170

Figure 3.19. Differentiation of kiPSCs towards NPCs following culture in mTeSR™ Plus / VTN culture system.....	171
Figure 4.1. Phase contrast images kiPSCs 96 h post seeding on native microcarriers for screening.....	188
Figure 4.2. Representative examples of Live/dead staining of kiPSCs at 48 h of the native microcarrier screening assay.....	189
Figure 4.3. Example phase contrast images of kiPSC and their initial attachment compared to established adhesion morphologies on VTN coated microcarriers. ....	192
Figure 4.4. Representative examples of Live/dead staining of kiPSCs at 48 h of the native microcarrier screening assay.....	193
Figure 4.5. Phase contrast images of VTN coated microcarrier screening after 96 h in culture.....	194
Figure 4.6. Viability and VCN/cm <sup>2</sup> of kiPSCs after harvesting from the screened VTN coated microcarriers.....	197
Figure 4.7. Growth kinetics of kiPSC during the screening of VTN coated microcarriers.....	198
Figure 4.8. Glucose concentrations of kiPSCs cultures during the screening of different VTN coated microcarriers.....	201
Figure 4.9. Lactate concentrations of kiPSCs cultures during the screening of different VTN coated microcarriers. ....	202
Figure 4.10. Comparison of the expected yield vs the actual yield of the harvesting process from the VTN coated microcarrier screening assay. ....	205
Figure 4.11. Viability and calculated growth kinetics of kiPSC harvested from VTN coated microcarriers, after culturing for 96 h in dynamic conditions. ....	209
Figure 4.12. Glucose concentration of kiPSC cultured on VTN coated microcarriers in dynamic conditions. ....	211
Figure 4.13. Lactate concentrations of kiPSC cultured on VTN coated microcarriers, throughout 96 h of expansion. ....	212
Figure 4.14. Comparison of the expected yield vs the actual yield of the harvesting process of kiPSC from VTN coated microcarriers in dynamic conditions. ....	215
Figure 4.15. Comparison of the (A) harvest efficiency and (B) total VCN/cm <sup>2</sup> on harvest between static and dynamic conditions.....	216
Figure 4.16. Representative SEM images at different magnification of VTN coated and non-modified plastic microcarriers.....	218
Figure 4.17. Morphology and pluripotency assessment of kiPSC cultured on VTN coated plastic microcarriers. ....	221
Figure. 4.18. Process workflow of the expansion and neural induction of kiPSC on VTN coated plastic microcarrier. ....	224
Figure 4.19. Assessment for the presence of Nestin following neural induction of kiPSC on 2D planar and 3D microcarrier platforms. ....	225
Figure 5.1. Comparing the effect of stirring speed and impeller configuration on the mixing time within the spinner flasks. ....	243

Figure 5.2. Expansion of kiPSC in spinner flasks for 96 h. kiPSCs were seeded at $4 \times 10^4$ cells/cm <sup>2</sup> onto 100 cm <sup>2</sup> of VTN plastic microcarrier and a maximum 20 mL working volume (mTeSR™ Plus)...	247
Figure 5.3. Assessment of the harvested cells after expansion of kiPSC in spinner flasks.....	248
Figure 5.4. Assessing the potential of kiPSC-laden microcarriers from the baseline scalable bioprocess to differentiate towards NPCs. ....	250
Figure 5.5. Comparison of 3 different impeller stirring speed on the growth of kiPSC with spinner flasks. ....	253

## List of Tables

Table 1.1. A table summarising examples of clinical trials from clinicaltrials.gov (last accessed 28th January 2022). ....	29
Table 1.2. Summary of the proposed requirements for clinical grade hiPSCs. The details of the recommended assays to test and validate the proposed CQAs are shown in this table.....	42
Table 1.3. Medium components of E8™ and mTeSR™1. The x indicates components present in the medium formulation.....	64
Table 1.4. List of different commercially available microcarriers and their properties. ....	87
Table 1.5. Examples of PSCs cultured in scalable culture systems. ....	91
Table 2.1 Details of the hiPSC lines used in this thesis. ....	103
Table 2.2. List of primary and secondary antibodies used for ICC experiments. ....	118
Table 3.1 Summary of the feeding strategies, showing the volumes of mTeSR™ Plus medium to be exchanged per well of a 6 well plate, at each timepoint of the cultures. ....	156
Table 3.2. Cost analysis of the different feeding regimes. ....	161

## Abbreviations

2D	two-dimensional
3D	three-dimensional
Abs	Antibodies
AD	Alzheimer's disease
ALS	amyotrophic lateral sclerosis
ASCs	Adult stem cells
ATMPs	Advanced therapeutic medicinal products
ATP	adenosine triphosphate
BBB	Blood-brain barrier
BMP	Bone morphonogenetic protein
CPP	Critical process parameters
CQA	Critical quality attributes
DA	Dopamine

DCX	doublecortin
DG	Dentate gyrus
DNA	deoxyribose nucleic acid
DO	dissolved oxygen
EDTA	ethylenediamine tetra-acetic acid
ESC	Embryonic stem cells
FTD	Frontotemporal dementia
GFAP	Glial fibrillary acidic protein
GMP	Good manufacturing practise
HD	Huntington's disease
HSA	Human serum albumin
HSCs	Hematopoeitic stem cells
ICC	Immunocytochemistry
ICM	Inner cell mass
IPCs	intermediate progenitor cells
iPSC	induced pluripotent stem cell
LIF	leukaemia inhibiting factor
LN	Laminin
mAbs	monoclonal Antibodies
MAPK	mitogen activated protein kinase
MS	Multiple sclerosis
MSC	Mesenchymal stem cells
Njs	speed required to just suspend
NP	Neural progenitor
NPC	Neural precursor cells
PAX6	Paired box protein 6
PD	Parkinson's disease
PLO	Poly-L-Ornithine
PSA-NCAM	Polysialyted neural CAM
PSCs	Pluripotent stem cells
RGCs	Radial glial cells
RNA	Ribose Nucleic Acid
RPM	Rotations per minute
SHH	Sonic hedgehog
SOX2	Sex determining region y-box 2
STB	Stirred tank bioreactor
SVZ	subventricular zone
TCA	Tricarboxylic acid
TDP	transactivation response deoxyribose nucleic acid
VEGF	Vascular endothelial growth factor
VTN	Vitronectin

# **1.Introduction**

## **1.1.General introduction**

Common to most neurodegenerative disorders is the progressive loss of function, structure, or number of neuronal cells within the central nervous system (CNS), including the brain and the spinal cord. In particular, it is the loss of a specific subset of neurons such as cholinergic, dopaminergic or motor neurons, that lead to the physically disabling and often fatal consequences (Heemels, 2016). Individuals living with neurodegenerative disorders experience a reduced quality of cognition, movement, and memory, further imposing health, social and economic burden. Neurodegenerative diseases that engender such disorders includes Parkinson's disease (PD) and multiple sclerosis (MS) reported to be at a global prevalence of 6.1 million individuals in 2016 and 2.2 million individuals worldwide (Ray Dorsey et al., 2018; Wallin et al., 2019), respectively; dementia as one of the leading causes of deaths in the UK currently.

The causes of neurodegenerative diseases remain largely unknown, although, environmental and lifestyle factors, combined with genetic susceptibility can increase the risk for certain neurodegenerative diseases. One of the most prominent risk factors for neurodegenerative diseases is ageing, since older nervous systems cannot effectively regenerate neuronal populations due to modifications over time of the niche microenvironments, ultimately preventing axonal repair (Jin *et al.*, 2003; Decimo *et al.*, 2012; Kovacs, 2018; Tonda-Turo *et al.*, 2018).

With the current ageing global population, the prevalence of neurodegenerative disorders is expected to increase. Cimler et al., (2019) performed computer simulations into the future to predict the costs of current therapies and care for patients suffering with Alzheimer's disease

(AD). Their predictions estimated the cost of therapies and care to reach around €509 (~£424) billion in 2030, €828 (~£689) billion in 2050, and a disturbing figure of approximately €1038 (~£864) billion in 2080. Without contemplating the significance of other neurodegenerative diseases (i.e., Huntington's disease (HD), amyotrophic lateral sclerosis (ALS) and frontotemporal dementia (FTD), to name a few) the gravity of the tribulations related to neurodegenerative disorders are already clearly conspicuous. To mitigate this looming burden and to better the global quality of life, there is an urgent need to develop sustainable and economical alternative therapies for neurodegenerative diseases.

## **1.2. Neurodegenerative diseases**

Common to most neurodegenerative diseases are fundamental processes of progressive neuronal dysfunction and cell death caused by protein abnormalities. The pathologies of protein abnormalities can be generally classified into amyloidoses (Shin and Robinson-Papp, 2012),  $\alpha$  synucleinopathies (McCann et al., 2014), taupathies (Kovacs, 2018) and transactivation response deoxyribose nucleic acid (DNA) binding protein 43 (TDP-43) proteinopathies (Lin *et al.*, 2009).

Briefly, amyloidosis is the aggregation or abnormalities related to insoluble fibrous proteins called amyloids within intracellular or extracellular structures of tissues and organs (Baker and Rice, 2012).  $\alpha$  synucleinopathies is characterised by aggregation within neurons, glia and oligodendroglia, of  $\alpha$  synuclein: a 140 amino-acid presynaptic protein that may contribute in synaptic vesicle trafficking (McCann et al., 2014). Taupathies are pathological accumulation of microtubule-associated phosphoprotein (i.e., Tau) within neurons and glia (Kovacs, 2018). Lastly, TDP-43 proteinopathies is caused by inclusions consisting of 43-kDa proteins known

as TDP-43, which normally operates as a transcription repressor, that can modulate gene splicing, RNA metabolism, and influence stress granules (Ratti and Buratti, 2016).

Subsequent broad effects of the aforementioned proteinopathies include increased oxidative stress, programmed cell death, neuroinflammation, and proteotoxic stresses, ultimately leading to neuronal atrophy (Baker and Rice, 2012; Shin and Robinson-Papp, 2012; W. Chen *et al.*, 2012). The loss of neurons and connections in the brain is the major cause for the clinical features of neurodegenerative diseases such as extrapyramidal, pyramidal, cognitive, or behavioural disorders, to name a few (Dugger and Dickson, 2017).

Diagnosis of neurodegenerative diseases is usually classified according to clinical features, anatomic distribution of atrophy, or principal molecular abnormalities. However, note that the onset of such clinical features does not always occur concurrently with the initial presence of protein abnormalities. To make matters more complex, it is also possible for a neurodegenerative disorder like AD, to display multiple protein abnormalities and pathologies, such as amyloid or senile plaque deposits in the parenchyma of the brain, neuronal tau inclusions, and amyloid angiopathy (Tagliavini *et al.*, 1988; Fukumoto *et al.*, 1996). Even within the same neurodegenerative disorder (e.g., parkinsonian disorders), there are clinical and pathological heterogeneity (Dugger *et al.*, 2014). Given the complexities of the neuropathologies and the general lack of specific understandings regarding neurodegenerative diseases, the current development of potential therapeutics is limited to an extent.

### **1.3.Current therapies for neurodegenerative diseases**

The overall complexity of multiple neuropathologies of neurodegenerative diseases, which lead to widespread neuronal cell death and the contradicting etiologies, creates major challenges in the efforts towards understanding their pathogenic processes. Consequently, the

validation of potential new molecular entities through new drug applications, or new biological products through biological license applications are impeded due to the lack of distinctive prognostic and diagnostic biomarkers for neurodegenerative diseases. Moreover, this presents a paradoxical challenge for new molecular entities or biological products to obtain approval from regulatory bodies like the Food and Drug Administration's (FDA) Centre for drug evaluation and Research (CDER) and Centre for biologics evaluation and research (CBER) in the United States (US). Other regulatory bodies include the Medicines and Healthcare Products Regulatory Agency (MHRA) in the United Kingdom (UK), and the European Medicines Agency (EMA) for the nations of the European Union (EU) (Iglesias-Lopez *et al.*, 2021). Despite these obstacles, the FDA recently approved 53 novel drugs and eight new biological license applications in 2020, and more than 31 novel drugs in 2021 including aducanumab and satralizumab-mwge for the treatment of AD and neuromyelitis optica spectrum disorder, respectively ([www.fda.gov](http://www.fda.gov)).

Unfortunately, the current therapies on offer are incapable of exhibiting complete reparative effects or functional replacement of damaged or lost neurons caused by degeneration. For example, pharmacological therapies for PD cannot deliver dopamine (DA), or replicate the normal release of DA, to the specific brain regions as needed (Fernandez-Muñoz *et al.*, 2021). Additionally, the majority of the available treatments are palliative without resolving the underlying multifactorial aetiology (Sulzer, 2007; Tonda-Turo *et al.*, 2018). In conjunction, pharmacological therapies like L-3-4-dihydroxyphenylalanine has been reported to cause hallucinations and dyskinesia side effects, whilst deep brain stimulation therapy pose risks of infections, brain haemorrhage or stroke (Goetz *et al.*, 2005; Deuschl *et al.*, 2006; Garitaonandia *et al.*, 2018).

Another major challenge for therapeutic developers is ensuring their bioavailability at the target site in organs or tissues. For many debilitating neurodegenerative diseases, the target site is the

parenchyma of the brain or usually tissues within the CNS. The challenge with treatment of neurodegenerative diseases is the delivery of therapeutic products across the blood-brain barrier (BBB): a physiological barrier composed of the cerebral capillary endothelium, basement membrane, neuroglial membrane, and podocytes, that regulates transportation of molecules between the cerebral capillary (blood) and the interstitial fluid of the brain. Typically, the composition of an intact BBB can limit the availability of therapies to the brain parenchyma to only molecules that are of low molecular weight (<400 – 500 Da) and lipophilic (Hou *et al.*, 2019). Regulators mainly deny potential therapeutic products due to their inability to cross the BBB, regardless of demonstrating safe use and efficacy (Leclerc, Dudonné and Calon, 2021).

Biological therapies such as antibodies (Abs; e.g. Humira®, Remicade® and Enbrel®) and gene therapies, are especially challenging to transport across the BBB due to their large molecular structures (Pardridge, 2020). The first FDA approved biologic capable of crossing the BBB was an adeno-associated-9-based gene therapy for the treatment of infantile spinal muscular atrophy (Pardridge, 2020). To date, there are no approved biological therapies specifically for neurodegenerative diseases that can penetrate the BBB through systemic administration (Tonda-Turo *et al.*, 2018; Cascione *et al.*, 2020; Pardridge, 2020; Seo and Park, 2021). Therefore, technologies which facilitate delivery of therapeutics across the BBB are a major research field. Some groups have developed carriers such as liposomes or nanoparticles that can assist in the delivery of therapeutics to typically restricted CNS locations (Modi *et al.*, 2010; Seo and Park, 2021).

Nonetheless, effective novel therapies with curative, regenerative or wide-spread reparative effect is needed. Hence, cell-based therapies have been identified as an exciting alternative treatment for neurodegenerative diseases that could overcome the limitations currently observed with the current therapy profile.

#### **1.4. Cell-based therapies as an alternative for treating neurodegenerative diseases**

Cell-based therapies classifies under the category of advanced therapeutic medicinal products (ATMPs), with great promise as treatments for neurodegenerative diseases. This therapeutic route relies on autologous or allogeneic cellular material directly transplanted to the patient, which in turn provides therapeutic effects through intrinsic cellular properties (Kim, 2013). In contrast to single target small molecule drugs, cell-based therapies can trigger a multitude of targets and active several therapeutic mechanisms which include regenerative, rejuvenating, or potentially curative outcomes. Cell-based therapies could also be applied to physically replace atrophied cells and tissues, or repair dysfunctional systems by integrating into the appropriate tissue networks.

Cell-based therapies can be divided into non-stem cell-based or stem cell-based. The former relies on differentiated somatic cells such as fibroblasts, hepatocytes, keratinocytes, T-cells, dendritic cells, natural killer cells, macrophages, and chondrocytes, or cells a like, to deliver therapeutic effects (Mount et al., 2015; El-Kadiry, Rafei and Shammaa, 2021). Differentiated somatic cells can offer specific therapeutic properties. For example, chondrocyte based therapies have been utilised as cellular scaffolds in symptomatic full-thickness cartilage defects of the knee (El-Kadiry, Rafei and Shammaa, 2021).

Stem cell-based therapy relies on cell types called stem cells. Stem cells can be administered directly into patients in stem cell therapies (Pittenger et al., 2019), or firstly differentiated towards target specific cell types, thus becoming stem cell-derived/based therapies. Such therapies have demonstrated promising outcomes as potential treatments for various conditions such as cardiovascular diseases, autoimmune disorders, graft-versus-host disease, diabetes and macular degeneration (*Mingliang et al., 2011; Prowse et al., 2011; Bartel, 2014; Gurusamy et al., 2018*). For neurodegenerative diseases, stem cells with neuroregenerative properties, or the

plasticity to commit towards the neural lineages, are the most promising (Joyce et al., 2010; Liu, Yang and Zhao, 2020).

### **1.5. General stem cell terminology**

Discernible by their attributes to proliferate indefinitely, self-renew and differentiate into various cell types, stem cells display potential versatility as a cell source for cell-based therapies, tissue engineering, disease modelling, and toxicological screening (El-Kadiry *et al.*, 2021).

The stem cell terminology is an umbrella term which encapsulates adult stem cells (ASC) and pluripotent stem cells (PSCs). Stem cells can be categorised according to their origin of source and developmental potency (totipotent, pluripotent, multipotent, oligopotent, and unipotent). Totipotent stem cells, like cells of the morula, can differentiate into all cell types of the human body including the extra-embryonic tissue. Pluripotent stem cells (PSCs) such as cells of the inner cell mass (ICM) of a developing blastocyst or induced pluripotent stem cells (iPSCs) can differentiate into all three germ layers thus giving rise to most cell types of the human body, however, they lack the capability to produce extraembryonic cells like the placenta (Prochazkova *et al.*, 2015). Most ASCs are multipotent and can differentiate towards lineages of a specific tissue or organ, exhibiting a more limited differentiation range. Mesenchymal stem cells (MSCs) are an example of multipotent ASCs which can only differentiate towards cells of the adipogenic, osteogenic and chondrogenic lineages. Oligopotent stem cells can differentiate towards several, but not all lineage of a tissue or organ, such as the common lymphoid progenitor cells. Finally, unipotent stem cells display the narrowest differentiation potential with only one lineage route; dermatocytes being a clear example (Singh *et al.*, 2016).

Nevertheless, the ability to self-renew, proliferate, and give rise to specialised cells is common amongst all stem cells. The potential for stem cells to differentiate towards therapeutically relevant cell phenotypes makes them an indispensable source material for cell-based therapies. The therapeutic benefits of each type of stem cell (i.e., types of ASC or PSC) are cell dependent. NPCs for example, were shown to display antiapoptotic effects and immunomodulatory properties, with superior effects on subject behaviour compared to that of MSCs, according to a meta-analysis of NPC treated subjects at preclinical stages (Janowski, Walczak and Date, 2010) Therefore, it is important to understand the different stem cell types to wholly utilise their specific potentials for treating neurodegenerative diseases.

### **1.6. Adult stem cells (ASCs)**

Amongst the differentiated cells in the human body are rare tissue specific stem cells known as ASCs. They reside as undifferentiated populations of cells in specialised vascular microenvironments, known as stem cell niches (Laperle *et al.*, 2015). The stem cell niche provides extrinsic determinants that regulate ASCs in an undifferentiated and long term self-renewing state. In tandem with intrinsic cell determinants such as epigenetic and molecular repertoires, ASCs respond to specific signals of the niche that can influence ASCs to proliferate, differentiate or remain quiescent.

The primary functions of ASCs are to sustain tissue homeostasis by replenishing aged cells, and to some extent, replace damaged or lost cells from disease or injury. The conservation of an ASC pool is achieved by their ability to undergo symmetric or asymmetric division (Faigle and Song, 2013). During symmetric division, ASCs produce identical copies of daughter cells which are either two identical ASCs leading to increased ASC population, or give rise to two identical differentiated cells, which in turn depletes the ASC population. In asymmetric

division, ASCs produce two non-identical daughter cells: one is influenced to commit towards a specific lineage, and the other being a stem cell. Asymmetric division leads to increased differentiated cell population, whilst maintaining the ASC pool (Pittenger *et al.*, 2019).

Depending on their origins, ASCs can display multi-, bi- or uni- potency. Typical ASCs possess differentiation potential towards cells related to their tissue of origin. For example, hematopoietic stem cells (HSCs) are ASCs which reside within the bone marrow, umbilical cord blood or in the peripheral blood. They typically reside in these niches in a quiescent state for prolonged periods. However, when induced to divide, they undergo asymmetric divisions giving rise to one new HSC and myeloid or lymphoid progenies, which eventually generates mature blood cell types such as white cells, red cells and platelets (Seita and Weissman, 2010; Lee and Hong, 2020). Asymmetric division allows for ASCs to replenish the stem cell pool. The properties of HSCs and MSCs have been exploited in blood related issues, with a long history of successful application as a cell-based therapy since 1957 (Thomas *et al.*, 1957).

Since ASCs display limited differentiation potential, their clinical relevance is dependent on the type of ASCs. Cardiac related disorders such as myocardial infarctions would require stem cells capable of differentiating into myocardial cells, smooth muscle cells or epithelial cells (e.g., cardiac stem cells) to restore compromised contractile functions, and/or promote angiogenesis (Mingliang *et al.*, 2011). Other applications of ASCs have been reported for eye and pancreatic disorders (see review by Gurusamy *et al.*, 2018). The most relevant ASCs to this thesis are those that possess intrinsic differentiation potential towards neural lineages, or ASCs that can exogenously activate the stem cell pools within the CNS, thus indirectly exhibiting regenerative properties. Examples of such ASCs include neural stem cells and neural progenitor cells (Nagoshi and Okano, 2018a).

### **1.6.1. Neural stem, Neural progenitor, and Neural precursor terminology**

Both populations of NSCs and NP cells are able to differentiate into various types of neurons (i.e., cholinergic, dopaminergic, gabanergic etc.), astroglia and oligodendrocytes (Shivraj Sohur et al., 2006). Adult NSCs are distinguished from adult NP cells by their ability to self-renew, produce equivalent progenies, and differentiate towards both the neuronal and glial lineages (Shivraj Sohur et al., 2006). Adult NP cells are also more restricted to commit to only one lineage and ultimately differentiate towards either cells of the neuronal or glial lineage. In addition, adult NP cells exhibit a finite cell division capacity (Gage, 2000). Collectively, NSCs and NP cells are termed neural precursor cells (NPCs) (Dibajnia and Morshead, 2013; Yap *et al.*, 2015).

The term NSC itself encapsulates several types of multipotent undifferentiated cells. Its terminology can often be confused throughout literature. NSCs exist in embryonic neurogenesis and in mature adult brains. During embryonic neurogenesis, neuroepithelial cells of the ventricular zone are considered NSCs. Similarly, radial glial cells (RGCs) derived from neuroepithelial cells, and the population of intermediate progenitor cells (IPCs) which originate from RGCs, are also deemed NSCs. IPCs, however, can only undergo one or two symmetrical divisions before differentiating into a neuron. In general, these terminologies arise due to discrepancies between the molecular, cellular or anatomical profiles of the cell populations. Nonetheless, all are considered NSCs.

More specifically, within the subventricular zone (SVZ) of the lateral ventricular and the subgranular zone (SGZ) of the dentate gyrus resides NSCs, which are considered radial glial-like (RG-like) cells (Dibajnia and Morshead, 2013; Garitaonandia *et al.*, 2018). These cells have a more restricted differentiation potential towards neurons and oligodendrocytes. Unlike RGCs, however, RG-like cells are more limited in their proliferation capabilities (Simons and Clevers, 2011). In the SVZ, these GFAP positive RG-like cells are termed Type B cells which

are slowly proliferating and can give rise to progenitor cells termed type C cells (neuronal precursor cells) (Morshead *et al.*, 1994). Neuronal precursor cells/Type C cells can transiently and rapidly amplify by symmetric division and instead are GFAP and Vimentin negative. Ultimately, Type C cells give rise to neuroblasts/Type A cells. Neuroblasts are discerned from their precursors by expression of doublecortin (DCX), polysialylated neural CAM (PSA-NCAM) and TuJ1 ( $\beta$ -tubulin) (Doetsch *et al.*, 1997; Francis *et al.*, 1999).

GFAP positive NSCs/RG-like cells of the SGZ of the dentate gyrus (DG) display a more limited self-renewal and multipotent capacities. These cells are positive for paired box protein 6 (PAX6), glial fibrillary acidic protein (GFAP), astrocyte specific glutamate transporter (GLAST), sex determining region y-box 2 (SOX2), Nestin and Vimentin, similar to that of embryonic RGCs in a developing embryonic brain (Urbán and Guillemot, 2014; Galiakberova and Dashinimaev, 2020a). They also differ to the RG-like population in the SVZ whereby, they mainly differentiate towards neurons and astrocytes. To distinguish NSCs/RG-like cells of the SGZ from RG-like cells in the SVZ or RGCs of the embryonic developing brain, they are termed Type 1 cells. Type 1 cells can generate IPCs known as Type 2 cells which are similar to Type B cells from the SVZ. Subsequently, Type 2 cells can differentiate to give rise to neuroblasts/Type 3 cells (Seri *et al.*, 2004; Sugiyama *et al.*, 2013; Galiakberova and Dashinimaev, 2020a).

Despite the many and subtle differences between NSCs in the SVZ and SGZ, both RG-like cells (i.e., Type B and Type 1 cells, respectively) express the molecules Nestin, SOX2 and GFAP.

### **1.6.2. Role of adult NPCs *in vivo***

Understanding the role and maintenance of adult NPCs *in vivo* provides exploitable information for their translation in *in vitro* culture. In the mammalian brain, NPCs are involved in adult neurogenesis, gliogenesis and the maintenance of the adult brain homeostasis (*Tang et al.*, 2019).

NPCs reside within the SVZ of the lateral ventricle and the SGZ of the dentate gyrus of the hippocampus (*Ahmed et al.*, 2011). The neurogenic niche maintains classical developmental morphogens such as Notch, Bone Morphogenetic Protein (BMP), Eph/ephrins, Noggin and Sonic hedgehog homolog (SHH) (*Decimo et al.*, 2012), which regulates differentiation of NPCs (*Decimo et al.*, 2012). For example, Notch signalling has been demonstrated to negatively regulate cell cycle exit and maintain NSCs in a stem cell state (*Breunig et al.*, 2007; *Corbin et al.*, 2008). Other extrinsic determinants that influences NPCs within the stem cell niche include oxygen tension, trophic factors, growth factors, resident niche cells, and extracellular matrix (ECM) components (*Decimo et al.*, 2012) (see Figure 1.1).

Although the function of NPCs in the adult SVZ remain unclear, they are able to generate GFAP<sup>+</sup> type B cells which migrate rostrally to the olfactory bulb (*Martínez-Cerdeño and Noctor*, 2018). Here, they differentiate towards interneurons and disperse within the neural network where it has been suggested that their function is for repair (*Carlén et al.*, 2009).

In adult brain, neurogenesis appears precisely only in the dentate gyrus and generates only one type of neuron known as granule cells which are derived from type 1 cells (*Martínez-Cerdeño and Noctor*, 2018). Adult neurogenesis occurs in four phases: 1) precursor cell phase, 2) early survival phase, 3) postmitotic maturation phase, and 4) late phase. In the precursor cell phase, the cells serves to expand the pool of cells that could differentiate into neurons. The onset of early survival phase is the exit of the precursors out of the cell cycle and the expression of

Calretinin and NeuN. Only a few new-born cells survive following this phase. During postmitotic maturation, functional connections, axonal and dendrite extension, and synapses are established. Then finally, during the late survival, connections are tuned, in all taking approximately 7 weeks to complete from neurogenesis (Kempermann *et al.*, 2015).

The extent of adult neurogenesis in the DG has been suggested important for cognitive and affective behaviours such as learning, memory retention and clearance, as well as recognition of patterns (Berg *et al.*, 2018).

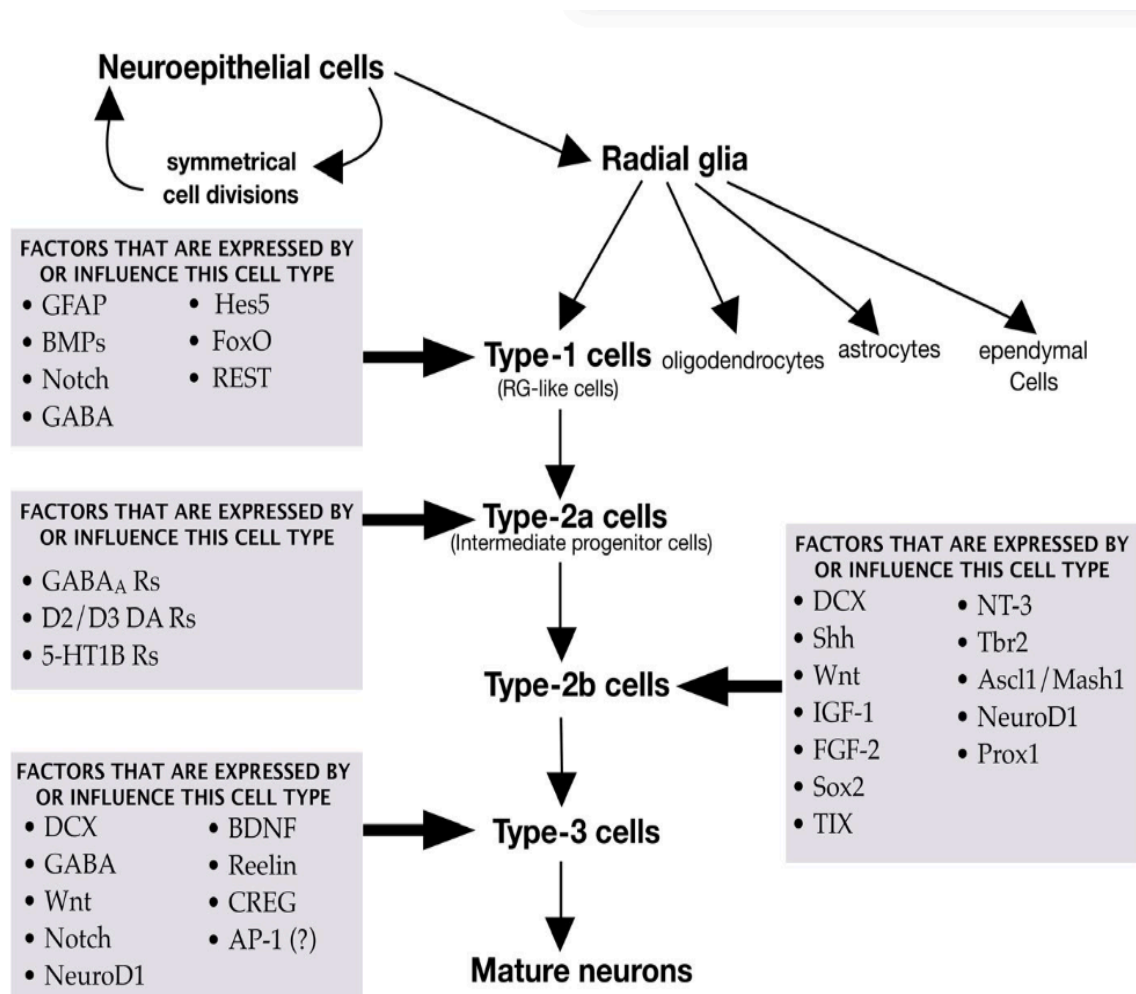


Figure 1.1. Diagram showing the factors involved in the differentiation steps from neuroepithelial cells to RG cells and their differentiation towards the neuronal and glial lineages. This diagram is adopted from Abbott and Nigussie (2020).

### **1.6.3. Clinical applications of NPCs**

As studies continue to unearth the mechanisms driving the regenerative properties of NPCs, their promise as a viable cell therapy is imminent. The path towards commercialisation, however, is long and requires stringent assessments of the candidate therapy; pre-clinical and clinical trials provide a framework to test the safety and efficacy of the candidate therapy prior to commercialisation.

After the discovery and identification of a potential therapeutic, it is first essential to demonstrate its safety in pre-clinical trials which usually employ animal test subjects. Following success in animal subjects, a submission for an investigational new drug (IND) application to regulators is submitted to gain permission to test in humans. Usually healthy volunteers, and subsequently diseased patients, are tested at the early-stage clinical trials, also known as clinical phase I/II. Early-stage clinical investigations are typically designed with the intentions to demonstrate product safety, determine dosage, and identify potential side effects (Jha *et al.*, 2021).

Further investigation into the efficacy of NPCs as a cell therapy would be the next steps. These are conducted at late-stage clinical trials, otherwise known as clinical phase III. Upon success of a phase III clinical investigation, regulators (e.g., FDA) review and decide on the release to commercialisation. With sufficient data and information, regulatory bodies can approve therapies for the commercialisation, which consequently enters it into phase IV clinical trials. At this stage, thousands of patients are monitored to further ensure safety and efficacy on a wider population (El-Kadiriy *et al.*, 2021; Jha *et al.*, 2021).

Importantly, the product CQAs and the critical process parameters (CPP) are defined and set throughout clinical trials so that it can be translated to commercial scale upon the success of the therapy.

At the time this thesis was written, 40 interventional clinical trial studies employing NPCs were identified from [clinicaltrials.gov](https://clinicaltrials.gov), some of which are summarised in Table 1.1. The majority of clinical trials identified were scheduled for phase 1 (I) or 2 (II), and only one was reported at phase 3 (III; NCT03128450). No studies were identified using the search criteria to be in phase 4 (IV; [clinicaltrials.gov](https://clinicaltrials.gov), 2022) and to date, there are no commercialised NPC cell-based therapies available.

Most reports published are from the findings of early-stage clinical trials. NPCs used in clinical trials currently are mainly foetal or embryonic tissue-derived. Riley *et al.* (2012) reported the safety of foetal-derived NSCs via intraspinal delivery in 12 patients with progressive MS, demonstrating no motor function decrement post-treatment. Similarly, a study by Mazzini *et al.*, (2015) exhibited the safe use of foetal-derived NSCs with no progressive development of the disease (ALS) in 6 patients. Madrazo *et al.*, (2019) later showed that the transplantation of NP cells were also safe with no adverse side effects in seven patients, most of which developed improved motor functionality and responsiveness to medication. Several other groups have reported the safe usage of foetal-derived NPCs for the treatment of various neurological disorders (Ferrari *et al.*, 2018; Pollock *et al.*, 2006; Stroemer *et al.*, 2009).

Interestingly, Kefalopoulou *et al.* (2014) conducted a study over 18 years reporting the motor improvement of two patients who received intrastriatal grafts of human foetal-derived DA neuroblasts. They reported long term improvement and sustained motor functionality in patients with PD, with no dependency on pharmacological dopaminergic therapy (Kefalopoulou *et al.*, 2014). Although, their study employed dopaminergic neuroblasts, NSCs

can also differentiate towards dopaminergic neuronal lineages and neuroblasts can therefore potentially offer similar therapeutic benefits to treat PD (Doetsch *et al.*, 1999; Sugiyama *et al.*, 2013; Lee *et al.*, 2019; Gilmozzi *et al.*, 2021).

In all, many phase I/II clinical reports suggested safe applications of NPCs in early phase clinical trials, with some studies suggesting signs of therapeutic benefits. While the underlying mechanisms of how NPCs ameliorate various pathological mechanisms of neurodegenerative diseases remain largely unknown, it is thought to be mediated through neurotrophic support, neuroregeneration and immunomodulation (Teng *et al.*, 2012). Still, regardless of success in the early clinical trials, most studies have not managed to then progress to later-stage clinical trials which would enable to further investigate the efficacy of the candidate NPC-based therapies using a larger volume of human patients and volunteers. The progression of studies through clinical trials are hindered by many factors, especially considering the complexity of NPC-based therapies. These challenges are further discussed in the next section.

Other potential applications of NPCs outside direct patient application include neurotoxicity/drug screening (Grainger *et al.*, 2018), pathological and developmental modelling (Williams *et al.* 2018), or the treatment of spinal cord injuries (Trawczynski *et al.*, 2019).

Table 1.1. A table summarising examples of clinical trials from clinicaltrials.gov (last accessed 28th January 2022). Inclusion criteria included the terms “neural stem cell”, “neural progenitor cell” and “neural precursor cells”. Only interventional study types were included. Trials with the status of terminated and no longer available were excluded from this search. Note that this is not the extent of clinical trials employing NPCs.

Condition or disease	Source of cells	Therapeutic cell type	Dosage	Mode of delivery	Phase	Clinical trials.gov identifier	References
Ischaemic stroke	Foetal	NSCs	20 x 10 <sup>6</sup> cells	Intracerebral	2	NCT03629275	Unknown
Progressive sclerosis (MS)	Multiple Foetal	NSCs	5.7 x 10 <sup>6</sup> ± 10% cells/kg	Intrathecal	1	NCT03269071	Unknown
Amyotrophic Sclerosis	Lateral Foetal	NSCs	4.5 x10 <sup>6</sup> cells	Intraspinal	1	NCT01640067	(Mazzini, Gelati, et al., 2015)
Secondary-progressive MS	Foetal	NSCs	20 x 10 <sup>6</sup> cells	Intraventricular	1	NCT03282760	Unknown

PD	Foetal	NSCs	>2 x10 <sup>6</sup> cells/vessel	Nasal delivery	drug 3	NCT03128450	Unknown
Ischemic stroke	hESC	NSCs	Not specified	Intracerebral	2	NCT04631406	Unknown
Spinal cord injury	hESC	NSCs	Not specified	Intrathecal	2	NCT04812431	Unknown
Spinal cord injury	Autologous MSC	NSCs	Not specified	Intraspinal	2	NCT02326662	Unknown
PD	Allogenic MSCs	NSCs	Not specified	Intrathecally	2	NCT03684122	(Jamali et al., 2021)
Progressive MS	Autologous MSCs	NP cells	10 x 10 <sup>6</sup> cells	Intrathecal	2	NCT01933802	(Harris et al., 2018)
PD	Human parthenogenetic PSCs	NSCs	70 x 10 <sup>6</sup> cells	Intracerebral	1	NCT02452723	(Garitaonandia et al., 2018)
PD	hESC	NPCs	Not specified	Intrastratial	2	NCT03119636	(Wang et al., 2018)

#### **1.6.4.Challenges with NPC-based cells as a cell therapy**

Several challenges hinder the progression of NPC-based therapies through clinical trials, further blocking their commercial availability. These bottlenecks can be split into three: ethical, biological, and manufacturing challenges.

##### **1.6.4.1.Ethical challenges**

First, most clinical trials currently use human foetal/embryonic-derived NPCs as therapeutic candidates for neurodegenerative diseases (see Table 1.1). Often, these are obtained from foetal tissues of elective or spontaneous abortions, with the former source causing major ethical concerns and opposition from religious and pro-life groups (Douglas and Savulescu, 2009). Furthermore, the use of any human foetal-derived NPCs in general have provoked restrictions imposed by regulatory boards and governments, rendering their use limited in some countries (Fernandez-Muñoz et al., 2021). Other methods of sourcing NPCs include surgical extraction from in vivo human niches which are complex, costly, inefficient, and poses high risks to the donor.

##### **1.6.4.2.Biological challenges**

Second, biological differences amongst candidate NPC-based therapies can lead to variation in clinical results. The causes of variation in NPC quality can be dependent on the tissue of origin, donor, and in vitro handling of the cells (i.e., method of cell delivery to the patients or in vitro culture systems). For example, cells derived from different physiological locations of a foetal tissue (i.e., brain vs spinal cord) from the same donor could possess different levels of intrinsic plasticity (Kim *et al.*, 2018; Zhang *et al.*, 2021). Similarly, NPCs derived from the same physiological location of foetal tissues, but from different donors, would display varying

genetic and epigenetic profiles. Additionally, NPCs obtained from the forebrain of foetal tissues leads to a collection of heterogenous NPC populations at different differentiation stages (Yin *et al.*, 2013).

NPC expansion is necessary to obtain sufficient quantities of cells at the therapeutic doses. This is especially true for NPCs derived from limited sources, such as foetal tissues. Through understanding the conditions maintaining NPCs *in vivo*, several *in vitro* culture systems have been developed for NPC expansion. Of note, biological changes can be induced in NPCs by factors of the culture system. For example, genetic aberration can occur due to cell stress from serial passaging. Thus, variations of *in vitro* culture systems amongst different laboratories (discussed in greater detail in Sections 1.8) of therapeutic developers can lead to variations in NPC quality. Ultimately, biological variations can affect the therapeutic effect of NPCs leading to contradictory clinical results (Ottoboni *et al.*, 2020).

#### **1.6.4.3. Manufacturing strategies**

Third, the requirement for large quantities of clinically relevant NPCs imposes manufacturing challenges. Progression of a candidate NPC-based therapy through clinical stages is permitted only by satisfactory safety and efficacy results. For early-stage clinical trials, progression could require satisfactory results from one to hundreds of volunteers. At late-stage clinical trials, this could increase to several thousand volunteers. Increased investments at late-stage clinical trials are necessary to accommodate for the increased NPC-based product doses per volunteer, in order to pass clinical trials. Mainly, investments are needed to cover the costs of the manufacturing process for clinical grade NPCs, whereby raw materials, labour, equipment, and manufacturing space play a significant influence.

Nonetheless, it is also necessary to contemplate the volume of patients that would eventually require the NPC-based treatments post clinical trials. For example,  $\sim 70 \times 10^6$  cells/patient are necessary to test the safety and efficacy of NSCs in patients with PD (Garitaonandia et al. 2018). If successful, manufacturing processes for NSCs will need to accommodate for more than 145,000 people living with PD in the UK alone as of 2020 ([www.parkinson.org.uk](http://www.parkinson.org.uk)), meaning more than an estimated  $1.015 \times 10^{13}$  cells would be required. Other studies have employed as much as  $5.7 \times 10^6 \pm 10\%$  human foetal-derived NSCs / kg of body weight for the treatment of MS (Clinicaltrials.gov: NCT03269071). Therefore, for a 70 kg patient, around  $3.99 \times 10^8$  cells would be required. The prevalence of MS is 110,000 people in the UK alone as of 2020 ([www.gov.uk](http://www.gov.uk)). Considering all the other types of neurodegenerative diseases and their prevalence, it is clear that manufacturing processes for NPC-based therapies should be at large or industrial scale.

#### **1.6.4.4. Addressing the current challenges with NPC-based therapies**

In summary, ethical, biological, and manufacturing challenges prohibit the progression of NPC-based therapy candidates through clinical stages, consequently hindering commercialisation. Alternative methods to obtain sufficient quantities of NPCs for clinical studies devoid the use of foetal or embryonic tissues would circumvent the ethical and legal issues. Furthermore, a standardised or universal culture systems for the generation of clinical-grade NPCs is needed to minimise biological variation in therapies. In fact, setting standardised criteria for quality validation of clinical-grade NPCs would further reduce confounding inferences of clinical results.

It is also vital to consider manufacturing strategies at the earliest onset of therapy development, which is usually disregarded by developers. Lab scale manufacturing processes that can be translated to large, industrial, and commercial scales positively influence the success of a therapy. Therefore, solutions towards a sustainable, cost-effective, and scalable manufacturing process to produce clinical-grade NPCs are timely necessary.

PSCs provide an alternative source for NPCs. Indeed, the property of PSCs to differentiate towards NPCs by neural induction in vitro is a promising route (Rogers, Moody and Casey, 2009; Robinton and Daley, 2012; Nakagawa *et al.*, 2014; Garitaonandia *et al.*, 2018). A manufacturing process, whereby clinical-grade NPCs are derived from PSCs, would need a different manufacturing process compared to foetal-derived NPCs. Broadly put, a manufacturing process from PSCs to NPCs would need to consider process steps such as: PSC manufacturing; followed by neural induction of PSCs; and finally, NPC manufacturing.

Therefore, a good understanding of PSC maintenance, neural induction mechanisms and NPC maintenance, would allow for a holistic approach to designing manufacturing processes for the production of hiPSC-derived NPC based therapies. The following sections will, therefore, explore PSC maintenance (section 1.7), the neural induction process (section 1.8) and NPC maintenance (section 1.9).

### **1.7.Pluripotent stem cells**

In 1998, Thomson *et al.*, (1998) reported the isolation of human embryonic stem cells (hESC) following successful extractions of the ICM from developing blastocysts. hESCs can differentiate towards the endoderm, mesoderm, and ectoderm lineages, hence, possessing pluripotent properties.

Another type of PSCs are human iPSCs (hiPSCs) which also exhibit similar properties to that of hESCs. Instead, hiPSCs are achieved by reverting adult somatic cells into a pluripotent state through reprogramming methods. This technique was firstly demonstrated using mouse somatic cells (Takahashi and Yamanaka, 2006) and then in humans shortly after by Takahashi et al. (2007). Essentially, reprogramming of somatic cells to a pluripotent state involves intracellularly introducing specific transcription factor genes collectively termed the Yamanaka factors which include: octamer-binding transcription factor 4 (OCT4); sex determining region box-2 (SOX-2); Kruppel-like factor 4 (KLF4); and cellular Myelocytomatosis (C-MYC) (Liu et al., 2008). As a result, transcriptome changes and chromatin restructuring occur. The expression of the Yamanaka factors leads to the synthesis of their respective transcription factor proteins. These transcription factors bind to pluripotency associated recognition sequences and creates an interconnected autoregulatory circuitry that induces and maintains the expression of other pluripotency associated genes (Takahashi and Yamanaka, 2016). Under appropriate exposure to the right conditions, hiPSCs can be maintained in a pluripotent and proliferative state in vitro. These conditions are detailed in the following sections.

Though, both hESCs and hiPSC have their own advantages and disadvantages as a cell source for cell therapies, only hiPSCs paves a route for personalised and patient specific PSC-based therapy.

### **1.7.1. Naïve vs primed PSCs**

PSCs can be in a naïve or primed state, which is defined by their developmental stage. However, defining human pluripotent states is proving difficult due to the ethical restrictions associated with hPSC research, in particular hESCs. Generally, naïve PSCs resemble

characteristics of cells within the inner cell mass of a human embryo at day (E) 6-7 preimplantation blastocysts (Ware *et al.*, 2014). Alternatively, primed PSCs resemble cells of post-implantation epiblast at later stages of embryo development.

Although recent molecular and phenotypic research on human embryos are starting to unveil specific characteristics of primed or naïve human pluripotent cells, current knowledge of this topic has mainly relied on the comparison of the morphologies and culture conditions between mouse PSCs to that of human PSCs (Martin, 1981; Thomson *et al.*, 1996; Nakamura *et al.*, 2016; Petropoulos *et al.*, 2016; Theunissen *et al.*, 2016). To name a few discrepancies, mESCs in culture heavily depends on growth medium containing leukaemia inhibiting factor (LIF), bone morphogenetic proteins (BMP) 4 and signal transducer and activator of transcription 3 (STAT3). In the absence of these supplements, the activation of the mitogen activated protein kinase (MAPK) pathway via the ligation of fibroblast growth factor 4 (FGF4) promotes the differentiation of mESCs (Kunath *et al.*, 2007). Thus, cultures of mESCs typically also include inhibitors of the MAPK and glycogen synthase kinase 3 (GSK3) which are PD0325901 and CHIRON99021 (2i) molecules, respectively (Ying *et al.*, 2008).

On the contrary, LIF is expendable for hESC cultures whilst BMP-4 drives the differentiation of hESCs into trophoblasts (Xu *et al.*, 2002). Similarly, the addition of 2i also causes the differentiation of hESCs (Ware *et al.*, 2014). Importantly, activation of signalling pathways related to basic fibroblast growth factor 2 (bFGF-2), Noggin, Activin/Nodal, and TGF- $\beta$  are imperative for promoting self-renewal of hESCs instead (James *et al.*, 2005; Xu *et al.*, 2005).

Furthermore, epigenetic signatures such as DNA hypomethylation is an indicator of naïve pluripotency in both human and mouse preimplantation embryos, where naïve hPSCs display around 70% global DNA methalomes. Another epigenetic hallmark for differentiation is the transcriptional inactivation of one of the X chromosomes, which is present only in primed

female hESCs and absent in naïve female hESCs (Hoffman *et al.*, 2005; Petropoulos *et al.*, 2016).

In general, specific hPSCs characteristics of a naïve state have been reported to adopt a domed appearance in culture, high single cell survival, low levels of methylation (~30%) and perform metabolism via oxidative phosphorylation. In contrast, primed state hPSCs have been reported to adopt a flat appearance, with low single cell survival rate, high methylation levels of global CpG (~80%) and reliant on glycolysis (Theunissen *et al.*, 2016).

Likewise, typical hiPSC cell lines display distinctly different culture requirements and morphology to that of naïve mESCs, whilst similar to that of primed hESCs. Thus, hiPSCs are often considered primed state and shares similar culture requirements to that of primed hESCs (Tchieu *et al.*, 2010).

Interestingly, conversion of primed hESCs or hiPSCs to a naïve state can be achieved using small molecules. For example, supplementation of GSK inhibitor (BIO), BMP signalling inhibitor (Dorsomorphin) and phosphatidylinositol 3 kinase (PI3K) inhibitor (PD0325901) to hESC media containing LIF allow for the conversion of primed hESCs to a naïve state (Chan *et al.*, 2013). This concoction is also known as 3iL. Another route for obtaining naïve hESCs is preculturing primed hESCs in histone deacetylase inhibitors (HDACi) and then in 2i medium supplemented with FGF2 (2iF). Theunissen *et al.* (2014) reported the successful conversion of hESCs from a primed to naïve state using 5 kinase inhibitors (5i) in addition with LIF and Activin A (5i/L/A).

Though these methods demonstrate different ways of reverting primed hPSCs to their naïve pluripotent states, is it even necessary to employ naïve PSC for cell-based therapy? The current literature suggests that the different pluripotent states can influence the intrinsic differentiation potential of PSCs. Indeed, from a therapeutic developer perspective, it would only be necessary

to revert primed hPSCs to a naïve state if the primed hPSCs cannot be differentiated towards the target therapeutic cell type. However, future studies would need to further investigate whether there are discrepancies in the quality or function of differentiated cells derived from naïve or primed hPSCs.

Furthermore, different pluripotent states (i.e., primed or naïve) impose different specific culture conditions in vitro to maintain the hPSCs in a proliferative, self-renewing and undifferentiated state. From a bioprocess developer perspective, the state of the PSCs can impact the bioprocess design in terms of operation modes (e.g., feeding regime) and process costs which are heavily influenced by the media composition; the more the media is composed of small molecules and expensive factors, the costlier the process become.

For simplicity, from here on, reference to PSCs, including hiPSCs and hESCs, shall refer to their respective primed pluripotent state, unless otherwise stated. Furthermore, since hESCs and hiPSCs are considered similar phenotypically, processes and methods developed for hESCs can also be considered applicable for hiPSCs, unless stated otherwise.

### **1.7.2.Limitations and safety concerns surrounding PSCs in cell-based therapies**

The use of either hESCs or hiPSCs as a cell source for cell-based therapies is tethered to their respective exclusive advantages and limitations. For instance, hESCs obtained from the ICM of a developing blastocyst do not require subsequent processing steps to obtain pluripotent cells. Whereas, reprogramming of somatic cells is necessary for obtaining hiPSCs. Also, hESCs do not typically display the extent of epigenetic modifications usually present in hiPSCs lines, especially when the hiPSCs are reprogrammed from aged somatic cells (Kim et al., 2010). These epigenetic differences could influence many attributes of the hiPSC cell line such reduce differentiation potential range or pluripotency gene expression.

However, hESCs pose potential risks to the patient such as immunological incompatibility as an allogenic treatments (Nie et al., 2010). Their use also elicits ethical and religious resistance due to the destruction of an embryo. and they are dependent on the availability of blastocysts, further presenting an impending sourcing constraint (Volarevic et al. 2018).

hiPSCs can overcome the limitations associated with hESCs (Takahashi et al., 2007). Ethical consent and derivation of hiPSCs can be achieved from healthy donors or patients. The latter route of obtainment allows for autologous, patient specific cell therapy. Autologous treatments have a reduced risk of immune rejection due to compatible human leukocyte antigen (HLA) system of the therapy to that of the patient (Madrid et al., 2021; Rehakova et al., 2020). However, partial reprogramming, de novo genetic mutations, and genetic instabilities within hiPSCs could trigger immune responses in transplanted recipients, regardless of using autologous sources. Furthermore, the use of vectors for hiPSC derivation (e.g., viral or non-viral vectors) can remain in the final product and be consequently delivered to the patient. This raises potential risks to the recipients' cells, especially when employing integrating viral vectors for the reprogramming which can cause genetic aberrations (Ben-David and Benvenisty, 2011).

Alternatively, clinically suitable reprogramming methods are viable routes to obtain clinical grade hiPSC. These reprogramming methods include the use of non-integrating vectors such as the negative single-stranded RNA Sendai-virus to introduce Yamanaka factors into the cells. Unfortunately, such methods yield low conversion efficiencies reported to be around 0.001% to 4% (Ban et al., 2011; Fusaki et al., 2009; MacArthur et al., 2012; Schlaeger et al., 2015; Seki et al., 2010). Other non-integrative methods without reliance on viral vectors include direct delivery of cytoplasmic RNA, episomal vectors, transposon vectors, recombinant proteins, microRNAs, liposomal magnetofection or polycistronic minicircle DNA vectors (Haridhasapavalan et al., 2019). Similarly, reprogramming using nonintegrating non-viral

methods have been reported to reach as low as 0.00033% for plasmid DNA (Si-Tayeb et al., 2010) and 0.005% for minicircle DNA vectors (Jia et al., 2010; Narsinh et al., 2011) as examples. Many factors affect the efficiency of reprogramming including the genetic and epigenetic makeup of the somatic cell type, and the reprogramming method used. Consequently, there remains focus on the development and improvement of reprogramming methods that appeases clinical and cGMP standards (Durruthy-Durruthy et al., 2014). A review by Haridhasapavalan et al., (2019) explores these strategies in greater detail.

Nonetheless, tumorigenic risks is a major concern for the use of either PSC type as they have the potential for unlimited division in vivo (Ben-David and Benvenisty, 2011). Therefore, it is crucial for manufacturing processes of PSC-based therapies to ensure the removal of undifferentiated cells prior to delivery into the patient.

Several strategies have been reported for selectively isolating and removing differentiated or residual PSCs. These include the induced expression of a suicide gene in PSCs (Schuldiner, Itskovitz-Eldor and Benvenisty, 2003), delivery of cytotoxic drug conjugated antibodies (Tan *et al.*, 2009), or magnetic activated cell sorter (Tsujiisaka *et al.*, 2022).

Other factors that make hiPSCs more attractive as a cell source for cell-based therapies instead of hESCs include their potential for allogenic as well as autologous treatment routes. hiPSCs can be easily sourced from more sustainable tissues compared to embryos. Nonetheless, autologous treatments would be the ideal therapeutic route especially for patients who are not currently covered by major HLA-matched haplobanks, patients with poor responses to immunosuppressors or those with chronic progressive diseases (Madrid et al., 2021b).

### **1.7.3. Towards clinical grade hiPSC-based therapies**

As with any therapeutic drug or biologics, quality control and quality assurance throughout the manufacturing process are vital to ensuring the safety of the products used in humans. Good manufacturing practise (GMP) is an FDA enforced system that imposes stringent regulations regarding people, products, processes, procedures, and premises within manufacturing facilities. The aim of implementing a GMP system for the bioprocessing of hiPSCs is to ensure the products are produced in a controlled, monitored, and standardised manner. In general, GMP standard requirements include employees to be trained in current GMP (cGMP) standards; products to be consistent and regularly checked; processes to be clearly documented and controlled; procedures must be standardised, and employees competently trained to perform; and the premises should promote aseptic processes especially when handling biological products to avoid cross-contaminations and accidents. Ultimately, cGMP systems are designed to protect the patients and plays an influential role in the holistic design of the bioprocess for hiPSC-based cell therapies from upstream to downstream and analytics.

Organisations such as the Global Alliance for iPSC Therapies aim to standardise stem cell manufacturing processes by defining the critical quality attributes (CQAs) for hiPSC-based cell therapies. Sullivan et al.( 2018) summarises the general CQAs consensus for clinical grade hiPSCs and the assays associated to test and assure their quality. Their report places importance on assuring hiPSC-based products are contaminant free (e.g., bacteria, mycoplasma, virus, endotoxin, and residual vector); karyotyped to show genetic stability; and characterised to show pluripotency markers (e.g., OCT4, SOX2, SSEA4, Nanog, TRA-1-60, TRA-1-80 etc.), differentiation potential and high cell viability (>60%), amongst other proposed assays (see Table 1.2 for full list).

**Table 1.2.** Summary of the proposed requirements for clinical grade hiPSCs. The details of the recommended assays to test and validate the proposed CQAs are shown in this table. Additionally, the acceptance criteria are also listed for each CQA. The details in this table are adopted from the report by Sullivan et al., (2018).

Attribute	Test	Status	Recommended analytical method	Acceptance criteria
Identity	Short tandem repeat (STR)	Mandatory	STR profiles Performed by accredited laboratory on donor starting material and lots	Identical
Microbiological sterility	Mycoplasma	Mandatory	Qualified qPCR or culture (broth/agar or Vero inoculation/DNA stain) method Use of pharmacopeial methods USP<63>, Ph.Eur.2.6.7 and JP17<G3>	Negative
	Bacteriology	Mandatory	Use of pharmacopeial methods USP<71> and <61>, Ph.Eur.2.6.27 and 2.6.1, JP17<4.05> and <4.06>	Negative
	Viral testing	Mandatory	Based on risk assessment of starting and raw materials Use pharmacopeial methods USP<1237>, Ph.Eur.2.6.16, JP17<G3>	Negative
Endotoxin	Endotoxin	Mandatory	Use pharmacopeial methods USP<85>, Ph.Eur.2.6.14, JP17<4.01>	Negative
Genetic fidelity & stability	Residual vector testing	Mandatory	Appropriate specific assay to be used	Negative

Attribute	Test	Status	Recommended analytical method	Acceptance criteria
	Karyotype	Mandatory	G Banding	Normal (diploid) ≥20 metaphases
	SNP arrays	For information		
	WGS/WES cancer associated panels and other genetic, and disease marker analysis	For information		
Viability	Viability	Mandatory	Dye exclusion test or flow cytometry Use pharmacopeial methods USP<1046>, Ph.Eur.2.7.29	>60%
	Doubling time	Not required Data may be added for information		
	Cell debris	Not required		
Characterization	Flow cytometry	Mandatory	A minimum of two markers from an accepted panel (SSEA4, TRA1-60, OCT4, Nanog, etc.). Use pharmacopeial methods USP<1027>, Ph.Eur.2.7.24	Markers should typically be positive on >70% of cells in the Master Cell Bank
	Immuno-cytochemistry	For information		

<b>Attribute</b>	<b>Test</b>	<b>Status</b>	<b>Recommended analytical method</b>	<b>Acceptance criteria</b>
	Differentiated cells	Not required, for information		
Potency	Phenotypic	Mandatory	EB formation and/or directed differentiation. Teratoma formation not required as a potency assay	Demonstration of cells from all three germ layers
	Molecular	For information	Pluritest™ or hPSC Scorecard™	

#### **1.7.4. Workflow of allogeneic and autologous hiPSCs based therapy**

Since hiPSCs can be generated from a donor or patient's somatic cells, the potential avenues for hiPSC-based therapies are both autologous or allogenic (Bravery, 2015). It is imperative for both avenues of treatment to expeditiously deliver the hiPSC-based product to patients. This is especially necessary for cases of neurodegenerative diseases, where patients may be seeking cell-based therapies as a last resort.

##### **1.7.4.1. Autologous workflow**

For autologous therapies, the general workflow can follow 8 steps from patient to product delivery: (1) acquirement of somatic cells, (2) expansion of somatic cells, (3) reprogramming to a pluripotent state, (4) creation and validation of a master cell bank (MCB), (5) expansion of hiPSCs, (6) differentiation towards the desired phenotype, (7) expansion and quality assurance of differentiated cells, and (8) delivery of the therapeutic cell-based products to the patient.

First, dividing somatic cells must be obtained from the patient. In theory, any dividing somatic cell can be acquired and reprogrammed to a pluripotent state, however, it is important to consider that different cell types have varying degrees of malleability for reprogramming due to differences in epigenetic profiles. Consequently, selection of slow growing cell types or those more resistant to reprogramming can slow down the manufacturing timelines.

The clinical method used to obtain the somatic cell from the patient (i.e., biopsy, surgery or intravenous extraction) must also be carefully deliberated. Methods that pose minimal risks to the patient health is preferred. For example, though fibroblast have been successfully reprogrammed by several groups and easily obtained from skin biopsies (Rodríguez-Pizà et al., 2010; He et al., 2014; Quintanilla et al., 2014), the damaging procedures to obtain skin biopsies

incites risks for infection and complications. Thus, obtainment of patient-derived peripheral blood mononuclear cells (PBMCs) using nominally invasive venipuncture procedures are now more commonly preferred (Zhang et al., 2017; Okumura et al., 2019; Vlahos et al., 2019). Note, however, that regulatory agencies have not yet outlined specific requirements or recommendations for the sourcing of somatic cells (Jha et al., 2021). It is therefore, still under the discretion of the therapeutic developer to decide on the source of somatic cells.

Once the somatic cells have been isolated, expansion is necessary to obtain sufficient starting material for reprogramming. The duration of this expansion step would be dependent on the somatic cell used. For example, PBMCs can require around 7 days of expansion (Eminli et al., 2009), whereas adherent cells like fibroblast can take >28 days (Takahashi et al., 2007).

Afterwards, a suitable reprogramming method that meets the safety and quality criteria for clinical applications is performed (Jha et al., 2021). As previously mentioned, reprogramming efficiencies are very low which are influenced by the source somatic cell type and the reprogramming method used. Additionally, the degree of reprogramming material transduced or transfected will also vary between cells even when exposed to the same reprogramming method. Therefore, often, a selection process is implemented to isolate only stably reprogrammed hiPSC populations from the partial (transient) or non-induced cells. Next, single clone selection is necessary to ensure that the hiPSC product for clinical use is from a homogeneous population with only clonal genetic identity. A hiPSC clone can be obtained by manual colony picking techniques or single cell sorting technologies (e.g. fluorescence-activated cell sorter or UP.sight from Cytex), and clone selection is based on ideal CQAs. Employment of clonal hiPSCs in a manufacturing process allows for a controlled and predictable production. Clonality is also important in terms of deriving safe hiPSC-based product.

Clones are then further expanded to create clonally derived MCBs. Cell banks are necessary as a back-up source, instead of requiring additional cell samples from the patient. To achieve sufficient quantities of hiPSCs for the creation of MCBs, expansion of the generated patient-derived hiPSCs is necessary. Current laboratory standard for the expansion of hiPSCs are usually achieved by sequential passaging of hiPSC using standard in vitro culture platforms such as tissue culture plastic (TCP) flasks (T-Flasks) and multi-well plates. Concomitantly, the sequential passaging allows for the gradual elimination of residual vectors and vector derivatives that could potentially harm the patient if administered.

Additionally, following MCB generation and validation, a working cell bank (WCB) could also be created, using similar expansion and banking procedures. CQA validation of the patient-derived hiPSC is performed using the quality assurance assays as previously mentioned. Overall, so far, from patient somatic cell to validated MCBs and WCBs, this process alone could take up to 6 months.

The following steps involve cell revival from MCBs or WCBs and subsequent expansion to required cell quantities for differentiation. The cell quantities required at this stage would be dependent on the target cell type and dosage of the treatment. For example, the clinical trial ID: NCT03128450 required  $\geq 1.6 \times 10^7$  cells/patient (administered at  $\geq 4 \times 10^6$  cells/treatment/week for 4 weeks) of hNSCs. Moreover, in this case, the differentiation timelines from hiPSC to hNSCs would be dependent on the quality of the generated hiPSCs and the differentiation strategy employed. Typically, however, hNSC derivation from hiPSCs can take from 7 to 28 days. Further expansion of differentiated cells may also be required to achieve the dose, prolonging the process timelines longer from initial donor cell extraction to the ready to administer cell treatment at the right dosage. This secondary expansion phase is dependent on the growth rates of the differentiated cells (e.g., hiPSC-derived NSCs in this case).

Finally, autologous hiPSC-derived cells will need to undergo safety and quality checks prior to transplanting back into the patient. Assays performed to assure the safety and quality of the cell product would be product and application dependent. Take for example the case of PD treatment with hNSCs (clinicaltrials.gov ID: NCT03128450): the hNSC product would need to demonstrate the potential of differentiation towards the neuronal or glial lineage, in particular towards midbrain dopaminergic neurons as these would function as cell replacements for degenerate DA neurons within PD patients. If hypothetically, the eventual cell therapy was applied to treat ALS, the required assay may evaluate for the hiPSCs-derived hNSCs' potential to differentiate towards motor neurons instead. In all, the differentiation phases of an autologous therapy workflow can take up to several months depending on the target cell type and quantity needed. Overall, the current processes from patient to product delivery could take several months to more than a year (Madrid et al., 2021a).

For autologous hiPSC-based therapy workflows, these face their own unique challenges and limitations. For one, there is a need to reduce manufacturing timelines to ensure the timely delivery of the therapies to patients. The major rate limiting steps of the workflow are the expansion phases for the patient derived somatic cells, as well as the expansion phase for hiPSCs and their derivatives. These upstream expansion steps are typically performed in open tissue culture vessels such as T-flasks, petri dishes, cell factories, cell bags, and other gas-permeable cell culture-ware (Abraham et al., 2018). Thus, these platforms limit cell expansion by the available surface area for growth.

Since autologous therapy workflows are essentially designed as one manufacturing process for one patient, significantly less cell quantities are therefore required per process compared to the production process of cells for commercial use in allogeneic workflows. Therefore, a more suitable route for reducing manufacturing timelines would be to scale out processes, rather than scale up.

#### **1.7.4.2. Allogeneic workflow**

Allogeneic hiPSC-based therapies can follow a similar workflow to that of autologous treatment. One major difference is that the somatic cells for reprogramming are instead sourced from a donor rather than the patient. This avenue presents several advantages over autologous therapies. First, sourcing from a donor is more suitable in cases where patients are unable to provide somatic cells due to logistical, medical, or biological complications. Second, with the freedom to select a donor, a more efficient manufacturing process can be designed by employing donors specifically with cells that are healthy, fast growing, easily reprogrammable and with high differentiation potential. Thirdly, allogeneic hiPSC-based therapies can target a wide range of compatible patients, therefore, typically requiring larger quantities of hiPSC-based products. Thus, scaled-up manufacturing processes of allogeneic products would provide a more economical strategy.

Nonetheless, there are some exclusive considerations for allogeneic therapy manufacturing processes. This includes the screening and selection of appropriate donors to ensure the highest level of compatibility to that of the receiving patient. For example, the selection of the donor could be based on the HLA profiles that matches with that of the patient (Taylor et al., 2012). However, in most cases of allogeneic therapy, immunosuppressive drugs are necessary to inhibit an immune response and rejection.

Allogeneic hiPSC-based therapies have the potential to be “off the shelf” therapeutic products. For this to realise, an industrial/large-scale manufacturing process is required. One strategy is to generate MCBs containing a variety of HLA-typed hiPSC lines that are compatible with the wider population; hiPSC banks would minimise the efforts in screening for compatible donors. The Korea National Stem Cell Bank (KSCB) organisation provides the infrastructure to easily accessible stem cell sources. The KSCB have been cryopreserving controlled and ethically sourced PSCs since 2012. Homozygous hiPSC lines with homozygous HLA haplotypes have

been gathered. As of 2021, 22 GMP-compliant hiPSC lines have been deposited into the KSCB which can match around 51% of the Korean population (Kim *et al.*, 2021).

Another interesting avenue is the creation of a universal hiPSC line which can be transplanted to any patient regardless of their HLA profile. The idea exploits the amenability of hiPSCs for genetic manipulation techniques to obtain engineered hiPSC lines that can avoid T cell recognition. This has been demonstrated by suppressing the expression of HLA class I and II using Clustered Regularly Interspaced Short Palindromic Repeats (CRISPR) - CRISPR associated protein 9 (Cas9) (CRISPR/Cas9) technology to delete  $\beta_2$  microglobulin and the class II major histocompatibility class activator genes, which are essential for HLA structures (Mattapally *et al.*, 2018). Although HLA downregulation allows evasion of T cell mediated immune responses, natural killer (NK) cells can recognise absence of HLA class I molecules and thereafter initiate an immune response (Lanier, 2008). To overcome this, several strategies have been reported that pave a way for NK cell invading hiPSC lines, which are explored in more detail elsewhere (Flahou *et al.*, 2021).

Ultimately, to materialise the idea of a widely accessible universal hiPSC line, MCBs of immune privileged hiPSCs lines will need to be generated and stored at logistically and strategically designated worldwide locations.

#### **1.7.4.3. Addressing the challenges in manufacturing of hiPSC-based therapies**

Allogeneic and autologous hiPSC-based therapies are promising routes towards an alternative treatment strategy for neurodegenerative diseases. They share key manufacture process steps, which are: the isolation of somatic cells; hiPSC reprogramming; hiPSC expansion; cell bank generation; hiPSC differentiation; differentiated cell expansion; delivery of therapy. Only

autologous therapies, however, would require performing independent manufacturing processes per patient, which can lead to long timelines and high manufacturing costs.

For allogenic workflows, establishment of a HLA matched hiPSC MCBs and/or immune privileged hiPSC MCBs, would permit patient access to already reprogrammed and validated allogeneic hiPSC lines. The challenge then is to minimise the manufacturing timelines from MCBs of allogeneic hiPSC to patient delivery of the hiPSC-based therapy.

Manufacturing costs is another hinderance towards the realisation of hiPSC-based therapies for neurodegenerative diseases. The development of a clinically suitable hiPSC cell line alone could cost around \$0.8 million US dollars (~£0.6 million) for its derivation, expansion and MCB/WCB creation along with other cGMP standard evaluations for tumorigenic hazards (Bravery, 2015). The high costs associated with hiPSC-based therapies are due to the technical manual labour, duration of process, raw materials and cost of space of the manufacturing facility required (Rafiq *et al.*, 2016; Abraham *et al.*, 2018). Reduction of manufacturing timelines would reduce overall operation costs, as well as endorsing the timely delivery of therapy to patients. Reducing the technical manual labour can be achieved through employment of automation technologies. Technologies and equipment that allow for manufacturing within a smaller facility space, especially scalable platforms such as bioreactors, could allow for efficient expansion of cells whilst saving on operation costs/unit space. Such examples of cost saving strategies are essential to ensure as many patients as possible can affordably access hiPSC-based therapies. To the best of the author's knowledge, however, no comprehensive cost analysis of manufacturing hiPSC-derived NPCs has been reported to date. The cost of generating a cell line alone, particularly for autologous therapies is unaffordable for most. Still, additional investments would also be needed for processes to differentiate hiPSCs towards the required cell type and patient care.

The largest impact on manufacturing timelines and costs are the expansion processes of hiPSCs and their differentiated derivatives (i.e., NPCs). The upstream expansion process steps consume the raw materials and the timelines are dictated by biological factors (i.e., growth rates of cells). Overall, cost and time persists to be the major issues hindering mainstream use of hiPSC-based products for the treatment of neurodegenerative diseases.

### **1.7.5. hiPSCs culture systems**

For a cost and time efficient manufacturing process of producing hiPSC-based products, an optimised hiPSC expansion process is key. Fundamental to bioprocess developers, therefore, is the understanding of the specific culture conditions involved in hiPSC cultures. A successful expansion process is one that promotes cell proliferation and maintenance of clinical grade hiPSC CQAs. This will be dependent on the culture system that the cells are exposed to.

Important to note is the pliability of hiPSC to be cultured as adherent cells on substrates or in suspension as cell aggregates. These two culture modes offer different culture systems. Critical culture system components that influence the quality of hiPSC includes the culture substrate, culture medium, cell density, and environmental conditions such as oxygen and temperature. In this section (1.7.5), these critical culture system components are discussed.

#### **1.7.5.1. Importance of cell-substrate interactions in adherent cultures**

Undifferentiated PSCs typically express cell adhesion molecules (CAMs) such as integrins ( $\alpha V\beta 5$ ,  $\alpha V\beta 3$ ,  $\alpha 6\beta 1$ , and  $\alpha 2\beta 1$ ), epithelial (E) - cadherins and heparan sulfate proteoglycans (Li, Bennett and Wang, 2012; Enam and Jin, 2015; Vitillo and Kimber, 2017). CAMs mediate juxtacrine cell-cell and cell-substrate interactions, which modulate self-renewing and pluripotent maintenance mechanisms (Figure 1.2). Most laboratory/research scale hiPSC

cultures exploit CAMs by culturing hiPSCs as adherent monolayers on relatively cheap and standardised planar TCP platforms such as T-flasks or multi-well plates under static conditions (Rowland et al., 2010; Si-Tayeb et al., 2010; Lam and Longaker, 2012; Wilmes et al., 2017). Importantly, the typical hydrophobic polystyrene surface of TCPs is an insufficient ligand for the CAM profile on hiPSCs, hence, they are unsuitable for hiPSC adherent cultures. Instead, the common practise is to coat TCP surfaces with suitable substrates that promote CAM activation (i.e., cell attachment and adhesion) therefore allowing adherent cultures systems of hiPSCs. Downstream of CAM ligation with appropriate substrates are intracellular pathways that maintain cell viability, pluripotency gene expression and self-renewing networks (Li, Bennett and Wang, 2012).

Early culture methods used irradiated mouse embryonic fibroblasts (Cheng et al., 2003; Takahashi et al., 2007) or human dermal fibroblasts (Ghasemi-Dehkordi et al., 2015) as substrates to support PSCs; these substrates are collectively termed feeder layers. The move towards feeder-free methods obviates the need for co-cultures leading to simplified culture processes.

Drawing from the role of ECM proteins in the stem cell niches of PSCs in vivo, allowed for development of ECM-based substrates for in vitro cultures of PSCs. Common ECM proteins include collagen, laminin (LN), proteoglycans, glycoproteins and vitronectin (VTN). Matrigel is a commonly used complex ECM product obtained from Englebreth-Holm-Swarm tumour cells in mice (Hughes et al., 2010) and is widely recognised as an alternative feeder-free substrate. Matrigel is a gelatinous protein compiled of various ECM proteins: primarily collagen IV, LN, heparin sulfate proteoglycans and enactin (Kleinman et al., 1982; Kleinman and Martin, 2005). Other components of Matrigel includes specific growth factors such as fibroblast growth factor (FGF), epidermal growth factor (EGF), insulin-like growth factor 1 (IGF1), transforming growth factor  $\beta$  (TGF- $\beta$ ), platelet-derived growth factor (PDGF), and

nerve growth factor (NGF) (Vukicevic et al., 1992). The true composition of ECM proteins, growth factors and other biological structures within Matrigel, such as enzymes (e.g., metalloproteinases [MMPs]), is largely undefined with unclear effects on PSC quality. Furthermore, the concentrations of the components in Matrigel can vary from batch to batch (Aisenbrey and Murphy, 2020).

From a clinical perspective, the employment of Matrigel as substrates for the production of clinical grade hiPSCs presents several major problems. First, its mice origin poses risks of product contamination with non-human derived biological material, potentiating xeno-induced immune responses when such contaminants are carried over in transplant. Reports of lactate dehydrogenase elevating virus traced in some batches of Matrigel also raises further safety concerns (Liu *et al.*, 2011). Second, the presence of active growth factors can impact the quality and behaviour of hiPSC, thus requiring increased quality and process controls. Thirdly, its undefined composition and batch to batch variability creates unpredictability, reduced reproducibility and risks robustness integrity of the manufacturing bioprocess, further complicating process validations and quality assurances of hiPSC-based products for clinical release (Higuchi et al., 2015). Lastly, the relatively costly manufacturing process of Matrigel renders it unsuitable for employment at commercial or large-scale manufacturing.

Xeno-free and defined substrates for adherent hiPSC expansion is ideal for clinical translation. Appropriate substrates for hiPSC cultures include xeno-free ECM proteins such as human LM, fibronectin, E-cadherins, collagen and VTN (Polanco et al, 2020). Each ECM protein interacts with CAMs in specific ways that ultimately influence cytoskeletal arrangements, expression of transcription factors and other mechanisms that control cell survival, proliferation, and differentiation. However, the extensive pathways of CAM activations have not yet been fully elucidated but this topic is explored elsewhere (Li et al., 2012; Enam and Jin, 2015). As an example, recombinant human VTN (rh-VTN) have been demonstrated to support hiPSC

cultures (Wang, B.-K. Chou, *et al.*, 2013; Parr *et al.*, 2016; Sara M Badenes *et al.*, 2016). The success of their employment is partly due to the arginine-glycine-asparagine (RGD) sequences present in the N-terminal of the VTN protein, which offers the binding sites for  $\alpha V\beta 5$  integrins (Rowland *et al.*, 2010). Conformational changes to integrin structures due to ligand binding (e.g., RGD sequence of rh-VTN) leads to the formation of active complexes, such as Talins and Kindlin (Abdal Dayem *et al.*, 2018), towards the cytoplasmic tail of the integrin heterodimers. These intracellular complexes are then able to bind with the cytoskeleton protein actin, initially forming small clusters, then maturing into sophisticated focal adhesion and eventually fibrillar adhesion (Geiger and Yamada, 2011; Abdal Dayem *et al.*, 2018). Moreover, integrin activity modulates the phosphoinositide 3 – kinase (PI3K) and focal adhesion kinase (FAK) pathways, which play significant roles in cell survival, self-renewal and proliferation (Zhao and Guan, 2011; Hemmings and Restuccia, 2012). Reviews by Lamshead *et al.*, (2013) and Abdal Dayem *et al.*, (2018) extensively describes the roles of other ECM proteins in the maintenance of PSCs.

Alternatively, synthetic substrates also allow for chemically defined and xeno-free culture systems. Synthemax II, fibronectin-derived motifs, and VTN-derived oligopeptide containing hydrogels, are a few examples of developed synthetic substrates that have been shown to support PSC cultures (Tucker *et al.*, 2013; Higuchi *et al.*, 2015; Dayem *et al.*, 2020).

Nevertheless, the employment of currently available recombinant human ECM proteins or synthetic substrates at large/industrial scale expansion processes is impractical due to the high costs associated with their manufacturing. This cost hinderance is even more profound with synthetic substrates due to their often-complex derivation processes.

### 1.7.5.2. Importance of cell-cell interactions in adherent culture systems

Equally important is the consideration for cell–cell interactions in the design of hiPSC culture systems. Establishment of cell-cell interactions are vital to hiPSC maintenance and expansion. Controlling these types of interactions in adherent hiPSCs culture systems can be achieved by adjusting seeding density and confluency parameters. Thus, optimisation of such parameters would contribute towards an efficient culture system through cell-cell interaction-induced maintenance of CQAs and cell expansion.

E-cadherins are the major CAMs involved in cell–cell interactions in PSCs (Figure 1.2). E-cadherins are transmembrane glycoproteins that permits homophilic cell–cell adhesion in the presence of  $\text{Ca}^{2+}$  ions. Ligand association to the extracellular component of E-cadherins allows for the binding of p120-catenin and  $\beta$ -catenin to its cytoplasmic structures, sequentially forming an intracellular complex with  $\alpha$ -catenin (Abdal Dayem et al., 2018). The cadherin-catenin complex associates with actin cytoskeleton, which contains non-muscle myosin II components. Though the mechanisms remain largely unclear, non-muscle myosin II are involved in self-renewal of PSCs (G. Chen et al., 2010; Xu et al., 2010). Additionally,  $\beta$ -catenin plays a central role in the canonical wingless-related integration site (WNT) signalling pathway that interlinks with the pluripotency network (e.g., OCT4, SOX2 and NANOG) (Angers and Moon, 2009; Zhang et al., 2013).

Another mechanism downstream of E-cadherin activation is the suppression of Rho and Rho-associated protein kinase (ROCK) pathways, which modulates cell survival mechanisms. Upon hiPSC dissociation (e.g., during cell passaging), cell-cell mediated adhesion of E-cadherin is disrupted, consequently permitting the activation of Rho/ROCK pathways which causes myosin light chain phosphorylation. Myosin hyperactivation and eventual increased actin-myosin contraction can lead to membrane blebbing, nuclear disintegration and cellular fragmentation (Croft et al., 2005; Shi and Wei, 2007). To mitigate these effects, especially in

single cell passaging of PSCs, supplementation of ROCK inhibitors (ROCKi) Y-27632 can promote cell survival in the absence of E-cadherin stimulation as seen in figure 1.2 (Watanabe et al., 2007).

An interesting approach could employ recombinant fusion proteins of E-cadherins as a substrate to support PSCs, like that demonstrated by Rodin et al., (2014). In their investigation, E-cadherin as a sole culture substrate was unable to support hESC expansion. However, they exhibited successful clonal derivation and long-term self-renewal of hESCs by using a combination substrate composed of LN-521 and E-cadherin (Rodin et al., 2014). The relevance of such findings suggests that E-cadherin activation or cell-cell contact alone is insufficient to maintain PSCs. Instead, this highlights the importance of combinatorial multiple CAM modulation for a viable PSC culture system.

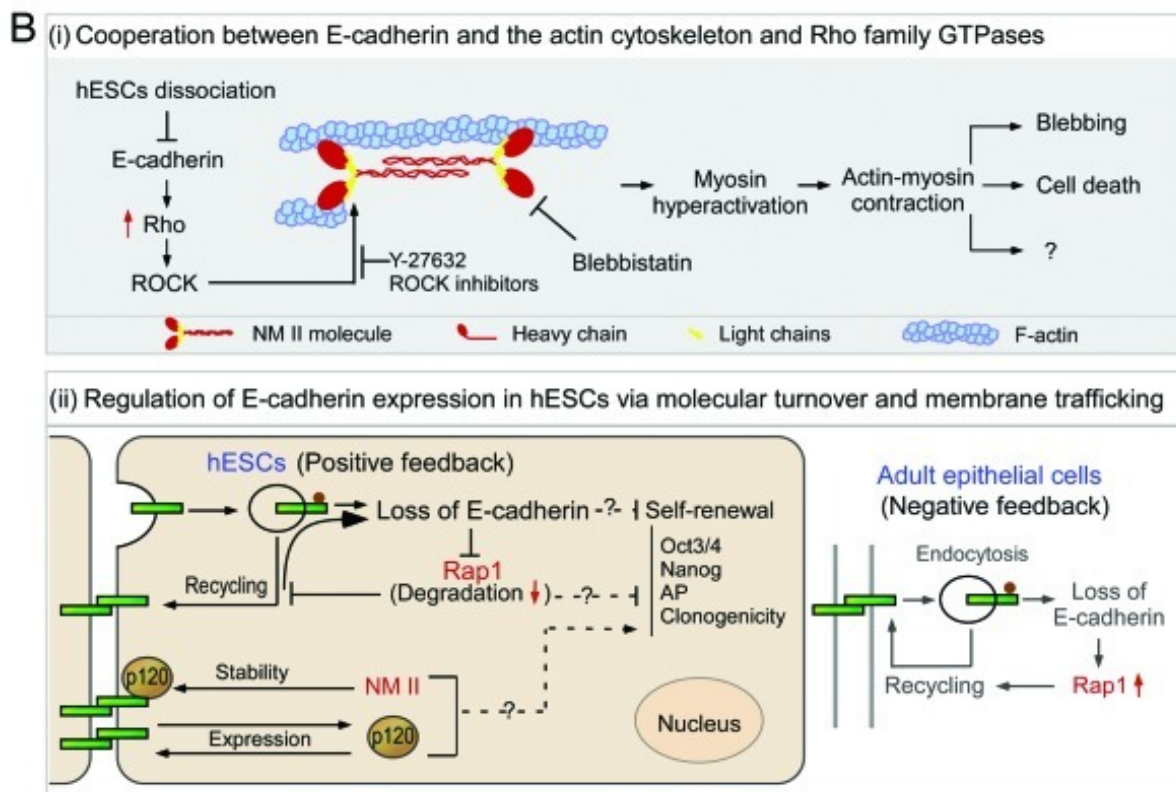
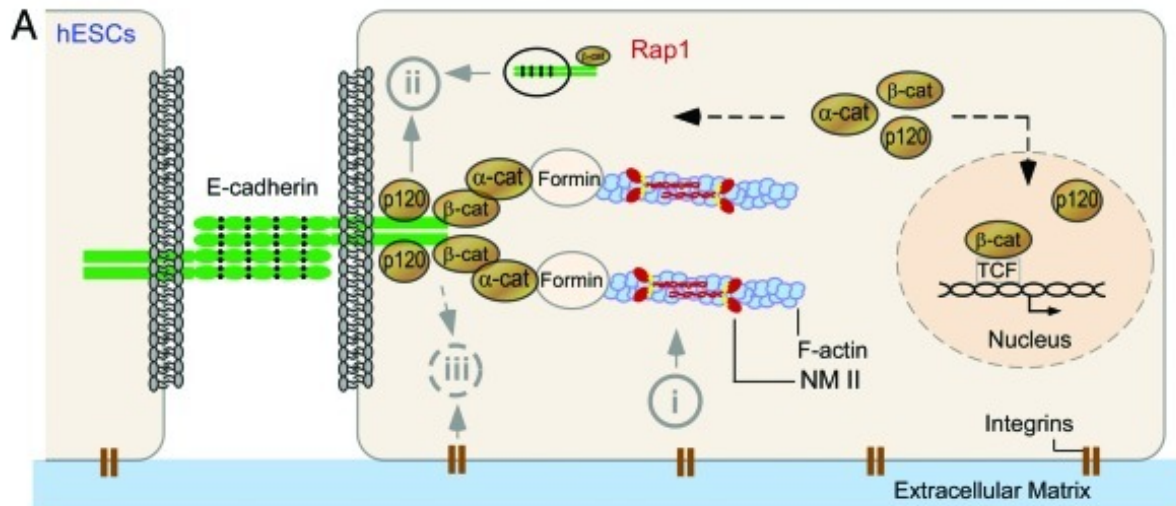


Figure 1.2. Schematic diagram of hPSC CAMs (E-cadherin and integrin) and their intracellular pathways leading to maintenance of pluripotency and cell survival. (A) follows interactions of E cadherin with other CAMs and integrin with extracellular matrix. (B) outlines the Rho-ROCK pathways and their influence with cytoskeletal proteins and downstream effect on PSC maintenance and survival. This diagram was adapted from Li, Bennett and Wang (2012).

### **1.7.5.3.Importance of cell-cell interactions in suspension culture systems**

hiPSC are also amenable for suspension culture systems due to their natural affinity to self-assemble and form free-floating aggregates in the absence of a suitable substrate (Olmer et al., 2012; Pettinato, Wen and Zhang, 2014; Schwedhelm, Zdzieblo, Appelt-Menzel, Berger, Schmitz, Schuldt, Franke, F.-J. Müller, et al., 2019). To achieve a suspension culture system, ultra-low attachment (ULA) T-flasks, ULA multi-well plates, Erlenmeyer flasks (E-flasks) and spinner flasks are commonly employed for laboratory scale production of hiPSCs (Stover and Schwartz, 2011; Pettinato *et al.*, 2014; Xie et al., 2017; Nogueira *et al.*, 2019; Schwedhelm *et al.*, 2019). hiPSC expansion can be achieved through propagation of cell aggregates through culture splitting. hiPSC aggregate suspension culture systems are devoid of additional surface substrates, offering a simplified and potentially cheaper culture system. Such systems provide relatively easier translational route to large /industrial scale manufacturing.

Under appropriate culture conditions, hiPSC CQAs can be controlled in suspension culture systems. Modulation of CAMs are key determinants of hiPSC quality in aggregate suspension cultures. Indeed, E-cadherins play a major role in establishing cell-cell interactions as per the mechanisms outlined in section 1.7.5.2. Physical forces and/or spatial proximity drive initial cell-cell interactions which can govern cell survival. These environmental factors have a profound significance in suspension cultures compared to adherent cultures due to the heavy reliance of cell-cell interaction-mediated mechanisms in suspension cultures. For example, prolonged inactivity of E-cadherin signalling due to cells being physically too far from one another, permits progression of Rho/ROCK pathways which follow the mechanisms towards cell death. To mitigate compromising hiPSC viability in suspension cultures, aggregate cultures are typically propagated by splitting and inoculating into new culture vessels as small cell aggregates with already established cell-cell networks (i.e., passaging as cell clumps).

Aggregated hiPSCs produce endogenous ECM in situ and constantly remodels the ECM throughout the development of the aggregate. This dynamic microenvironment stimulates CAMs further activating their respective pathways (Laperle, Masters and Palecek, 2015; Kim et al., 2019). Upon initial cell-cell interactions, early ECM like collagen type I, are synthesised and secreted between the cells. ECM proteins such as LM, nidogen and fibronectin are secreted as the aggregates develop. These endogenous ECM serves as suitable substrates for more CAMs, thus regulating mechanisms which modulate self-renewal, proliferation and expression of pluripotent associated transcription factors such as OCT4 (Sart et al., 2017). Note that adherent monolayer cultures of hiPSCs also deposits ECM proteins and remodels the culture substrate microenvironment using enzymes such as MMPs (Nie et al., 2021).

The optimal expansion of hiPSCs as aggregates relies on process controls that determine the size of the aggregates (Sart et al., 2017). Of course, as cultures progress and cells continue to proliferate, the size of the aggregates would increase. The increasing size of the PSC aggregates over time can lead to formation of necrotic cores due to gas (i.e., O<sub>2</sub> and CO<sub>2</sub>) and nutrient (i.e., growth factors) concentration gradients. Differentiation due to concentration gradients presents another technical issue associated with aggregate suspension cultures. Furthermore, cells located at different positions of larger aggregates are exposed to different concentration gradients, whereby cells closer to the core are exposed to lower concentrations of gases and nutrients compared to cells closest to the outer layer of the aggregates. Thus, a heterogenous population of varying cell quality is often observed in larger aggregates (Clark *et al.*, 2004; Van Winkle *et al.*, 2012; Xie *et al.*, 2017).

To control aggregate size, different approaches have been reported, including the addition to the culture medium of heparin (Li L. et al., 2011) or dextran sulphate (Lipsitz et al., 2018). Others use agitation to physically break down the aggregates (Olmer *et al.*, 2012; Takahashi *et al.*, 2017).

#### **1.7.5.4.Importance of hiPSC culture media components**

The exogenous factors of culture media for hiPSC cultures play a critical role in their maintenance. Especially for large scale hiPSC productions, culture media will majorly impact the process costs, operation modes, and the CQAs of hiPSCs and their derived products. Since the isolation of hESCs and their culture in feeder layers with foetal bovine serum (FBS) (Thomson *et al.*, 1998), media development have steered towards cheaper, more defined and xeno-free media compositions, with the aim of aligning to clinical and cGMP regulatory requirements. Two breakthrough media compositions, amongst many proposed formulations, had been developed: the widely used mTeSR<sup>TM</sup>1 (StemCell Technologies) medium, which is a modification of the TeSR<sup>TM</sup> formula containing 19 components (Ludwig *et al.*, 2006; Ludwig and A. Thomson, 2007); and Essential 8 (E8) (ThermoFisher), a chemically defined, xeno-free and simplified medium containing only 8 components (G. Chen *et al.*, 2011). Table 1.3 lists the components in both media for comparison. mTeSR<sup>TM</sup>1 and E8 media have been demonstrated to support the proliferation and maintenance of undifferentiated PSCs in cultures mainly at laboratory scale (Meng *et al.*, 2008; Nie *et al.*, 2010; Wang *et al.*, 2013; Zhang *et al.*, 2017; Horiguchi *et al.*, 2018b; Le and Hasegawa, 2019).

However, the accumulation, depletion, or changes in concentration of several key components in the culture medium are reported to have profound effects on the cell's CQAs. These components include growth factors, glucose, glutamine, metabolic waste products, and oxygen.

##### **1.7.5.4.1 Growth factors**

FGF2, TGF- $\beta$ 1/Activin and insulin/IGF are the main influencers of the signalling pathways that affect CQAs of PSCs. These growth factors are commonly incorporated in commercially

available PSC media (Lu et al., 2006; Wang et al., 2007) including mTeSR<sup>TM</sup>1 and E8<sup>TM</sup> medium.

The molecular mechanisms of FGF2, TGF- $\beta$ 1/Activin and insulin/IGF and their signalling pathways reveal how hiPSC are maintained undifferentiated and in a self-renewal state in vitro (Romito and Cobellis, 2016). FGF2 binds to FGF receptors (i.e. FGFR1/FGFR4) initiating PI3K/AKT/mammalian target of rapamycin (mTOR) (PI3K/AKT/mTOR) pathways, as well as the MAPK/extracellular-signal-regulated-kinase (MAPK/ERK) pathways, which modulates cellular proliferation, differentiation and cell survival (Zhang and Liu, 2002; Porta, Paglino and Mosca, 2014). TGF- $\beta$ 1/Activin binds to TGF- $\beta$ 1/2 and activin receptors, respectively, activating the TGF- $\beta$  signalling pathways which similarly regulates cellular processes and pluripotency maintaining network of PSCs (Massagué, 2012). Insulin binds to insulin receptors signalling the PI3K/AKT pathways and promotes cell survival and growth.

Though commercially available media such as mTeSR<sup>TM</sup>1, E8<sup>TM</sup>, and TeSR<sup>TM</sup>-E8<sup>TM</sup> (StemCell Technologies) have demonstrated robust and reliable laboratory scale cultures of hiPSCs, their implications in industrial manufacturing platforms are hindered by the high manufacturing costs, subjected to the associated costs for growth factor production (Specht, 2020). Hence, other media development research groups have aimed to replace some or all of the growth factors with small molecules (Yao et al., 2006; Tsutsui et al., 2011; Yasuda et al., 2018). However, reduced growth factor media has not successfully translated to widespread use in research or industry. This may be due to reports of compromised PSC properties such as slower cell growth and colony outgrowth (Yasuda et al., 2018).

Slow growth kinetics have major implications at large scale cultures such as increased manufacturing timelines and production costs. Further optimisation studies are required for the field of hiPSC media development to mature towards a chemically defined, xeno-free and cost-

effective (i.e., reduced growth factors) medium for PSC expansion. Importantly, optimised hiPSC medium should not compromise the CQAs. In all, it is apparent that current media compositions like mTeSR™1, E8™, and other PSC medium with reduced growth factors, are not optimised for large/industrial scale manufacturing of hiPSCs-based therapies. Also, note that basic FGF (bFGF) in typical hiPSC culture conditions of 37°C are unstable with a short half-life (Levenstein *et al.*, 2006; Furue *et al.*, 2008; G. Chen *et al.*, 2012). Reliable manufacturing processes must ensure the constant availability of functional growth factors to the hiPSC in culture to assure CQAs.

Table 1.3. Medium components of E8<sup>TM</sup> and mTeSR<sup>TM</sup>1. The x indicates components present in the medium formulation.

<b>Media components</b>	<b>E8<sup>TM</sup></b>	<b>mTeSR<sup>TM</sup>1</b>
DMEM F-12	<b>x</b>	<b>x</b>
L-ascorbic acid	<b>x</b>	<b>x</b>
Selenium	<b>x</b>	<b>x</b>
NaCHO <sub>3</sub>	<b>x</b>	<b>x</b>
Insulin	<b>x</b>	<b>x</b>
FGF2	<b>x</b>	<b>x</b>
TGF-β1	<b>x</b>	<b>x</b>
Transferrin	<b>x</b>	<b>x</b>
L-Glutamine		<b>x</b>
Thiamine		<b>x</b>
Trace elements B		<b>x</b>
Trace elements C		<b>x</b>
B-Mercaptoethanol		<b>x</b>
Bovine serum albumin (BSA)		<b>x</b>
Glutathione		<b>x</b>
Pipecolic Acid		<b>x</b>
LiCl		<b>x</b>
γ-aminobutyric acid		<b>x</b>
H <sub>2</sub> O		<b>x</b>

#### **1.7.5.4.2 Glucose and glutamine**

The depletion of medium components throughout cultures of hiPSCs can be a limiting factor of cell growth (Horiguchi et al., 2018a). Several studies demonstrate the reliance of hiPSCs on aerobic glycolysis as the primary mode of energy metabolism (Tsutsui et al., 2011; Varum et al., 2011; Panopoulos et al., 2012; Lees, Gardner and Harvey, 2017). In glycolysis, glucose firstly undergoes a series of phosphorylation, followed by lysis into two molecules of 3 carbon which are eventually converted to 2 pyruvate molecules. Pyruvate is then processed through the tricarboxylic acid (TCA) cycle to produce adenosine triphosphate (ATP) molecules. (Varum et al., 2011; Zhang et al., 2012; Greuel et al., 2019; Schwedhelm et al., 2019). hiPSC are highly metabolically active and require high glucose content in the medium. High glucose concentrations have also been shown to improve cell growth and expression of pluripotency markers, but exactly how glucose moderates these effects remain unclear (Madonna et al., 2014; Horiguchi et al., 2018b). Thus, depletion of glucose in culture medium could drive hiPSCs to differentiate and reduce growth.

Glutamine also plays an essential role in maintaining hiPSC survival and pluripotency. Oxidative phosphorylation of glutamine contributes to nucleotide and glutathione synthesis. Sustained production of glutathione via oxidation of glutamine helps maintain the stability of OCT4 in hPSCs. Otherwise, in the absence of glutamine, oxidation of OCT4 cysteine residues preside causing OCT4 degradation (Warburg, 1956; Tanosaki et al., 2021). Glutamine support for survival is achieved through ATP generation as a result of glutamine metabolism. This mechanism acts as an energy production “safety net” in the case of complete glucose depletion (Tohyama et al., 2016).

#### 1.7.5.4.3 Metabolic waste

Metabolic waste products like ammonium and lactate, can have adverse effects on hiPSC CQAs. Lactate is produced as a byproduct of glycolysis, even in the company of abundant oxygen available to the hiPSCs in culture (Teslaa and Teitell, 2015; Nishimura *et al.*, 2019). Lactate builds up in the culture medium as cells metabolise glucose, which in turn can decrease the pH of the culture medium, ultimately presenting a more acidic environment for the cells. The reductions in pH as a result can impose detrimental effects on enzyme activity, protein conformations, cell quality and cell viability (Chen *et al.*, 2010). Interestingly, Horiguchi *et al.*, (2018b) reported that although culture media was adjusted, the growth rate of PSCs did not improve, suggesting lactate may have a direct effect on cell proliferation.

However, other reports have suggested beneficial effects of lactate and lactic acid. Lactic acid is an uncharged small molecule capable of permeating the lipid bilayers of the cells and have been demonstrated to possess antioxidative effects and promoted cell proliferation (Lampe *et al.*, 2009). Lactate can be internalised through the monocarboxylate transporter protein shuttle system (Philp *et al.*, 2005), and once internalised lactate can be oxidised to pyruvate and subsequently to acetyl-CoA then used as a substrate for TCA cycles, providing more energy sources for the cell.

Regardless, the removal of metabolic wastes is an imperative process operation for hiPSCs cultures. Typical cultures of hiPSCs *in vitro* require constant and periodic medium exchanges to remove such metabolic wastes and replace the depleted growth factors, such as glucose and glutamine which are essential for hiPSC maintenance. At laboratory scale, the use of standard planar platforms for hiPSCs cultures would require medium exchanges to be performed by trained laboratory technicians daily. This incites poses high risk of contamination due to manual handling of an open culture system, and increases costs of operations.

#### **1.7.5.4.4 Oxygen**

Oxygen plays a major role in the maintenance of PSCs. Typical research scale cultures of hiPSCs are usually incubated inside humidity and gas-controlled incubators set at 95% humidity in an atmosphere of 5% CO<sub>2</sub> in air. Oxygen is delivered to the cells from air at normoxic concentrations of ~21%. Gases are able to enter the culture systems through diffusion, especially when culture in standard planar culture platforms like multi-well plates or T-flasks.

Recapitulation of the hypoxic (<5% O<sub>2</sub>) in vivo conditions of PSC niches can also offer a suitable in vitro culture condition for the maintenance of hiPSCs. Studies have suggested that oxygen concentrations influence multiple PSC functions such as differentiation, genetic stability, and maintenance of pluripotency (Ezashi *et al.*, 2005; Yoshida *et al.*, 2009; Eliasson and Jönsson, 2010; Sugimoto *et al.*, 2018). Hypoxic conditions, have been demonstrated to support hiPSC culture with improved genomic stability (Kuijk *et al.*, 2020), reprogramming efficiency (Yoshida *et al.*, 2009) and expression of pluripotency markers (Guo *et al.*, 2013). Nonetheless, contradicting reports demonstrating hypoxic effects on hiPSCs have also been reported. For example, Guo *et al.*, (2013) saw reduction in the expression of some pluripotency markers such as *OCT4* compared to normoxic conditions, whilst Sugimoto *et al.*, (2018) reported increased markers of pluripotency and cell growth.

### **1.8.NPCs: neural induction and maintenance**

Since hiPSCs possess the potential to differentiate towards the ectoderm lineage, they can be utilised as a sustainable and ethical source of NPC-based therapies. The differentiation of hiPSCs towards NPCs can be achieved by an in vitro technique known as neural induction.

Neural induction is a process describing the commitment of PSCs to differentiate towards the neural lineage (Stern, 2006; Rogers *et al.*, 2009). In embryogenesis, neural induction more specifically describes the onset of primitive dorsal ectoderm cells committing towards a neural fate. Unravelling of the neural induction mechanisms were pioneered through developmental studies of amphibian, avian, and mammalian models; the studies collectively emphasised the dependency of the embryonic neurogenesis process on the spatial and temporal manipulation of cells by gradients of different morphogens and signalling molecules (Piccolo *et al.*, 1996; Zimmerman *et al.*, 1996; Wilson and Edlund, 2001). The mechanisms of these morphogens and signalling molecules in the patterning and development of the mammalian embryonic brain is reviewed elsewhere (Stern, 2006; Urbán and Guillemot, 2014).

How NPCs are maintained and activated in the adult stem cell niches, remains largely elusive due to the complexities of *in vivo* assays with the human brain. Nonetheless, some key signalling pathways have been identified, which are further discussed in section 1.8.1. By exploiting the known *in vivo* mechanisms in embryonic neurogenesis, and the maintenance and neurogenesis of adult NPCs, several *in vitro* neural induction strategies have been developed for PSC cultures (Nakayama *et al.*, 2004; Eiraku *et al.*, 2008; Elkabetz *et al.*, 2008; Chambers *et al.*, 2009; Koch *et al.*, 2009; Morizane *et al.*, 2011; Reinhardt *et al.*, 2013).

Importantly, these developed neural induction methods provide the foundations for manufacturing strategies to derive NPCs from hiPSCs. A successful manufacturing process should efficiently convert hiPSCs to NPCs, whereby the culture system during neural induction must be capable of inducing and orchestrating the signalling pathways which modulate pluripotency related genes in hiPSCs and simultaneously activate specifying genes for neural lineage. Indeed, the success of such processes rely on specific environmental and biological factors. Thus, understanding the culture system conditions that drive neural induction is essential for the development of a hiPSC-derived NPC production process.

### 1.8.1. The molecular mechanisms that drive neural induction

WNT/ $\beta$ -catenin pathway, TGF $\beta$  pathways (i.e., BMP/SMAD signalling), SHH signalling, and neural-cadherin (N-cadherin) signalling are some of the key pathways that regulate the fine balance between pluripotency and neural commitment (Patten and Placzek, 2000; Corbin *et al.*, 2008; Decimo *et al.*, 2012; Abbott and Niggussie, 2020).

The activation of canonical WNT signalling pathway leads to the stabilisation of intrinsic  $\beta$  catenin molecules which plays a role within the pluripotency network as previously mentioned.  $\beta$  catenin also enters the nucleus and eventually targets genes like *c-MYC* and *cyclin D1*, in turn permitting the progression of the cell state through G1 to S phase of the cell cycle (Hadjihannas *et al.*, 2012). Thus, activated canonical WNT signalling in PSCs may promote pluripotency and self-renewal properties. Blocking the canonical WNT signalling pathway would destabilise  $\beta$  catenin, and in turn promote the differentiation of PSCs (James *et al.*, 2005; Zhang *et al.*, 2013).

The TGF $\beta$  family proteins can instigate pathways such as the canonical BMP signalling (Hata and Chen, 2016). This pathway recruits SMAD proteins which regulate cell proliferation, differentiation, and cell death such as apoptosis in PSCs (James *et al.*, 2005; Massagué, 2012; Osnato *et al.*, 2021). Canonical BMP/SMAD signalling within PSCs prohibits their differentiation towards the “default model”: the neural lineage. Thus, canonical BMP-signalling is an exploitable mechanism for in vitro neural induction strategies of hiPSC culture.

The BMP signalling pathways can appear perplexing since the activation of different BMP receptors (eg., BMPR Ia, Ib or II), in combination with different BMPs, can lead to multiple and contradicting effects on PSCs and NPCs. For example, in the SGZ of the dentate gyrus, NSCs are maintained in a dormant or quiescent state by BMP/SMAD signalling which reduces cell proliferation (Mira *et al.*, 2010). However, signalling via BMP/SMAD 1/5/8 promotes

neuronal differentiation, maturation and specification of embryonic NPCs (Hegarty, O’Keeffe and Sullivan, 2013; Galiakberova and Dashinimaev, 2020). Therefore, careful consideration in the manipulation of this pathway is essential for ensuring the correct phenotype of NPCs is achieved after the neural induction process.

One method is to block BMP/SMAD signalling to permit neural commitment of PSCs. Noggin, a well-known inhibitor of BMP4 (Zimmerman *et al.*, 1996), has been used to obtain PSC-derived NPCs in vitro (Chambers *et al.*, 2009; Morizane *et al.*, 2011; Shi *et al.*, 2012). Noggin inhibits the BMP pathways by binding directly to BMP4 in the extracellular space, disallowing the propagation of the SMAD 1/5/8 mediated signalling (Goldman *et al.*, 2009). Chambers *et al.*, (2009) showed that the small molecule SB431542 was also able to modulate the TGF- $\beta$  signalling pathway through inhibition of SMAD signalling by regulating the phosphorylation of ALK5, ALK4 and ALK7 receptors (Chambers *et al.*, 2009; Chandrasekaran *et al.*, 2017). The combined use of Noggin and SB431542, commonly termed the dual SMAD inhibition, have been reported to efficiently induce neural differentiation of PSCs with high efficiencies (Chambers *et al.*, 2009; Grainger *et al.*, 2018; Pauly *et al.*, 2018; Vlahos *et al.*, 2019).

Similarly, the SHH signalling protein is also involved in cell proliferation and maintenance of NSCs in the adult stem cell niche (Machold *et al.*, 2003). The presence of exogenous SHH in cultures of NPCs promotes cell proliferation. Blocking the SHH-signalling pathways lead to slow proliferation rates and premature differentiation of NPCs in culture (Balordi and Fishell, 2007). SHH also play a crucial role in driving PSCs towards the neural fate (Crompton *et al.*, 2013). Thus, SHH has been employed in some neural induction media to obtain more differentiated (late-stage) NPCs, particularly towards neuronal progenitors (Elkabetz *et al.*, 2008; Fedorova *et al.*, 2019).

FGF2 has been demonstrated to play a key role in embryonic neurogenesis (Jin *et al.*, 2003). FGF2 signalling via FGFR sustains NSC survival in the presence of IGF (Drago *et al.*, 1991). Furthermore, EGF and FGF2 induction can be used to promote NSC proliferation in vitro. In fact, FGF2 is capable of promoting NSC proliferation in the absence of EGF. Because of this, FGF2 has been employed extensively in various neural induction and neural maintenance media concoctions (Nakayama *et al.*, 2004; Eiraku *et al.*, 2008; Elkabetz *et al.*, 2008; Koch *et al.*, 2009; Reinhardt *et al.*, 2013)

Furthermore, the neural induction media can be specifically formulated to induce PSC towards specific subtypes of NPCs. For example, low concentrations of CHIR99021, an activator of the WNT pathway, directs the neuroepithelial cells to become NP cells of the posterior forebrain. Higher concentrations of CHIR99021 leads to NP cells with hindbrain, midbrain, and anterior spinal cord identities (Kirkeby *et al.*, 2012; Lu *et al.*, 2016).

Another influential molecule is retinoic acid (RA) which ligates RA receptors, consequently activating intracellular pathways leading to the direct modulation of several neural commitment genes including *SOX6* and *WNT1*. RA is also an antagonist of  $\beta$  catenin. Furthermore, RA mediated pathways indirectly targets the family neurogenic differentiation genes (*NeuroD*) which promote neuronal differentiation (Tu tukova, Tarabykin and Hernandez-Miranda, 2021). Hence, RA is usually employed at later stages of neural differentiation when the target cell type for example are neurons (Shi *et al.*, 2012).

In all, an effective NPC-based therapeutic product must possess the right qualities specific to the type of neurodegenerative disease. For example, NPCs that give rise to DA neurons are suitable for replacing damaged DA neurons in PD. Therefore, specific NPC CQAs are dependent on the target cell type, and the target neurodegenerative disease to treat. Nonetheless, typical characteristics of general NPCs include expression of N-cadherin, PAX6,

SOX2, MUSASHI and NESTIN. Functional assays are also performed to confirm differentiation potential towards neuronal lineages and glial lineages.

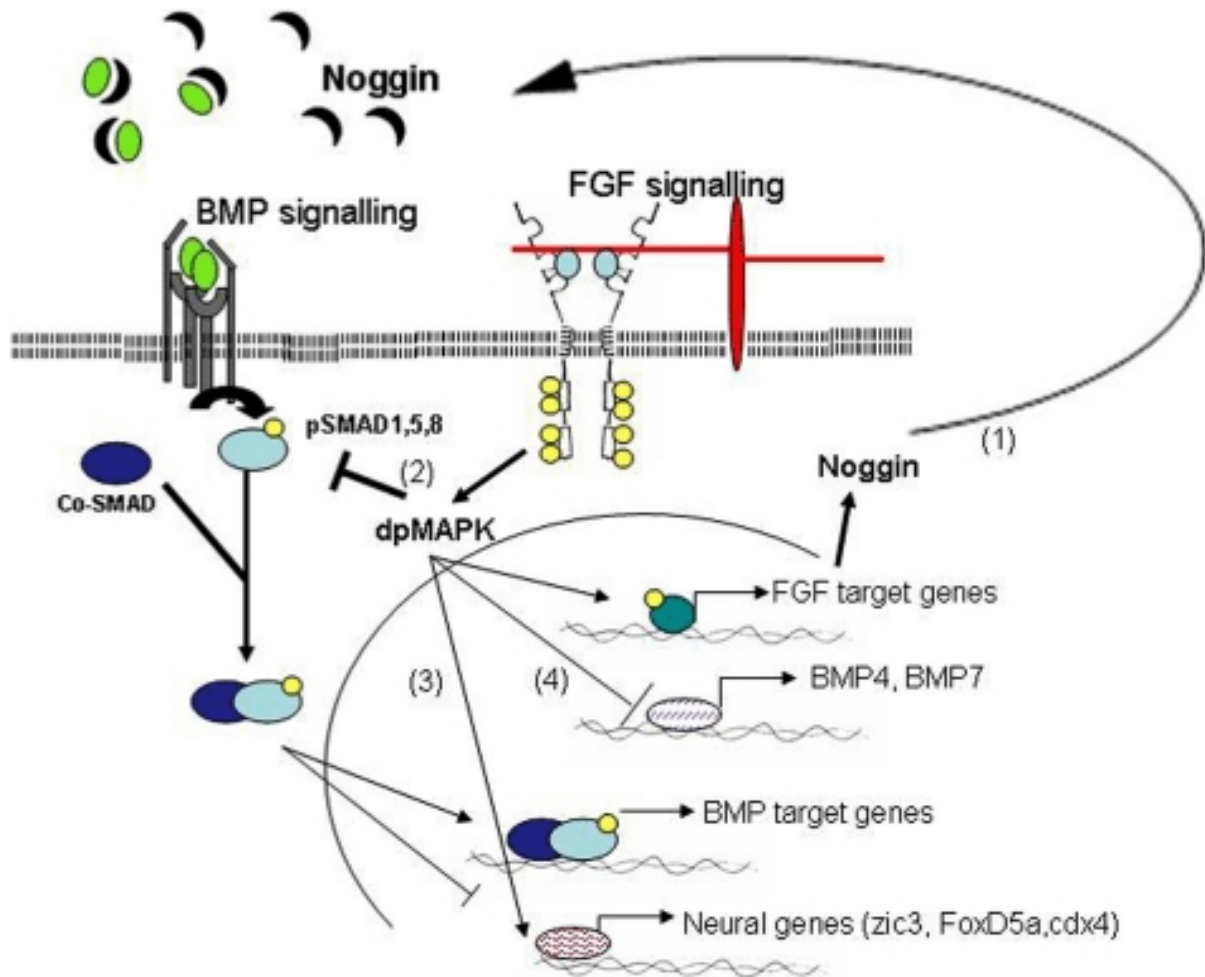


Figure 1.3. Schematic diagram of key signalling pathways during neural induction. Diagram is adopted from Pownall and Isaacs, (2010) .

### **1.8.2. Consideration of the culture substrate during neural induction**

It is also important to consider the substrate of a culture system for neural induction of hiPSCs. This is because the CAM profiles of PSCs change during differentiation to NPCs, thus potentially requiring different substrates for the maintenance of hiPSCs and NPCs in vitro. For example, PSCs typically express E-cadherins and integrins  $\alpha V\beta 5$ ,  $\alpha V\beta 3$ ,  $\alpha 6\beta 1$ , and  $\alpha 2\beta$  (Vitillo and Kimber, 2017), but as a result of neural commitment,  $\alpha V\beta 5$  integrins are reduced whilst  $\alpha 6\beta 1$  integrins are increased (Morante-Redolat and Porlan, 2019). Though both  $\alpha V\beta 5$  and  $\alpha 6\beta 1$  can be activated by VTN,  $\alpha 6\beta 1$  has a higher preference for LN-511 substrates, thus may prefer culture systems employing LN-511 as a substrate (Vitillo and Kimber, 2017).

Furthermore, the expression of E-cadherin in undifferentiated PSCs during neural induction is reduced. Instead, N-cadherin is expressed which plays an important role in maintaining NPCs (Stern, 2006; Singh *et al.*, 2010; Fernandez-Muñoz *et al.*, 2021). Substrates that can support N-cadherin CAMs, such as recombinant N-cadherin may support an efficient neural induction process. Additionally, it is also important to account for the endogenous ECM deposited by hiPSCs in culture. Because of this ECM deposition, it could help prime the substrate to support the neural induction process. Nevertheless, more studies are required to understand the role of CAMs during neural differentiation.

In all, a suitable substrate must be identified and employed for a successful neural induction process within a manufacturing workflow for adherent cell-based processes. These substrates includes Matrigel, LN, collagen, VTN, fibronectin, and PLO to name a few (Li et al, 2014). For example, due to the complex ECM components of Matrigel, it has been used in a previous study for the production of hiPSCs-derived NPCs (Bardy et al., 2013). However, the use of Matrigel is tethered with major limitations for large-scale clinical applications. While NPC

maintenance requires substrates such as collagen, fibronectin, PLO, LN or poly-D-lysine (Khlongkhlaeo *et al.*, 2016; Abdal Dayem *et al.*, 2018; Gilmozzi *et al.*, 2021) these may be costly to implement in large-scale processes due to the material manufacturing costs. Nevertheless, the most ideal substrate for production of clinical grade hiPSC-derived NPCs, without having to change to the substrate, would be of the nature that is xeno-free, defined and contains the ligands to maintain both hiPSCs and NPCs.

### **1.8.3. Neural induction using suspension culture systems**

From the learnings of neurogenesis within developing embryos, various *in vitro* neural induction methods for PSC cultures were developed, traditionally using suspension culture systems (Alam *et al.*, 2004; Jensen and Parmar, 2006; Stern, 2006; Kumar *et al.*, 2007; Corbin *et al.*, 2008; Faigle and Song, 2013; Galiakberova and Dashinimaev, 2020a). These methods rely on the ability of PSCs to form cell aggregates in the absence of a substrate. Subsequently, indirect differentiation occurs, caused by concentration gradients of pluripotency maintaining medium components across the 3 dimensional (3D) structure (Li *et al.*, 2014; Rivera-Ordaz *et al.*, 2021). The resulting heterogeneous cell aggregates are known as embryoid bodies (EBs), which contains sub-populations of ectodermal committed cells amongst other differentiated cell types. EBs can autonomously produce ECM and endogenous proteins such as SHH (Crompton *et al.*, 2013) which can help promote neural induction. With the addition of specific neural inducing factors, cells of the EB can be committed towards the neural lineage more efficiently. Figure 1.4 shows the different strategies for obtaining NPCs by neural induction of PSCs.

To isolate cells committed to the neural lineage, EBs are usually re-plated onto a culture system which support neural induction and neural lineage maintenance. These culture systems provide

a suitable substrate such as laminin (LN), to accommodate neural lineage specific CAMs (Gunther, 2016). Typically, after EB replating and under appropriate culture conditions, rosette-like cell arrangements are observed. These structures, termed neural rosettes, indicate a population of early neural committed cells displaying polar morphologies akin to that of the developing neural tube (neuroepithelial cells) in embryogenesis (Koch *et al.*, 2009; Fedorova *et al.*, 2019).

However, neural induction of suspended hiPSC cultures via EB formation can be inefficient. Firstly, necrotic core formations risks cell viability and quality (Van Winkle *et al.*, 2012). Secondly, the differentiation efficiency of the aggregates towards neural commitment is highly dependent on their density, size, shape and aggregate morphology meaning such parameters are a necessity to control during the neural induction process (Guo *et al.*, 2020). Thirdly, additional processing steps are needed for the re-plating of EBs onto a secondary platform/substrate, in order to isolate the neural rosettes. Finally, the heterogenous nature of EBs creates a hinderance for their applicability as a mediator for NPC-based therapies, due to the possibility of product contamination with unwanted cell types.

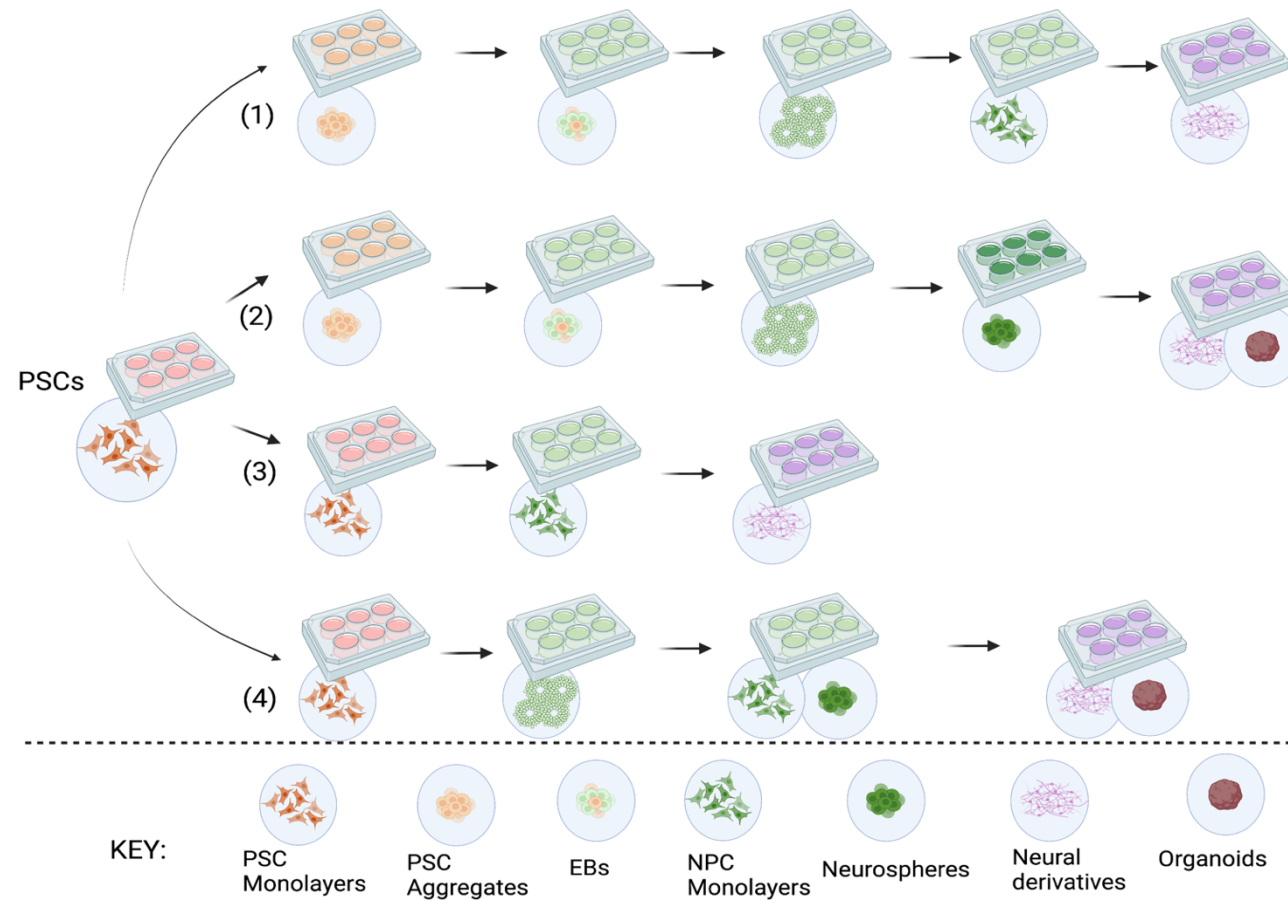


Figure 1.4. The different methods of neural induction. Methods (1) and (2) mediate the neural induction process through EB formation and neural rosettes. Methods (3) and (4) requires monolayer cultures of PSCs. Stages which show two types of cell type implies two possible culture routes for that particular stage.

#### **1.8.4. Neural induction using adherent culture systems**

An alternative method of neural induction, also commonly practised, is the direct neural induction method. The starting point for this process is an adherent monolayer culture of PSCs typically on planar platforms coated with Matrigel or VTN substrates (see methods 3 and 4). Subsequently, PSCs are differentiated towards NPCs by changes in the culture systems' environmental cues. These cues can be delivered to the cells through medium exchange with relevant factors such as morphogens and inhibitors, whilst adhered on a suitable substrate composition as described earlier in sections 1.8.1 and 1.8.2.

Neural induction is typically initiated at a point when PSCs are most prone to differentiate. This point has been previously identified as the G1 phase of the PSCs cell cycle (Wu, Fan and Tzanakakis, 2015). PSCs are known to have a short G1 phase (Zaveri and Dhawan, 2018). However, it can be prolonged by contact inhibition, which is achieved in culture systems with planar platforms by allowing the cultures to reach confluence (Zaveri and Dhawan, 2018). At this point, the neural inducing factors can be added to effectively differentiate the PSCs towards NPCs.

In direct neural induction processes, the generation of neural rosettes is dependent on the differentiation morphogens, factors and inhibitors used. When generating neuroepithelial like neural precursors or early neural precursors, the formation of neural rosettes are typical morphological indicators of successful PSC commitment towards the neural lineage (Stiles and Jernigan, 2010; Khlongkhlaeo *et al.*, 2016; Lukovic *et al.*, 2017; Fedorova *et al.*, 2019). Subsequently, the neural rosettes give rise to the targeted NPC types, which is achieved by repeated selective sub-culture techniques to eliminate undifferentiated PSCs or unwanted differentiated cells. These techniques include manual selection of the rosettes or the use of selective dissociation reagents (Khlongkhlaeo *et al.*, 2016). Thus, hiPSC-derived NPCs generated in the initial platform/substrate are sub-cultured onto a second culture system, which

is usually designed to maintain and expand NPCs. These secondary culture systems would usually employ specific substrates such as LN and PLO (Zhang *et al.*, 2001; Khlongkhlaeo *et al.*, 2016)

However, for culture systems using neural inducing cues to generate NP cells or late neural precursor populations, neural rosettes are not typically observed (Galiakberova and Dashinimaev, 2020). This offers for a process which can reduce the need for neural rosette subculturing.

### **1.9. Scalable strategies to produce clinical-grade hiPSC-derived NPCs**

Although hiPSC-derived NPCs pave a promising avenue towards an ethical and sustainable therapy for neurodegenerative diseases, several major barriers hinder their commercialisation, which have been identified and discussed so far in this chapter. Of note are the challenges involved in their progression through the different stages of clinical trials, including commercialisation (phase IV). To progress hiPSC-derived NPCs from preclinical to clinical stages, and then eventually to commercialisation, approvals from local regulators are mandatory at each stage.

The safety and efficacy data of a candidate therapy are obvious influencers towards the decision of regulators. However, often overlooked are the manufacturing process information, which are also equally pivotal within regulatory decisions. It is important to reassure regulators that product CQAs are consistent at all stages of the clinical trials, thus making the product predictable and consistent. Therefore, CPPs of the manufacturing process for a candidate therapy are typically set from the onset of clinical trials to ensure consistent and reproducible product CQAs.

Importantly, note that at each stage of the clinical trials, progressively larger quantities of the therapeutic product are required, thus necessitating adaptations of manufacturing processes to cope with the demands. For example, pre-clinical and early-stage clinical investigation of a potential hiPSC-derived NPC therapy targeting neurodegenerative diseases, would require a small-scale manufacturing process capable of producing enough NPCs to test several hundred volunteers. Employing a large-scale manufacturing process at these early stages would be unnecessary, costly, and impractical. For late-stage clinical investigations, larger quantities of the same quality NPCs are required to accommodate for a much larger user-group, thus a large-scale manufacturing process would be then more suitable. Hence, different manufacturing strategies may be applied at different stages of clinical trials.

To avoid resistance from regulators, the manufacturing information submitted should detail the strategies to reassure consistent CQAs at all scales of manufacturing. The problem arises when the CPPs within the submitted manufacturing information are set for non-scalable processes. Progression of such submissions are usually hindered because of inadequate manufacturing information to reassure consistent CQAs at all production scales.

Furthermore, the procedures involved in obtaining NPCs from hiPSCs via neural induction, inherits unique manufacturing challenges compared to the bioprocessing of other stem cell-based therapies. MSC therapies for example, can employ just a single process unit for cell expansion in their manufacturing workflows. However, in the case of hiPSC-derived NPC production, the manufacturing workflow would need to recognise 3 imperative upstream processing stages: (1) hiPSC expansion, followed by (2) neural induction, and finally (3) expansion of NPCs. One systematic approach is to chain 3 individual processing stages, with each processing unit dedicated to a process stage. This strategy could be considered an direct translation of a typical laboratory scale production process for hiPSC-derived NPCs in T-flasks or multi-well plates. In these cases, the initial culture system is specifically designed for hiPSCs

expansion, followed by hiPSCs transfer into a different culture system specific to neural induction processes, and then finally, the hiPSC-derived NPCs would then be subsequently transferred into another culture system specific for NPC expansion.

Employment of chained processing units to produce hiPSC-derived NPCs at the upstream manufacturing workflow, however, requires stringent CPPs and increased process validation and CQA assessments due to very complex procedures involved (e.g., harvest, neural induction, cell transfer etc.). Additionally, chained processing units would increase the risks of batch failures and require dedicated equipment per process unit that would increase costs and investments.

Integrating the 3 key process steps (hiPSC expansion, neural induction, and NPC expansion) into one single process unit is advantageous since equipment and procedures can be reduced for a manufacturing workflow, thus offering a potentially faster, cheaper, more manageable, and robust process. In other words, the success of this approach relies on a single culture vessel which allows for the 3 key processing stages to proceed.

Despite the advantages of a single culture vessel for the entirety of the manufacturing workflow, major biological and logistical challenges arise. For one, different culture systems are required for hiPSC expansion, neural induction, and NPC expansion stages, thus an approach to integrate the transition from one culture system to the next within the same vessel is needed. The following sections describes how strategies and scalable technologies can be utilised to realise a scalable integrated culture system for the production of hiPSC-derived NPCs.

### 1.9.1. Scale-out and scale-up strategies

Conventional laboratory scale methods for producing hiPSC-derived NPCs are difficult to apply in large-scale manufacturing processes. This is due to their reliance on traditional static and planar platforms for cell culture. Such platforms can yield hiPSC monolayers from  $3 \times 10^5$  to  $1 \times 10^6$  cells/cm<sup>2</sup> (Tohyama *et al.*, 2017), and would require expansive surface areas to accommodate the demands of production at commercial scale which requires billions of cells. However, most planar platforms can be scaled-out to obtain larger quantities of NPCs by simply employing more planar platforms, thus essentially running multiple manufacturing processes in parallel to obtain more product. Scale-out enabling technologies include cell stackers and automated robotic arms for cell culture handling (Terstegge *et al.*, 2007; Wilmes *et al.*, 2017; Daniszewski *et al.*, 2018). For autologous therapies, a scale-out approach would suffice since the manufacturing process only requires production of enough cell-based product for one individual.

Nevertheless, a scale-out approach has several caveats. The need to use multiple culture vessels simultaneously increases utility of manufacturing facility space; increases the technical manual labour required; risks consistent process control due to potential variation in the handling amongst culture vessels; and increases risks of batch variability and failures. These identified shortcomings of a scale-out approach translate to higher costs of manufacturing, which consequently inflicts a premium on the overall cost of therapy (Abraham *et al.*, 2018). Therefore, a scale-out of the current laboratory scale production for hiPSC-derived NPCs are unsuitable for large-scale production.

A scale-up strategy provides another method for obtaining large quantities of hiPSC-derived NPCs. Essentially, the scaling up of a culture system would involve switching the culture platform to a large culture vessel of similar or proportional geometries, to maintain a linear relationship between the different culture scales. However, traditional static planar platforms

for cell culture are not practically amenable for scale-up. Only suitable culture systems can be scaled up; these scalable culture systems require scalable technologies such as bioreactors and microcarriers (Badenes *et al.*, 2016; Koenig *et al.*, 2018), which are discussed more in the following sections.

Within upstream, scale-up can be achieved by transitioning from small scale or benchtop bioreactors (typically 10 mL – 10 L capacity) to large-scale or industrial bioreactors (> 50 L capacity). An advantage of scalable manufacturing processes is the ability to linearly scale procedures and CPPs. This ensures to maintain consistent product CQAs amongst all production scales. Scale-up also offers improved product homogeneity per batch, less manufacturing space required, and less risks of contaminations or failures when compared to a scale out approach.

### **1.9.2. Bioreactor platforms**

Bioreactors are a well-established scalable platform for culturing cells, with a successful history in manufacturing processes of large scale bioproduction. For example, bioreactors are robust platforms for cultures of Chinese hamster ovary (CHO) cells to manufacture recombinant mAb, fusion proteins, and other protein-based molecules. Comparatively fewer reports which employ bioreactors for bioprocessing of cell-based therapeutic products have been published; this is certainly true for hiPSC-derived NPCs products.

Bioreactors are commercially available in different modalities including packed bed bioreactors, vertical-wheel bioreactors, wave bioreactors, hollow fibre bioreactor and stirred tank bioreactors (STB). In most cases, these bioreactors are suited for suspension culture systems. Note that the cell phenotypes involved in the production of hiPSC-derived NPCs are adherent cell types which can be cultured in suspension as cell aggregates. Therefore, bioreactors are considered suitable platforms for hiPSC-derived NPC manufacturing processes.

### 1.9.2.1. Stirred tank bioreactors

Of particular promise for the bioproduction of hiPSCs-derived NPCs are STBs: a scalable culture vessel configured with an internal impeller. The impeller is mechanically rotated to physically agitate the culture environment, thus causing the necessary uplift for a dynamic and homogenous culture system. Benchtop and larger STBs (>2 L capacity) are typically closed systems with ports available for probes to monitor CPPs such as pH, glucose, metabolites, or dissolved O<sub>2</sub>. Important gases like O<sub>2</sub> can either be delivered into the headspace of the vessel or sparged from the bottom of the vessel and directly into the medium; both methods rely on the dynamic environment of STBs for gases to efficiently dissolve into the medium. Temperature is regulated by heating/cooling jackets. Addition and removal of culture components (e.g., medium exchanges) is achieved through the configured inlets/outlets of the STBs. These are usually sterile connected to an external system via tubing and regulated by a physical mechanism (e.g., pumps). Because of their scalable designs and the potential for a controlled and monitored dynamic culture system, they are an attractive platform for the production of NPC-based therapies at clinical stages.

Different scales of STBs have been successfully applied for multiple applications such mAb production, viral production, bacterial culture, MSC expansion, PSC expansion and NPC expansion, to name a few (Kehoe *et al.*, 2010; Abbasalizadeh *et al.*, 2012; Rafiq *et al.*, 2013; Petry *et al.*, 2016; Schnitzler *et al.*, 2016; Fan, Zhang and Tzanakakis, 2017). Nonetheless, the employment of benchtop and larger STBs for PSC and NPC culture is one of the least investigated compared to other mammalian culture systems such as CHO or HEK cells. This is likely due to the costs of performing process development experiments at large scale and the relative infancy of the field.

### **1.9.2.2. Spinner flask**

Spinner flasks are considered small-scale STBs. They have been utilised as platforms for the expansion of several cell types, including PSCs and NPCs. Due to their modality and design, they hold potential for scale-up towards benchtop and larger STBs. Additionally, spinner flasks require low working volumes ranging from 10 mL (e.g., Ambr® 15, Sartorius) to 1000 mL (e.g., 1L disposable Spinner flask, Corning), making them economically ideal for process development projects. Spinner flask vessels can be made of autoclavable glass or non-autoclavable plastic which are suited for multi-use and single use, respectively. Usually, they are designed as open culture systems with side arms to allow for gassing, medium exchanges, and sampling. A magnetic bar and impeller are also often configured in spinner flasks, which can be magnetically induced to rotate by a magnetic stirrer platform. The agitation as a result, provides a similar dynamic culture system to that achieved in benchtop and larger STBs.

Nevertheless, spinner flasks have several inherent limitations. First, spinner flasks are a semi-controlled culture platforms which rely on the incubator conditions for gas and temperature control. Second, most spinner flasks cannot be configured with sensors or probes to monitor CPP thus requiring offline manual sampling. Third, medium exchanges, sampling, feeding and other necessary manipulations of hiPSC or NPC cultures, risks contamination and error due to the open system nature of spinner flasks. Lastly, although scalable, spinner flasks are difficult to automate therefore requiring technical manual labour to operate. There are, however, several systems that provide an automated spinner flask/dynamic small-scale platform for cell culture, which includes the Ambr®15 and Ambr®250 from Sartorius, and the c.bird™ and S.bird™-systems from Cytex. Although allowing for high throughput and automated process developments, such systems of automated dynamic culture platforms come at a premium cost.

### 1.9.3. Microcarrier technologies

Microcarriers are an enabling technology that allows for anchorage dependant cultures to be adapted into suspended cultures. Microcarriers are micrometre-sized polymeric particles typically composed of a core material and often layered with a substrate coating. Commercially available microcarriers range in sizes, core material, substrate coatings and porosity amongst several other features (see Table 1.4). Several groups have employed microcarriers as physical platforms for anchorage dependent cells to attach onto and combined these technologies with STBs (Phillips *et al.*, 2008; Eibes *et al.*, 2010; Rafiq *et al.*, 2013; Badenes *et al.*, 2015; Lam *et al.*, 2015, 2016; Nienow *et al.*, 2016; Fan *et al.*, 2017; Yuan *et al.*, 2018; YekrangSafakar *et al.*, 2018; Hanga *et al.*, 2021). Importantly, cells adapted to the suspended culture system in STBs can reap the benefits of a dynamic, homogenous, and controlled culture environment.

Furthermore, due to the size and geometries of microcarriers, they offer a large surface area for cell growth within a relatively small volume space of the STBs. This allows for efficient medium utility. Hence, the employment of microcarrier platforms for cell expansion processes could overcome the culture area and the manufacturing space limitations associated with the use of conventional planar platforms.

Microcarrier porosity determines the available surface area allowed for cell attachment. For macroporous microcarriers such as Cultispher S and Cultispher G, the available surface area is increased significantly by the crevices within the structure. Although promising, macroporous microcarriers are difficult to estimate the available surface area, and pose problems of pore fouling leading to inefficient media diffusion. Additionally, cell detachment from porous microcarriers could be difficult in the downstream processing, whereby cell dissociation is typically mediated by chemical or enzymatic means.

Furthermore, specific uplift force is required to suspend microcarriers within STB culture environment (Nienow *et al.*, 2016). Since the hydrodynamics within STBs is regulated by the impeller speed, the density of the microcarriers will influence the impeller speed parameter of the culture system, whereby heavier microcarriers would require faster impeller rotation speeds, and vice versa (Li et al, 2015; Chen X-Y et al, 2020).

Table 1.4. List of different commercially available microcarriers and their properties.

Microcarrier	Manufacturer		Diameter range (µm)	Core material	Substrate coating	Surface charge	Porosity	Average density g/cm <sup>3</sup>	Surface Area/gram cm <sup>2</sup> /g
Collagen	SoloHill Inc.	Eng.	125-212	Polystyrene	Type I Porcine	None	Non-porous	1.04	360
Cultispher-G®	Percell Biolytica		130-380	Crosslinked gelatine	No	None	Macroporous	1.04	N/A
Cultispher-S	Percell Biolytica		130-380	Crosslinked gelatine	No	None	Macroporous	1.02-1.04	N/A
Cytodex 1™	Sigma-aldrich		147-248	Dextran	DEAE	Positive	Non-porous	1.03	4400
Cytodex 3™	Sigma-aldrich		130-138	Dextran	Type I porcine collagen	None	Microporous	1.04	2700
Dissolvable microcarrier	Corning		200-300	Polygalacturonic acid polymer chains cross linked via calcium ions	Corning™ Synthemax II	None	Non-porous	1.02-1.03	5000
FACT III	SoloHill Inc.	Eng.	125-212	Polystyrene	Type I Porcine	Positive	Non-porous	1.02	360
Hillex®	SoloHill Inc.	Eng.	160-180	Dextran	Cationic trimethyl ammonium	Positive	Non-porous	1.11	515
Plastic	SoloHill Inc.	Eng.	125-212	Crosslinked polystyrene	No	None	Non-porous	1.02	360
Plastic Plus	SoloHill Inc.	Eng.	125-212	Crosslinked polystyrene	No	Positive	Non-porous	1.02	360
Pronectin® F	SoloHill Inc.	Eng.	125-212	Polystyrene	Recombinant fibronectin	None	Non-porous	1.02	360
Synthemax™II	Corning		125-212	Polystyrene	Corning™ Synthemax II	None	None-porous	1.02	360

#### **1.9.4. Scalable culture systems**

The utilisation and advancements of scalable technologies in the recent years have allowed for work towards the development of scalable culture systems for expanding PSCs. In most cases, the expansion processes developed have been designed to harvest PSCs as the product (Fan, Zhang and Tzanakakis, 2017; Chan, Rizwan and Yim, 2020)(Krawetz *et al.*, 2009). Although such contributions are welcomed, it is important to remember that the eventual product for cell-therapies are the differentiated cells that are derived from PSCs. In fact, the administration of PSCs into humans is a risk for tumorigenesis, thus regulators require for the removal undifferentiated PSCs from the final cell-based product (Jha *et al.*, 2021).

Similarly, advancements towards the development of scalable culture systems for NPC expansion have been made in the recent years (Baghbaderani *et al.*, 2008, 2010; Miranda *et al.*, 2016; Song *et al.*, 2016).

Neural induction methods are predominantly performed under static conditions using planar platforms; these methods are reviewed extensively by Galiakberova and Dashinimaev (2020). To the best of the author's knowledge, only the study by Bardy *et al.*, (2013) has attempted to perform neural induction of hiPSCs whilst suspended on microcarriers within spinner flasks and this paper is discussed in great detail in section 1.9.5. Several others have performed neural induction of PSC aggregates cultures in STBs (Rigamonti *et al.*, 2016; Miranda *et al.*, 2016)

##### **1.9.4.1. Expansion of hiPSCs as suspended cell aggregates**

The expansion of PSCs in different scales of STBs have been demonstrated (Abbasalizadeh *et al.*, 2012; Wang *et al.*, 2013; Abecasis *et al.*, 2017; Nogueira *et al.*, 2019). STBs are the most common scalable platforms for PSC cultures. There are two dominating methods for employing STBs in the expansion of PSCs: either as cell aggregates or as anchorage dependent cell layers

on microcarriers. Table 1.5 summarises some examples of the achieved cell densities using STBs for aggregate or microcarrier based culture systems.

Expansion of hiPSCs as aggregates in STBs provides several advantages over microcarrier based culture systems, if the target product is purely the PSCs. For one, the implementation of such approach in the manufacturing of PSCs will bypass the additional processing steps associated with microcarrier preparation and microcarrier filtration (Singh *et al.*, 2010; Lam *et al.*, 2016; Abecasis *et al.*, 2017). Also, this strategy omits the need for additional substrate coatings such as Matrigel or VTN which are usually essential for planar platforms and most microcarrier platforms (Oh *et al.*, 2009; Jenkins and Farid, 2015;Badenes *et al.*, 2016). Thus, without the required microcarrier and coating resources, such a manufacturing process would appear to be more economical for production of PSCs compared to microcarrier dependent processes.

However, for the generation of PSC derived products such as NPCs, layers of additional process complexities need to be considered. For example, although the generated hiPSCs aggregates are co-operative with aggregate/EB mediated neural induction protocols to generate EBs or neurospheres, these differentiated heterogenous aggregates typically require replating and further isolation of the desired neural population, often and classically performed manual by colony picking (see section 1.8.3 and 1.8.4). Thus, translation of these manual selections steps to scalable process is necessary when implementing an aggregate based expansion of PSCs, which is difficult to achieve.

In addition, there are several other logistical and biological challenges with the cultures of aggregates expansion approach as mentioned previously in this chapter, such as formations of necrotic cores due insufficient mass transfers of gases and nutrients the cell layers inside large aggregates. Ultimately, process parameter optimisation and aggregate control is key to

achieving clinically and economically feasible bioprocesses for expanding suspended PSC aggregates. A review by Jenkins and Farid (2015) discusses various process development considerations for a scalable and cost-effective manufacturing strategy of PSCs.

One method for controlling aggregate size is by mechanical regulation through hydrodynamic forces caused by mechanical mixing as impellers rotate. Several studies have suggested that hydrodynamic forces can cause shear stress to the cells, thus inducing stress mediated cell death mechanisms or compromise the critical cell attributes (Wolfe *et al.*, 2012; Chen *et al.*, . Encapsulation of the cells/aggregates using hydrogels offers an alternative strategy to control aggregate size (Enam, 2015; Higuchi *et al.*, 2015). The encapsulating hydrogel creates a physical barrier between the cells and hydrodynamic forces of the culture environment, essentially buffering the cells within and reducing exposure to shear stress. The effect of dynamic environments and shear stress on the cells are further discussed in section 1.10.2.

Hydrogels have been shown to promote the expansion of PSCs as uniform aggregate sizes whilst maintaining their pluripotency qualities. This is achieved by the permeance of the hydrogel which allows for the diffusion of essential medium components to reach the cell, and similar for the metabolic wastes to exit the encapsulation (Horiguchi and Sakai, 2015; Sara M. Badenes *et al.*, 2016; Gilmozzi *et al.*, 2021). Another advantage of hydrogel encapsulation is the ease of cell extraction at the downstream process, typically completed by chemical or enzymatic degradation, consequently releasing the cell content for harvest (Andersen *et al.*, 2015). Furthermore, the use of hydrogels to generate uniform and controlled aggregates may pave a way towards generating homogenous aggregates of NPCs such as neurospheres.

Table 1.5. Examples of PSCs cultured in scalable culture systems.

Cell type	Platform	Culture system	Microcarrier/additional coating	Working volume (mL)	Medium	Maximum cell density (cells/mL)	Reference
<i>Aggregates</i>							
<b>hESCs</b>	Spinner flask	Aggregates	N/A	50	KO-SR medium, mTeSR1	2.4 x 10 <sup>6</sup>	(Singh <i>et al.</i> , 2010)
<b>hESCs</b>	Spinner flask	Aggregates	N/A	60	StemPro/mTeSR1	1 x 10 <sup>6</sup>	(V. C. Chen <i>et al.</i> , 2012)
<b>hESCs</b>	Spinner flaks	Aggregates	N/A	100	mTeSR1	2 x 10 <sup>6</sup>	(Olmer <i>et al.</i> , 2012)
<b>hESCs</b>	STBs	Aggregates	N/A	100	mTeSR1	0.45 x 10 <sup>6</sup>	(Krawetz <i>et al.</i> , 2009)
<b>hiPSCs</b>	Spinner flasks	Aggregates	N/A	45	E8	1.7	(Kehoe <i>et al.</i> , 2010)
<b>hiPSCs</b>	STBs	Aggregates	N/A	100	mTeSR1, E8	3.01 x 10 <sup>6</sup>	(Silva <i>et al.</i> , 2015)
<i>Microcarrier</i>							
<b>hESCs</b>	Spinner flasks	Microcarrier	DE-53/Matrigel	50	Conditioned medium	3.5 x 10 <sup>6</sup>	(Oh <i>et al.</i> , 2009)
<b>hESCs</b>	Spinner flasks	Microcarrier	Cytodex 3/Matrigel	100	KO medium	1.22 x 10 <sup>6</sup>	(Serra <i>et al.</i> , 2010)
<b>hiPSCs</b>	Spinner flask	Microcarrier	DE-53/Matrigel	50	mTeSR1	6.1 x 10 <sup>6</sup>	(Leung <i>et al.</i> , 2010)
<b>hiPSC</b>	Spinner flask	Microcarrier	Plastic/vitronectin	50	E8	1.4 x 10 <sup>6</sup>	(Sara M Badenes <i>et al.</i> , 2016a)
<b>hiPSC</b>	Spinner flask	Microcarrier	Synthemax II	100	mTeSR1	3 x 10 <sup>6</sup>	(Silva <i>et al.</i> , 2015)
<b>hiPSC</b>	Spinner flask	Microcarrier	Plastic/PLL + vitronectin	50	TeSR2	1.6 x 10 <sup>6</sup>	(Fan <i>et al.</i> , 2014)

#### **1.9.4.2. Expansion of hiPSCs as adherent cultures on suspended microcarriers**

hiPSCs can use microcarriers as a physical substrate to attach and grow on. These hiPSC-microcarrier conjugates can then be suspended in the dynamic environment of STBs, thus exposing the cells to a dynamic homogeneous environment. This is certainly an advantage over aggregate culture methods since cells can grow as monolayer on the surface and access nutrients and gases of the medium more readily.

Nonetheless, there are challenges tethered with the use of commercially available microcarriers for hiPSC cultures. For one, commercially available microcarriers were mainly tailored towards cell types with the likes of fibroblast, CHO and HEK. Thus, there is a lack of commercially available ready to use microcarriers optimised to support hiPSC and their pluripotent and self-renewing qualities. Second, undifferentiated PSCs tend to self-aggregate in suspension, therefore, a suitable microcarrier should promote cell attachment and overcome the tendency of hiPSCs to aggregate (Olmer et al., 2012).

For a successful microcarrier-based bioprocess, the identification of a suitable microcarrier is key. In an attempt to establish which microcarrier best supported PSC expansion, Chen *et al.*, (2011) performed a screening study of various commercially available microcarriers, and investigated the cell attachment efficiency, growth rate, and their effects on cell integrity. Their work showed that positively charged microcarriers (DE53, QA52, Cytodex 1) allowed efficient cell attachment at more than 60% of the initial cell inoculation density, whereas negatively charged microcarriers (CM-52) showed lower attachment efficiency (Chen *et al.*, 2011). The higher attachment efficiency of these PSCs to positively charged microcarriers was likely due to the electrostatic attraction between the positively-charged microcarrier and the relatively negative charge of the cells (Chen *et al.*, 2013).

However, conflicting observations have been reported regarding the use of some microcarriers. For example Cytodex 3 has been shown to support mouse PSC expansion (Gupta *et al.*, 2016) which is believed to be mediated by the denatured collagen coating that bind to  $\alpha 2\beta 1$  integrins present on the cell surface membranes of mouse PSCs. However, some groups have reported that although Cytodex 3 promoted cell attachment, harvested human PSCs cells failed to express adequate pluripotency markers such as Tra-1-60 post-microcarrier culture, along with slow growth rates and loss of self-renewing attributes (Kehoe *et al.*, 2010; Nie *et al.*, 2010; Chen *et al.*, 2013). This is potentially due to the different developmental stages of mouse PSCs and human PSCs.

Because of the lack of readily available microcarriers for PSCs, several groups modified the surfaces of microcarriers by coating with suitable substrates. Matrigel is one such coating that was shown to support attachment, ECM deposition, growth and maintenance of undifferentiated PSCs in microcarrier cultures (Oh *et al.*, 2009; Nie *et al.*, 2010). However, Matrigel is poorly defined, and is not a suitable substrate for the production of clinical-grade PSCs as mentioned previously in section 1.7.5 (Hughes *et al.*, 2010; Higuchi *et al.*, 2015).

Therefore, more defined and xeno-free coatings such as rh-VTN and LN have been identified as suitable for PSCs in microcarrier-based cultures (Fan *et al.*, 2014; Enam, 2015; Lam *et al.*, 2015; Badenes *et al.*, 2016). As a result, research groups have focused on developing and utilising defined surface coatings capable of supporting PSCs. For example, a study by Badenes *et al.* (2016) shows the suitability of rh- VTN as a coating for microcarriers. In their study, E8<sup>TM</sup> culture medium was used.  $\alpha v\beta 5$  and  $\beta 1$  integrins on the surfaces of PSCs have been shown to ligate VTN and promote cell attachment and proliferation (Rowland *et al.*, 2009; Braam *et al.*, 2008).

Fan, et al., (2017) investigated the potential of VTN and VTN crosslinked with human serum albumin (HSA) as coatings on plastic microcarriers. They reported that plastic microcarriers coated with only VTN had an attachment efficiency of around 25% but were unable to maintain cell attachment during a 5-day agitated spinner flask culture. Due to the lack of protein supplements in the TeSR™-E8™ medium, the group supplemented the medium with HSA in an attempt to increase cell attachment. VTN coated plastic microcarriers were conditioned in TeSR™-E8™ medium supplement with HSA. To further increase the seeding efficacy, they crosslinked the HSA to the vitronectin coating using ultraviolet light. Another effect of crosslinking is to expose active molecules from the matrix proteins such as RGD targets, which can subsequently promote cell attachment, adhesion and spreading. Their results suggested that UV crosslinked vitronectin-HSA coated microcarriers increased attachment efficiency to around 35% in agitated culture (Fan *et al.*, 2017).

Lam et al. (2015) developed a xeno-free culture system utilising plastic and plastic plus microcarriers coated with different isoforms of LN-521 and LN-5111 (Lam et al., 2015). LN-521 is expressed during early embryonic development and shows a higher affinity towards the cell adhesion molecule integrin  $\alpha6\beta1$  compared to LN-111. Their study showed that LN-521 coated Plastic microcarriers supported human PSC attachment similarly compared to Plastic Plus microcarriers coated with LN521 (Lam et al., 2015). This highlights the importance of the interaction between CAMs and the surface chemistry of microcarriers which in this case was further enhanced with protein coatings.

Customised synthetic microcarriers have also be used to culture PSCs. Kolhar et al., (2010) synthesised polystyrene microcarriers with surfaces decorated with cyclic RGD peptides and investigated the adhesion of PSCs (Kolhar et al., 2010). An approximate 4 fold higher increase in cell attachment efficiency was obtained compared to PSCs cultured on polystyrene microcarriers with linear RGD peptides (Kolhar et al., 2010).

Other modes of bioreactors have also been implemented into an expansion process for hiPSCs, including vertical wheel single use bioreactors which was reported capable of generating cell densities of  $2.3 \pm 0.2 \times 10^6$  cells/mL by Nogueira et al., (2019). Davis et al., (2018) reported an average fold increase of 5.7 in cell numbers using rocking motion bioreactors. Olmer et al., (2012) utilised Cellferm® Pro parallel bioreactor systems (DASGIP AG) which generated  $2 \times 10^6$  hiPSCs/mL, equivalent to a 5.5-fold increase within 7 days. They also highlighted the importance of aggregate size control to avoid formation of necrotic cores and concentration gradients, thus resulting in variation in cell quality.

#### **1.9.5. Scalable neural induction and NPC culture strategies**

PSC aggregates can be directed to commit down the neural lineage through the formation of neurospheres, a term that describes a structure of free-floating aggregates of NPCs. By removing the factors from the media that maintains pluripotency whilst subsequently introducing neural inducing morphogens and factors, PSC aggregates can differentiate to form neurospheres in suspension (Serra *et al.*, 2009). Xie *et al.*, (2017) reported the importance of controlling the size, shape and rate of the aggregate formation as it can influence a certain lineage bias. However, these neurospheres typically have slow proliferative rates, a heterogenous population of NPCs and post-mitotic neurons and glia, and an uncontrollable spontaneous differentiation when above 150  $\mu\text{m}$  in diameter (Deleyrolle *et al.*, 2009). Nonetheless, Serra *et al.*, (2009) developed a two-step bioprocess for the generation of PSC derived neurons utilising bioreactors, by firstly expanding the PSCs as aggregates, followed by the generation of neurospheres, and finally demonstrated their capability to differentiate into neurons.

In an application note, DASbox® mini bioreactor system (Eppendorf) has been reported to be capable of expanding PSCs as aggregates in suspension as well as an integrated neural induction step. This system was shown to obtain  $2 \times 10^8$  cells as neurospheres (Koenig et al., 2018). This protocol took > 32 days from PSC inoculation to the harvest of neurospheres.

However, as mentioned, it was only Bardy *et al.*, (2013) who had demonstrated an integrated bioprocess to obtain hiPSC-derived NPCs using microcarriers. Their process requires a 7 day expansion of PSCs in spinner flasks, with a twice daily feeding strategy using mTeSR1 medium, followed by an 18 day integrated neural induction process, in differentiation media containing antibiotics such as penicillin and streptomycin. Using such processes, they were capable of generating 333 PSA-NCAM positive NPCs per hiPSCs or 371 NPCs per hESCs. Still, the process by Bardy et al. (2013) is established with the employment of DE-53 large positively charge cylindrical microcarriers, and Matrigel ECM coating which are undefined animal products unsuitable for clinical applications. The NPCs produced were then characterised and differentiated towards neural derivatives such as neurons, oligodendrocytes, and astrocytes to successfully demonstrate their functionality (Bardy *et al.*, 2013). More work is needed towards the development of a neural induction process using similar platforms, with consideration towards a clinical applications.

There are several advantages of performing neural induction on hiPSC monolayers adhered to microcarriers compared to hiPSC aggregates. First, hiPSC are homogenously exposed to the morphogens and inhibitors within the medium. This leads to a more efficient utilisation of the medium components and promotes a homogenous differentiation effect across the cell population. Second, direct neural induction of monolayer PSCs can typically require less time than that of aggregate neural induction. Third, the EB generation and neural rosette isolation with aggregate mediated neural induction processes requires re-plating steps and specific dissociation of neural lineage committed cells, which may prove difficult to perform within

STBs. With the case of direct neural induction of monolayer hiPSCs on microcarriers, the need for re-plating can be omitted.

However, with microcarrier expansion, the available surface area becomes a limitation of cell growth. In order to propagate the cells further, new surface area must be introduced, which can be achieved through passaging the cells onto new fresh microcarriers, or addition of microcarriers.

## **1.10. Other bioprocessing considerations using STBs**

### **1.10.1. Operation mode**

PSCs are rapidly dividing cells with high metabolic activity. PSCs have preference for glucose as an energy source, but also rely on glutamine metabolism to support cell growth and proliferation, as well as to minimise reactive oxygen species production (Lees et al., 2017; Tsogtbaatar et al., 2020). As a result of their metabolism, end-products such as lactate and ammonium are produced which if uncontrolled can inhibit cell growth and quality (Freund and Croughan, 2018). The depletion of essential nutrients, along with the build-up of metabolites pose multiple biological and bioprocessing challenges. These can be minimised through feeding regimes or operation modes which have been explored in the past for mammalian cultures in bioreactors (Le et al., 2012; Kropp et al., 2016). The different operation modes include batch, fed batch, repeated batch, and perfusion.

Due to the high sensitivity of PSCs to their culture environment and the build-up of metabolic wastes, the batch and fed batch operation modes are considered unsuitable for long term maintenance of PSCs. This can cause spontaneous differentiation of PSCs and reduced viability. Instead, several groups have attempted optimising the repeated batch operation mode for the expansion of PSCs in bioreactors (Krawetz et al., 2009; Olmer et al., 2012; Chen et al.,

2012; Ismadi et al., 2014). This strategy involves the partial or full replacement of the spent culture medium with fresh medium at interval timepoints of the culture. Spent medium containing metabolic end-products is removed and the addition of fresh medium replenishes the nutrients consumed.

However, only the perfusion operation mode can ensure the maintenance of a steady state providing the cells a constant reserve of nutrients whilst continuously removing waste products. Only a few studies have explored perfusion systems for the expansion of PSCs (Fong et al., 2005; Serra et al., 2010; Yoshimitsu et al., 2014; Kropp et al., 2016). Furthermore, only a limited number of studies have described perfusion cultures of NSCs (Simao et al., 2016; Song et al., 2016). Though perfusion systems may be advantageous compared to other operation modes, the current cost of expansion and differentiation media, combined with the large volumes required to operate are major hinderances in their implementation within laboratory processes.

### **1.10.2. Mixing speed**

STBs are designed with mechanically driven impellers that ensure mixing. Mixing facilitates the diffusion of gases such as O<sub>2</sub> into the medium. The agitation speed can be adjusted to optimise PSC expansion as well as influence their differentiation potential. For example, Correia *et al.*, (2014) found that agitation supported the differentiation of hiPSCs to cardiomyocytes at faster and with higher conversion yields (Correia *et al.*, 2014). However, for neural commitment, more studies are needed to investigate the effect of mixing speed on the differentiation potential of hiPSC towards NPCs.

Furthermore, the combination of stirring speed and impeller design should be set to produce enough uplift to keep cell-laden microcarriers or cell aggregates in suspension (Fridley *et al.*,

2012). However, as the cells proliferate, the cell aggregates will increase in diameter; similarly, microcarriers will become more confluent, thus the buoyancy of the aggregates/cell-laden microcarriers would change throughout the culture. This would influence the stirring speed to maintain the correct up lift. Ensuring a homogenous distribution of suspended cells throughout the culture maintains an efficient mass transfer.

However, it is also important to be aware of the fluid shear stress created and experienced by cells in such dynamic environments. Shear stress is the mechanical force induced by tangential flow movement of liquid particles (friction) against the cell surface membranes. Several reports have suggested that fluid shear stress can affect the expression of pluripotency markers or even their ability to differentiate since such forces can stimulate stress signals and further influence intracellular pathways (Gareau *et al.*, 2014; Wolfe *et al.*, 2012). Stem cells in particular are susceptible to mechanical stresses. To recapitulate stem cell environments in the body, values of 0.5 to 120 dyn/cm<sup>2</sup> is the known physiological range of shear stress (Lindner *et al.*, 2021).

Studies exploring the effect of shear stress on PSCs have suggested that exposure to certain values of shear (e.g.,  $1 \times 10^4 - 1.5 \times 10^4$  N/cm<sup>2</sup>) can cause cells to differentiate, particularly towards endothelial cells (Zhong *et al.*, 2001; Huang *et al.*, 2005; Marchand *et al.*, 2014; Sivarapatna *et al.*, 2015). Mechanosensitive cell surface membrane molecules such as Notch1/4, integrins and VEGFR respond to shear stress by cytoskeletal reorganization (i.e., through VEGFR-Notch-EphrinB2 signalling or FAK-RhoA-Ras signalling; Zhong *et al.*, 2001; Sivarapatna *et al.*, 2015) and affects downstream intracellular pathways as mentioned in section 1.7.5. Ultimately, this influences the expression of pluripotency maintenance factors, and upregulation of specific differentiation factors.

Stirring speeds have also been used to control the aggregate size of PSC suspension cultures (Abbasalizadeh *et al.*, 2012; Wu *et al.*, 2014) and this is important as specific aggregate sizes

possess an intrinsic bias to differentiate towards certain lineages. Prolonged cultures of larger aggregates with diameters bigger than 300  $\mu\text{m}$  are prone to ineffective mass transfers as diffusion becomes inefficient and can therefore lead to necrotic cores which are highly undesirable (Nogueira et al., 2019).

### **1.10.3.Overall literature summary**

The current therapies for neurodegenerative diseases are unable to offer complete amelioration of the associated neuropathies. hiPSC-derived NPCs are a promising therapeutic alternative. However, current common methods for obtaining hiPSC-derived NPCs by neural induction are incompatible for scale-up strategies which is an essential approach towards commercialisation of NPC-based therapies. Only a few studies so far have worked towards an integrated bioprocess approach using scalable platforms such as STBs. Thus, this thesis aims to contribute towards the process development of an integrated bioprocesses for NPC production from ethically sourced hiPSCs.

### **1.11.Aims and objectives**

The overall aim of this thesis is to develop an integrated bioprocess for the production of hiPSC-derived NPCs using scalable technologies. However, it is important to note, that the aim of this thesis is not to develop a fully cGMP compliant bioprocess, for reasons of budget, time, equipment and infrastructure limitations. Instead, the work completed in this thesis will consider and implement, where possible, standards for clinical production. This approach differs to the work described by Bardy et al. (2013) who also reported an integrated bioprocess for NPC production using Matrigel coated DE53 microcarriers in non-xeno free and antibiotic containing culture systems, which are not compatible for clinical release.

To achieve these aims, specific objectives were set for this project:

1. To establish a baseline bioprocess for the expansion and neural induction of hiPSCs on standard planar platforms.
2. To translate the established baseline integrated bioprocess to suspended culture systems using suitable scalable technologies.
3. To design and develop a bioprocess for the expansion and differentiation of hiPSCs towards NPCs on scalable STB platforms.

## **2. General materials and methods**

### **2.1. Chemical reagents, consumables, and equipment**

A full list of equipment used to carry out this work is provided in Appendix 1. All reagents were purchased from Sigma unless otherwise specified. All reagents and materials used for cell culture (e.g., microcarriers) were sterilised prior to use by either autoclaving at 121°C for 30 minutes or by filtering through a 0.22 µm pore sized filter (Millipore, UK). The water used for preparation of various solutions was obtained from the Elga Purelab water purification system.

### **2.2. Cell lines**

Two hiPSC lines were used, both purchased from Public Health England (UK). The specific details of each hiPSC line are given in Table 2.1. The necessary ethical approvals and a Material Transfer Agreement (MTA) were put in place for their purchase. Cell line HPSI0714i-kute\_4 and HPSI1113i-podx\_1 will be referred to as kiPSC and piPSC respectively, throughout this thesis.

Cord blood CD34<sup>+</sup> derived NPCs (Ax0013) of a healthy new born donor were obtained from Axol Biosciences (Cambridge, UK) and used in these studies as a control cell line.

Table 2.1 Details of the hiPSC lines used in this thesis.

Name given	Cell line	Disease status	Donor sex	Donor ethnicity	Donor age	Tissue of origin	Reprogramming method
kiPSC	HPSI0714i-kute_4	Normal	Female	Caucasian	25-29	skin	Non-integrating virus (sendai)
piPSC	HPSI1113i-podx_1	Normal	Female	Undisclosed	65-69	skin	Non-integrating virus (sendai)

## 2.3. Preparation of cell culture media

### 2.3.1. hiPSC maintenance media

hiPSCs were mainly cultured in either TeSR<sup>TM</sup>-E8<sup>TM</sup> (Stem Cell Technologies, UK) or cGMP-grade mTeSR<sup>TM</sup> Plus (Stem Cell Technologies, UK) with increased FGF stability, which are based, respectively, on the xeno-free E8<sup>TM</sup>, and mTeSR1<sup>TM</sup> formulations. Both medium compositions used are fully defined and serum free. A series of experiments were conducted comparing the mTeSR<sup>TM</sup>- Plus with TeSR<sup>TM</sup>-E8<sup>TM</sup> media.

Both types of media were handled according to the manufacturer's instructions. Both TeSR<sup>TM</sup>-E8<sup>TM</sup> and mTeSR<sup>TM</sup>- Plus were ordered as kits comprising of two parts: a Basal Medium and a supplement. The TeSR<sup>TM</sup>-E8<sup>TM</sup> kit consisted of a 450 mL Basal Medium and a 10X supplement, whilst the mTeSR<sup>TM</sup> Plus kit consisted of a 400 mL Basal Medium and a 5X supplement. The Basal Media was stored in the fridge whilst the supplements were stored in -20°C. For the preparation of the medium, the Basal Medium was warmed for at least 1 hour (h) at room temperature. The respective supplements were thawed at either room temperature or overnight in the fridge at 4°C. Once thawed, it was then immediately supplemented to the Basal Medium to make complete hiPSC maintenance medium. Complete media was stored in the fridge at 4°C for up to 2 weeks. Otherwise, aliquots of complete media were stored in the freezer

at -20°C for up to 6 months. Complete media were thawed and warmed at room temperature when required, and additional freeze thaw cycles were prohibited.

### **2.3.2. Preparation of neural induction media**

Two media compositions were tested for the neural induction of hiPSCs: STEMdiff™ Neural induction Medium (Stem Cell Technologies, UK) and STEMdiff SMADi Neural Induction kit (Stem Cell Technologies, UK) was used which are defined, serum-free media that enables the generation of NP cells from PSC. The neural induction medium can be applied to either hiPSCs aggregate cultures via EB formation or monolayer culture routes. The STEMdiff™- SMADi Neural induction medium was constituted according to the manufacturer's instructions. Briefly, both the basal medium (250 mL) and the STEMdiff™ SMADi neural induction supplement (0.5 mL) were thawed at room temperature and then mixed thoroughly. The complete neural induction medium was then used, or aliquoted and stored in the -20°C freezer for up to 6 months. These neural induction medium compositions direct the differentiation of PSCs towards PAX6, SOX1 and Nestin positive CNS-type NPCs.

## **2.4. Preparation of cell culture substrates**

### **2.4.1. Vitronectin**

hiPSCs were routinely cultured on multi-well plates (Corning, UK) coated with Vitronectin XF™ (VTN; Stem Cell Technologies, UK). A solution of 10 µg/ml VTN was prepared in Cell Adhere Buffer Solution (Stem Cell Technologies, UK). 0.105 mL/cm<sup>2</sup> of VTN solution was used per well in multi-well plates which is the equivalent of 1 mL/well of a 6 well plate. The plates were left to coat inside a biological safety cabinet (BSC) for at least 1 h at room temperature, after which the excess solution was removed, and the surfaces were gently washed

with Cell Adhere Buffer solution once. Coated plates were either used immediately or stored in Cell Adhere Buffer solution up to 1 week in the fridge.

In some cases of neural induction process, higher concentrations of VTN (20 µg/mL) were used at the same 0.105 mL/cm<sup>2</sup> of surface area.

#### **2.4.2. Matrigel**

Matrigel (Corning, UK) polymerizes above 4°C. As a result, it is critical that its handling is carried out at a temperature below that to avoid formation of clumps and an uneven coating. For this reason, pipettes, pipette tips, tubes and plates were cooled for at least 24 h in a -20°C freezer prior to use. Matrigel was aliquoted in batch specific volumes recommended by the manufacturer and stored at -20°C. All pre-cooled necessary materials were then transferred onto an ice bucket placed inside the BSC where all the manipulation of Matrigel was carried out. A Matrigel solution was made in DMEM/F-12 (Corning) to achieve a concentration of 3 mg/mL. Surfaces were then quickly coated with around 0.105 mL/cm<sup>2</sup> of Matrigel solution equivalent to 1 mL per well in a 6 well plate. Plates were left to coat for at least 1 h inside the BSC at room temperature, then gently washed twice with DMEM/F-12 to remove excess Matrigel. Coated plates were either used immediately or stored at 4°C for up to 1 week.

#### **2.4.3. Poly-L-Ornithine and Laminin**

For the maintenance of NPCs, PLO and LN substrates were used to coat multi-well plates. Briefly, 15 µg/mL PLO solution was made in Ca<sup>2+</sup> and Mg<sup>2+</sup> free Dulbecco's phosphate buffered saline (DPBS; Lonza, UK). Multi-well plates were coated with PLO solution at a volume of 0.105 mL/cm<sup>2</sup>. The PLO solution was left to incubate for at least 2 hours at room temperature or overnight in the fridge at 4°C. The PLO solution was then removed, and the surfaces were gently washed twice with DPBS and once with DMEM/F-12. LN was prepared

in DMEM/F-12 to reach a final concentration of 10  $\mu\text{g}/\text{mL}$ , then added to the PLO coated wells at 0.105  $\text{mL}/\text{cm}^2$ . LN solution was left to incubate on the plates for at least 2 h in room temperature or overnight in the fridge at 4°C. LN solution was then removed and washed with DMEM/F-12 three times. Coated plates were used immediately or stored in the fridge with DMEM/F-12 for up to 1 week.

## **2.5.Preparation of cell culture platforms**

### **2.5.1.TCP planar platforms**

hiPSCs were routinely cultured on planar platforms such as 6, 12 and 24 well plates. To support hiPSCs, surfaces were coated with either VTN or Matrigel as per sections 2.4.1 and 2.4.2, respectively.

### **2.5.2.Microcarrier platforms**

Eight commercially available microcarriers were used: Plastic, Plastic Plus, Cytodex 1 Cytodex 3, Collagen, Hillex, Pronectin and Fibronectin. Their characteristics are shown in Chapter 1, Table 1.4. According to the manufacturer's instructions and using the nominal surface area, the weight required to achieve the surface area needed for each experiment was calculated. The microcarriers were weighed using an analytical balance and resuspended in magnesium and calcium free DPBS to achieve a 9.5  $\text{cm}^2/\text{mL}$  stock. The microcarriers were then sterilised by autoclaving at 121°C and 1.5 atm for 15 minutes.

### 2.5.3. Spinner flask platforms

Prior to use, the spinner flasks were siliconized using Sigmacote (Sigma Aldrich, UK) to avoid cell attachment to the glass of the vessel and to only promote cell attachment to the microcarriers. Briefly, 10 mL of Sigmacote solution was pipetted onto the walls of the spinner flask. This step was performed multiple times to ensure full coverage of the glass surface. The remaining Sigmacote solution was then removed, and the spinner flask was left inside the BSC for 5 minutes under the air flow without the top lid to allow evaporation of the remaining Sigmacote. The spinner flask was then disassembled and washed thoroughly with tap water, then left overnight to air dry. Then the spinner flask would be autoclaved at 121°C and 1.5 atm for 15 minutes.

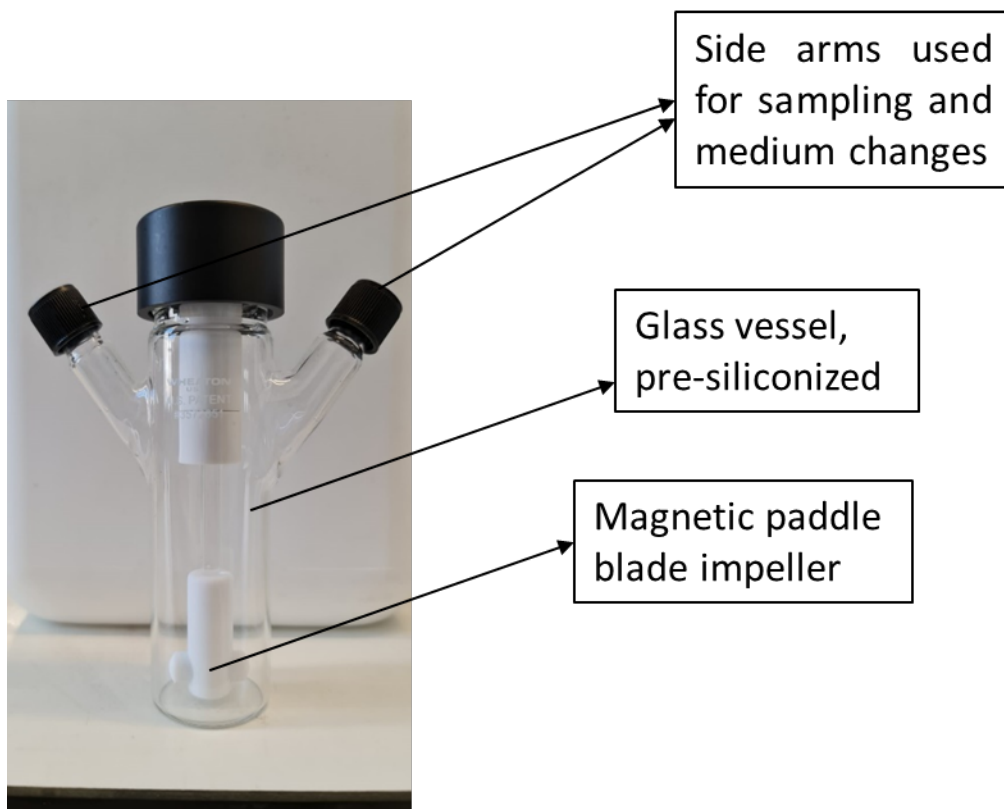


Figure 2.1. Photograph of 50 mL spinner flask (Wheaton). Spinner flask features are labelled

## **2.6. General cell culture procedures**

### **2.6.1. Monolayer cultures of hiPSC on planar platforms**

For the general maintenance of hiPSCs, cells were cultured in TeSR™-E8™ or mTeSR™ Plus media on VTN coated 6 well plates and passaged when cells reached around 80% confluency. hiPSCs were passaged as cell clumps at a split ratio of 1:6. This was performed by firstly washing the cells with Ca<sup>2+</sup> and Mg<sup>2+</sup> free DPBS, then treating the cells with 1 mL/well of 0.5 mM EDTA for 7 min at room temperature inside a BSC. EDTA solution was then removed following incubation and the cells were gently dissociated mechanically by pipetting 3 mL/well of medium. The cell suspension was then split into a ratio of 1:6 per well. The working volume of medium of cultures within multi-well plates was 0.105 mL/cm<sup>2</sup>.

For single cell passaging, cells were pre-treated with 10 µM Y-27632 (Stem Cell Technologies) for 1 h prior to passage. Spent medium was then removed, and the cells were carefully washed once with Ca<sup>2+</sup> and Mg<sup>2+</sup> free DPBS. Cells were then treated with 0.105 mL/cm<sup>2</sup> accutase for 7 min at 37°C inside an incubator. Following treatment with accutase, mechanical dislodgement of the cells from the substrate was achieved by gentle pipetting. After, accutase activity was quenched by diluting 1:5 in DMEM/F-12 containing 10 µM Y-27632 and the cell suspension was centrifuged at 250 g for 5 min to obtain a cell pellet. The supernatant was carefully aspirated and discarded without disturbing the cell pellet. The cell pellet was then resuspended in a known volume of mTeSR™ Plus or TeSR™-E8™ supplemented with 10 µM Y-27632 and counted. hiPSC were seeded at 40,000 cells/cm<sup>2</sup> onto VTN-coated well plates. Daily medium exchanges were performed without Y-27632 supplementation. Cells were routinely monitored under a phase contrast microscope (EVOS, Thermofisher) to visualise cell morphology and colony growth. Well plates were kept at 37°C in a humidified incubator in an air atmosphere supplemented with 5% v/v CO<sub>2</sub>. At day 4 in culture, confluency was achieved as indicated by merging of colonies when cell passage was performed.

### **2.6.2. Suspended aggregate cultures of hiPSCs on planar platforms**

hiPSCs in culture were dissociated from the planar platform substrates either with 0.5 mM EDTA for clump inoculations or accutase for single cell inoculations, similarly to the passaging method described in section 2.6.1. However, for aggregate cultures, following the dissociation and resuspension steps in section 2.6.1, cells were instead seeded onto ultra-low attachment well plates (ULA; Corning, UK) supplemented with or without 10  $\mu$ M Y-27632. Daily medium exchanges were performed by carefully tilting the plates about 45° to its side and leaving the plate undisturbed for at least 5 min to allow the cell aggregates to deposit into a corner of the well. With care, 80% of the spent medium was removed, as not to aspirate the suspended aggregates. An equal volume of fresh medium was then added. Aggregates were routinely monitored under a phase contrast microscope to visualise aggregate morphology and size.

### **2.6.3. Monolayer cultures of hiPSC on microcarrier platforms in static conditions**

For cultures of hiPSC as monolayers on microcarriers under static conditions, microcarriers were firstly prepared as per section 2.5.2. After sterilisation, some of the microcarriers were coated with VTN. For this, 1 mL of sterile microcarriers from the stock were transferred to 1.5 mL microcentrifuge tubes (Eppendorf). Two washes of the microcarriers were performed. To perform washes, the microcarriers were settled for at least 5 min and then 500  $\mu$ L of the excess solution was removed ensuring not to aspirate the settled microcarriers. Then, 500  $\mu$ L of washing buffer (in this case Cell adhere buffer solution) was added, ensuring to mix gently the microcarriers. At the last wash, 500  $\mu$ L of solution was removed and replaced with 500  $\mu$ L of 20  $\mu$ g/mL VTN solution to make a final concentration of 10  $\mu$ g/mL VTN. The tubes containing microcarriers in the VTN solution were then housed inside 50 mL Falcon tubes and placed on

a roller mixer (Stuart) to promote a homogenous coating. Microcarriers were left overnight at room temperature to coat. Following the coating, microcarriers were washed twice with DMEM/F-12 and once with mTeSR™ Plus containing 10 µM Y-27632. At the final wash 500 µL of excess solution was removed and replaced with 500 µL of mTeSR™ Plus containing 10 µM Y-27632. This created coated microcarriers solution of 9.5 cm<sup>3</sup>/mL in mTeSR™ Plus supplemented with 10 µM Y-27632. From this, 3 cm<sup>2</sup> (320 µL) of microcarrier surface area was calculated and transferred to wells of 24 ULA well plates. This provides an available microcarrier surface area of 3 cm<sup>2</sup>/well. 3 cm<sup>2</sup> per well of a 24 well plate was chosen as this was the observed suitable concentration of microcarriers to completely cover the surface area of the well in a homogenous fashion with minimal stacking of microcarriers, thus allowing for visualisation using microscopy techniques throughout the culture.

For single cell inoculation onto the microcarriers, cultures of hiPSCs were passaged with accutase and 4 x 10<sup>4</sup> cells/microcarrier surface area were subsequently seeded into the wells (i.e., 1.2 x10<sup>5</sup> cells/well). The working volumes of the wells were then made up to 500 µL with mTeSR™ Plus supplemented with 10 µM Y-27632. 50% daily medium exchanges were performed without Y-27632 in the medium. 50 µL samples for nutrient and metabolite analysis were taken from the discard during medium exchange and from the culture system after medium exchange.

#### **2.6.4. Monolayer cultures of hiPSC on microcarrier platforms in dynamic conditions**

For the cultures of suspended hiPSC-laden microcarriers on planar platforms, under dynamic conditions, the plates and microcarriers were prepared similarly to that in section 2.6.3. Here, instead, the plates were placed on a rocking platform (Stuart, UK) set at 30 rotations per minute

(RPM) and installed inside a humidified incubator at 37°C with 5% CO<sub>2</sub>. Monitoring of the cells were performed the same as static conditions.

#### **2.6.5. Microcarrier culture in agitated conditions in spinner flasks**

Spinner flask were prepared as per section 2.5.3 and an image of the spinner flask used in this thesis is shown in Figure 2.1. Photograph of 50 mL spinner flask (Wheaton). Spinner flask features are labelled . Microcarriers were prepared as per section 2.5.2, with the exception that the stock microcarrier concentration was instead made to 10 cm<sup>2</sup>/mL in DPBS. To coat the microcarriers, 10 mL of the 10 cm<sup>2</sup>/mL stock microcarrier mixture was transferred to a 15 mL centrifuge tube and allowed to settle to the bottom for at least 10 min due to the volume of microcarriers inside a BSC. 8 mL of the excess DPBS was removed and replaced with Cell Adhere Buffer solution. The mixture was then made to 10 µg/mL of VTN in 10 mL of Cell Adhere Buffer solution and microcarrier mixture. The tube was then placed on a roller mixer overnight at room temperature. Following coating, microcarriers were washed with Cell Adhere Buffer solution twice and then once with DMEM/F-12. VTN-coated microcarriers were then resuspended into a total volume of 10 mL of mTeSR<sup>TM</sup> Plus containing 10 µg/mL Y-27632 and transferred into an already prepared spinner flask. The spinner flask and microcarriers were then conditioned for at least 30 min inside a humidified incubator at 37°C and 5% CO<sub>2</sub>, on a magnetic platform set to stir at 30 RPM. To allow for gases to equilibrate the culture system within the spinner flasks, one of the side arm screw caps were unscrewed by 1 and a half turns, ensuring to keep the cap on and not compromising the sterility of the system. After conditioning, spinner flask culture systems were then inoculated with cells through the side arms and made up to the working volume. Inoculated cells at day 0 were cultured in medium containing 10 µg/mL Y-27632 which was then removed from the medium for the following daily medium exchanges. Medium exchange was only achievable by carefully

removing the spinner flask lid along with the impeller and aspirating the spent medium directly from the top. This was due to the configuration of the side arms being unable to fit the standard pipettes. Nevertheless, addition of fresh medium could be performed using the side arms. Daily monitoring of the cultures were performed by taking samples for visual assessment using phase contrast microscopy, cell counts, pH, glucose and lactate readings. Live/Dead staining was also performed on certain days to visually assess the growth of the cells on microcarriers.

#### **2.6.6. Cell harvest from microcarriers in ULA well plates platforms**

For cultures of hiPSCs on microcarriers in ULA multi-well plates, cells were harvested using accutase and separated from the microcarriers using 100 µm cell strainers (Appleton Woods, UK). Briefly this involved, treating the cells with 10 µM Y-27632 1h prior to harvest. The medium was removed from the wells carefully without disturbing the microcarrier/cells. Microcarriers were then washed twice with Ca<sup>2+</sup> and Mg<sup>2+</sup> free DPBS and then cells were incubated in accutase for 7 min at 37°C inside an incubator. Afterwards, DMEM/F-12 containing 10 µM Y-27632 was added into each well to dilute the accutase activity by 1:4, whilst pipetting up and down several times to mechanically dislodge the cells from the microcarriers. Cell and microcarrier suspensions were then filtered through a 100 µm cell strainers and further washed with extra DMEM/F-12 containing 10 µM Y-27632 to harvest potentially trapped cells. Here, cells pass through the pores of the strainer whilst microcarriers are retained. The cell suspension collected in 50 mL falcon tubes was then centrifuged at 250 g for 5 min to obtain a cell pellet and the supernatant removed. The pellet was then resuspended in hiPSC maintenance medium containing 10 µM Y-27632 in a known volume and cell counts are performed.

### **2.6.7. Cell harvest from microcarriers in spinner flask platforms**

On the day of spinner flask harvest, cells within the spinner flasks were treated with 10 mM Y-27632 1 h prior to harvest. First, the side caps of the spinner flask were tightened. Spinner flasks were then removed from the magnetic platform inside the incubator and transferred into a BSC. The main cap was then carefully loosened ensuring that it remains covering the culture within the vessel of the spinner flasks. The microcarriers were settled to the bottom of the vessel by leaving the spinner flask undisturbed for at least 5 min or until the microcarriers are no longer visibly floating. Spinner flasks were not left outside the incubator longer than 15 min. Once the microcarriers have settled, the main cap was gently removed, along with the impeller, without disturbing the microcarriers. 80% of the medium is then aspirated and replaced with  $\text{Ca}^{2+}$  and  $\text{Mg}^{2+}$  free DPBS. The spinner flask main cap was then returned in place and the spinner flask was transferred back onto a magnetic platform within a 37°C humidified incubator. Once inside the incubator, one of the lids of the side arms was loosed 1 and a half turns and the magnetic platform was set at 40 RPM for 5 min to wash the cells. This washing step was repeated twice. After the second wash, as much of the wash solution was removed and 10 mL of accutase was added. The spinner flasks were then returned inside the incubators onto the magnetic platforms and set at 150 RPM for 10 min to dislodge the cells from the microcarriers. Following incubation with accutase, spinner flasks were transferred into the BSC and a 10 mL stripette was used to pipette the culture up and down, to further assist the dislodgement of cells from the microcarriers. 40 mL DMEM/F-12 was then added to dilute the accutase activity. The contents of the spinner flasks were then filtered using a 100  $\mu\text{m}$  cell strainer to separate the microcarriers from the cells. Cells were collected in the flow through into a 50 mL falcon tube which were subsequently spin down at 250 g for 5 min using a centrifuge. As much of the supernatant was aspirated whilst ensuring the pelleted cells were

undisturbed. Cell pellets were then resuspended in a known volume of mTeSR<sup>TM</sup> Plus medium supplemented with 10  $\mu$ M Y-27632.

### **2.6.8. Cell storage and thawing**

hiPSCs were stored in a cryopreservation media composed of 10% Dimethyl sulfoxide (DMSO) in mTeSR<sup>TM</sup> Plus or TeSR<sup>TM</sup>-E8<sup>TM</sup>. Cryovials containing cells were carefully recovered from liquid nitrogen and quickly transferred to a 37°C pre-set water bath until only a small lump of ice could be seen. Working under aseptic conditions, 1 mL of pre warmed DMEM/F-12 media was transferred dropwise, directly onto the cell solution, to avoid osmotic shock. The 2 mL cell suspension was further transferred dropwise into 8 mL of pre-warmed DMEM /F-12. Cell suspension was then centrifuged at 250 g for 5 min to obtain a cell pellet. Cells were then resuspended in a known volume of mTeSR<sup>TM</sup> Plus containing 10  $\mu$ M Y-27632 and counted using Nucleocounter NC-3000 (Chemometec; detailed in section. 2.7.1

## **2.7. Analytical techniques**

### **2.7.1. Cell counting**

Cell counts were performed using the Nucleocounter NC-3000 (Chemometec). For cell counting directly onto microcarriers the manufacturer's reagent A100 and reagent B protocol was used. Briefly, the cell-microcarrier suspension was diluted in a 1:3 ratio with reagent A100 (lysing agent) and then reagent B (stabilizing agent). The resulting suspension was then loaded onto a Via-1 Nucleocassette containing acridine orange and DAPI and placed in the Nucleocounter. This protocol has been successfully used before to count cells directly on microcarriers (Hanga *et al.*, 2020, 2021).

To determine the cell density of the resuspended cells, homogenous samples of cell solution (~200 µL) were taken and placed into microcentrifuge tubes. Before sampling, the microcentrifuge tubes were briefly vortexed to ensure homogeneity and the samples were loaded onto a Vial-Cassette™ then analysed using a Nucleocounter NC-3000 following a Viability and Cell count Assay protocol. This analysis provided cell count, viability, cell diameter, and aggregation information.

Solution 13 containing acridine orange and DAPI in conjunction with NC-slide A2™ and/or NC-slide A8™ was also used following a preadjusted “Viability and Cell count Assay” protocol. Similarly, this provided cell count, viability, cell diameter and aggregation information.

### **2.7.2. Live/dead staining for viability assessment**

Cell viability/cytotoxicity was assessed by using the Live/Dead Viability/Cytotoxicity kit for mammalian cells (Thermofisher, UK). This kit allows for simultaneous visualisation of live and dead cells. This is particularly useful for microcarrier culture especially when using opaque microcarriers such as Plastic or Plastic Plus that don't allow cell visualisation when using phase contrast microscopy. The Live/dead staining kit uses fluorescent probes that measure recognized parameters of cell viability and plasma membrane integrity. Live cells are distinguished by the presence of ubiquitous intracellular esterase activity. In live cells, the virtually non-fluorescent calcein-AM which is cell permeant is converted enzymatically to the intensely fluorescent calcein, thus showing live cells in green fluorescence channel (Excitation ~495 nm; Emission ~515 nm). Dead or damaged cells will appear in the red fluorescence channel (Excitation ~ 495 nm; Emission ~ 635 nm) when stained with ethidium homodimer-1 (EthD-1). This dye is excluded by the live cells with intact membranes, and it will only enter

the cells with damaged membranes when it will undergo a 40-fold enhancement of fluorescence upon binding to nucleic acids. Background fluorescence levels are inherently low with this assay because the dyes are virtually non-fluorescent before interacting with cells. However, some background fluorescence is registered when staining cells on microcarriers.

Fresh solutions were prepared for each staining. In 10 mL of sterile Ca<sup>2+</sup> and Mg<sup>2+</sup> free DPBS, 20 µL of the supplied 2 mM EthD-1 stock solution were first added and mixed to achieve a working concentration of 4 µM EthD-1. In the same solution, 5 µL of the supplied 4 mM calcein-AM stock solution were added to achieve a working concentration of 2 µM calcein-AM. The working solution was then added directly to the samples and incubated at 37°C for 40 minutes in the dark. The samples were then visualized on a fluorescence microscope (EVOS M5000, Thermofisher, UK).

### **2.7.3. Metabolic analysis**

Spent medium samples were collected before and after medium exchanges and analysed for glucose and lactate concentrations on a handheld, point-of-care device (AccuTrend Plus meter; Roche). Positive control strips and parameter recognition were used for calibration. Briefly, a drop of spent medium was carefully added to the pre-loaded test strip. Lactate analysis was carried out in 60 s, while glucose analysis in 10 s. Fresh growth medium was used as a baseline control.

### **2.7.4. Immunocytochemistry staining for marker assessment**

For the general immunocytochemistry (ICC) staining procedures, cells were fixed for 15 min with 4% v/v paraformaldehyde (PFA) at room temperature. The PFA solution is then removed, and the cells washed 3 times with DPBS. Fixed cells were then permeabilised for 5 min using Perm Wash (Biolegend, UK) followed by 2 further washes with DPBS and a final wash with cell staining buffer (Biolegend, UK). The fixed cells were then incubated in normal serum

block (Biolegend, UK) for 45 min in the dark. Afterwards, a maximum of two primary (i.e., for co-staining) antibodies were added and left to incubate in the dark overnight in the fridge at four degrees (see **Table 2.2**). The primary antibody solution was then removed, and the wells washed thoroughly 3 times with cell staining buffer. When necessary, secondary antibodies were then added and left to incubate for at least 2 hours at room temperature in the dark by covering the plates with foil. Following incubation, wells were again washed 3 times with cell staining buffer and the cells were then incubated with 300 mM working solution of DAPI for 5 min at room temperature, to stain for nuclei. DAPI solution was then removed, and the wells washed 3 times with cell staining buffer. Stained cells were then imaged using a fluorescent microscope and stored in cell staining buffer.

To assess for non-specific immunoreactivity of secondary antibodies, cells were fixed as above, and stained with secondary antibody only for 45 min in the dark. DAPI was then used to visualise cell nuclei. An example is shown in Figure 2.2. All secondary antibodies were tested at least N=1 and no immunoreactivity was observed.

Table 2.2. List of primary and secondary antibodies used for ICC experiments.

<b>Antibody</b>	<b>Expres sion</b>	<b>Species (Primary)</b>	<b>Dilution (Primary)</b>	<b>Secondary Antibody</b>	<b>Dilution (Second ary)</b>
<b>OCT4 (ThermoFi sher Scientific)</b>	Pluripot ency Marker	Rabbit	1:200	Alexa Fluor™ 594 Donkey Anti-Rabbit	1:250
<b>SOX2 (ThermoFi sher Scientific)</b>	Pluripot ency Marker	Rat	1:100	Alexa Fluor™ 488 Donkey Anti-Rat	1:250
<b>SSEA4 (ThermoFi sher Scientific)</b>	Pluripot ency Marker	Mouse	1:100	488 Goat Anti-Mouse IgG3	1:250
<b>TRA-1-60 (ThermoFi sher Scientific)</b>	Pluripot ency Marker	Mouse	1:100	Alexa Fluor™ 555 Goat Anti-Mouse IgM	1:250
<b>Pax 6 (Biolegend)</b>	Neural precurs or marker	Rabbit	1:100	Alex Fluor™ 488 Donkey Anti-rabbit IgG	1:100
<b>Nestin (Biolegend)</b>	Neural precurs or marker	Mouse	1:100	Alexa Fluor™- 647 Goat Anti-Mouse IgG	1:100
<b>SOX1 (R&amp;D Systems)</b>	Ectoder m	Goat	1:10	*conjugated NL493	N/A
<b>Otx-2 (R&amp;D Systems)</b>	Ectoder m	Goat	1:10	*Conjugated NL557	N/A
<b>Brachyury (R&amp;D Systems)</b>	Mesode rm	Goat	1:10	*Conjugated NL557	N/A
<b>HAND1 (R&amp;D Systems)</b>	Mesode rm	Goat	1:10	*Conjugated NL637	N/A
<b>GATA-4 (R&amp;D Systems)</b>	Endode rm	Goat	1:10	*Conjugated NL493	N/A
<b>SOX17 (R&amp;D Systems)</b>	Endode rm	Goat	1:10	*Conjugated NL637	N/A

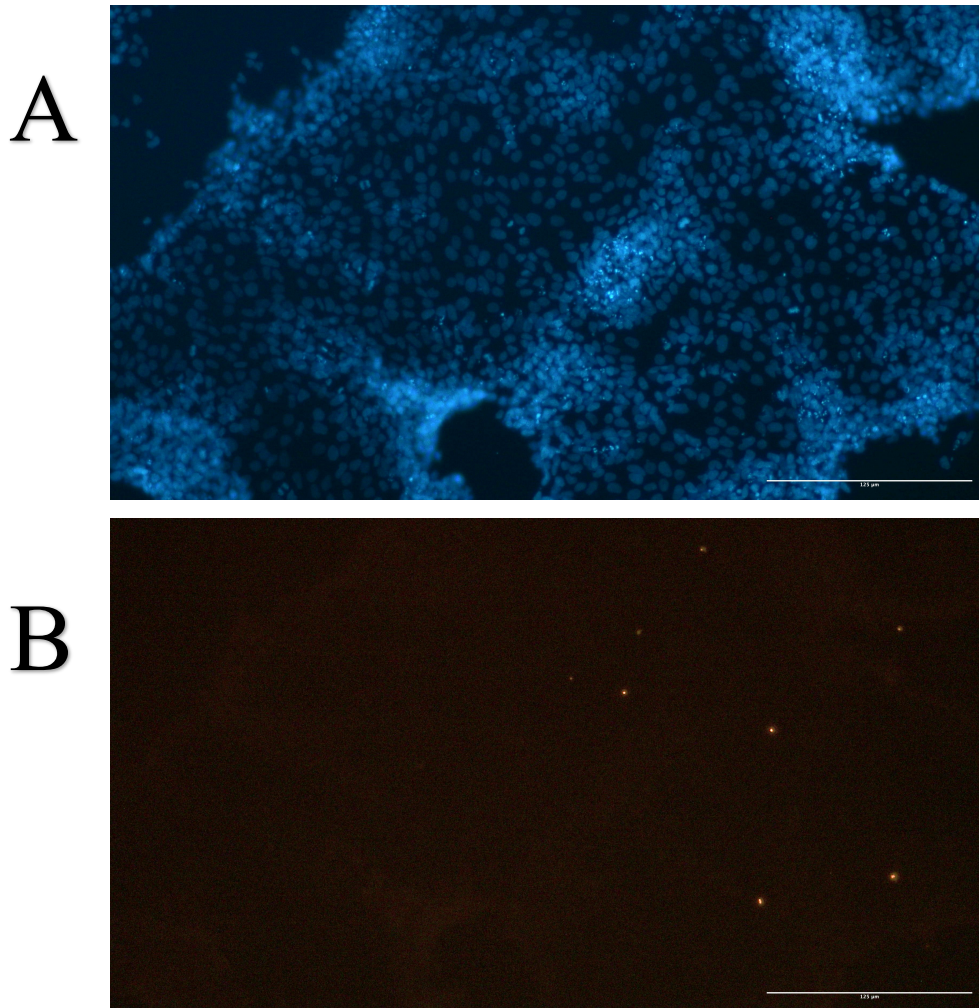


Figure 2.2. Illustrative example of control for secondary antibodies to assess for non-specific binding. Cells were stained with DAPI and secondary antibody only. In this example, kiPSCs were cultured for 4 days, fixed and stained with DAPI (A) and Alexa Fluor<sup>TM</sup> 594 Donkey Anti-Rabbit (B).

### **2.7.5. Trilineage differentiation of hiPSCs**

To assess for the differentiation potential of hiPSCs, cells were passaged from the culture systems and seeded as single cells on 24 well plates coated with 20 µg/mL VTN at 0.105 mL/cm<sup>2</sup>. Cells were seeded at different seeding densities depending on lineage commitment of the differentiation. For ectodermal and endodermal lineage commitment, hiPSCs were seeded at 2 x 10<sup>5</sup> cells/cm<sup>2</sup> and cultured in PSC maintenance media containing 10 µM Y-27632 for the first 24 h. Afterwards, the medium was exchange to either StemDiff trilineage Ectoderm Medium for ectodermal commitment, or StemDiff trilineage Endoderm medium for endoderm lineage. For mesodermal lineage differentiation, hiPSCs were seeded at 5 x 10<sup>4</sup> cells/cm<sup>2</sup> in PSC maintenance medium with 10 µM Y-27632 for the first 24 h and then changed to StemDiff trilineage mesoderm medium. Medium exchanges were performed daily. Cultures were differentiated for 5 days towards endodermal and mesodermal lineages, whilst ectodermal lineage differentiation took 7 days.

### **2.7.6. Scanning electron microscope imaging**

Scanning electron microscope imaging was used to assess the surface morphology of uncoated and coated microcarriers. Microcarriers were prepared and coated and given to a trained technician to acquire SEM images.

### **2.7.7. Quantification by Image J analysis**

The cell marker expression assessed qualitatively by immunocytochemistry staining was then quantified by Image J analysis. Image J is a public, free, Java-based image processing program. Images were obtained in separate fluorescent channel, as well as merged. The blue channel images obtained for DAPI staining of the nuclei were used to obtain total cell counts, whilst

nuclei stain with specific markers using green or red fluorescent channels were used to manually count the number of cells that positively expressed the assessed marker. The positive expression percentage was then calculated using the following formula:

$$\% \text{marker expression} = \frac{\text{number of positive cells}}{\text{total number of cells}} \times 100 \quad [\text{eq. 1}]$$

Briefly, the acquired images were imported into Image J software. Images were then converted to 8-bit greyscale. The threshold was then adjusted so that all stained areas were clearly visible. Images were then converted to binary. The software allows manual corrections if not all nuclei were fully filled. In some cases, particularly when cells are at a high level of confluency, the nuclei can touch each other. For a more accurate counting in such a case, watershed functions were applied to automatically separate the borders of the nuclei to be counted. The software also allowed for manual corrections if the automatic function of watershed wasn't satisfactory. Binary images were then analysed to count stained areas with specific size ranging from 5-50 $\mu\text{m}$  and circularity of  $>0.5$ . This analysis technique was used to quantitate the positively stained nucleus for nuclear proteins such as OCT4, SOX2 and PAX6. To count the total number of cells, DAPI positive stained cells were also counted. The counts were then exported to an Excel spread sheet and equation 1 was used to determine marker expression. Prism 9 was used to determine statistical analysis as outlined in section 2.9. At least 2 images per well per biological repeat was used for analysis.

## **2.8.Engineering characterisation of bioreactors**

### **2.8.1.Mixing studies**

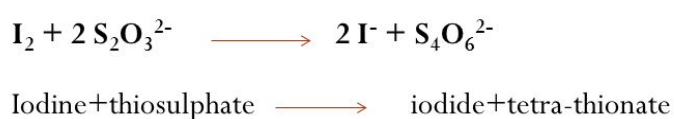
It is widely recognised that the performance of a bioreactor depends largely on the mixing characteristics (Bailey and Ollis 1986; Kawase and Moo-Young, 1989; Nienow 2006). Mixing

times are useful for indicating the length of time of inhomogeneities as the mixing time denotes the time required for the vessel to achieve homogeneity following a tracer pulse. They can also be used to characterise the flow and mixing within the vessel, and identify the extent of potential concentration gradients and dead zones (Hadjiev, Sabiri and Zanati, 2006).

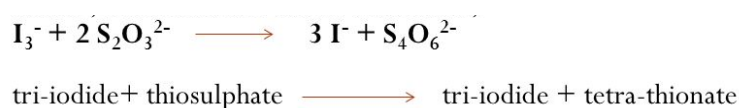
The mixing characteristics of a bioreactor can be quantified by determining the mixing time has which is defined as the time necessary to achieve a specified degree of homogeneity in a mixed liquid after a tracer pulse has been added. Mixing time is dependent on the:

- ✓ working volume;
- ✓ impeller type;
- ✓ agitation speed.

To determine the  $t_m$  in a bioreactor, a decolourisation indicator reaction technique can be used. The reaction between sodium thiosulfate ( $\text{Na}_2\text{S}_2\text{O}_3$ ) and iodine ( $\text{I}_2$ ) in the presence of starch is the most satisfactory decolourization reaction, with a strong colour change from deep blue to clear. Sodium thiosulfate ( $\text{Na}_2\text{S}_2\text{O}_3$ ) is used as a reducing agent in redox titration of iodine. The reaction between iodine and sodium thiosulfate is:



Since iodine ( $\text{I}_2$ ) is present as a tri-iodide ( $\text{I}_3^-$ ) in aqueous solutions containing iodide, the reaction can also be written as:



Initially a 2M iodine solution was prepared by dissolving 400 g of iodate-free potassium iodide in 0.5 L of distilled water. To this solution, 254 g of iodine was added and agitated until all the

iodine has dissolved, then cooled to room temperature and stored in the dark to prevent deterioration. Iodine is insoluble in water. However, it can be solubilised in a potassium iodide solution due to the formation of the soluble potassium tri-iodide. Then a 1M solution of sodium thiosulfate was prepared by dissolving 248 g of sodium thiosulfate pentahydrate in 1 L of distilled water. In parallel, the starch indicator was prepared by making a thick paste containing 10 g of soluble starch in a small volume of distilled water. This paste was then added dropwise to 1 L of boiling water while stirring constantly until a clear liquid was obtained. The starch indicator solution was then cooled to the ambient temperature and 20 g of potassium iodide were added. This solution was then used immediately or prepared fresh on the day of the experiments.

To determine the mixing time, 18 mL of distilled water was added to the spinner flask with 2 mL of the starch indicator solution. Iodine solution (100  $\mu$ L) was then added for a dark blue starch-iodine complex to form. When sodium thiosulfate ( $\sim$ 200  $\mu$ L) was added, the complex was reduced resulting in decolourisation of the solution. After adding the sodium thiosulfate solution, the time was measured until the intense blue colour disappeared completely and that represented the mixing time( $t_m$ ).

## **2.9. Statistical analysis**

All cell culture experiments on well plates were performed in triplicate wells as a minimum, unless otherwise stated; this is considered the technical replicates. Biological repeats (N numbers) are considered biologically independent when the cells have been revived and sourced from different starting vials. Cell counts for each timepoint were acquired using two independent samples from each technical replicate. Data was expressed as mean  $\pm$  SD. Statistical analysis was carried out using the GraphPad Prism v9 software. For comparison

between two data sets, statistical significance was determined by using the Student's two-tailed t-test. For comparison of more than two data sets, significance was calculated by the one-way or two-way ANOVA, with either Tukey's or Sidak's multiple comparison test. Significance was determined at  $p \leq 0.05$ .

## 2.10. Other equations used

Based on the cell counts performed, the following parameters were calculated:

Specific growth rate

$$\mu = \frac{\ln(Cx(t)/Cx(0))}{\Delta t} \quad [\text{eq. 2}],$$

Doubling time

$$DT = \frac{\ln 2}{\mu} \quad [\text{eq. 3}],$$

Fold increase

$$FI = \frac{Cx(t)}{Cx(0)} \quad [\text{eq. 4}],$$

Where:  $\mu$  is the specific growth rate ( $\text{h}^{-1}$ );

$t_d$  is doubling time (h);

FI is fold increase,

$Cx(t)$  and  $Cx(0)$  represent cell numbers at the end and start of the exponential growth;

$t$  represents time in culture (h).

### **3. Establishing a baseline integrated bioprocess for the production of hiPSC-derived NPCs on planar platform**

#### **3.1.Introduction**

The current available drug-based treatments for neurodegenerative diseases fail to completely ameliorate the pathologies leading to neuronal death and the clinical deterioration of patients. NPCs are a promising therapeutic alternative for neurodegenerative diseases. The widespread application of NPCs as commercially available treatments, however, is hindered by several challenges. For one, the field of NPC-based therapies are relatively still immature with many unknown mechanisms and effects that still need to be investigated. Secondly, there is lack of feasible bioprocessing strategies for the generation of clinically relevant quantities of NPCs.

hiPSCs are potentially an unlimited source for NPCs (Nagoshi and Okano, 2018b; Galiakberova and Dashinimaev, 2020b). Thus, accessibility to an abundance of hiPSCs would contribute significantly towards realising NPC-based therapies. Current methods for generating and expanding hiPSCs typically rely on in vitro culture systems using planar platforms. Similarly, neural induction processes are usually conducted on planar platforms. Essentially, an ideal process workflow would consist of firstly the propagation of hiPSCs to achieve enough cells, followed by neural induction, to then commit the hiPSCs towards the neural lineage. This approach considers that some NPCs like primitive NP cells cannot proliferate indefinitely and, therefore, propagation is limited once the hiPSC have been differentiated. However, such processes carried out on planar platforms like TCP multi-well plates or T-flasks are impractical for achieving the required cell quantities of cell-based therapies at a commercial scale (>trillions of cells).

The path towards commercially available hiPSC -derived NPCs is dependent on large-scale bioprocesses capable of producing sufficient quantities to appease material demand as stated in Chapter 1 of this thesis. To establish such bioprocesses, bioprocess development is necessary; this involves identifying specific process parameters to robustly produce the desired yield and quality/purity of a bioproduct, which in this case are NPCs. The first step in bioprocess development is to establish a baseline bioprocess. Therefore, with consideration of the overall thesis aim, it was imperative to firstly establish a robust baseline bioprocess for obtaining hiPSC-derived NPCs using planar platforms. The processes established in this chapter will later be used as the base model to be translated to scalable platforms and eventually implemented into dynamic scalable culture systems.

### **3.1.1. Establishing the baseline bioprocess**

For the baseline bioprocess, two independent key processes were identified: the expansion of hiPSCs and the neural induction process to commit the cells towards the neural lineage. Essentially, the process would involve with hiPSCs as the starting material whilst NPCs are the end-product. Compared to other bioprocesses for cell-based production (i.e., hMSCs production), whereby, the starting material and the end-product are the same cell type, the bioprocess in this case contains added complexities as two different cell types (hiPSC and NPCs) will need to be considered and at different stages of the bioprocess.

#### **3.1.1.1. hiPSC baseline expansion bioprocess**

The first step was to establish a baseline bioprocess for the expansion of hiPSCs; the literature was reviewed, and suitable culture components were identified for in vitro maintenance of HiPSCs. rh-VTN was identified as a suitable substrate for hiPSC as it is xeno-free and defined

which can stimulate the appropriate CAMs to maintain hiPSC CQAs such as pluripotency and self-renewal (Parr *et al.*, 2016; Sara M Badenes *et al.*, 2016; Fan *et al.*, 2017). In combination with TeSR™-E8™ medium, a xeno-free and defined culture system would be offered for the maintenance of hiPSCs on planar platforms (Chen *et al.*, 2011; Wang *et al.*, 2013). Therefore, as a starting point, the TeSR™-E8™ / VTN culture system was deemed suitable for hiPSC culture.

After identifying a suitable culture system, it was imperative to determine the quality of hiPSC within the designed culture systems. Several techniques are usually employed to assess the quality of hiPSCs in culture including cell and colony morphology, pluripotency markers and functional assays such as differentiation towards the three-germ layers: endoderm, ectoderm and mesoderm.

Here, optimisation of the expansion culture system was also performed to efficiently expand hiPSCs with regards to time and costs, as these can have a significant impact later on when translating to scalable culture systems or larger scale. Critical culture factors such as cell seeding density, culture duration, medium compositions and feeding regimes were explored to assess their effect on the growth and quality of hiPSCs. Following these experiments, an optimised culture system on planar platforms and expansion process was obtained.

### **3.1.1.2. hiPSC expansion and differentiation - baseline integrated bioprocess**

Once the optimised culture system was obtained, it was then important to assess whether the hiPSCs cultured in such culture systems could be differentiated towards the target cell type: NPCs. For the neural induction bioprocess, it was identified that hiPSCs would require differentiation cues such as morphogens and inhibitors to drive neural commitment (Cohen *et al.*, 2007; Chambers *et al.*, 2009; Morizane *et al.*, 2011). These cues could be delivered through

the media. After market research, commercially available formulations from StemCell Technologies were identified to be suitable for driving neural commitment towards “predominantly” CNS-like NP cells. Because the neural induction process cannot assure 100% conversion of hiPSC to CNS-like NP cells, and subpopulations of NSCs or more naïve NP cells could arise, the collective term for both NSC and NP cell populations will be used in this chapter (i.e., neural precursor cells or NPCs) to describe the derived cell populations from the neural induction process using the StemCell Technologies neural induction medium.

Most differentiation protocols of neural induction (including StemCell Technologies’) require the replating of PSCs onto a new culture vessel (e.g., onto new multi-well plates at day 0 of neural induction) to initiate neural induction (Gunther, 2016; Nagoshi and Okano, 2018c; Pauly *et al.*, 2018). Implementing the re-plating methods at large-scale manufacturing may be laborious, complex, and risks introducing contamination or error, especially when employing closed system platforms such as bioreactors. Therefore, an integrated bioprocess where the expansion of hiPSCs and their differentiation towards NPCs, within a single culture vessel, could potentially mitigate the aforementioned problems at large scale production. Thus, here, it was tested whether the baseline bioprocess for the differentiation of hiPSC towards NPCs could be integrated with the optimised expansion bioprocess to create a single planar platform-based bioprocess for NPC production.

### 3.1.2. Chapter aims and objectives

The overall aim of this chapter is to establish an integrated bioprocess on planar platforms, starting from the expansion of hiPSCs and ending at the point of NPC derivation by neural induction. To realise this aim, several objectives were set:

1. To determine the quality and growth characteristics of two available hiPSC lines (kiPSC and piPSC) when propagated in the TeSR™-E8™ / VTN culture system. This will provide the baseline quality and quantity of cells when expanded in such processes on planar platforms. Quality assessment is also necessary to distinguish if cell lines possess unwanted properties (e.g., slow growth, or spontaneous differentiation) that would make them unsuitable for further process development work.
2. To optimise the baseline expansion process for hiPSC on planar platforms with respect to investigating the effects of medium composition and feeding regimes on cell growth, cell quality and the process cost. This will enable the utilisation of a cost-effective and efficient process for expanding hiPSCs and will be considered the optimised expansion process.
3. To develop an integrated bioprocess on planar platforms which incorporates two processes: (1) the optimised expansion process for hiPSCs and (2) the differentiation process of hiPSCs towards NPCs via neural induction.

## **3.2.Results**

### **3.2.1.Quality assessment of hiPSC lines in TeSR™-E8™ / VTN culture systems**

By adapting StemCell Technologies' protocol for the culture of hiPSCs, a suitable culture system and procedures for culturing hiPSCs on 2D static planar platforms was identified. This consisted of employing standard TCP multi-well plates coated with xeno-free rh-VTN substrates, along with the xeno-free and defined TeSR™-E8™ medium. Together they offer a xeno-free and defined culture system (TeSR™-E8™ / VTN) for the maintenance of hiPSCs. hiPSCs were dissociated from the culture substrates using chemically defined 5 mM ethylenediamine tetra-acetic acid (EDTA) to propagate the cells through passaging as cell clumps.

To determine the quality of the two hiPSC lines when cultured using the EDTA procedure as and the TeSR™- E8™ culture system, the cell and colony morphologies, pluripotency marker expression, and differentiation capacity of the cells were assessed and are reported in the following sections.

### 3.2.1.1. Morphological assessment of kiPSC and piPSC

First, both cell lines were adapted to the culture system by culturing the cells in the TeSR™-E8™ / VTN culture system for at least 2 passages using clump passaging method following revival from cryovials. The morphologies of the cells and colonies in culture were qualitatively assessed by phase contrast microscopy and compared to typical morphologies of human PSC cultures. Both kiPSCs and piPSCs lines were capable of proliferating within the culture system as more surface area of the culture platform were occupied by cells as the culture duration progressed. Cell clumps from initial seeding eventually formed large colonies with clearly defined borders (Figure 3.1): a typical characteristic of hiPSC colonies. Cells from both cell lines displayed epithelial-like morphologies with visible and large nucleoli depicted by dark spots within the cytoplasm. Small floating cell debris were also observed, especially at later stages of the culture. Cell debris were removed with each medium exchange but would be seen to accumulate again as cultures progressed.

Differences in cell and colony morphologies were noticeable between the two cell lines. Colonies formed by kiPSCs were densely packed at the centre with comparatively spikier border edges. In comparison, piPSCs displayed rounder colony border edges of tightly packed rounder cell morphologies.

Notably, a higher degree of spontaneous differentiation was identified in piPSC cultures, as indicated by cells surrounding the colonies with distinguishably larger cytoplasm to nucleus ratio, and a more fibroblastic morphology as shown by the arrows in Figure 3.1. Due to the identification of spontaneously differentiated cells amongst the piPSC line, a decision to remove the differentiated population was made. To isolate the hiPSCs from differentiated cells, piPSC cultures were passaged with ReLeSR™ (StemCell Technologies). ReLeSR™ is an agent which specifically detaches the hiPSC population from a substrate whilst leaving the

spontaneously differentiated population attached. StemCell Technologies' protocol for ReLeSR™ was used.

Up to 3 serial passaging with ReLeSR™ was required to eliminate most of the differentiated cells. kiPSC required no treatment with ReLeSR™ as no spontaneous differentiation could be observed when culturing these cells at early passage numbers 10-14 (cells were bought in at passage 10). In comparison, the passage number of piPSC used in this assessment was above 40, since the cells were only available at an already late passage number of 37.

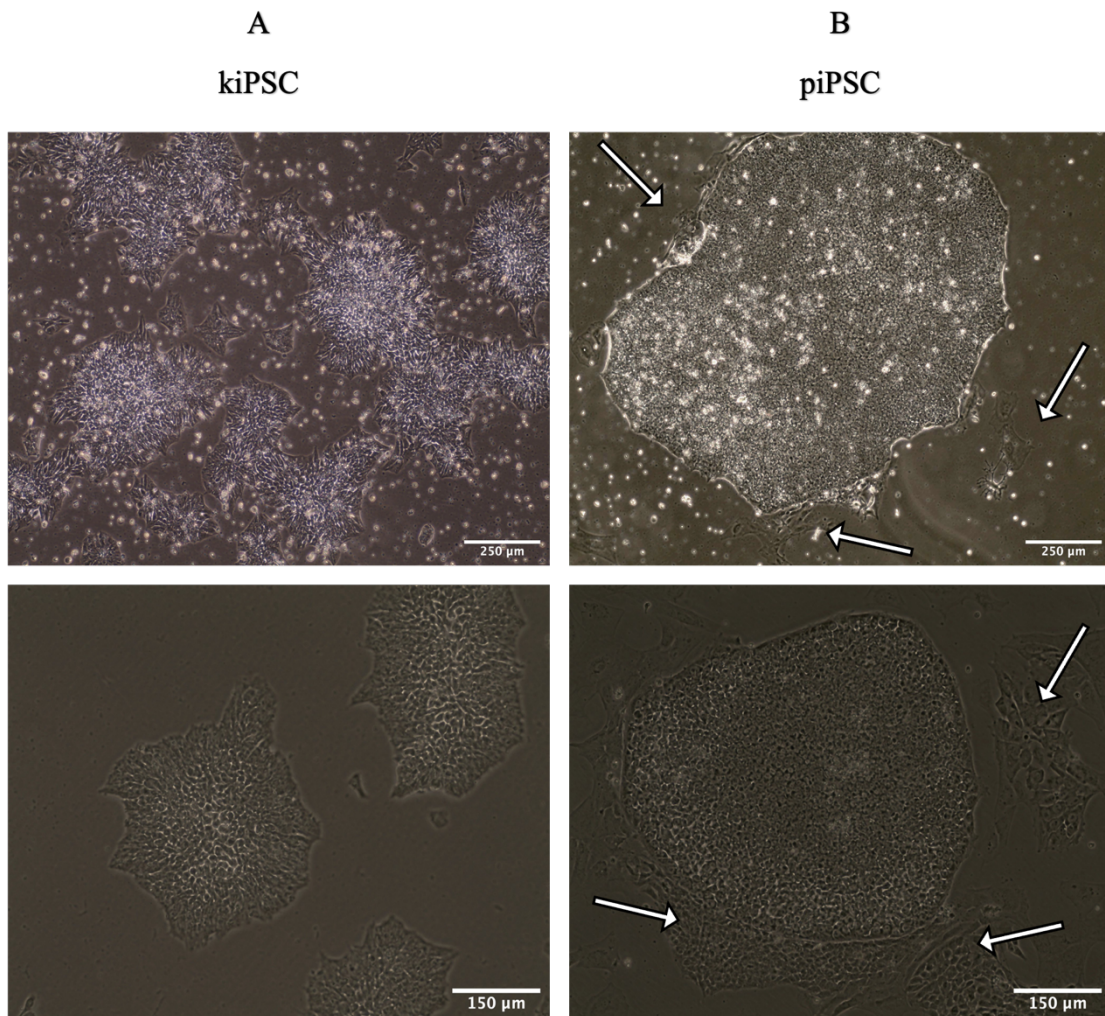


Figure 3.1. Representative phase contrast images of hiPSC colonies in TeSR™-E8™ / VTN culture systems. Phase contrast images of kiPSCs (A) and piPSCs (B) colonies showing colony morphology differences and levels of spontaneous differentiation. kiPSCs cultures systems were imaged between passage 10 and 14. piPSCs were used between passages 40 to 44. Cells were passaged at 60-80% confluency at a 1:6 split ratio using EDTA. Images were taken at day 4 of cultures after passage. N=4, biological repeats.

### 3.2.1.2.Pluripotency assessment of kiPSC and piPSC lines

After removal of the differentiated cells from hiPSCs cultures by ReleSR™, it was important to check the quality of the hiPSC lines by assessing for their expression of pluripotency markers. Using clump passaging method as mentioned earlier, cells were expanded for 120 h in the TeSR™-E8™ / VTN culture system, then fixed and prepared for ICC. Cells were assessed for the presence of nuclear factors of pluripotency: OCT4 and SOX2. Similarly, the presence of cell surface markers indicative of pluripotency was evaluated: TRA1-60 and SSEA4. Cells within the population of the kiPSC and piPSC line displayed OCT4 and SOX2 localised in the nuclei as indicated by their correlation with the DAPI<sup>+</sup> nuclei staining. kiPSC and piPSCs were also positive for the cell surface markers SSEA4 and TRA-1-60 as shown in Figure 3.2 (A-D).

However, not all DAPI positive cells were stained for OCT4 or SOX2 in both hiPSC lines. After image analysis to determine the number of DAPI<sup>+</sup> cells compared to OCT4<sup>+</sup> cells, it was calculated that  $59.93 \pm 11.98$  % of the cells were OCT4<sup>+</sup> in piPSC cultures whilst kiPSC was calculated at  $64.64 \pm 4.01$ % (no significant difference; Figure 3.3 E). Additionally, it was calculated that  $74.06 \pm 20.65$  % of the cells in piPSC cultures were positive for SOX2 whilst kiPSC cultures were similar at  $75.50 \pm 15.22$  % (Figure 3.2E). In general, no significant difference was found between the two cell lines in terms of detectable pluripotency markers regardless of the morphological difference seen in Figure 3.1.

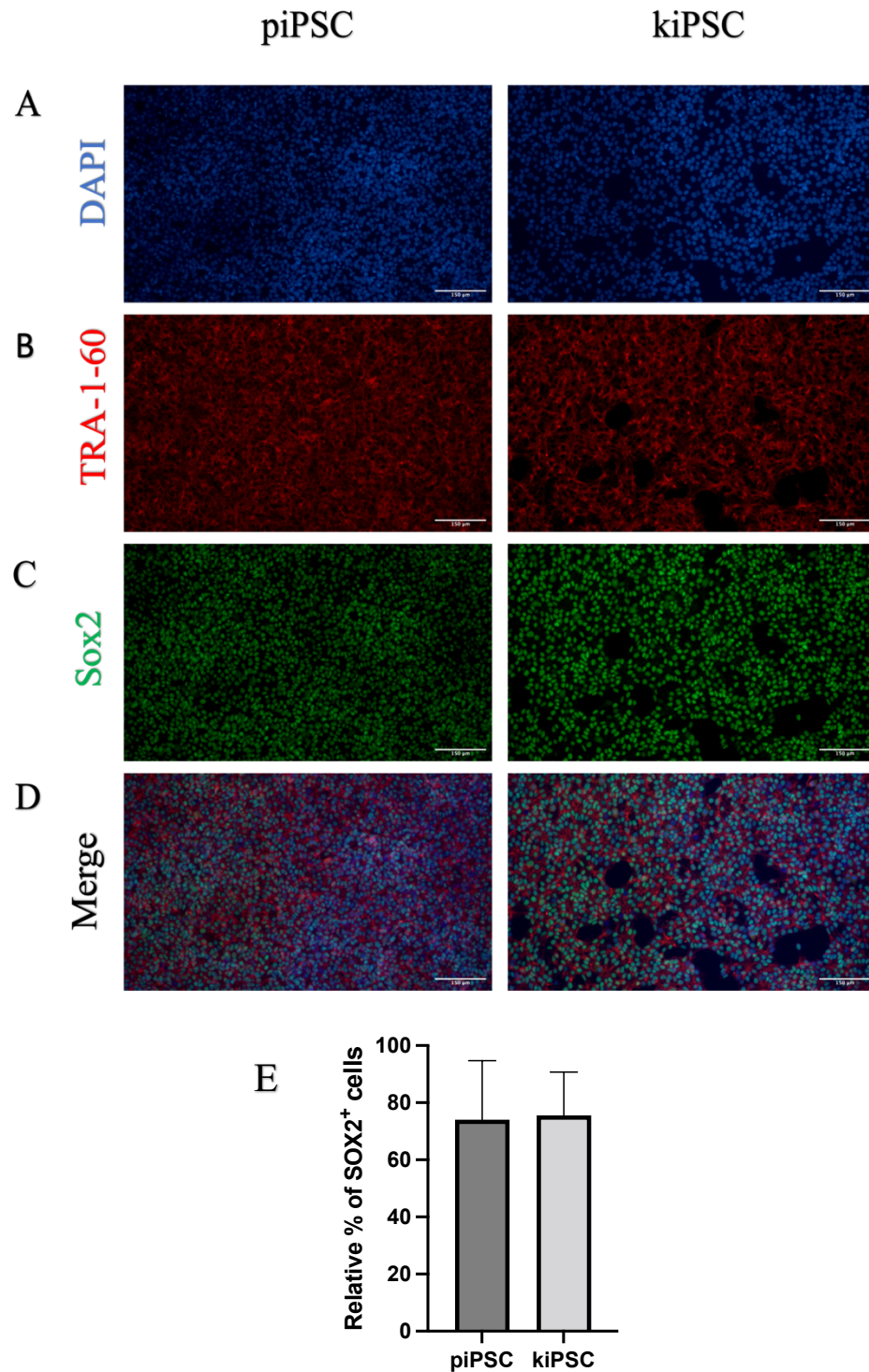


Figure 3.2. Assessment of piPSCs and kiPSCs for the presence of SOX2 and TRA-1-60 markers when cultured on VTN and TeSR™- E8™ culture system. ICC was performed to assess the expression of pluripotency markers after 120 h in culture. (A) Nuclei was stained with DAPI (Blue). Pluripotency markers TRA-1-60 (B; red) and SOX2 (C: Green). (D) Merged image of A, B and C. Scale bar: 100  $\mu$ m. The percentage OCT4+ cells were calculated relative to DAPI+ cells shown in (E) as mean  $\pm$  SD. N=3, biological repeats.

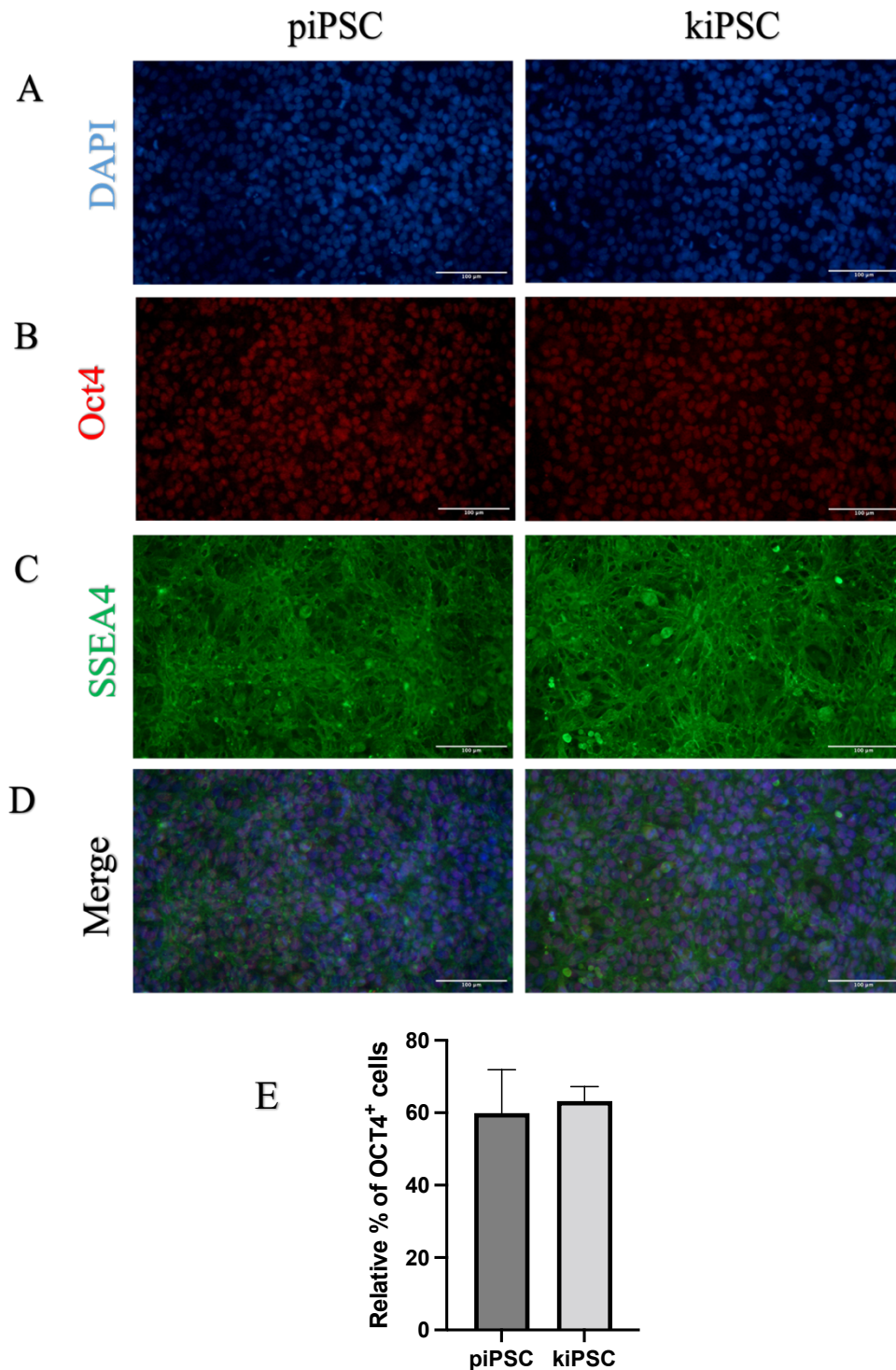


Figure 3.3. Assessment of piPSCs and kiPSCs for the presence of SSEA4 and OCT4 markers when cultured on VTN and TeSR™- E8™ culture system. ICC was performed to assess the presence of pluripotency markers after 120 h in culture. Nuclei was stained with DAPI (A; Blue). Pluripotency markers OCT4 (B; Red) and SSEA4 (C; Green) were detected. (D) Merged image of A, B and C. Scale bar = 100  $\mu$ m. The percentage SOX2<sup>+</sup> cells were calculated relative to DAPI<sup>+</sup> cells shown in (E) as mean  $\pm$  SD. N=3, biological repeats.

### **3.2.1.3. Trilineage differentiation assessment of kiPSC and piPSC**

Another assay to test the potency of the hiPSC lines is the trilineage differentiation assay. This assesses the potency of the cell lines to differentiate towards the three germ layers to confirm pluripotency which are: endoderm, mesoderm and ectoderm lineages.

The initial trilineage differentiation experiments were performed according to StemCell Technologies protocol, with modification of the substrate used. Instead of using Matrigel, the differentiation of kiPSC and piPSCs were attempted on 1.05  $\mu\text{g}/\text{cm}^2$  VTN coated 24 well plates, since these replicated the conditions of which the cells are expanded in.

Phase contrast microscopy of hiPSCs plated for trilineage differentiation assays were visibly observed to attach onto the substrate within 24 h of seeding. However, when cells reached around 72 h – 120 h in the trilineage differentiation medium, cells would detach from the substrate and cell death was indicated by noticeable floating cells and debris, especially for STEMdiff™ Trilineage Mesoderm Medium (appendix 1). Cells which remained attached became confluent causing formation of cell sheets. These cell sheets were very sensitive to culture manipulations such as medium exchanges and would often detach. This was seen in most trilineage differentiation assays attempted regardless of using either piPSC or kiPSC cell line.

Therefore, the differentiation protocol was adjusted and hiPSCs were differentiated on increased VTN concentration of 2.10  $\mu\text{g}/\text{cm}^2$  to help support attachment and reduce cell detachment. Cells were able to attach onto the substrate, proliferate and survive when incubated with differentiation medium for the duration of the experiment. Detection of fluorescence showed that cells from both hiPSC lines were only partially positive for endoderm markers SOX17 and Gata4, mesoderm marker brachyury and ectoderm marker Otx2, since DAPI positive cells clearly indicated that not all cells expressed these lineage specific nuclear

markers. Additionally, the mesoderm marker HAND1 and the ectoderm marker SOX1 were not detected in either cell lines.

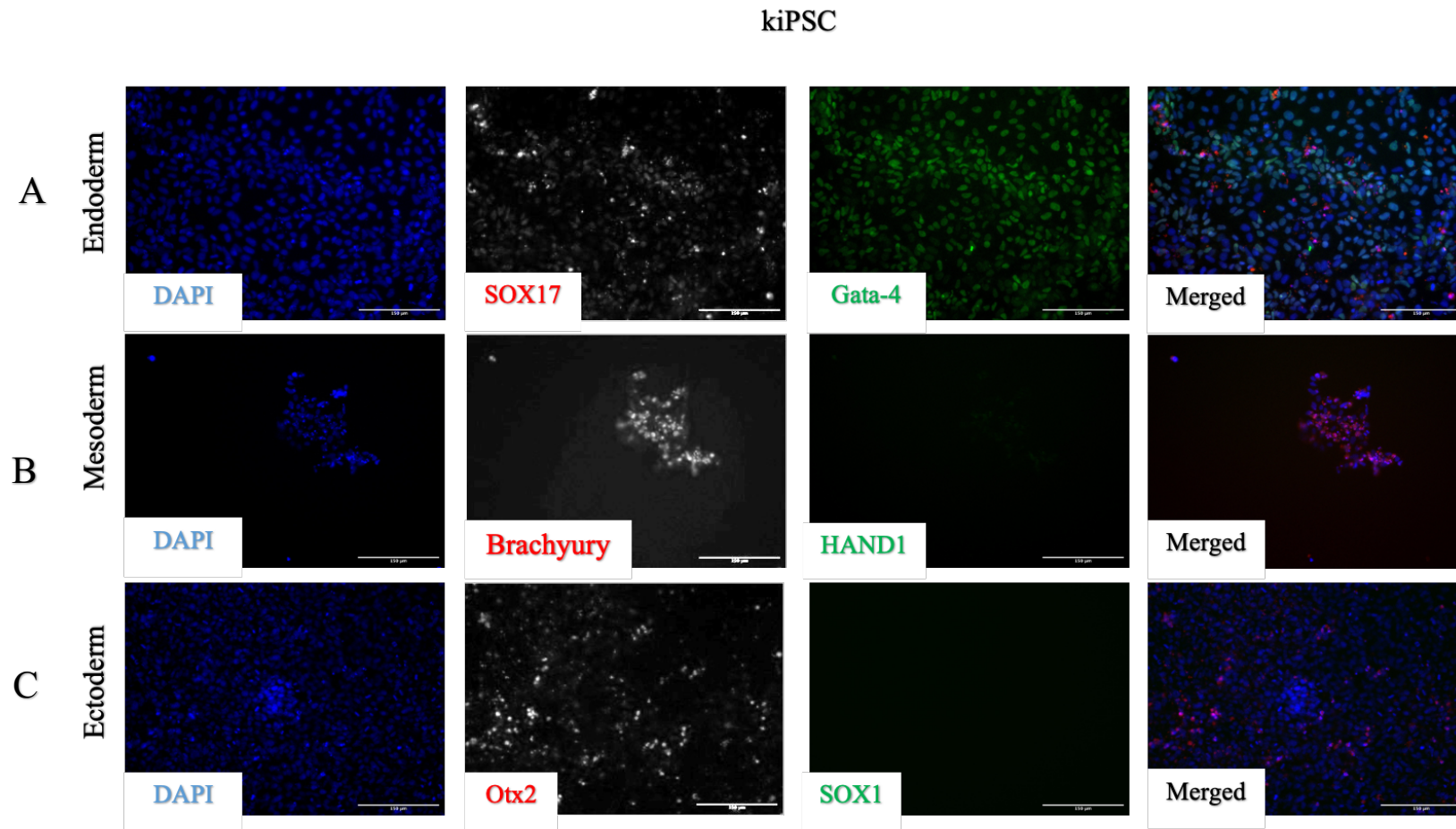


Figure 3.4. Trilineage assessment of kiPSC after culturing in TeSR™-E8™ / VTN culture systems. kiPSCs were directed to differentiate towards endoderm for 5 d (A), mesoderm for 5 d (B) and ectoderm (C) for 7 d by culturing in specific differentiation medium. Cells were then fixed and prepared for ICC. 2 Random areas of the wells were imaged under a fluorescence microscope to detect for endoderm markers (SOX17 and Gata4), mesoderm markers (Brachyury and HAND1) and ectoderm markers (Otx2 and SOX1). Nuclei was stained with DAPI (blue) and the images obtained from the red, green and blue channels were merged. N=2, biological repeats. Scale bar =150 µm.

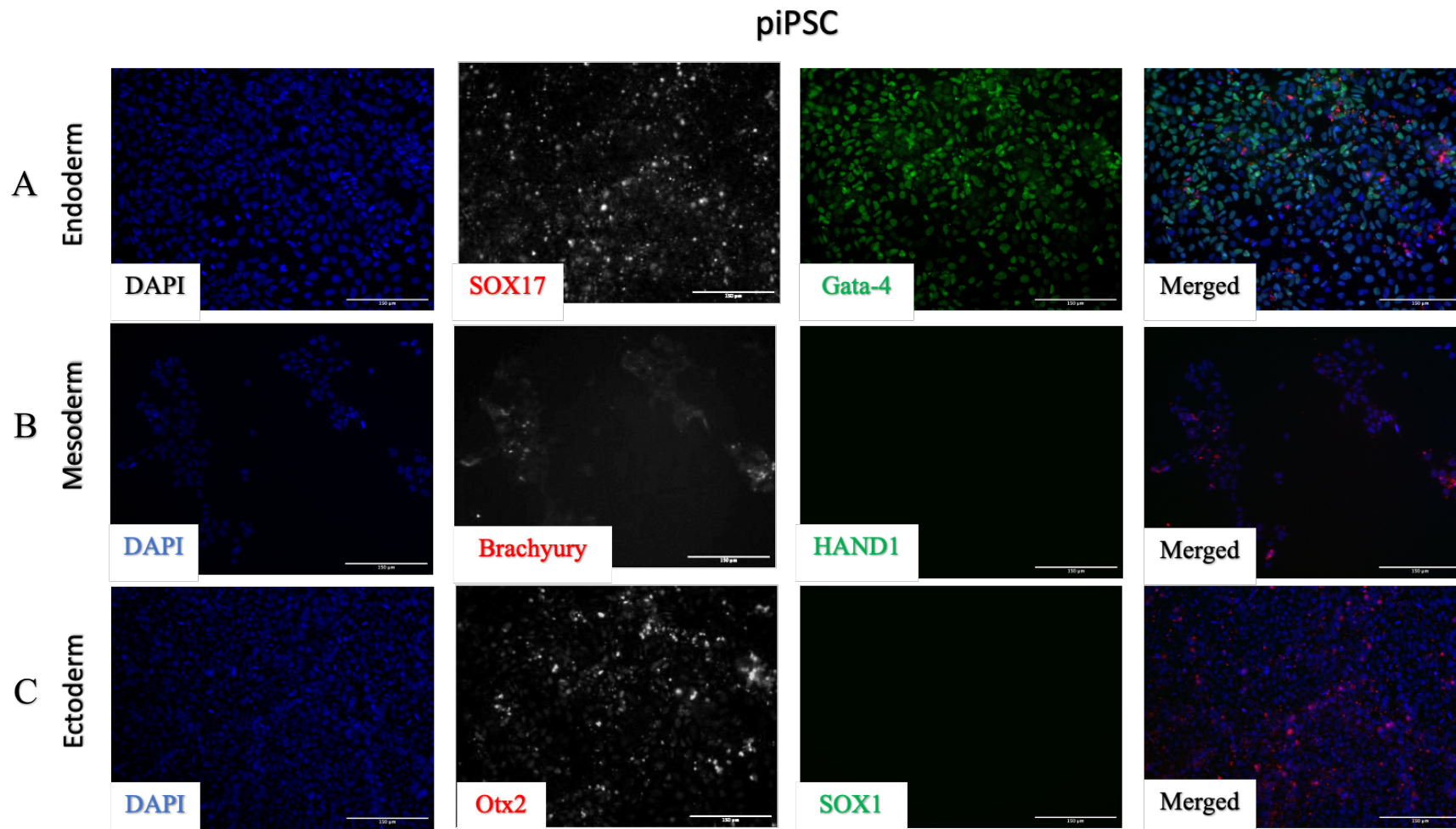


Figure 3.5. Trilineage assessment of piPSC after culturing in TeSR<sup>TM</sup>-E8<sup>TM</sup> / VTN culture systems. piPSCs were directed to differentiate towards endoderm for 5 d (**A**), mesoderm for 5 d (**B**) and ectoderm (**C**) for 7 d by culturing in specific differentiation medium. Cells were then fixed and prepared for ICC. 2 Random areas of the wells were imaged under a fluorescence microscope to detect for endoderm markers (SOX17 and Gata), mesoderm markers (Brachyury and HAND1) and ectoderm markers (Otx2 and SOX1). Nuclei was stained with DAPI (blue) and the images obtained from the red, green and blue channels were merged. N=2, biological repeats. Scale bar =150 µm.

### **3.2.2. Growth characteristics of kiPSC and piPSC in TeSR™-E8™ / VTN culture system**

Initial comparative studies of best practises for single cell passaging were also explored. It was clear that single cell passaging with accutase required the supplementation of Y-27632 for 24 h post passage to ensure cell survival as cells failed to form aggregates 24 h post single cell inoculation (Figure 3.6).

To determine the growth characteristics of the cell lines, cells were seeded at  $2 \times 10^4$ ,  $4 \times 10^4$  and  $6 \times 10^4$  cells/cm<sup>2</sup> in triplicate wells of 12 well plates coated with VTN. Cells were seeded as single cells, as previously mentioned, to determine the viable cell number (VCN) seeding density more accurately on the Nucleocounter 3000. A daily 100% medium exchange (1 mL) was performed every 24 h to replenish the nutrients and remove metabolic waste. 3 wells per condition were sacrificed and harvested every 24 h to be obtain two independent cell counts per well. This provided data at each harvest timepoint, up to 120 h in culture, of the cell viability, VCN, specific growth rates (SPGR), doubling time (DT) and fold increase (FI). These data were then compared between the two cell lines at each seeding density condition (Figure 3.7 and 3.8).

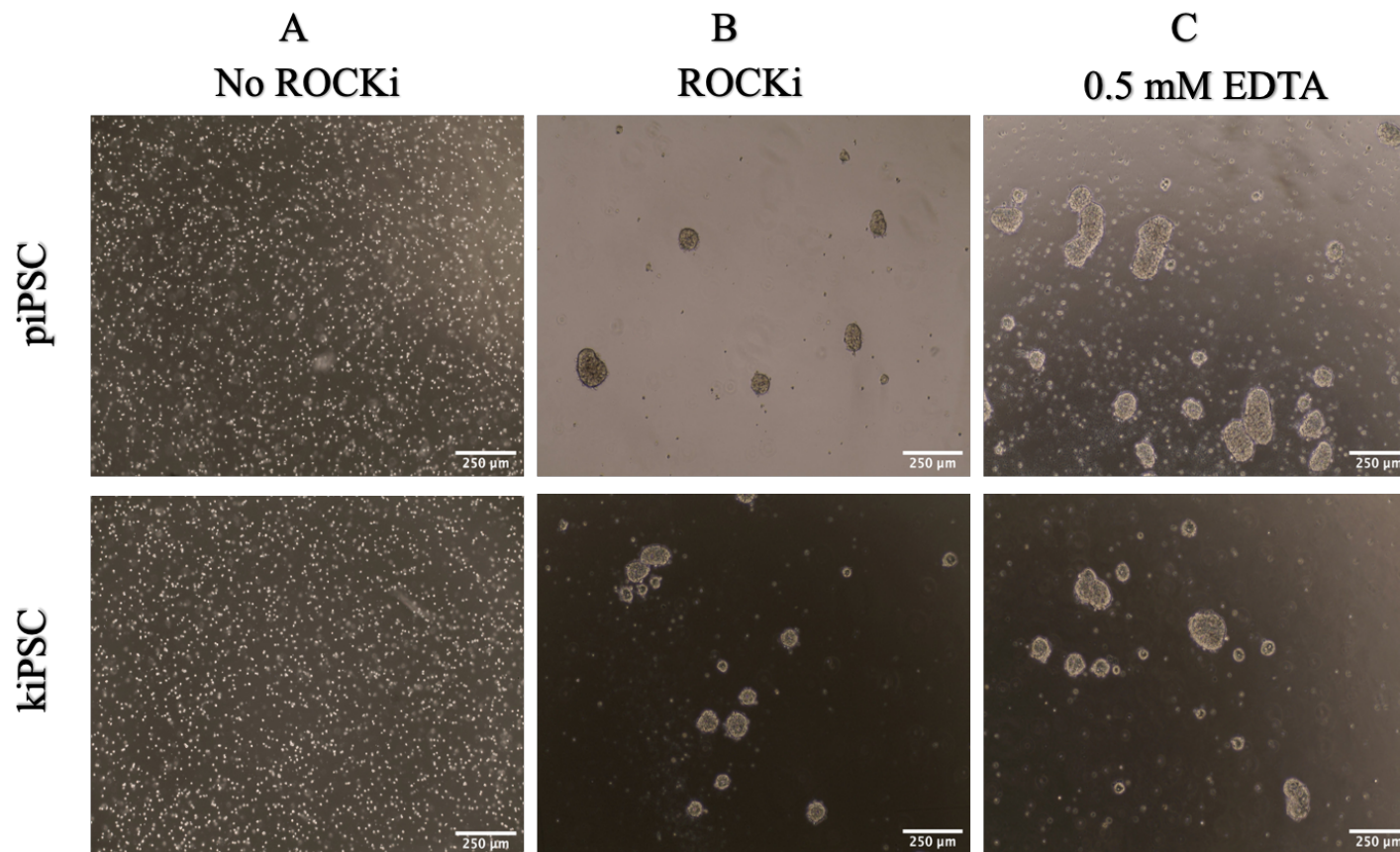


Figure 3.6. Representative images of kiPSC cells passaged with different techniques. A) shows images of kiPSCs passaged using accutase after 24 h without ROCKi. B) shows the formation of aggregates 24 h after passaging with Accutase and treating with Y-276321. C) is the control EDTA passage method showing aggregation of cells. kiPSCs were unable to form cell aggregates without Y-2776321 supplementation for the first 24 h following single cell dissociation. N=3, biological repeats.

### 3.2.2.1. Cell viability of hiPSC lines in TeSR™-E8™/VTN culture system

Cell viability of kiPSCs and piPSCs in the TeSR™-E8™ and VTN culture system was obtained at different timepoints of the culture, and the data shown in Note, that the cell viability criteria to initially seed the cells for these experiments (at 0 h timepoint) was set at >80 % across all conditions (Figure 3.7)

Both kiPSCs and piPSCs seeded at  $2 \times 10^4$  cells/cm<sup>2</sup> were shown to decrease in cell viability after 24 h to  $55.66 \pm 8.73\%$  and  $54.73 \pm 5.10\%$ , respectively, following harvesting from the plates as single cells (Figure 3.7). Although, no significant difference in cell viability between the two cell lines, this is a considerable drop from the initial cell viability at the point of seeding.

In comparison, cultures seeded at either  $4$  or  $6 \times 10^4$  cells/cm<sup>2</sup> and harvested after 24 h in the culture system, recorded higher cell viability (>60%). In particular, kiPSCs seeded at  $4 \times 10^4$  cells/cm<sup>2</sup> showed significantly higher viability ( $p = 0.038$ ) 24 h after compared to that of piPSC seeded at the same density. No other significant differences were observed between the two cell lines under any other seeding condition at the 24 h harvest point.

After 48 h in culture, the cell viability of kiPSC and piPSC cultures increased to > 84% under all conditions. At this time point, no significant difference was detected between the two cell lines under any seeding condition. This high viability (>84%) was maintained by all cultures for the duration of the culture period.

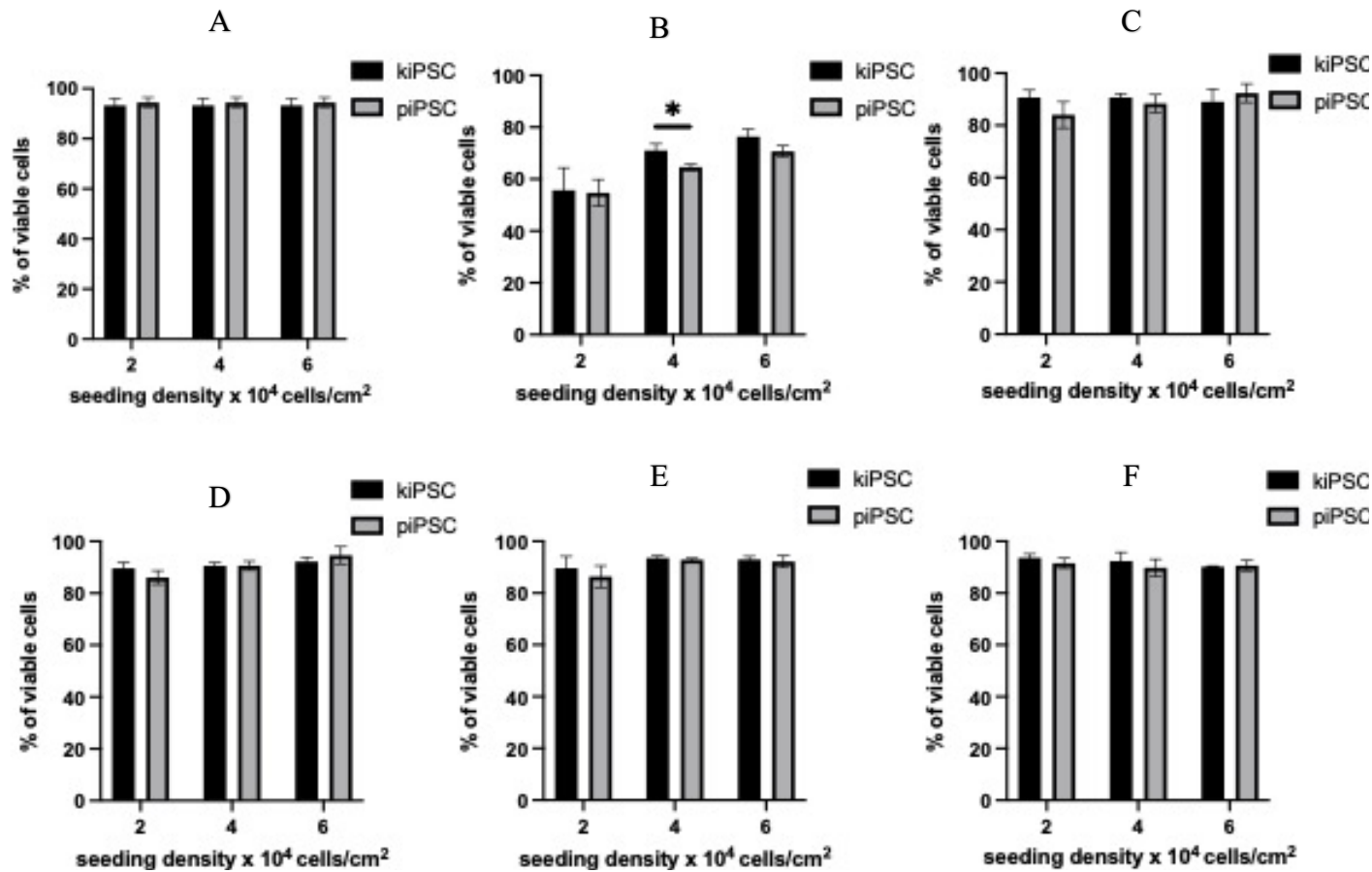


Figure 3.7. Measured cell viability of kiPSC and piPSC cell lines when seeded at different seeding densities and cultured over 120 h. Cells were seeded at 3 different seeding densities: 2, 4 and 6 x 10<sup>4</sup> cells/cm<sup>2</sup>. After seeding at 0 h (A), cells were harvested from culture every 24 h to determine cell viability at different timepoints: 24 h (B), 48 h (C), 72 h (D), 96 h (E) and 120 h (F). Measurements were taken from the average of triplicate wells. Data presented as mean ± SD. N=3, biological repeats \*p ≤ 0.05, multiple unpaired T- test.

### 3.2.2.2. Viability and growth kinetics hiPSC lines in TeSR™-E8™/VTN culture system

VCNs were obtained every 24 h up to 120 h in culture (Figure 3.8). The initial number of cells seeded at 0 h for  $2 \times 10^4$ ,  $4 \times 10^4$  and  $6 \times 10^4$  cells/cm<sup>2</sup> conditions, were  $7.8 \times 10^4$ ,  $1.56 \times 10^5$ , and  $2.34 \times 10^5$  VCN, respectively, in 12 well plates (3.9 cm<sup>2</sup>/well surface area).

After 24 h, piPSC and kiPSC seeded at  $2 \times 10^4$  cells/cm<sup>2</sup> reduced in VCN by >80 % to  $1.4 \pm 0.16 \times 10^4$  and  $1.79 \pm 0.72 \times 10^4$  VCN, respectively (Figure 1.). Such a large decrease in VCN was not observed in cultures of either hiPSC lines seeded at  $4 \times 10^4$  or  $6 \times 10^4$  cells/cm<sup>2</sup> conditions; instead, for example, the VCN of piPSC and kiPSC seeded at  $4 \times 10^4$  cells/cm<sup>2</sup> were comparable to the initial seeding VCN at  $1.37 \pm 0.15 \times 10^5$  cells and  $1.53 \pm 0.16 \times 10^5$  VCN, respectively, after 24 h in culture (Figure 3.8 E and I). DT could not be calculated from the VCN data obtained at 0 h to 24 h, since cells did not increase in VCN compared to the seeding VCN, under any condition.

After 48 h in culture, piPSCs seeded at  $2 \times 10^4$  cells/cm<sup>2</sup> were counted at  $1.62 \pm 0.13 \times 10^5$  VCN whilst kiPSC cultures of the same condition yielded significantly more VCN at  $2.58 \pm 0.22 \times 10^5$  ( $p = 0.027$ ; Figure 3.8). The calculated DT after 48 h in culture was significantly larger for piPSCs at  $45.80 \pm 4.87$  h compared to  $27.93 \pm 1.91$  h for kiPSCs ( $p = 0.004$ ; Figure 3.8)

For culture conditions at  $> 4 \times 10^4$  cells/cm<sup>2</sup> initial seeding density of both hiPSCs line, no significant difference was observed in terms of DT and FI, which were calculated to range from ~23 – 28 h and ~3 – 4 times, respectively, after 48 h in culture.

After 72 h in culture, both cell lines under all conditions were highly proliferative in all seeding conditions with DTs between  $\sim 20 - 25$  h; the shortest DT recorded was for kiPSC cultures seeded at  $4 \times 10^4$  cells/cm<sup>2</sup> (DT =  $20.70 \pm 0.66$  h). No significant difference in the growth characteristics of the hiPSC lines were observed at this timepoint.

After 96 h of culture, however, kiPSCs seeded at  $4 \times 10^4$  cells/cm<sup>2</sup> yielded significantly larger VCN ( $2.60 \pm 0.19 \times 10^6$ ) compared to piPSCs seeded at the same density which yielded  $2.11 \pm 0.09 \times 10^6$  VCN, ( $p = 0.015$ ). The derived SPGR, DT ( $23.66 \pm 0.60$  h) and FI ( $16.66 \pm 1.19$  times) at 96 h were all significantly better for kiPSCs compared to piPSCs (where  $p = 0.013$ ,  $0.012$ , and  $0.015$ , respectively). Interestingly, no other significant differences were observed amongst other conditions.

By 120 h, kiPSC and piPSC cultures yielded VCN of  $3.36 \pm 0.22 \times 10^6$  cells/well ( $\sim 8.84 \times 10^5$  cells/cm<sup>2</sup>) and  $3.28 \pm 0.02 \times 10^6$  cells/well ( $\sim 8.66 \times 10^5$  cells/cm<sup>2</sup>), respectively. Similar VCN could be achieved when expanding initial cultures of  $6 \times 10^4$  cells/cm<sup>2</sup> for 120 h.

The highest FI was obtained from seeding kiPSCs at a density of  $2 \times 10^4$  cells/cm<sup>2</sup> and harvesting at 120 h which yielded  $28 \pm 2.48$  times more than the initial seeding VCN; though, the VCN was considerably lower at  $2.21 \pm 0.19 \times 10^6$  compared to the other seeding conditions counted at the same timepoint for the same cell line, which in general reached  $>2.9 \times 10^6$  VCN per well of a 12 well plate.

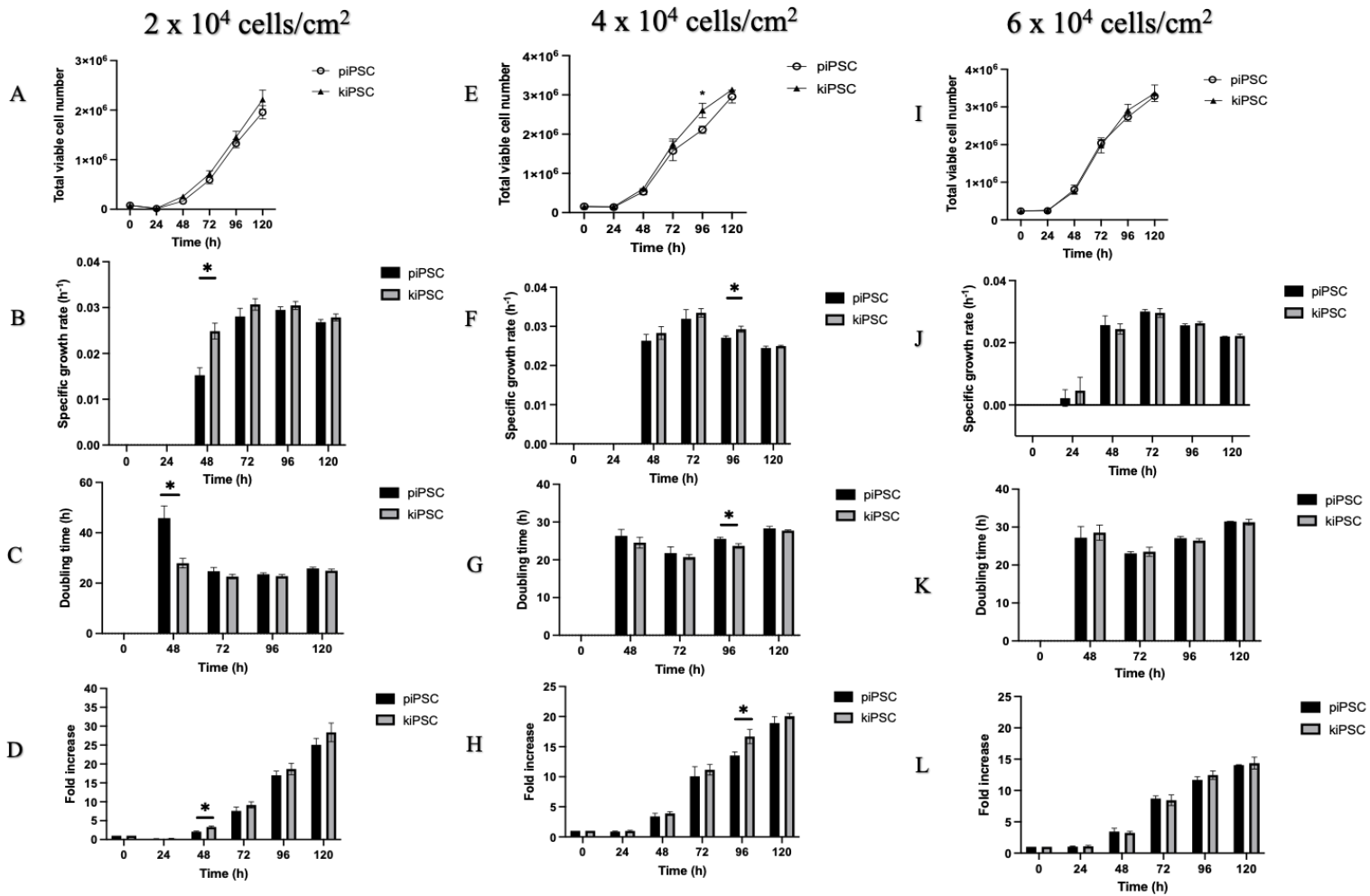


Figure 3.8. Measured VCN, SPGR, DT and FI of hiPSCs when seeded at different seeding densities over 120 h incubation in TeSR™-E8™/ VTN culture system. VCN, SPGR, DT and FI at different time points of the 120-h culture duration are shown for initial seeding conditions at  $2 \times 10^4$  cells/cm<sup>2</sup> (A-D),  $4 \times 10^4$  cells/cm<sup>2</sup> (E-F) and  $6 \times 10^4$  cells/cm<sup>2</sup> (I-L). Cells were seeded in triplicate wells and each time point is obtained from the average of the triplicate wells. Data is shown as mean  $\pm$  SD. N=3, biological repeats. \*p $\leq$ 0.05, multiple unpaired T-test.

### 3.2.2.3. Glucose and lactate profiles of hiPSC lines in TeSR<sup>TM</sup>-E8<sup>TM</sup>/VTN culture system

To understand the general metabolic activity of the cell lines in the TeSR<sup>TM</sup>-E8<sup>TM</sup> / VTN culture system, glucose and lactate concentrations were obtained before and after each medium exchanges. Common to all seeding conditions of both hiPSC lines was an overall decreasing trend of glucose concentration and a general increasing trend of lactate production as the cultures progressed (Figure 3.9 A -C). This further correlates with the increase in VCN as the culture progressed, as shown in (Figure 3.8). The graphs in figure 3.9 show sharp increases of glucose concentration following medium exchanges, whilst lactate sharply decreases (medium exchanges are indicated by arrows in figure 3.9 A-C). This is expected as the medium exchange procedure replenishes glucose, whilst removing the by-product lactate. Concentration of the stock TeSR<sup>TM</sup>- E8<sup>TM</sup> medium was measured to contain ~15 mM of glucose.

For cultures of piPSC and kiPSC seeded at  $2 \times 10^4$  cells/cm<sup>2</sup>, only a small drop in glucose concentration was observed after 24 h to  $14.1 \pm 0.3$  and  $13.8 \pm 1.3$  mM, respectively. After 48 h in culture, glucose concentration would drop by ~27% for both hiPSC lines (Figure 3.9A). At 72 h, glucose depleted by 45% and 40% for kiPSC and piPSC, respectively. Eventually at 96 h, glucose dropped to around 3 mM for both cell lines and following medium exchange, completely depleted by 120 h timepoint, regardless of medium exchanges.

In comparison, piPSCs and kiPSCs seeded at  $6 \times 10^4$  cells/cm<sup>2</sup> experienced larger glucose concentrations depletion to  $11.6 \pm 0.8$  mM and  $10.7 \pm 0.8$  mM, respectively, after 24 h At 48 h, glucose concentration was depleted by 40% in both kiPSC and piPSC cultures, whilst at 72 h, glucose was depleted by 87% and 77%, respectively. Glucose was fully depleted by 96 h and 120 h, regardless of daily medium exchanges.

The lactate profiles of the cells under different seeding conditions were also observed. The general pattern for all conditions was an increasing trend in lactate production as the cultures

progressed, in correlation with the increasing VCN obtained at each time point (Figure 3.8). At each medium exchange, the control TeSR™- E8™ medium was measured to contain undetectable concentrations of lactate (< 0.8 mM).

After 24 h in culture, lactate is at detectable levels in all conditions yet remained at very low concentrations (<3 mM). After each medium exchange (indicated by the arrows in Figure 3.9) the lactate levels sharply drop below the limit of detection. No significant differences were observed in the lactate profiles of the two cell lines when seeded at the same initial cell density. It is important to note, that the general lactate yield was calculated to be ~ 2 mM per 1 mM of glucose, which is typical of glycolysis, and the main pathway for the breakdown of glucose molecules by PSCs.

Overall, no significant difference was observed in the patterns of glucose and lactate consumption between the two cells line when seeding at 2, 4, or 6 x 10<sup>4</sup> cells/cm<sup>2</sup> and expanded for 120 h.

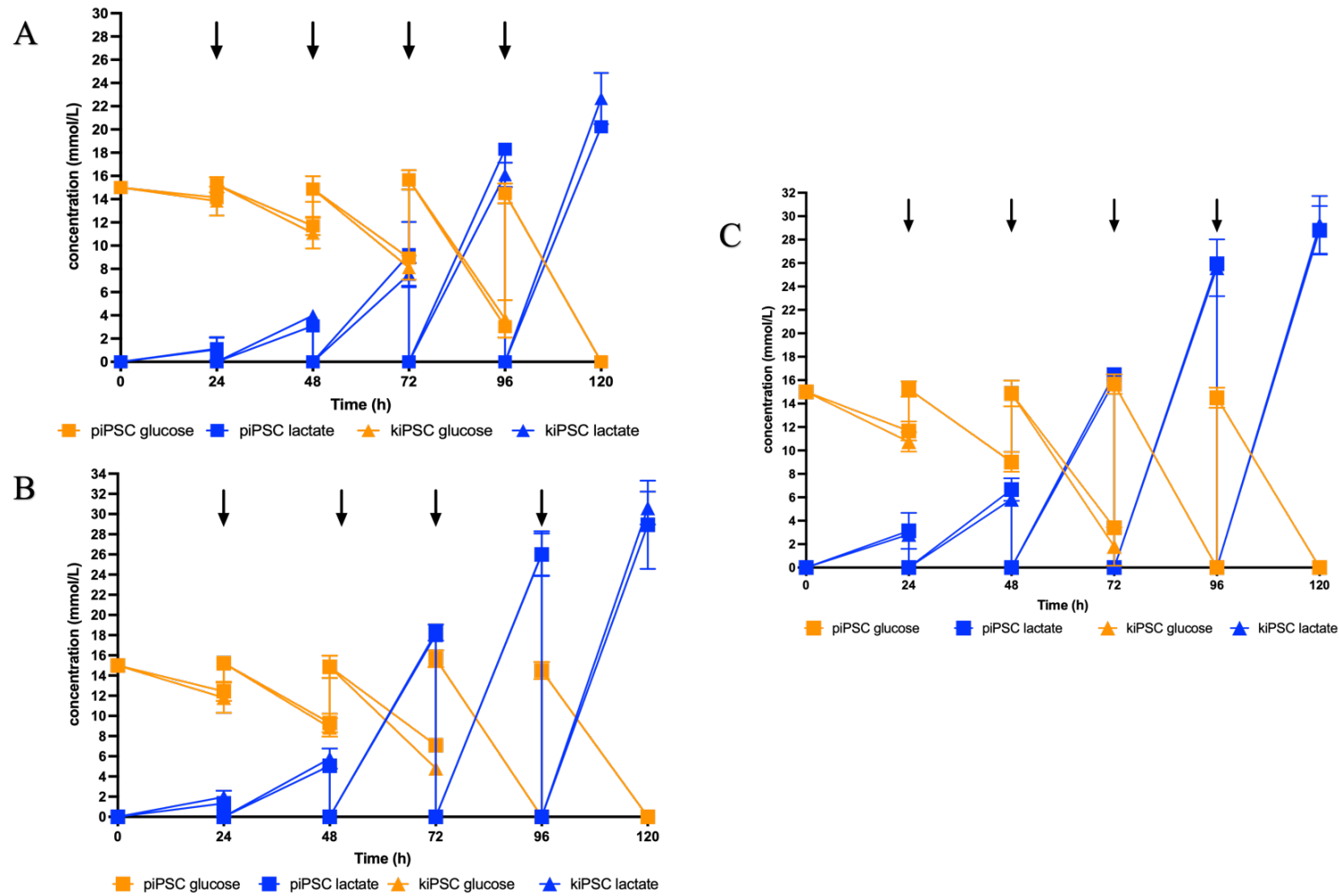


Figure 3.9. Glucose and lactate profiles of kiPSCs and piPSCs over 120 h of culture, when seeded at different seeding densities. Glucose and lactate concentrations were obtained before and after medium exchanges. Glucose and lactate for  $2 \times 10^4$  cells/cm<sup>2</sup> (A),  $4 \times 10^4$  cells/cm<sup>2</sup> (B) and  $6 \times 10^4$  cells/cm<sup>2</sup> (C) are shown as an average from three replicate wells of 3 independent studies. Data is shown as mean  $\pm$  SD. N=3, biological repeats, multiple unpaired T-test.

### **3.2.3. Comparison of TeSR™-E8™ with a newly developed mTeSR™ Plus medium composition**

Experiments conducted in sections 3.2.1 and 3.2.2 showed that the TeSR™-E8™ / VTN culture system demonstrated to support both hiPSCs line and their expansion. The next steps were to determine if the culture system could be improved in terms of efficient expansion.

At the time the experimental work in this thesis was conducted, the mTeSR™ Plus medium was released by StemCell Technologies. The formulation of this medium is an adaptation of the classic mTeSR™1 formula with improved and stabilised basic FGF and buffer system, for longer medium quality in typical 37 °C incubation cultures. Furthermore, mTeSR™ Plus is cGMP grade which would ease its translation when employed for clinical grade productions. Therefore, the mTeSR™ Plus medium was considered a potentially suitable medium for improving the culture systems to expand hiPSC. Hence, the next series of experiments compares the ability of mTeSR™ Plus medium with the TeSR™-E8™ medium in terms of cell growth and cell quality.

#### **3.2.3.1. Comparison of hiPSC growth when cultured in mTeSR™-Plus or TeSR™-E8™**

Both cell lines were cultured in static conditions on 6 well plates coated with VTN and incubated with 2 mL of mTeSR™ Plus or TeSR™-E8™ medium. 100% medium exchanges were performed daily, and the cells were harvested after 96 h of expansion. VCN were measured at this time point and no significant differences were found. VCN of kiPSC after 96 h expansion was  $9.62 \pm 0.96 \times 10^6$  in mTeSR™ Plus cultures, which were comparable to cultures in TeSR™-E8™ yielding  $8.48 \pm 7.51 \times 10^6$  VCN. The same comparability is true for piPSCs cultured in the two media. SPGR, DT and FI were all comparable.

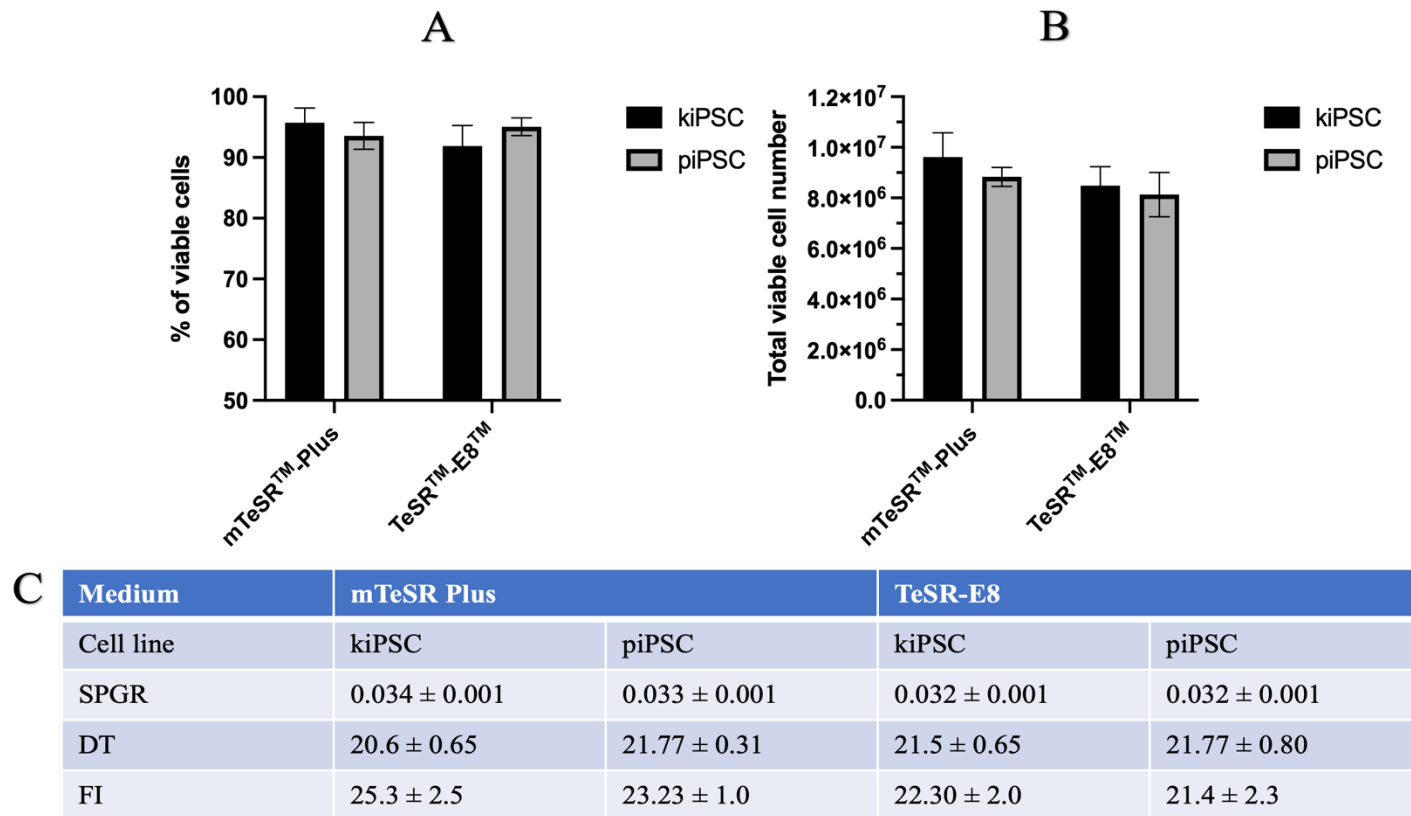


Figure 3.10. Viability, VCN and growth kinetics of hiPSCs in different media. kiPSC and piPSC were cultured in mTeSR™ Plus or TeSR™-E8™ for 96 h. Cell viability (A) and VCN (B) were obtained at harvest. Values of SPGR, DT and FI were derived from the VCN. piPSCs and kiPSCs passage numbers used in this study were 44 and 15 respectively. Mean ± SD. N = 3, biological replicates, multiple unpaired T-test.

### **3.2.3.2. Quality of kiPSC in the mTeSR™ Plus / VTN culture system**

mTeSR™ Plus / VTN cultures systems were previously shown to be comparable to the TeSR™-E8™ / VTN culture system in terms of promoting cell growth and expansion (section 3.2.3). It was therefore decided to further assess whether the mTeSR™ Plus / VTN culture system could support hiPSCs CQAs.

At this point, the kiPSC line were chosen as the cell line model for further bioprocess developmental work since the piPSC were more prone to spontaneous differentiation as a result of serial passaging.

To determine whether the mTeSR™ Plus / VTN culture system could support the maintenance of kiPSC qualities, the next step was to assess for the presence of pluripotency marker OCT4 and SSEA4. In this experiment, kiPSCs were expanded on planar platforms using the mTeSR™ Plus / VTN culture system. A full 100% daily medium exchange was performed throughout 96 h of culture. On the 4<sup>th</sup> day of expansion cells were fixed and stained with fluorescent markers for OCT4 and SSEA4 detection. Cells grown in this culture system showed positive expression of OCT4 ( $46.59 \pm 17.28$  % of N=2 biological repeats) and SSEA4 (Figure 3.11). Noticeably, more nuclei were stained with DAPI compared to OCT4. These are comparable to the percentage of OCT<sup>+</sup> expressing cells in TeSR™-E8™ / VTN culture as shown earlier in Figure 3.11.

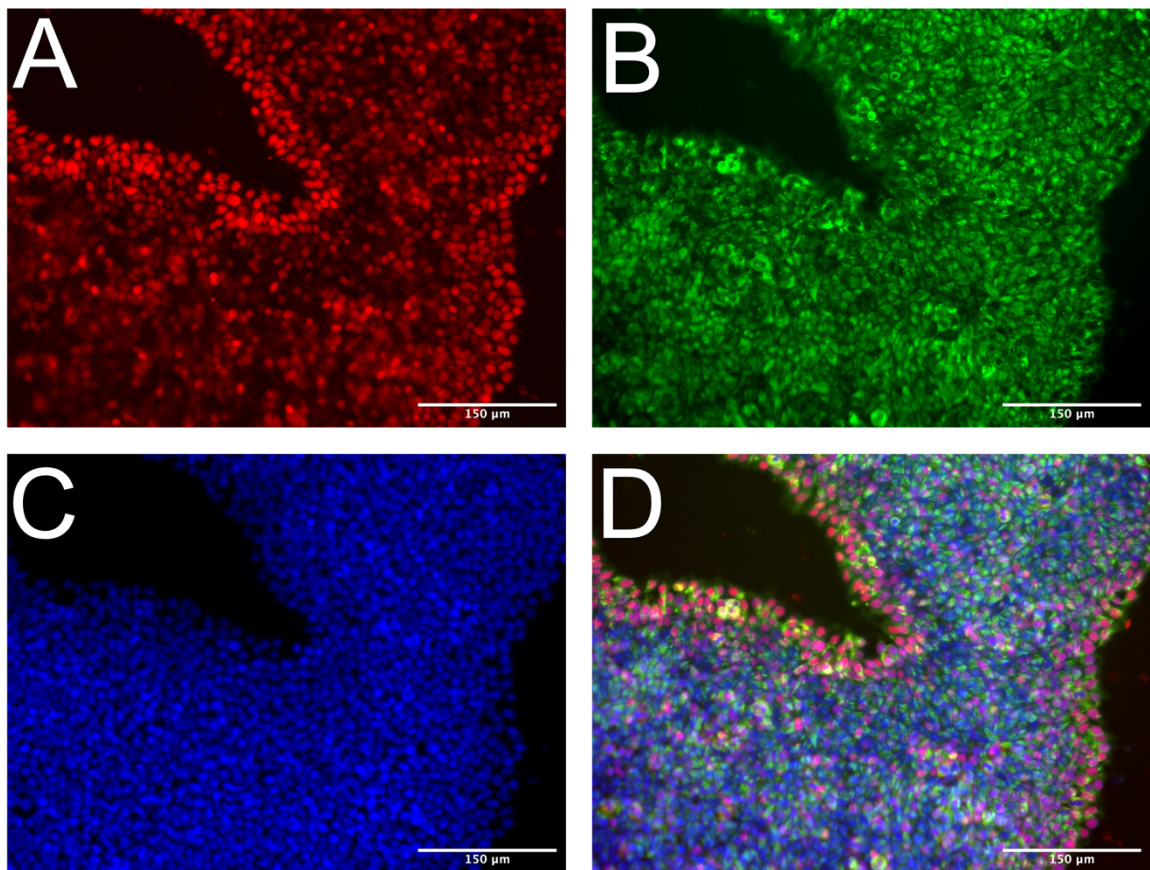


Figure 3.11. Pluripotency assessment of kiPSCs in mTeSR<sup>TM</sup> Plus / VTN culture system using fluorescent imaging. kiPSCs were grown in 48 well plates and cultured for 96 h. Cells were then fixed for ICC and 2 random areas of the well were captured. The pluripotency markers OCT4 (A; red) and SSEA4 (B; green) were detected, whilst the nuclei were stained with DAPI (C; blue). Images were then merged to show localisation of pluripotency markers within the cell (D). Representative of N = 2, biological replicates, Scale bar = 150 µm.

### **3.2.4. Optimisation of mTeSR<sup>TM</sup> Plus / VTN culture system by feeding regime**

The employment of mTeSR<sup>TM</sup> Plus for a hiPSC culture system has several advantages over TeSR<sup>TM</sup>-E8<sup>TM</sup>. For one, mTeSR<sup>TM</sup> Plus is manufactured to the standard of cGMP grade therefore facilitating its transition into clinical production scale. Second it contains stabilised basic FGF, an advantage over TeSR<sup>TM</sup>-E8<sup>TM</sup> due to its amenability to be implemented into a periodic feeding regime, allowing for skipped feeds, thus potentially reducing labour costs. Such a feeding regime was tested here to investigate its effect on the hiPSCs' expansion characteristics. In addition, two other feeding strategies were tested (Table 3.1). For the control feeding strategy, the same feeding regime in section 3.2.3.1 was used where a routine 100 % medium (2 mL) exchange is performed every 24 h until harvest day. Briefly, for feeding strategy 1, intermittent feeding is mimicked by skipping a scheduled feed on the 48 h; feeding strategy 2 was designed to reduce the total volume of medium required by 50% compared to control; and feeding strategy 3 is tailored to the growth profile of hiPSCs recorded in Figure 3.8, whereby hiPSC enter exponential growth phase only after day 1 in culture, therefore requiring more nutrients to support their higher metabolic activity.

Table 3.1 Summary of the feeding strategies, showing the volumes of mTeSR™ Plus medium to be exchanged per well of a 6 well plate, at each timepoint of the cultures.

Time of culture (h)	Control	Feeding strategy 1	Feeding strategy 2	Feeding strategy 3
0	2 mL	2 mL	1 mL	1 mL
24	2 mL	2 mL	1 mL	1 mL
48	2 mL	N/A	1 mL	2 mL
72	2 mL	2 mL	1 mL	2 mL
96	Harvest	Harvest	Harvest	Harvest

#### 3.2.4.1. Effect of feeding regime on the viability and growth kinetics of kiPSCs

After 96 h of culture with different feeding regimes, kiPSCs were harvested to obtain the viability and VCN (Figure 3.12). It was observed that Feeding strategy 1 yielded cells with significantly lower viability ( $87 \pm 1.0 \%$ ) compared to the control ( $94 \% \pm 2.8$ ;  $p = 0.016$ ), whilst no significant difference was detected amongst other feeding strategies. Nonetheless, all Feeding strategies yielded cells of  $>85\%$  viability (Figure 3.12 C)

For control cultures, VCN was measured at  $9.2 \pm 0.30 \times 10^6$ . Feeding strategies 2 and 3 were comparable to the control with VCNs of  $8.2 \pm 0.49 \times 10^6$  and  $9.07 \pm 0.73 \times 10^6$ , respectively. Feeding strategy 1 harvested the lowest VCN out of all conditions at  $7.62 \pm 0.20 \times 10^6$ , significantly lower than that of the control ( $p = 0.0076$ ); the derived SPGR, DT and FI for Feeding strategy 1 were significantly affected compared to the control ( $p$  values = 0.007, 0.004 and 0.007, respectively).

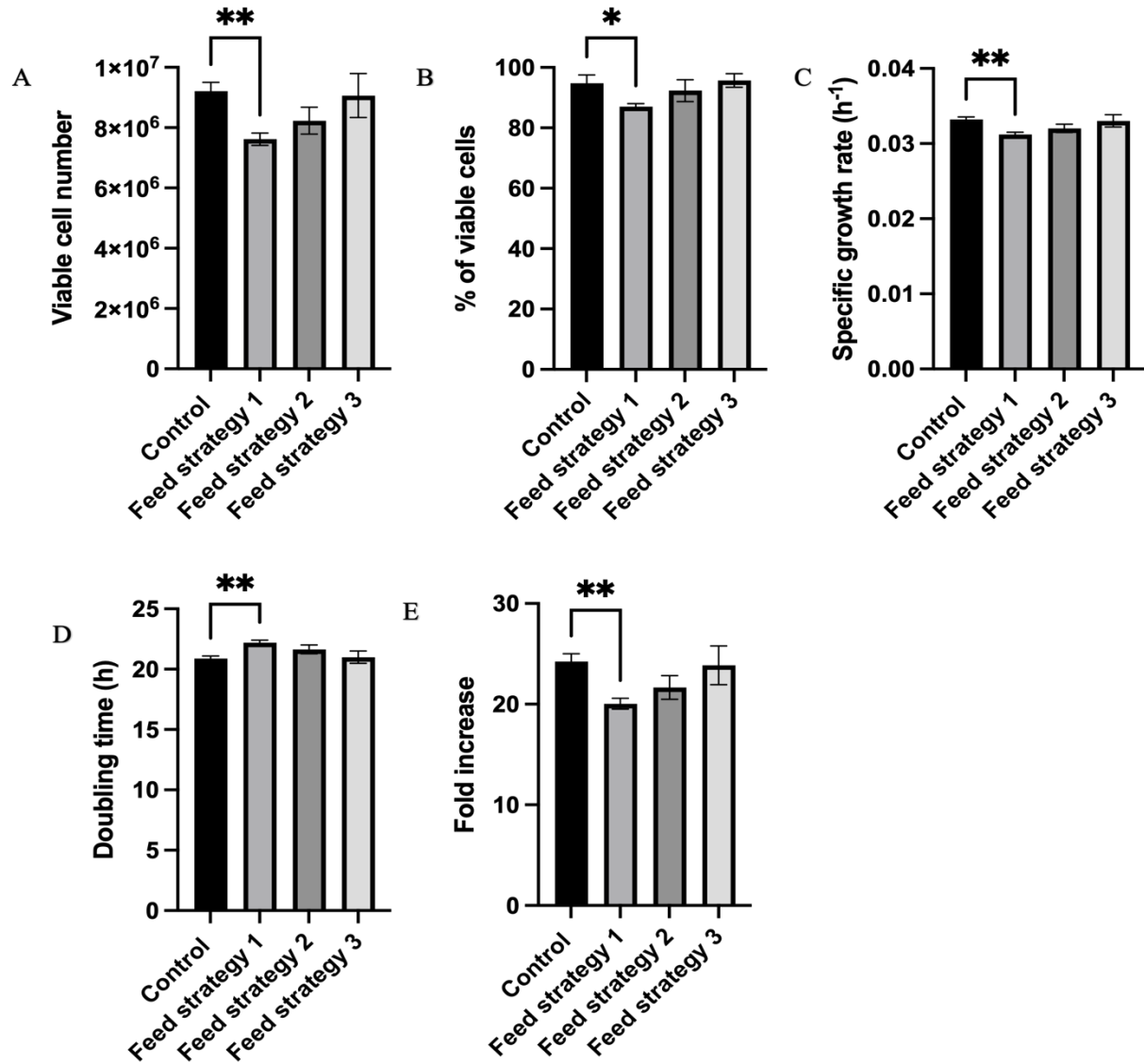


Figure 3.12. Viability, VCN and growth kinetics of kiPSCs under different feeding strategies. Cell counts were obtained after 96 h in different feeding strategies from three replicate wells of 6 well plates. Data shown here is the mean  $\pm$  SD. N = 3. \* $p \leq 0.05$ , \*\* $p \leq 0.01$

### 3.2.4.2. Effect of feeding regime on glucose and lactate profiles of kiPSCs

Glucose and lactate concentrations were monitored every 24 h throughout the different expansion culture conditions. Since hiPSC are known to predominantly metabolise glucose through glycolysis, the expected lactate yield from 1 molecule of glucose is 2 molecules of lactate. Here, the average lactate yield from glucose was measured across all timepoints then averaged for control, feeding strategy 1, feeding strategy 2 and feeding strategy 3 conditions; these were calculated at  $2.0 \pm 0.4$ ,  $2.6 \pm 1.0$ ,  $2.8 \pm 1.4$  and  $2.2 \pm 0.1$ , respectively. In general, cultures in all feeding conditions yielded  $\sim 2$  molecules of lactate from 1 molecule of glucose.

The metabolic behaviour of the kiPSCs under each feeding strategy was characterised. First it was seen that after medium exchanges (indicated by the arrows in Figure 3.13) glucose returned to concentrations of  $\sim 12$  mM whilst lactate returned to 0 mM indicated by the sharp peaks. Since medium exchanges were not performed at 48 h to mimic weekend feeding for cultures in feeding strategy 1, the glucose and lactate concentrations remained the same at  $3.7 \pm 2.6$  mM and  $12.5 \pm 2.9$  mM, respectively. Thus, cells cultured with feeding 1 strategy do not receive replenishment of glucose compared to other feeding strategies. Further, toxic metabolites such as lactate are kept in the culture.

By 72 h, glucose concentrations under feeding strategy 1 depleted to 0 mM. In comparison to other feeding strategies and the control, detectable levels of glucose were still obtained by 72 h, although very low ( $\sim < 1$  mM). By 96 h, glucose depleted completely in all culture conditions, and signified the point of harvest.

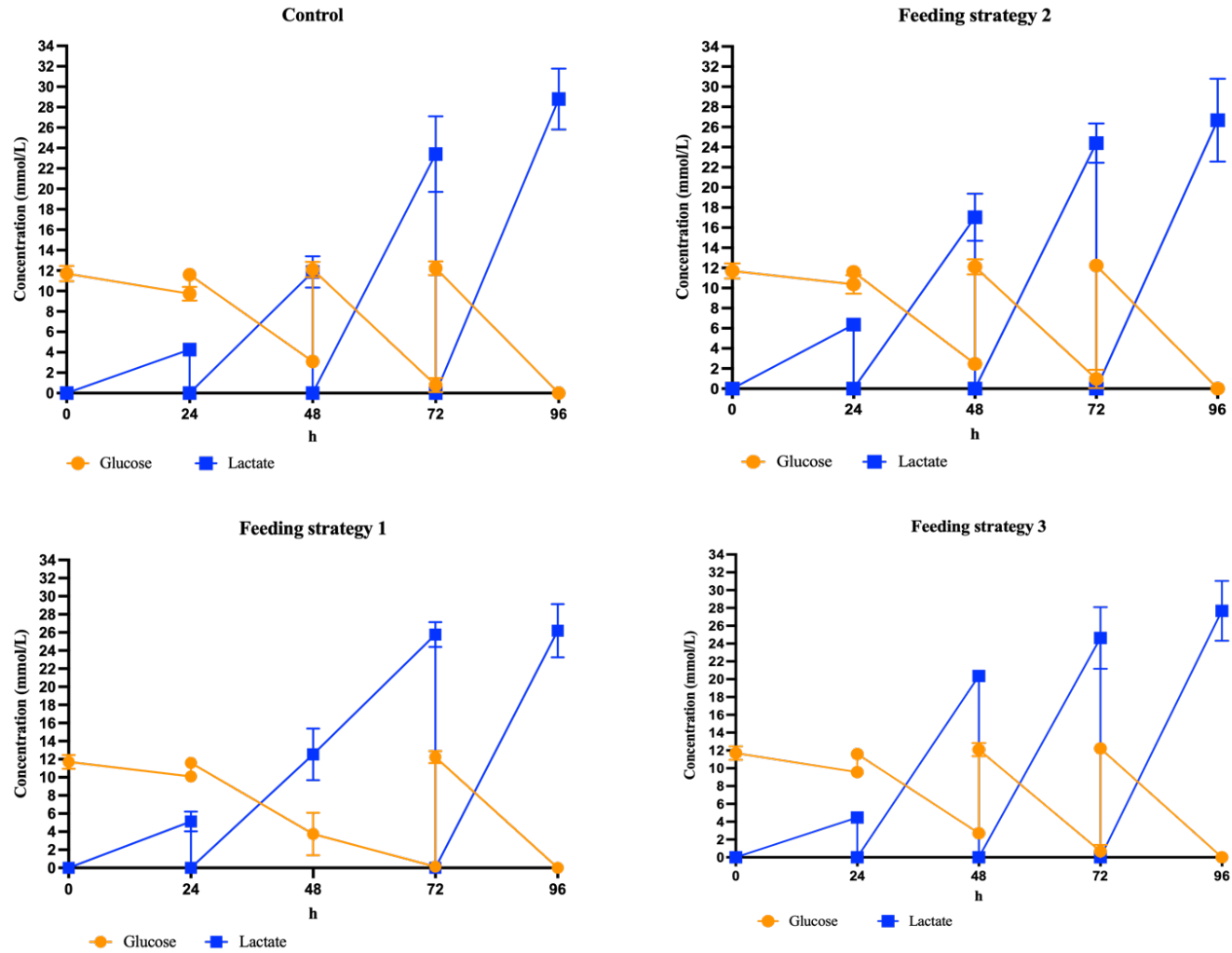


Figure 3.13. Glucose and lactate profiles of kiPSC cultures in different feeding regimes. The glucose and lactate concentrations for control feeding regime (A), was compared to 3 other feeding strategies 1 (B), 2 (C) and (3) throughout a 96 h culture in 6 well plates. Readings were taken at each time point and before and after each medium exchange. Data here is shown is the average of triplicate wells per condition as mean  $\pm$  SD. N = 3.

### 3.2.4.3. Effect of feeding regime on the operation cost for expanding kiPSC

To further assess the suitability of mTeSR<sup>TM</sup> Plus medium as a replacement for TeSR<sup>TM</sup>-E8<sup>TM</sup>, a cost analysis of each feeding strategy was performed with respect to the cost of medium per VCN obtainable, and these are shown in Table 3.2. For the previously established TeSR<sup>TM</sup>-E8<sup>TM</sup> / VTN culture system, the expansion of kiPSCs to clinically relevant dose quantities of  $1 \times 10^8$  cells, would cost ~ £36.21 in terms of medium alone (adjusted accordingly to the retail price of the TeSR<sup>TM</sup>-E8<sup>TM</sup> at the time of analysis). Note, that these calculations disregard other associated costs of the expansion process including equipment, other raw materials, facility rent and labour.

The VCN generated from each feeding strategy was used to obtain the cost of medium per viable cell harvested. The cost of medium per cell was then multiplied to obtain the cost of  $1 \times 10^8$  viable cells. This is a clinically relevant number to generate enough cell product for some doses of NPC therapies as discussed in Chapter 1. The cost of each feeding strategy, if directly scaled out to generate such quantities, are shown in Table 3.2. It was calculated that each tested feeding strategy would cost significantly less than the control method (p values are shown in Table 3.2). This was, however, expected as the control strategy process required the most medium in all condition tested.

Feeding strategy 2 was the cheapest strategy ( $p < 0.0001$ ) at an estimated cost of  $£23.17 \pm 1.22$  to generate  $1 \times 10^8$  viable cells (Table 3.2). Whilst feeding strategy 1 and feeding strategy 3 required the same volume of medium to operate, feeding strategy 3 was cheaper at  $£31.63 \pm 2.44$  per  $1 \times 10^8$  cells. Feeding strategy 3 would also require less 6 well plates than feeding strategy 1 and 2 to generate the same quantity of cells.

Table 3.2. Cost analysis of the different feeding regimes.

	<b>Control</b>	<b>Feeding strategy 1</b>	<b>Feeding strategy 2</b>	<b>Feeding strategy 3</b>
Total viable cells harvested (x 10 <sup>6</sup> )	9.21 ± 0.30	7.62 ± 0.20	8.23 ± 0.45	9.07 ± 0.73
Total volume of medium required	8	6	4	6
Estimated medium cost to generate 1 x 10 <sup>8</sup> hiPSCs (£)	41.35 ± 1.35	37.51 ± 1.00 (p=0.045)	23.17 ± 1.22 (p<0.0001)	31.63 ± 2.44 (p=0.0002)
Equivalent number of wells (6 well plates) to generate 1 x 10 <sup>8</sup> hiPSCs	10.86	13.12	12.15	11.03

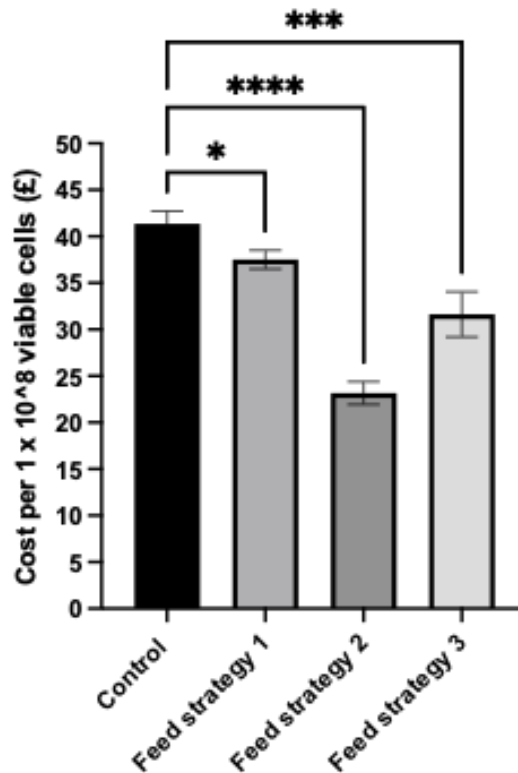


Figure 3.14. Cost analysis of the different feeding strategies. The costs calculated here are based on the VCN obtained from each condition after 96 h in culture, and the cost of the medium used for the process. This is adjusted to the cost for generating 1 x 10<sup>8</sup> viable cells. Data is shown as mean ± SD. N =3. \*p ≤0.05, \*\*\*p<0.001 and \*\*\*\*p<0.0001, one-way ANOVA, multiple t-test.

#### 3.2.4.4. Growth behaviour of kiPSCs over multiple passage in mTeSR™ Plus / VTN /

##### Feeding strategy 3

The work so far has demonstrated that the mTeSR™ Plus / VTN culture system can support kiPSCs in the short term. To validate a cost-efficient feeding strategy for its employment in the expansion of hiPSC, it was important to test if the cell quality and growth properties of kiPSCs are maintained in prolonged cultures using the identified cost-efficient feeding strategies. In this case, feeding strategy 3 was employed due to being significantly cheaper compared to the control feeding strategy, without compromising viability or the growth characteristics of kiPSCs.

First, kiPSCs were thawed from frozen cryovials and seeded at  $4 \times 10^4$  cells/cm<sup>2</sup> into triplicate wells of a 6 well plate precoated with VTN (seeded at passage 12). kiPSCs were expanded for 96 h with medium exchanges performed as per feeding strategy 3. After 96 h of cell propagation, cells were harvested from the culture system as single cells. Cell counts were taken per well and then averaged for the passage number. Cells were then re-seeded at  $4 \times 10^4$  cells/cm<sup>2</sup> onto fresh VTN coated plates, and the process was repeated up to passage 19. The collected VCN and viability of each passage in the sequential passaging are shown in Figure A and B.

kiPSCs seeded from thaw and harvested after 96 h (passage 12) displayed significantly reduced VCN compared to harvested VCN at passage 14 and beyond ( $p$  values were all  $<0.05$ ), as shown in (Figure 3.15). Because of the significantly lower VCN, kiPSC from thaw (passage 12) calculated significantly lower FI ( $14.5 \pm 0.88$  times), compared to passage 14 and beyond which was calculated at around 21-fold after 96 h. The DT of kiPSC from thaw ( $24.93 \pm 0.56$  h) was significantly higher to that obtained from passage 14 and above which averaged around 21 h. Interestingly, no significant difference was observed in the viability of the cells across all passages.

Another interesting growth characteristic observed was the growth of kiPSC one passaged after thaw (passage 13). The growth kinetics of the cells at passage 13 were not significantly different to that of passage 14 and beyond. However, similarly, they were also not significantly different to that of passage 12.

Although, critical process parameters such as seeding density, substrate concentration, medium volume and time of incubation were tightly controlled, variability in harvested VCN after each passage was still observed as indicated by the error bars (SD) in (Figure 3.15 A).

Importantly, cells appear to maintain the expression of OCT4 over several passages as seen in (Figure 3.16), whilst the colony morphology of kiPSCs appear to show compact centres with clearly defined borders, a feature of typical hiPSC cultures (Figure 3.17). Thus, the mTeSR™ Plus / VTN culture system with feeding strategy 3 was established capable of supporting and expanding kiPSC, and from here on, was routinely employed for the general maintenance of kiPSCs.

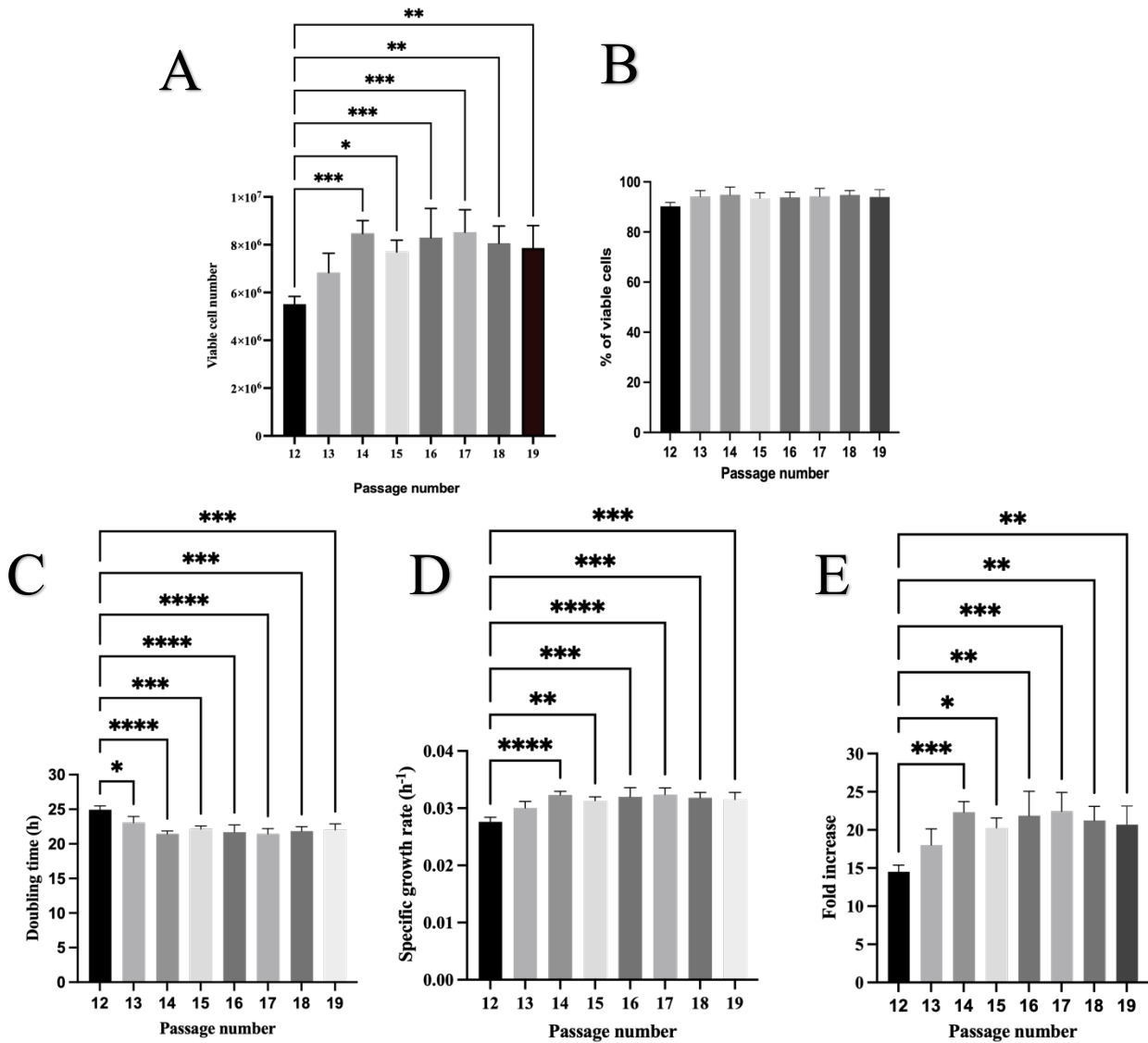


Figure 3.15. Viability and growth kinetics of kiPSC over 8 consecutive passages. Cells were thawed at p12 and seeded at  $4 \times 10^4$  cells/cm<sup>2</sup> in the mTeSR™ Plus /VTN culture system in 6 well plates. After 96 h in culture, cells were harvested with accutase the viability and number of cells were measured on the nucleocounter 3000. VCN (A) and cell viability (B) of the cells throughout the serial passage are shown here. The derived DT (C), SPGR (D) and FI (E) are also displayed for each passage. kiPSCs were cultured in three replicate wells and the measurements were obtained from 2 technical repeats per well. The average of all three triplicate wells were taken to provide an N=1. Data shown here is the mean  $\pm$  SD. N=3, biological replicates \*p<0.05, \*\*p<0.01, \*\*\*p<0.001 and \*\*\*\*p<0.0001. One-way anova, multiple t-test.

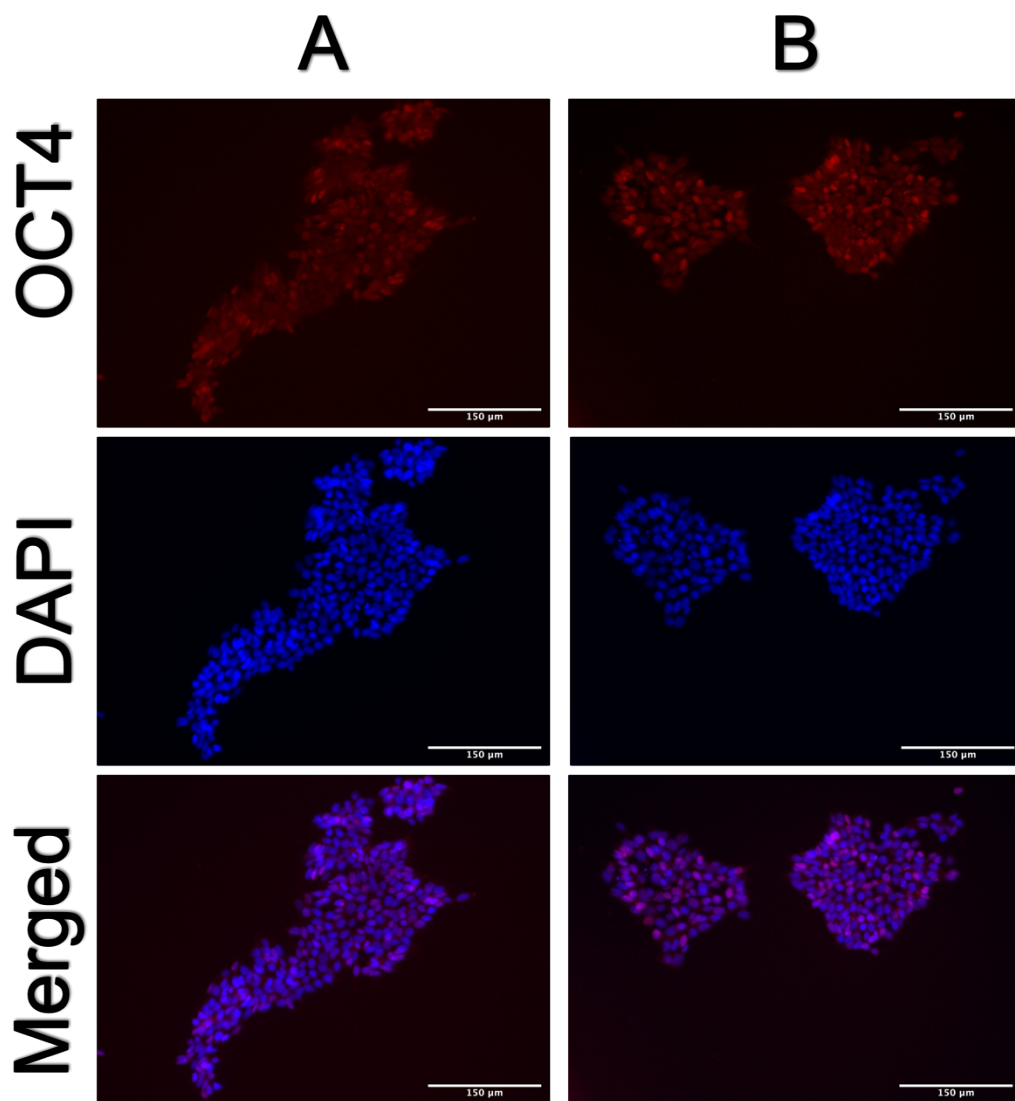


Figure 3.16. Pluripotency assessment of kiPSCs after multiple serial passaging. Cells were prepared for ICC following passage 12 (A) and passage 19 (B). The pluripotency markers OCT4 (red) was stained. The nucleus was stained for DAPI (blue). The images were then merged. N=1.

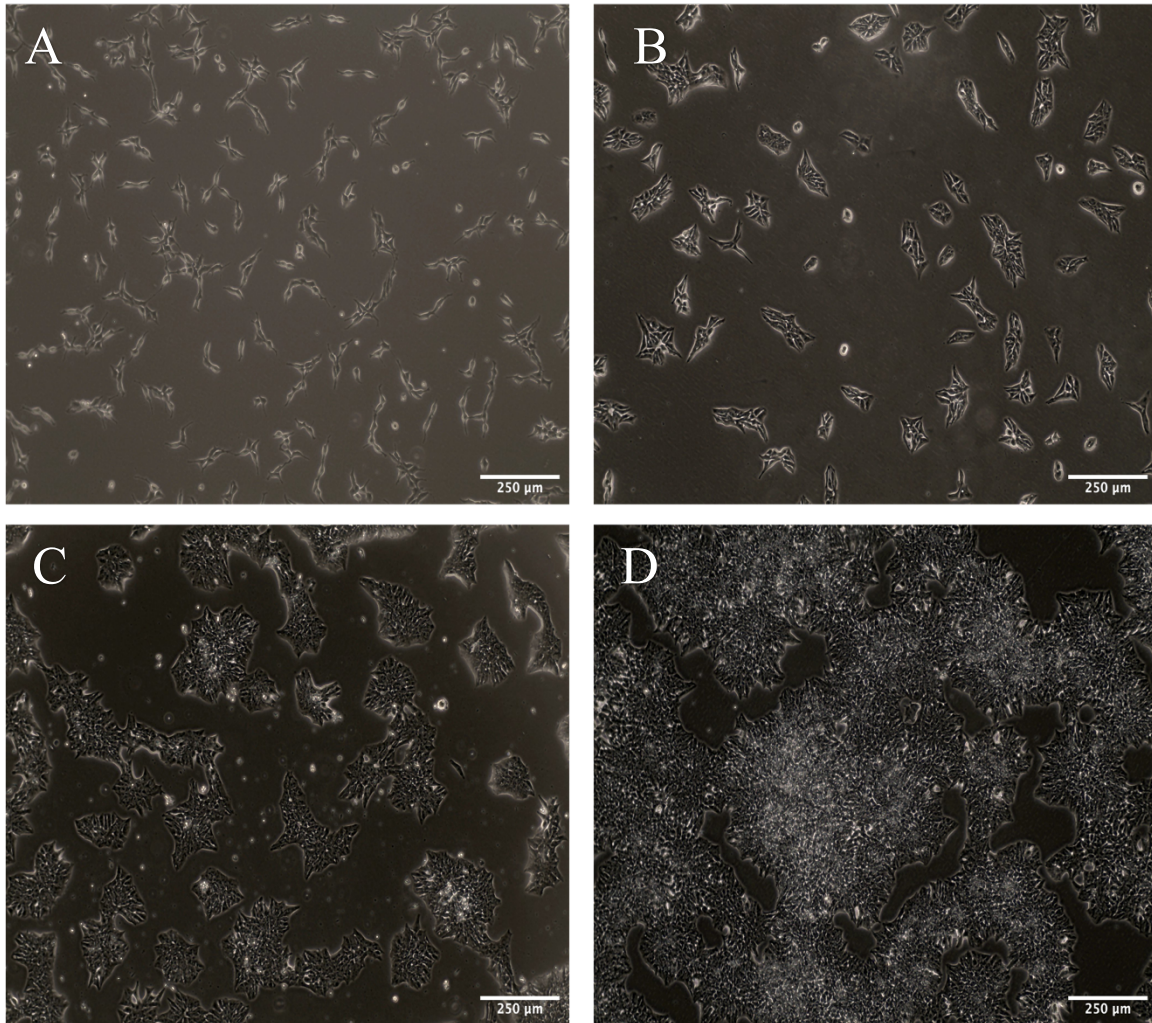


Figure 3.17. Representative images of cell and colony morphologies of kiPSC cultures after passage 14 in mTeSR<sup>TM</sup>Plus / VTN culture system up to passage 19. 24 h post seeding (A). 48 h into the culture (B). After 72 h in culture (C). At 96 h, end of culture (D). Scale bar = 250 µm

### 3.2.5. Neural induction of hiPSCs towards NPCs following their expansion in mTeSR<sup>TM</sup> / VTN culture system

Crucially, it was important to demonstrate that the kiPSC line could differentiate towards NPCs after culturing in the mTeSR<sup>TM</sup> Plus /VTN system. The next experiment was therefore designed to assess the ability of kiPSCs to commit towards the neural lineage following culture in the optimised baseline expansion process.

First, kiPSCs were propagated in the optimised baseline expansion process (section 3.2.4.4) for at least 2 passages following thaw to ensure that the growth behaviour of the cells normalised. The kiPSCs used for these experiments were between passage 14 – 16.

To initiate the neural induction process, the mTeSR™ Plus medium was replaced with neural induction medium instead of performing a passage (or harvest) on day 4 of the expansion. This was to test whether a single culture platform for both the expansion and the differentiation of hiPSC was feasible. At the time of initiating the neural induction process, the borders of the kiPSC colonies were observed to be touching (Figure 3.18). As explained earlier in this thesis, contact inhibition can promote better differentiation of cells. This explains why standard neural induction methods of PSCs are typically performed on densely seeded populations of PSCs. For example, the neural induction process recommended by StemCell technologies requires seeding at  $2 \times 10^5$  cells/cm<sup>2</sup> to initiate neural induction. Here, the Stemdiff™ neural induction medium (SNIM) and SNIM + SMADi were initially used to test the differentiation potential. Both medium compositions are proprietary formulations of StemCell Technologies but are based on (Chambers *et al.*, 2009). Both media claims to drive differentiation of PSCs towards PAX6<sup>+</sup> CNS-NP cells. However, SNIM alone was unable to differentiate the kiPSC to PAX6<sup>+</sup> cells. kiPSCs in these experiments were incubated in SNIM + SMADi for a further 6 days, with daily full 100% medium exchange. Following the neural induction process, cells were harvested and re-plated for ICC staining and imaging. VTN was not a suitable substrate to support the reattachment of neural induced kiPSCs as they would form sheets and detach from the substrate. Matrigel and PLO/LN coated well plates, however, could allow the differentiated cells to attach (Galiakberova and Dashinimaev, 2020a). Hence, PLO/LN was used to reattach differentiated kiPSCs following neural induction.

PAX6 was used as a marker of neural lineage commitment. Ax0013, an established hiPSC-derived NPC line, was used as a positive control for PAX6 (Grainger, 2020). kiPSC which

was not cultured in SNIM + SMADi was used as a negative control for PAX6. kiPSC-derived differentiated cells after the neural induction process were then stained for PAX6 markers.

kiPSC-derived differentiated cells were shown positive for PAX6 (Figure 3.19) similar to the control Ax0013 cells. Non-differentiated kiPSCs did not stain for PAX6 as expected.

After 6 days of neural induction, cells were detached from the culture substrate and the viability and VCN was obtained. Cell viability was recorded at  $90.44 \pm 3.99$  %. The total obtainable VCN from a single 6 well plate was  $1.63 \pm 0.26 \times 10^7$ , a  $42.83 \pm 6.87$  FI compared to the initial VCN seeded ( $4 \times 10^4$  cells/cm<sup>2</sup>). However, it was found that  $72.07 \pm 12.69$  % of cells replated from the differentiation process were PAX6<sup>+</sup>.

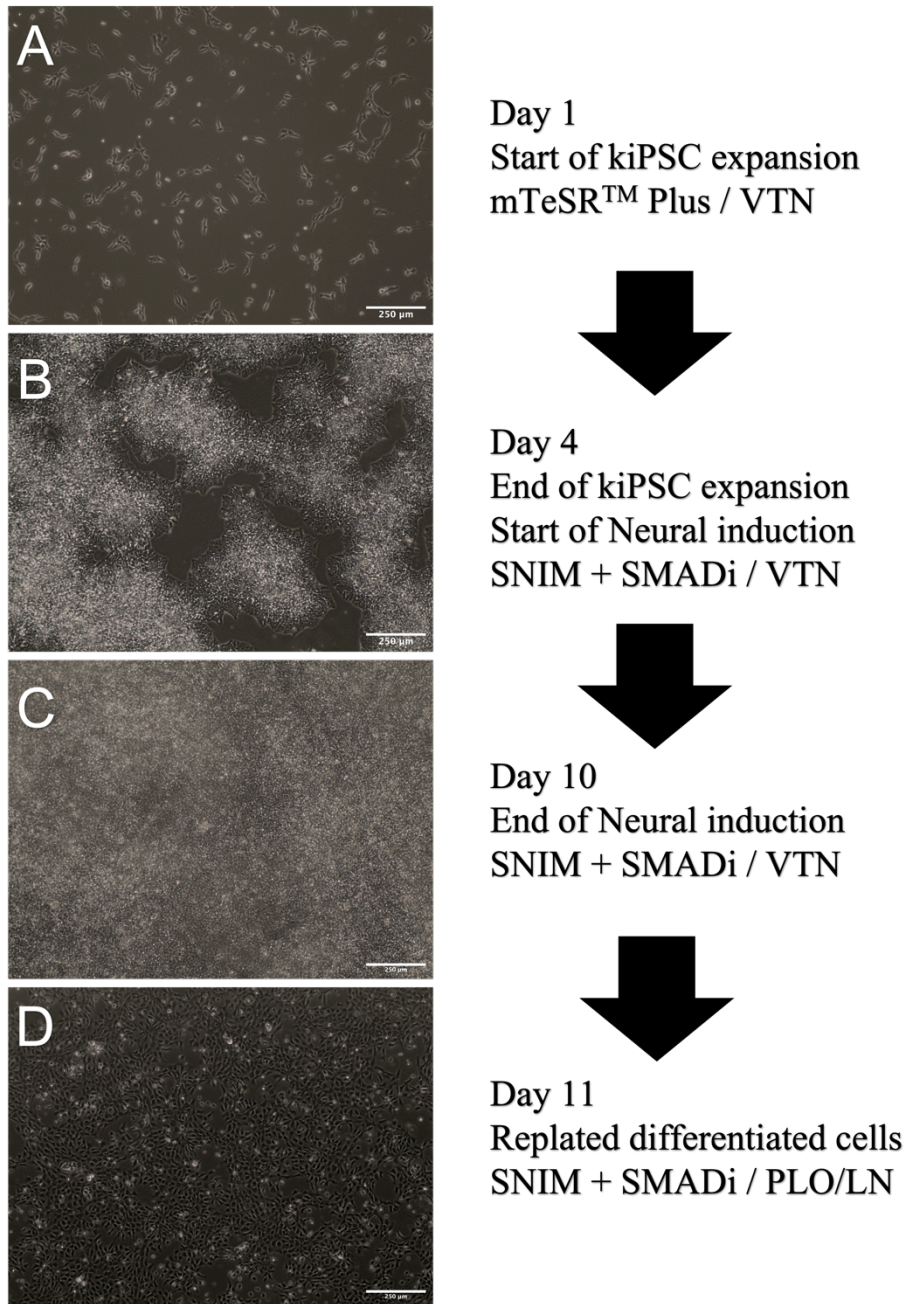


Figure 3.18. Process workflow of the integrated bioprocess for deriving NPCs from kiPSCs. Cells were cultured in mTeSR™ Plus containing 10 μM Y-27632 for the first 24 h post seeding (A). kiPSCs were cultured in mTeSR™ Plus until day 4 post seeding, when SNIM + SMADi was then used to exchange the medium (B). Cells were differentiated for a further 6 d (C) in SNIM + SMADi. Cells were then replated on PLO/LN coated well plates and imaged 24 h post seeding (D). Images are representative of 2 random areas of the wells at each stage of the process. N=3, biological repeats. Scale bar = 250 μm

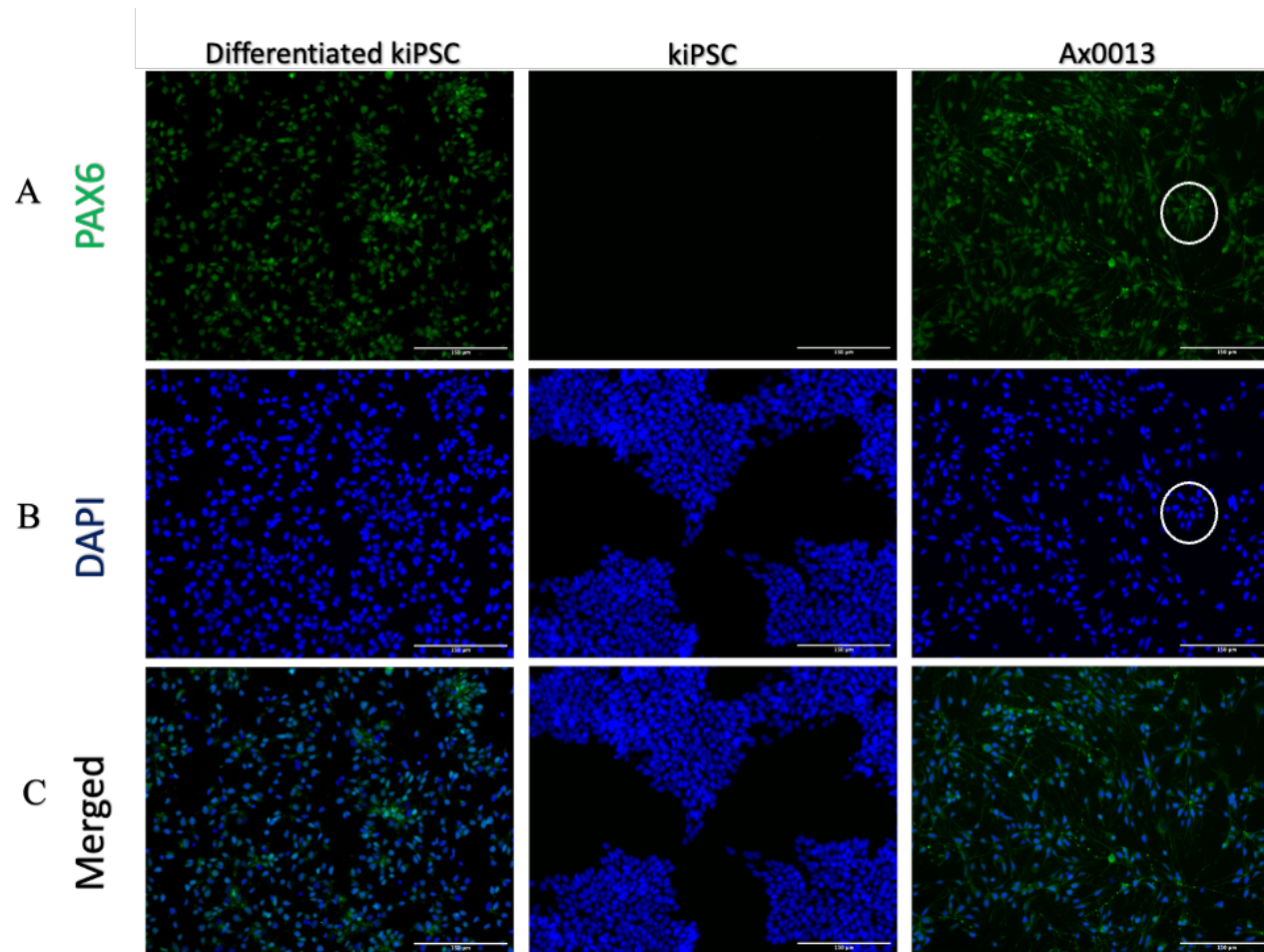


Figure 3.19. Differentiation of kiPSCs towards NPCs following culture in mTeSR™ Plus / VTN culture system. On day 4 of kiPSC cultures (P14 -16) following propagation, the media was exchanged to SNIM + SMADi to initiate neural induction. Cells were then harvested 6 days after the initiation of neural induction and plated onto PLO/LN coated plates. 48 h post plating cells were prepared for ICC. Neural lineage committed kiPSC-derived cells stained positive for PAX6 (A; green). DAPI staining was performed for nuclei identification (B; blue). PAX6 and DAPI images were merged in C. Negative control kiPSCs were not differentiated and instead cultured in mTeSR™ Plus and then fixed. Ax0013 cells were plated on PLO/LN plates and then fixed 24 h after seeding for ICC. White circles indicate rosette like organisation of cells. N=3, biological repeats. Scale bar = 150 μm

### 3.3.Discussion

Common methods for obtaining NPCs from sources such as foetal tissues are considered unethical and limited. hiPSCs provide an alternative unlimited source for NPCs by neural induction. Further advantages of hiPSC-derived NPCs include their amenability for autologous therapies. Since hiPSC are promising sources for obtaining large quantities of NPCs, accessibility to an abundance of hiPSCs would play a significant role towards realising NPC-based therapies for neurodegenerative diseases, as well as other applications such as drug discovery, disease modelling, tissue engineering, or neurotoxicity screenings. Thus, the ability to expand hiPSCs in vitro is a crucial process for obtaining large quantities of hiPSCs.

Importantly, expansion processes should not only generate the target cell quantities but also ensure the retention of desirable quality attributes of hiPSCs, such as pluripotency and self-renewal. Several culture systems have been developed to maintain adherent cultures of hiPSCs in a self-renewing and pluripotent state. These include the employment of planar platforms and varying combinations of substrates and media, dependent on different applications and research groups (Ghasemi-Dehkordi *et al.*, 2015; Lam *et al.*, 2015; Abdal Dayem *et al.*, 2018).

Here, TeSR<sup>TM</sup>-E8<sup>TM</sup> / VTN culture systems were identified suitable for the culture of hiPSCs owing to their defined and xeno-free compositions. Thus, the initial experiments performed in this chapter were designed to assess, first, whether the culture system could support pluripotency and self-renewal qualities of the hiPSC lines, and second, whether there were major differences in the growth characteristics and quality profiles between the two hiPSC lines.

### **3.3.1. kiPSCs was chosen as the model cell line for further bioprocess development**

The first set of experiments were designed to assess and compare the morphologies of cells and colonies of the two cell lines when cultured in the TeSR™-E8™ / VTN culture system, using phase contrast microscopy and imaging. As seen in Figure 3.1, the TeSR™-E8™ / VTN culture system could support the attachment and adhesion of both the hiPSC cell lines, and encouraged the formation of colonies that are morphologically typical of PSCs adherent cultures (Okumura *et al.*, 2019; Liszewska *et al.*, 2021).

However, morphological differences were observed between the colonies of the two cell lines. kiPSC colonies displayed “spikey” borders whilst piPSC formed colonies with smoother and rounder edges. Using cell and colony morphologies as a criterion of cell quality is challenging since it is subjective. Nonetheless, several classification systems to categorise PSC quality based on morphology have been suggested by some research groups. Kato *et al.*, (2016), for one, developed methods to assess PSC colony morphologies and reported that morphological features may be indicative of the quality of the PSCs in culture. Similarly, Wakui *et al.*, (2017) described morphological classifications distinguishing undifferentiated and differentiated human PSCs. Their report suggested that undifferentiated PSC colonies should have prominent nucleolus, are flat, with well-defined borders, and the cells tightly packed. In contrast, differentiating or differentiated PSCs colonies would have irregular spaces between cells, low nucleus to cytoplasm ratio and contains a darker nucleus since the chromatin undergoes a change in structure to become heterochromatin, consequently losing the transparency in the nuclei, thus masking nucleoli structures. Both the kiPSCs and the piPSCs colonies observed in these early experiments clearly displayed features of undifferentiated PSCs.

Some colonies of piPSCs from passage 38 onwards were observed to host visible spontaneously differentiated cells. This extent of differentiated cell contamination was not observed in kiPSC cultures even after serially passaging up to 4 times (from passage 12 to F.D., de la Raga, PhD Thesis, Aston University, 2022

passage 16). Although, low levels of differentiated cells are commonly found by other groups, owing to the sensitivity of PSCs to their environment (Sathananthan and Trounson, 2005; Nie *et al.*, 2010). Regardless of efforts attempted to remove the differentiated cells from piPSC cultures using ReleSR™, spontaneously differentiated cells continued to occur following serial passaging. Several consecutive passaging with ReleSR™ was required to remove and minimise differentiated cell populations. Differentiation of cells within piPSC cultures could be due to their high passage number. It is known that prolonged cultures of PSCs are prone to acquiring chromosomal aberrations such as chromosomal duplication and deletions (types of aneuploidies). For example, copy number gains of chromosome 12 (or parts of the structure) was reported by Mayshar *et al.*, (2010) to occur as a result of prolonged PSC cultures. Nevertheless, the use of high passage piPSC line was unavoidable as the cells were only available from passage number 37 onwards. Because chromosomal assessment by karyotyping, a technique typically employed to determine chromosome copies, was not performed here for either cell line due to budget and time constraints, it cannot be, therefore, truly confirmed whether chromosomal aberrations are the cause of spontaneous differentiation within the hiPSC cultures.

To further assess the quality of the cells, ICC was used to detect the presence of pluripotency markers. The results showed that both cell lines were positive for OCT4, SOX2, SSEA4 and TRA-1-60 from qualitative assessment of the fluorescent images acquired. However, when quantifying the nuclear markers of pluripotency (OCT4 and SOX2), it was found that cells from both cell lines were less than 70% and 80% positive for OCT4 and SOX2, respectively. This suggests that not all DAPI stained cells expressed these pluripotency markers, therefore, some cells could not be truly considered pluripotent (i.e., could be differentiated cells). Other groups who have employed hiPSCs in TeSR™-E8™ / VTN medium reported > 90%

expression of pluripotency markers such as OCT4 and SSEA4 (G. Chen *et al.*, 2011; Sara M Badenes *et al.*, 2016).

The quality of the hiPSC lines were also confirmed to be poor by low detection of lineage specific markers after directly differentiating towards the three germ lineages: ectoderm, mesoderm, and endoderm. Other cell lines have been reported for trilineage differentiation (Warren *et al.*, 2012; Okumura *et al.*, 2019; Cruvinel *et al.*, 2020). Potentially, the reason for ineffective trilineage differentiation seen in this chapter could be attributed to the employment of VTN as the substrate, which may not have the correct ligands or stimuli to facilitate differentiation of hiPSCs (Smith, Cho and Discher, 2018), especially as cell detachment was observed. A Matrigel substrate control for the differentiation of the cell lines would have been useful to assess whether the VTN substrate was the inhibitory factor for trilineage differentiation.

The growth patterns of the cell lines during 120 h cultures, when seeded at different seeding densities were also observed. Common to all seeding conditions and cell line, was the presence of a lag phase following initial seeding at 0 h. During the lag phase, cells did not expand. In the case of seeding either cell line at  $2 \times 10^4$  cells/cm<sup>2</sup>, VCN decreased following seeding, suggesting that the seeding conditions were suboptimal to support the survival of the hiPSCs. The duration of the lag phase between the different seeding densities were different. Cells seeded at  $2 \times 10^4$  cells/cm<sup>2</sup> had a longer lag phase of ~48 h compared to the ~24 h lag phase seen in the higher seeding densities. kiPSCs also appeared to exit the lag phase earlier than piPSC as suggested by the significantly different DT calculated at 48 h harvest timepoint. This difference was not observed in higher seeding densities. In bioprocesses using cells, the lag phase of cell growth can majorly impact process lengths and timelines, hence, affecting costs of the process. An exponential growth phase was observed following the lag phase, where the VCNs rapidly increase over time.

The results suggested that seeding kiPSCs at  $4 \times 10^4$  cells/cm<sup>2</sup> and expanding for 96 h in the TeSR™-E8™ / VTN culture system would lead to significantly higher quantities of cells compared to piPSC cultures in the same condition.

No significant difference was observed between the growth profiles of the two cell lines after 96 h in culture when initially seeding at  $\geq 4 \times 10^4$  cells/cm<sup>2</sup> condition. This is likely due to colonies enlarging, merging, and saturating the available surface area; hence, the growth curve begins to plateau which is observed when cells are seeded at  $6 \times 10^4$  cells/cm<sup>2</sup> after 96 h in culture. Thus, this demonstrated that the expansion of adherent hiPSC cultures in multi-well plates is limited by the available surface area of the platform. For the continuous propagation of hiPSCs, reaching confluent cultures is detrimental to the quality of the cells, as they would experience contact inhibition consequently reducing their capacity to self-renew and maintain essential intrinsic pluripotency networks (Pavel *et al.*, 2018). Therefore, for the general maintenance and propagation of hiPSC, it was important to passage the cells during their exponential growth phase, disallowing cultures to reach full confluency.

Glucose and lactate concentrations of the medium can affect the expansion potential of hiPSCs (Horiguchi *et al.*, 2018a). Since hiPSC mainly rely on aerobic glycolysis for their ATP generation (Varum *et al.*, 2011; J. Zhang *et al.*, 2012), glucose was used in these experiments as an indicator of cell metabolism (Greuel *et al.*, 2019; Schwedhelm *et al.*, 2019). As a result of aerobic glycolysis, lactate is produced even in the company of abundant oxygen (Teslaa and Teitell, 2015; Nishimura *et al.*, 2019). Metabolic waste products such as ammonium and lactate can have adverse effects on hiPSCs since they can become inhibitory of cell growth.

Generally, both hiPSC lines, regardless of seeding density conditions, displayed similar glucose and lactate profile patterns. When cells undergo the exponential growth phase, ATP demands rise to accommodate for the high energy demanding process of cell division. Glucose

in the medium is metabolised to pyruvate and further into lactate and ATP in the glycolysis cycle. This explains the reduction in glucose concentrations in the medium and higher lactate concentrations. The more cells conducting aerobic glycolysis, the higher the glucose consumption rate is, and the higher the lactate production. The general metabolite trends reported here also follow those described by Horiguchi et al., (2018a).

The overall results from the first set of experiments suggested that the cell population of the kiPSC and piPSC lines may not have been completely homogenous or clonal hiPSCs. It was deemed that both cell lines were generally of poor quality. It was also demonstrated that both cell lines were unable to differentiate effectively towards the germ lineages when reseeded on VTN substrates upon initiation of differentiation. Furthermore, piPSCs showed more spontaneous differentiation and a slightly inferior growth kinetics when compared to that of the kiPSC lines. The employment of poor quality hiPSCs for the production of cell-based therapies poses several issues: (1) it can impact the robustness and reliability of the bioprocess due to the unpredictability of differentiated hiPSC populations; (2) the presence of undesired cell qualities risks product contamination with unwanted or even harmful bioproducts; (3) low quality hiPSCs could lead to inefficient product yields which influence negatively on the costs of the process. Hence, of the two available cell lines, kiPSCs were selected as the more suitable cell line, though not particularly ideal.

### **3.3.2. Establishing the baseline expansion process for kiPSC**

The baseline expansion process was also identified from these experiments. The process consisted of seeding kiPSCs as single cells at  $4 \times 10^4$  cells/cm<sup>2</sup> onto VTN coated well plates and provided with TeSR™-E8™ medium supplemented with 10 μM Y-27632 only for the first 24 h post seeding, to reduce cell death by anoikis. Then, daily 100% medium exchanges were

to be performed up to the point of harvest at 96 h, to avoid reaching 100% confluency and inducing contact inhibition. With this process employed for kiPSCs expansion, a FI of up to  $16.66 \pm 1.19$  times and  $22.30 \pm 1.95$  times can be achieved in 12 well and 6 well plates respectively.

Kato et al., (2018) reported greater FI of 26-28 times when seeding at lower seeding densities of  $1 \times 10^4$  cells/cm<sup>2</sup>. This difference may be due to their use of mTeSR1™ as the growth medium as well as a different substrate (iMatrix-511), different culture lengths and seeding densities.

### **3.3.3. Cost optimisation of the baseline bioprocess**

After establishing the baseline expansion process for hiPSCs, optimisation experiments were performed. These experiments were designed to compare two commercially available medium: TeSR™-E8™ and mTeSR™ Plus. To the best of the author's knowledge, no comparison between TeSR™-E8™ and mTeSR™ Plus medium have been reported in the literature specifically investigating their effects on hiPSC growth kinetics. However, a study comparing mTeSR™ Plus with mTeSR1™ (StemCell technologies) demonstrated that the hiPSCs growth characteristics were relatively the same or improved in mTeSR™ Plus culture systems (Kardel et al., n.d.). A technical bulletin article from StemCell Technologies reported a study comparing mTeSR1™ and TeSR™-E8™ and showed better or comparable results in mTeSR1™. From the experiments conducted in this chapter, the growth characteristics of the hiPSC lines were comparable in mTeSR™ Plus to that of TeSR™-E8™. Cells also expressed the pluripotency markers OCT4 and SSEA4 similarly to that of kiPSCs cultured in TeSR™-E8™ based culture system.

Interestingly, no significant difference in growth characteristics was observed between the two cell lines when cultured using the baseline expansion process using 6 well plate platforms (9.5 cm<sup>2</sup>/well), whereas significant difference was previously observed when using 12 well plate scale (3.9 cm<sup>2</sup>/well). A possible explanation may be due to the different manufacturing standards of different multi-well plates. For example, it was noticed that when seeding cells in different sizes of multi-well plates, cells appeared to pool in the middle of the well or migrate to the corners of the well, rather than being evenly distributed, depending on the size of the well. More studies are needed to investigate whether brand and sizes of the well affect the growth characteristics of hiPSCs.

To decide which medium could efficiently expand hiPSCs, the advantages and disadvantages were identified. First, advantages of the TeSR<sup>TM</sup>-E8<sup>TM</sup> medium included its xeno-free composition and cheaper price (correct at the time of employment for the experiments). The advantages of the mTeSR<sup>TM</sup> Plus medium included its cGMP standard and stabilised growth factors and buffer system to allow for intermittent medium exchange. Hence, several feeding strategies were tested to optimise the cost efficiency of the process.

Data shown in 3.14 implies that the expansion of kiPSCs using feeding strategy 3 resulted in similar VCN yields compared to the control. Though daily medium exchanges were performed in the case of feeding strategy 2, and regardless of removing the metabolic waste products from the culture and simultaneously replenishing the nutrients as frequently as the control, the available nutrients in the reduced volume of medium per culture can affect the expansion of the cells. This may explain the lower harvested VCN at the end of the expansion process under feeding strategy 2 conditions. This data further suggests that nutrient availability is essential to the cells during their exponential growth phase (after 48 h) since increased demands for nutrients are proportional to the increasing number of actively metabolising cells.

When employing mTeSR™ Plus in conjunction with feeding strategy 3, the obtainable total VCN were comparable to the baseline mTeSR™ Plus expansion process. Indeed, the process utilising feeding strategy 3 was significantly more cost effective, thus this was considered the optimised expansion process capable of achieving  $23.86 \pm 1.92$  FI. When propagating kiPSCs through consecutive passaging whilst using the optimised expansion process, no impact on the growth rates of long-term single cell passaging was observed. Cruvinel et al., (2020) who performed similar studies of prolonged sequential single cell passaging also confirmed no significant impact on the growth kinetics of hiPSC over time. It was also demonstrated here that cells maintained the expression of OCT4 over 8 consecutive passages, though this study was only performed at N=1. More repeats of the ICC staining are needed to confirm stability. It would also be beneficial to perform other assays as listed earlier, to fully assure the CQAs of the hiPSCs expanded under this culture system.

#### **3.3.4. kiPSC expanded by the optimised expansion process could differentiate towards NPCs in an integrated bioprocess on planar platforms**

Preliminary neural induction experimental work was conducted but not included in this thesis. Briefly, initial neural induction of kiPSCs were performed according to StemCell Technologies protocol, with slight modifications. VTN was used instead of the recommended PLO/LN or Matrigel. kiPSCs were seeded at  $2 \times 10^5$  cells/cm<sup>2</sup> onto 10 µg/mL VTN coated well plates. kiPSCs were firstly cultured in mTeSR™ Plus medium containing 10 µg/mL Y-27632 for the first 24 h to ensure cell attachment and survival on the substrate. Neural induction was then initiated at day 1 post seeding by replacing the PSC maintenance medium with SNIM + SMADi. As the continued to proliferate under the neural induction conditions, cells eventually became confluent and formed cell sheets which started to detach by day 6 of the neural

induction process. Doubling the VTN concentration to 20  $\mu\text{g}/\text{mL}$  improved the problem with detachment.

In an attempt to reduce the cost of the neural induction process, SNIM medium without SMADi was tested. However, cells fixed for ICC under these conditions did not stain for PAX6 (data not shown here).

From the studies in this chapter, kiPSCs could be expanded using the optimised expansion process on planar platforms in a cost-effective manner, without compromising cell growth kinetics. It was then essential to examine whether the cells expanded in such processes retained the ability to differentiate towards NPCs. The results shown in section 3.2.5 demonstrated that kiPSC can indeed be expanded for 96 h, and subsequently differentiated towards PAX6<sup>+</sup> NPCs in SNIM + SMADi for a further 6 days, as confirmed by ICC after replating the cells onto PLO/LN. However, only  $72.07 \pm 12.69$  % of the cells were PAX6<sup>+</sup>. This was then considered the integrated bioprocess for the production of hiPSC-derived NPCs in planar platforms. Interestingly, cell detachment was not observed, regardless of using 10  $\mu\text{g}/\text{mL}$  of VTN to coat the surfaces of the plates for the expansion phase. It is possible that the substrate was reinforced by the in situ ECM deposition of the proliferating kiPSCs and remodel my MMP activity (K. G. Chen *et al.*, 2014).

The results of this chapter highlight the concerns regarding the quality of the available hiPSC lines. Nevertheless, it was demonstrated that kiPSCs can be expanded and differentiated towards NPCs in a single culture platform.

## **4. Expansion and neural induction of hiPSC on microcarrier platforms**

### **4.1.Introduction**

Using 2D planar platforms to generate clinically relevant quantities of hiPSC-derived NPCs, would require extensive laboratory space to accommodate the proportional numbers of incubators required. Employment of such scale-out strategies to produce hiPSC-derived NPCs at large-scale will be challenging due to the cost of space and the need for technical operators or advanced robots to manipulate multiple culture vessels. In turn, these poses risks of contaminations and mishandling, as well as product quality inhomogeneity due to the potential of batch-to-batch variation amongst different culture vessels.

To circumvent such dilemmas, several groups have developed suspended culture systems which offer efficient utilisation of facility space for cell production (Kumar *et al.*, 2007; Kehoe *et al.*, 2010a; Fan *et al.*, 2014; Andersen *et al.*, 2015; Tohyama *et al.*, 2017; Lavon, Zimmerman and Itskovitz-Eldor, 2017; Sart, Bejoy and Li, 2017; Koenig *et al.*, 2018; Pauly *et al.*, 2018; Chan, Rizwan and Yim, 2020; Miranda *et al.*, 2022). The next steps of this thesis was, therefore, an investigation into whether the integrated expansion and neural induction bioprocesses established in 3 (also referred to in this thesis as the baseline integrated bioprocess), could be translated into an integrated bioprocess utilising 3D suspended culture technologies.

#### **4.1.1.Microcarriers – an enabling technology for scalable culture systems**

Several suspension culture strategies were carefully considered at early stages of this project including expansion and differentiation for hiPSCs as aggregates or on microcarriers.

Considering the limitations of each approach, as outlined in Chapter 1, it was ultimately

decided to explore the microcarrier technologies due to their potential to eliminate the manual picking aspect for replating of aggregates necessary with suspended aggregate expansion and neural induction.

Also, the baseline integrated bioprocess established in 3 was performed on monolayer adherent cultures of hiPSCs using planar platforms. Microcarriers would therefore offer a logistically direct approach to adapt the baseline integrated process into a suspension adherent culture system. Advantageously, key medium components for cell growth, differentiation and/or cell quality maintenance can be homogeneously distributed across the adhered cell monolayers, minimising cell quality variation within the same batches and the formation of necrotic cores.

#### **4.1.2. Choosing a suitable microcarrier**

Although several groups have employed microcarriers for PSC cultures, the rationale behind their choice of microcarrier is often not disclosed or minimally discussed. Some groups have attempted to screen microcarrier to determine the most suitable candidate for PSC cultures, and these have been mainly performed using hESCs, or microcarriers/coatings unsuitable for clinical applications (Phillips *et al.*, 2008; Nie *et al.*, 2010; Bardy *et al.*, 2013; Badenes *et al.*, 2016; Fan *et al.* 2017). The outcomes of these screenings have varied between groups. For example Nie *et al.*, (2010) reported the suitability of Cytodex 3 microcarriers to support hESCs, which have also been confirmed by other groups (Gupta *et al.*, 2016). In contrast, Phillips *et al.*, (2008) reported the poorest growth on Cytodex beads in their screening assays. Other groups have employed different microcarriers such DE53, Plastic and Synthemax II, with varying surface modifications such as addition of ECM protein coating or functionalisation with small molecules and engineering to further improve PSC attachment (Kehoe *et al.*, 2010b; Bardy *et al.*, 2013; Fan *et al.*, 2014; Gupta *et al.*, 2016).

The current literature suggests that the suitable microcarrier for hiPSCs may be cell line and culture system dependent, thus in this chapter, a systematic microcarrier screening was performed in order to identify the suitable microcarrier specifically for the maintenance of the kiPSC line. The screening process of 8 commercially available microcarriers were performed in 3 steps. First, the microcarriers, in their native non-modified state, were tested for their ability to support kiPSC attachment and growth in static conditions. Second, it was investigated whether the addition of VTN to the native surfaces of different microcarriers could further support the growth of kiPSCs in static conditions. Finally, the screening of VTN coated microcarriers were then performed in rocking conditions to investigate whether dynamic conditions could further improve cell growth.

To fully translate the baseline integrated bioprocess from Chapter 3 to microcarrier platforms, it was also important to consider the neural induction process. Thus, the microcarrier of choice was assessed for its ability to support neural induction of the kiPSC line towards NPCs in this chapter.

#### **4.1.3. Chapter aims and objectives**

The main aim of this chapter is to develop an integrated bioprocess for the expansion and neural induction of hiPSCs on microcarriers. This would enable the development of a process using dynamic 3D suspended culture systems and STBs, which are scalable and relevant for clinical productions of hiPSC-derived NPCs.

To realise this aim, several objectives were set for this chapter:

- 1) To identify a suitable microcarrier for kiPSC expansion by performing systematic screenings of 8 commercially available microcarriers. The selection of the suitable microcarrier will be based on a set of criteria verified by analytical techniques such as

phase contrast microscopy, cell counting, live/dead staining, metabolite analysis and

ICC. The suitable microcarrier should be able to:

- i. support kiPSC attachment and adhesion,
  - ii. promote kiPSC expansion,
  - iii. maintain kiPSC pluripotency during expansion,
  - iv. be amenable for a defined and xeno-free culture system,
- 2) To assess the potential of the identified suitable microcarrier as a platform for the neural induction of kiPSC. The selected microcarrier should also be able to allow for neural lineage commitment of kiPSCs and confirmed by the expression of neural lineage markers.

## **4.2.Results**

### **4.2.1.Screening of commercially available non-modified microcarriers in static conditions**

The first steps towards development of a 3D suspension culture system, was to identify a suitable microcarrier for the expansion and differentiation of the kiPSC line, according to the set of criteria mentioned previously. Thus, screening assays of commercially available microcarriers were performed. Briefly, 3 cm<sup>2</sup> of Collagen, Cytodex 1, Cytodex 3, Fact III, Hillex, Plastic, Plastic Plus and Pronectin were prepared on ULA 24 well plates for screening. kiPSCs (from passage 14 – passage 16) were seeded at 4 x 10<sup>4</sup> cells/cm<sup>2</sup> into wells with microcarriers and imaged using a phase contrast microscope throughout 96 h in culture. 3cm<sup>2</sup> was chosen as this concentration of microcarriers covered the well surface without forming multiple layers of beads that would distort and block visualisation of cultures using the microscope. Control wells contained no microcarriers and any suspended cells were removed from the wells 24 h by a complete 100 % medium exchange. This was performed to demonstrate that cells do not adhere onto the surface of the ULA plates and confirmed by the absence of attached cells in Figure I for control wells. The positive control were kiPSCs grown in the optimised baseline expansion process to confirm the functional attribute of the kiPSC used to attach, adhere, and spread onto standard TCP planar platforms coated with VTN.

#### **4.2.1.1.Morphology of kiPSCs on commercially available non-modified microcarriers in multi-well plates**

Phase contrast images of kiPSCs 96 h after seeding into wells with native microcarriers showed successful attachment and adhesion onto Collagen, FACT III and Hillex microcarrier surfaces Figure 4.1. Both Collagen and FACT III have type I porcine collagen coatings. PSCs are expected to bind to collagen substrates via  $\beta$ 1 integrins when associated with  $\alpha$ 1,  $\alpha$ 2,  $\alpha$ 10, and

$\alpha 11$  subunits (Santoro *et al.*, 2019), therefore it was anticipated that kiPSCs would attach onto Collagen and FACT III microcarriers. Interestingly, Cytodex 3 which are also coated with type 1 porcine collagen, did not efficiently promote kiPSC attachment.

In the case of Hillex microcarriers which are not coated with type 1 porcine collagen, kiPSCs were able to attach and adhere onto its native surface chemistry made of cationic trimethyl ammonium. kiPSCs formed large cell-microcarrier complexes with Hillex microcarriers after 96 h in culture. Hillex microcarriers also absorbed the phenol red indicator components of the medium, leading to the red tint to the microcarriers under phase contrast imaging as seen in Figure 4.1.

kiPSCs did not establish successful attachment and adhesion onto native Cytodex 1, Cytodex 3, Plastic, Plastic Plus, and Pronectin microcarriers. Instead, cell-cell aggregates formed in between microcarriers as indicated by the orange arrows in Figure 4.1 B, C, F, G and H. Live/dead staining of cultures at 48 h in culture also confirms that cell-cell aggregates remained viable as shown by the green fluorescent markers indicating Calcein AM in Figure 4.2. Ethidium homodimer staining in the same figure indicated the presence of some dead cells which were mainly found within cell-cell or cell-microcarrier aggregates.

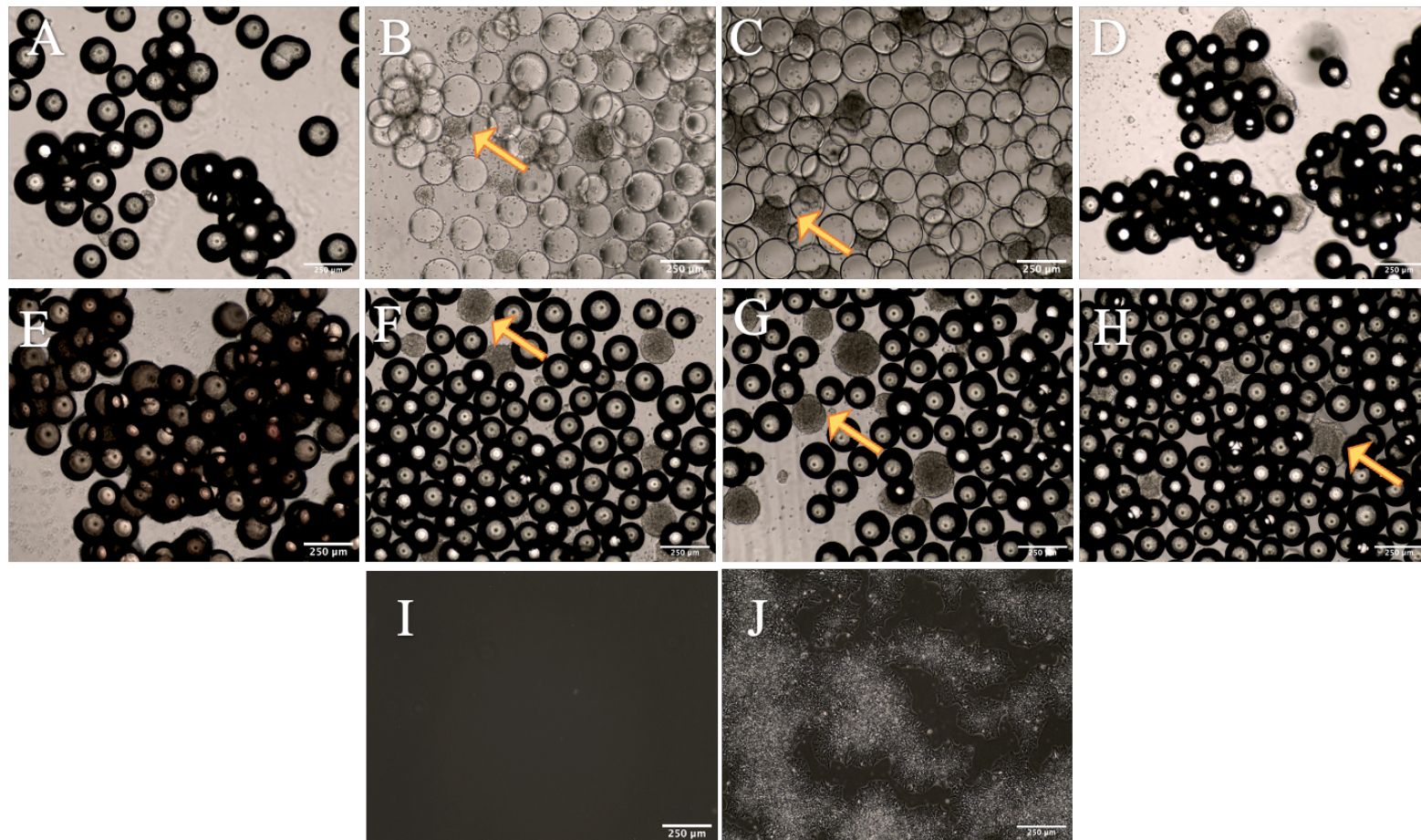


Figure 4.1. Phase contrast images kiPSCs 96 h post seeding on native microcarriers for screening. Images are representative of commercially available microcarrier seeded with  $4 \times 10^4$  cells/cm<sup>2</sup> kiPSCs and taken from 2 random areas at the centre of the well. The microcarriers shown include Collagen (A), Cytodex 1 (B), Cytodex 3 (C), FACT III (D), Hillex (E), Plastic (F), Plastic Plus (G), and Pronectin (H). The negative control wells contained no microcarriers (I). Images for the positive control wells (J) were taken after 96 h c on VTN coated well plates seeded at the same density. Scale bar = 250 µm. N=3, biological repeats.

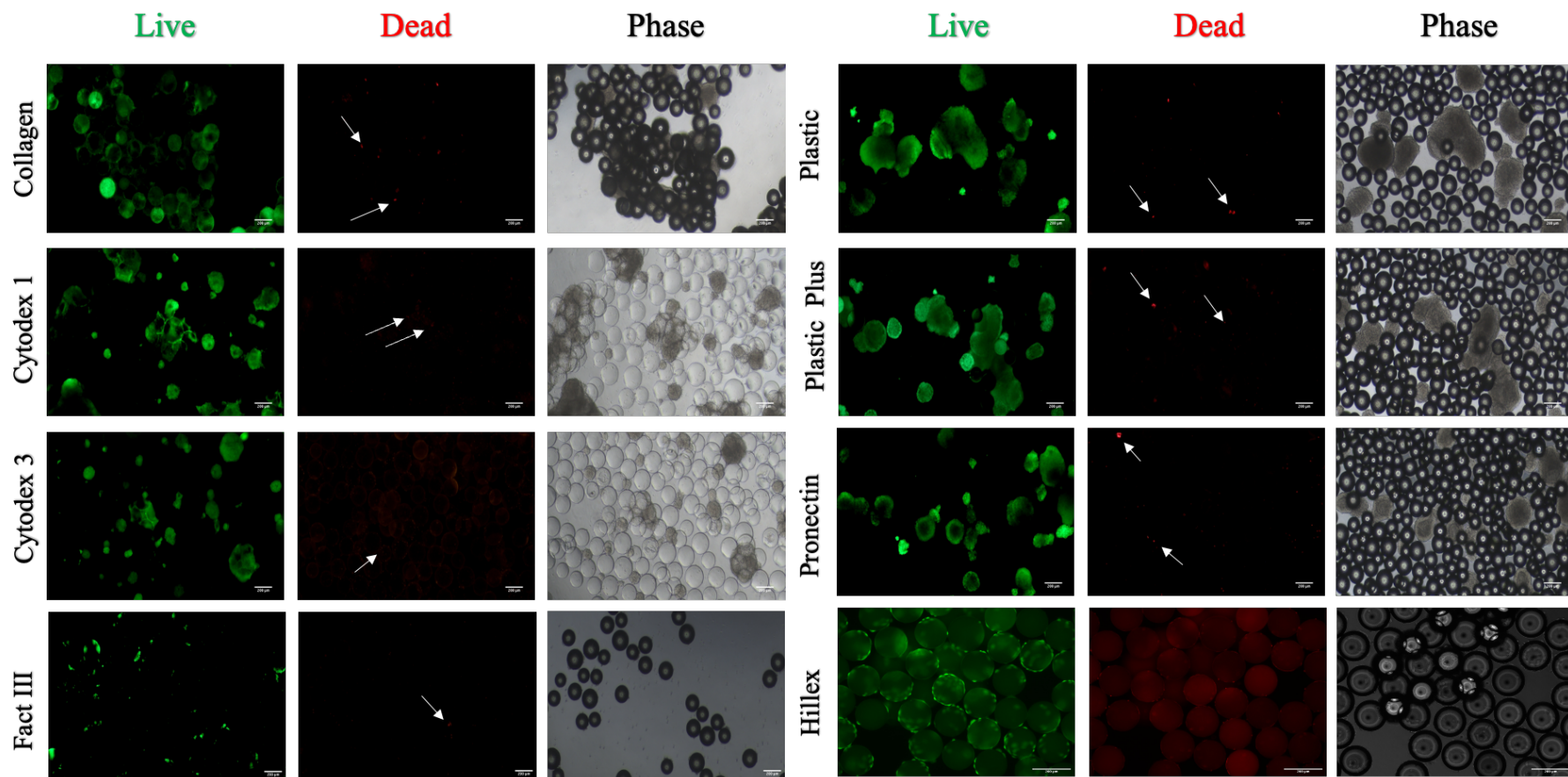


Figure 4.2. Representative examples of Live/dead staining of kiPSCs at 48 h of the native microcarrier screening assay. Green fluorescent cells indicate live/viable due to the uptake of Calcein AM. Cells in red are stained with ethidium homodimer indicating compromise of cell surface membrane integrity and loss of viability. Images are representative of 2 random areas taken from the centre of the wells. N=1 biological repeat.

#### **4.2.2. Screening of VTN coated microcarriers under static conditions**

After the initial screening experiments using native microcarriers, which showed poor cell attachment on most microcarriers, the next avenue was to investigate whether cell attachment and adhesion could be improved by modifying the microcarrier surfaces with the addition of VTN substrates. Recombinant VTN was chosen due to suitability in xeno-free cultures systems as compared to Matrigel or Geltrex. A similar screening assay to that conducted in section 4.2.1 was performed with VTN coated microcarriers. The passage number of the kiPSC used in these experiments were between passaged 12 to 14. The negative control wells which contained no microcarriers, again showed no cells, whilst the positive control wells demonstrated the ability of kiPSC to attach, adhere, spread, and form colonies on VTN coated TCP multi well plates

Following 96 h of incubation, a total cell count (TCC) was obtained using the count of aggregated cell reagent A100 and B protocol on the Nucleocounter. This was also compared with the TCC obtained after performing the microcarrier harvest process described in 2.6.6. This was conducted to assess whether the harvest process caused cell loss, hence the harvesting efficiency later reported within this section.

##### **4.2.2.1. Morphology of kiPSCs on VTN coated microcarriers in static conditions**

When visualised under a phase contrast microscope 1 h post seeding, the single cell seeded kiPSCs appeared to attach onto all VTN coated microcarrier in static conditions as seen in Figure 4.3A. Images of initial kiPSC attachment onto VTN microcarriers reveal the rounded shape of cells during initial attachment, appearing to have little cell-microcarrier contact. Examples of these rounded cell morphologies 1 h after seeding are shown in Figure 3A for Plastic and Cytodex 1 microcarriers. These cell morphologies at 1 h were similar across all VTN coated microcarriers.

Once cells establish attachment and adhesion after 24 h, cell spreading was observed as indicated by a change from the round cell morphologies at the 1 h timepoint to a flatter morphology on the bead surfaces as indicated by the arrows in Figure 4.3B. Again, this change in cell shape was observed across all microcarrier types.

Live/dead images of cells at 48 h in culture further confirmed the flat morphologies of the cells on the surfaces of VTN coated microcarriers (Figure 4.4). Dead cells were marked with ethidium homodimer (red staining) and are found also attached onto the surface of some microcarriers, mainly Cytodex microcarriers (Figure 4.4).

By 96 h in culture, kiPSC formed large cell-microcarrier aggregate complexes which varied in size and observed across all VTN coated microcarriers screened (Figure 4.5). VTN coated Plastic, Plastic Plus, Pronectin, Cytodex 1 and Cytodex 3 supported cell attachment, adhesion and cell expansion shown by the phase contrast images and live/dead staining throughout the timepoints of the screening. This contrasts with their native or non-modified state reported in Section 4.2.2. Interesting to note was the observation of cell-microcarrier aggregates collecting in the centre of the well forming aggregates larger than 250  $\mu\text{m}$ .

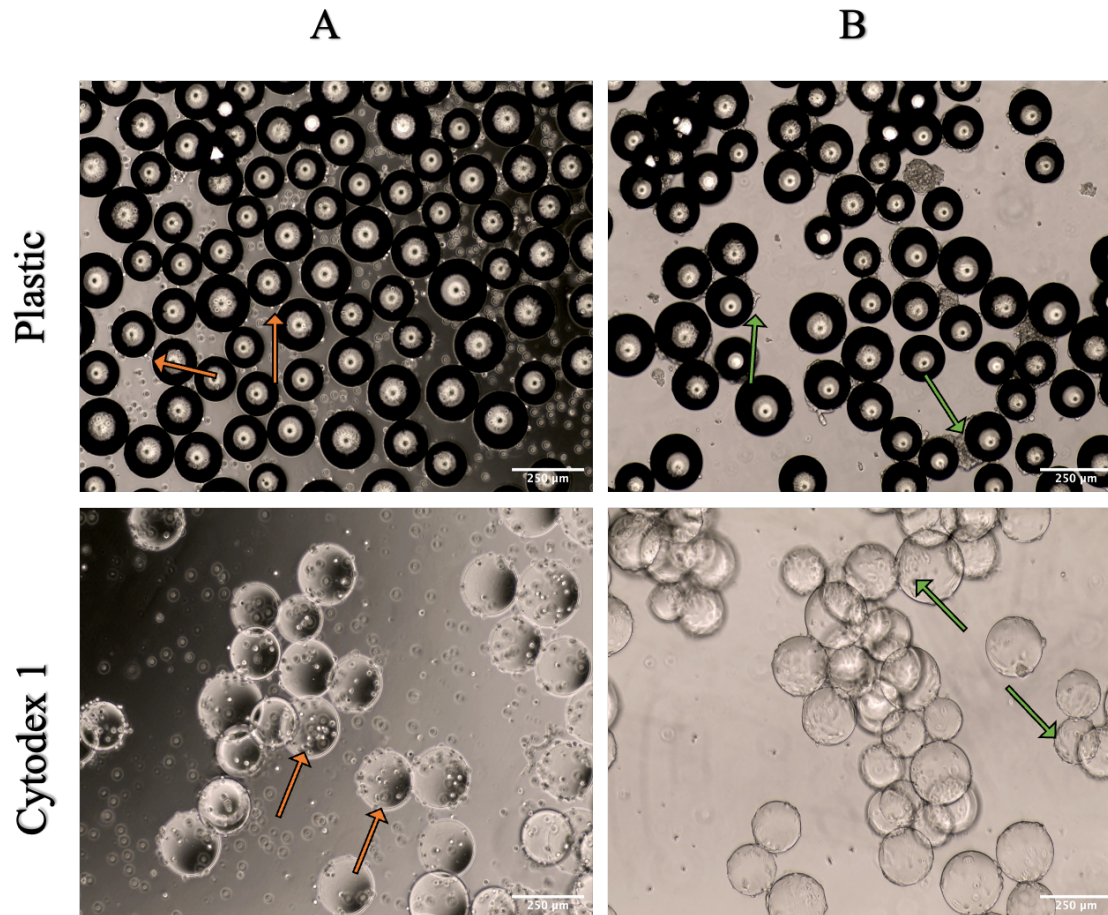


Figure 4.3. Example phase contrast images of kiPSC and their initial attachment compared to established adhesion morphologies on VTN coated microcarriers. Images were obtained 1 h (A) and 24 h (B) post seeding of kiPSCs at a density of  $4 \times 10^4$  cells/cm<sup>2</sup> on 3 cm<sup>2</sup> surface area of VTN coated Plastic and Cytodex 1 microcarriers. Plastic and Cytodex 1 were chosen as representatives for polystyrene and dextran core microcarriers, respectively. Cell morphologies at these timepoints were similar across all microcarrier types. Orange arrows indicate initial cell attachment and rounded cell morphologies. Green arrows indicate adhered kiPSCs which are flatter and spread on the surface. Bridging of two or more microcarriers by cells in between can also be observed at 24 h in culture (green arrow). N=3, biological repeats.

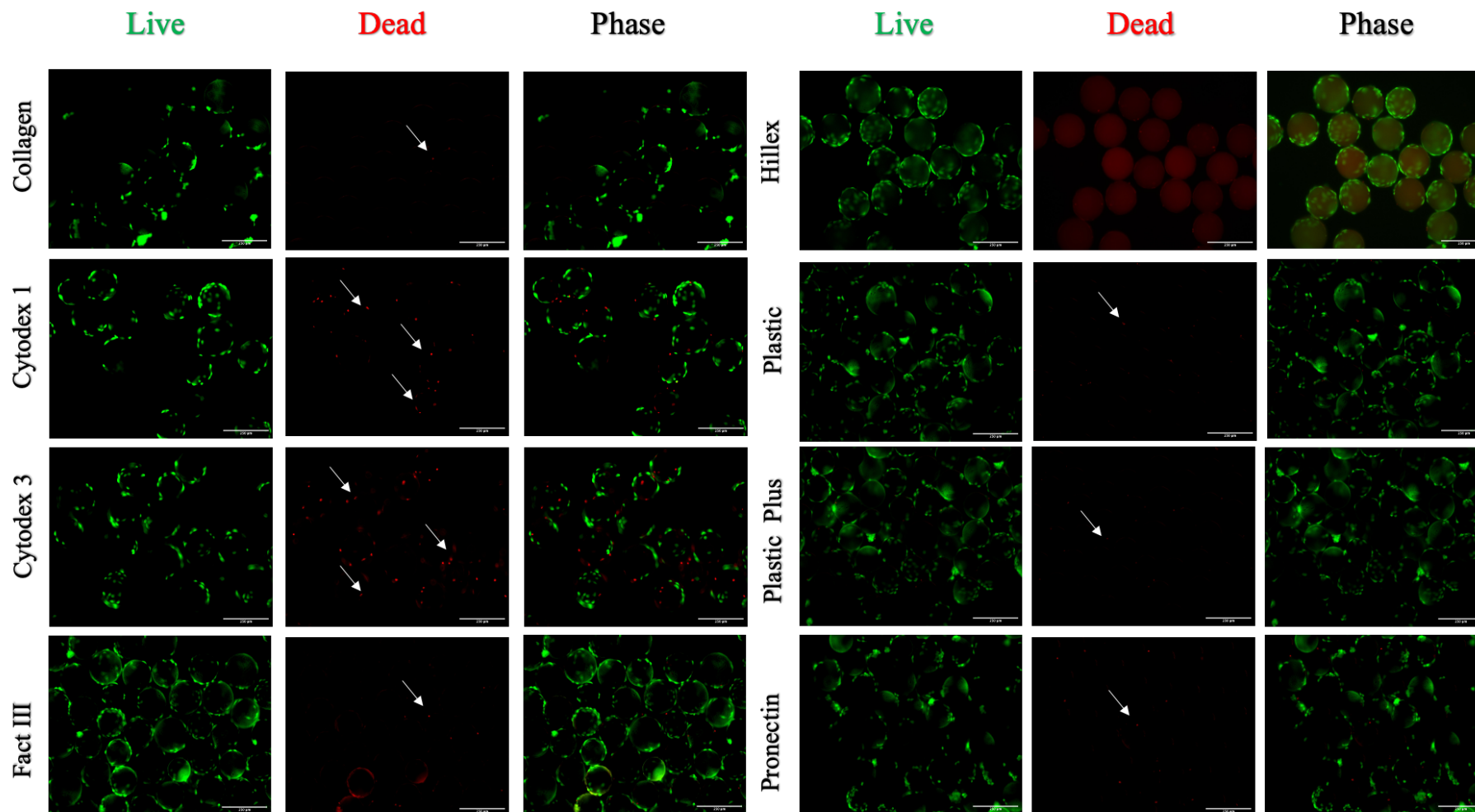


Figure 4.4. Representative examples of Live/dead staining of kiPSCs at 48 h of the native microcarrier screening assay. Green fluorescent cells indicate live/viable due to the uptake of Calcein AM. Cells in red are stained with ethidium homodimer indicating compromise of cell surface membrane integrity and loss of viability. Images are representative of 2 random areas taken from the centre of the wells. N=2 biological repeat

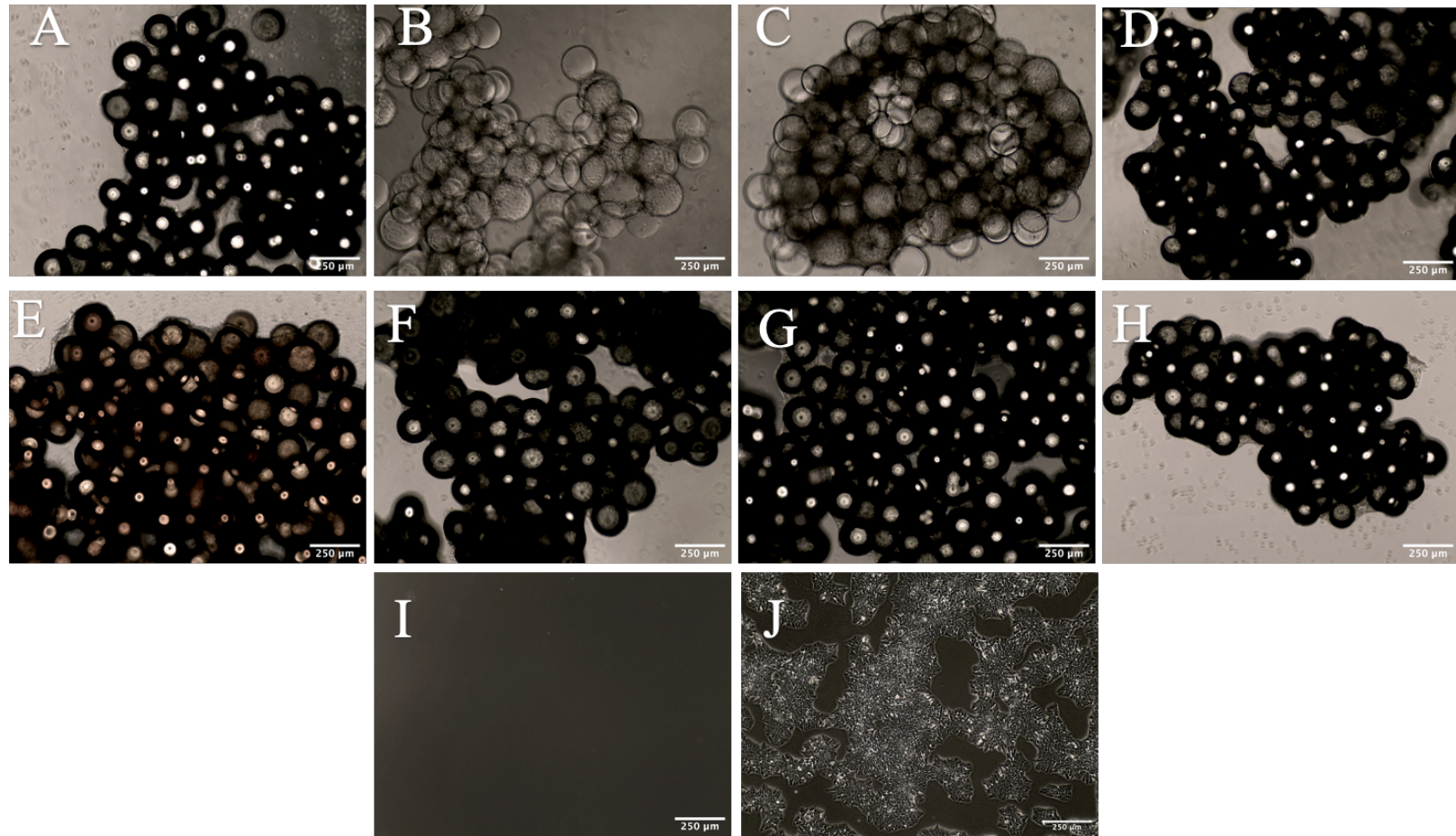


Figure 4.5. Phase contrast images of VTN coated microcarrier screening after 96 h in culture. Images are representative of VTN coated microcarrier seeded with kiPSC at a density of  $4 \times 10^4$  cells/cm<sup>2</sup> and taken from 2 random areas at the centre of the well at 96 h in culture. Images were obtained at two random locations at the centre of the wells. The microcarriers used include Collagen (A), Cytodex 1 (B), Cytodex 3 (C), FACT III (D), Hillex (E), Plastic (F), Plastic Plus (G), and Pronectin (H). The negative control wells contained no microcarriers (I). Images for the positive control wells (J) were taken from cultures of kiPSC on VTN coated TCP multi-well plates. Scale bar = 250 µm. N=3, biological repeats.

#### **4.2.2.2. Viability and growth kinetics of kiPSCs on VTN coated microcarriers in static conditions**

kiPSCs were visually confirmed to be attached and adhered onto VTN coated microcarriers using phase contrast microscopy. After 96 h incubation, the viability and VCN, adjusted to the VCN per cm<sup>2</sup> (VCN/cm<sup>2</sup>), were obtained post-harvest from VTN coated microcarrier and the results are shown in Figure 4.6. The negative control wells confirmed no cell growth on the ULA well plate surfaces as no cell viability of VCN was measured. Thus, growth kinetic calculations for the negative control wells are not applicable.

Cell viabilities from all microcarrier conditions, except Cytodex 3 ( $79.67 \pm 11.45$  %) and Cytodex 1 ( $64.80 \pm 19.51$  %; significantly lower compared to most microcarriers), were on average above 85% after harvesting. This was comparable to the positive control on the standard TCP well plates ( $94.37 \pm 4.3$  %). Cell viability from VTN coated Cytodex 1 cultures was shown to be the only condition significantly lower than the control ( $p < 0.0001$ ).

The VCN/cm<sup>2</sup> obtained from VTN coated Collagen ( $2.91 \pm 0.42 \times 10^5$ ), Cytodex 3 ( $2.20 \pm 0.58 \times 10^5$ ), Fact III ( $3.23 \pm 0.62 \times 10^5$ ), Hillex ( $3.22 \pm 0.12 \times 10^5$ ), Plastic ( $3.78 \pm 0.56 \times 10^5$ ), Plastic Plus ( $3.76 \pm 0.71 \times 10^5$ ) and Pronectin ( $3.16 \pm 0.18 \times 10^5$ ) were all comparable to each other as no significant differences were found. VCN harvested from VTN coated Cytodex 1 ( $1.30 \pm 0.36 \times 10^5$  VCN/cm<sup>2</sup>) were significantly lower compared to all other microcarriers except Collagen and Cytodex 3 (Figure 4.6). Nonetheless, all VTN coated microcarriers yielded less VCN/cm<sup>2</sup> compared to the positive control well on standard TCP VTN coated planar platforms which provided a harvest of  $8.92 \pm 1.20 \times 10^5$  cells/cm<sup>2</sup>.

The SPGR of kiPSC on all VTN coated microcarriers were significantly lower than the positive control ( $0.033 \pm 0.001$ ), with Collagen, Cytodex 1 and Cytodex 3 being the most significant

( $p < 0.0001$ ). VTN coated Plastic was the least significantly different to the positive control ( $0.024 \pm 0.001$ ;  $p = 0.0014$ ; Figure 4.7A)

kiPSC DT were calculated for all microcarriers and control after 96 h. The positive control DT was calculated at  $21.09 \pm 0.59$  h which was significantly faster than Cytodex 1 ( $42.33 \pm 8.09$  h;  $p < 0.0001$ ) and Cytodex 3 ( $35.62 \pm 7.48$  h;  $p = 0.0058$ ). Generally, the DT of kiPSC on VTN coated Cytodex 1 were poorer when compared to other microcarriers. Although the DT data in Figure 4.7B shows differences of  $\sim 10$  h when comparing the positive control to the conditions of non-Cytodex based microcarrier, the statistical analysis One-way Anova, with Tukey's multiple comparison test, found no significant difference.

kiPSC growth on VTN coated Cytodex 1 were significantly smaller compared to growth on VTN coated Plastic and Plastic Plus microcarriers. This is indicated by the smaller FI calculated for kiPSCs on VTN coated Cytodex 1 ( $3.25 \pm 0.90$  times) compared to kiPSC on VTN coated Plastic and Plastic Plus which reached FIs of  $10.36 \pm 1.00$  ( $p = 0.011$ ) and  $10.13 \pm 1.72$  ( $p = 0.016$ ), respectively (Figure 4.7C). However, all microcarrier conditions yielded significantly lower FI compared to the positive control ( $23.57 \pm 2.07$  FI;  $p < 0.0001$ ).

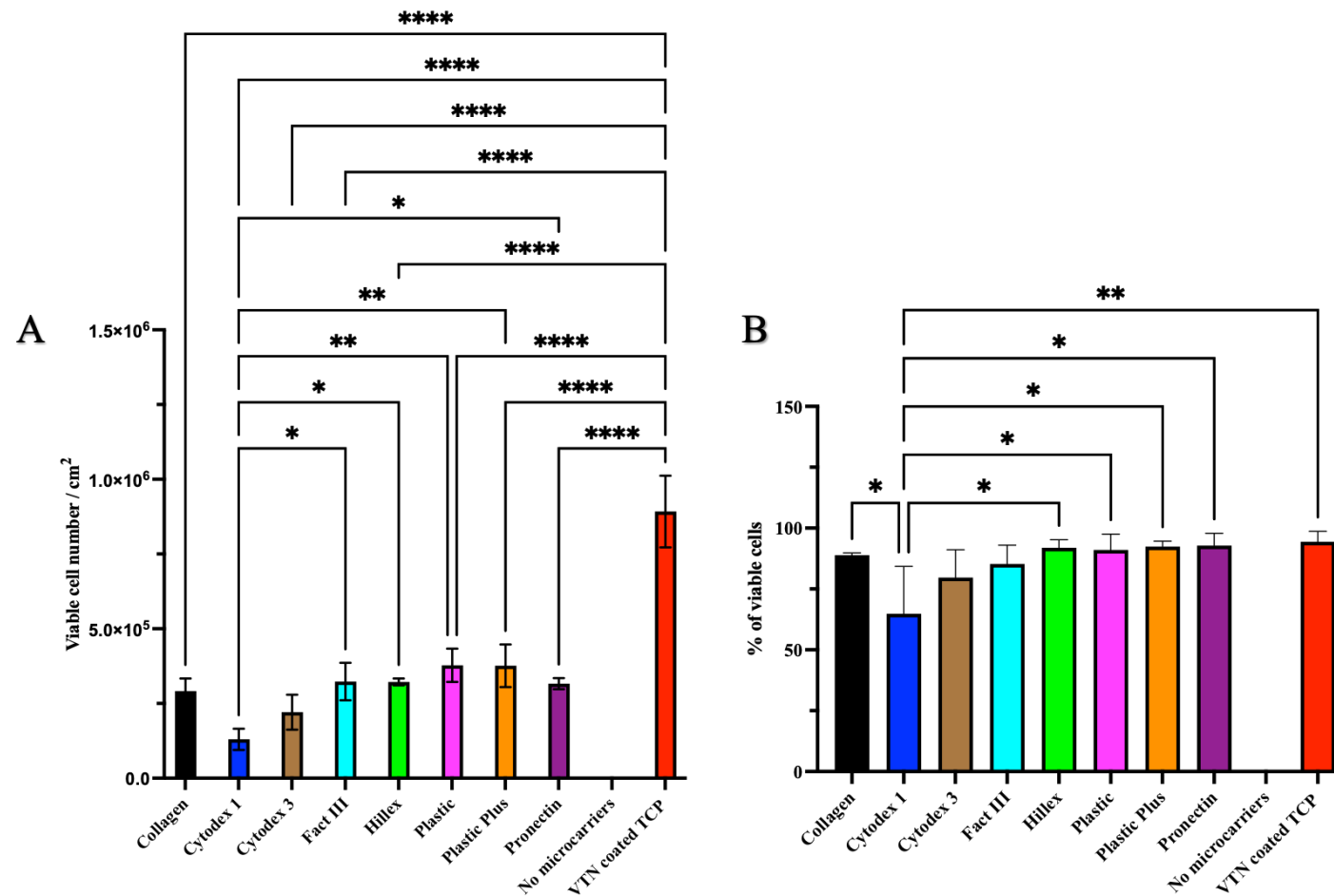


Figure 4.6. Viability and VCN/cm<sup>2</sup> of kiPSCs after harvesting from the screened VTN coated microcarriers. kiPSC were harvested 96 h after seeding onto 8 different VTN coated microcarriers and the viability and VCN were obtained. Negative control were ULA wells seeded with kiPSC at 0 h, followed by the removal of suspended cells at 24 h. No cells were detected attached onto the ULA. The positive control were cultures of kiPSCs on TCP multi-well plates coated with VTN and harvested after 96 h in incubation. The VCN were adjusted to VCN/cm<sup>2</sup> and shown in (A). The viability of the cells was also obtained (B). The data is presented as mean  $\pm$  SD. N = 3, biological repeats \* $p \leq 0.05$ , \*\*\* $p < 0.001$  and \*\*\*\* $p < 0.0001$ , one-way ANOVA, Tukey's multiple t-test.

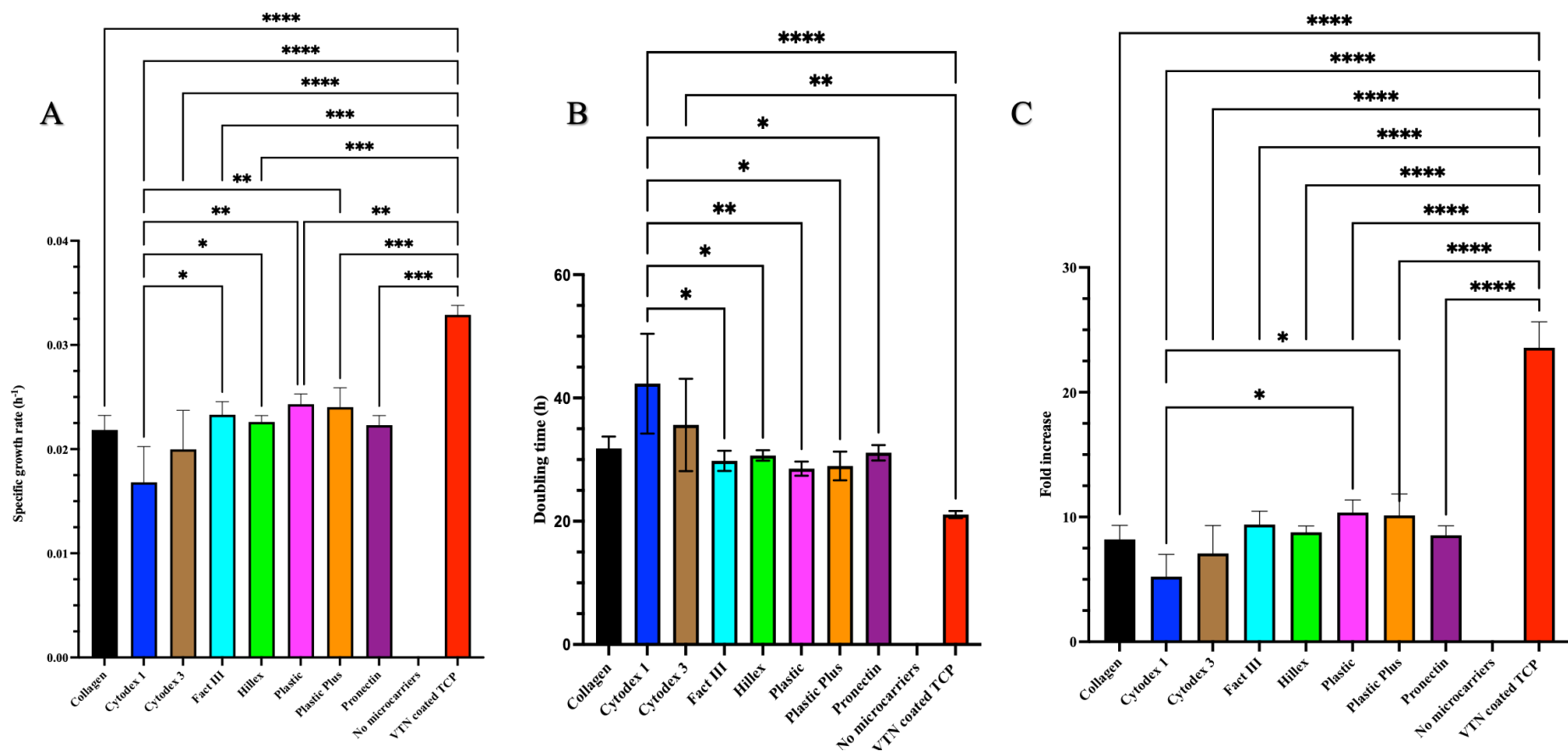


Figure 4.7. Growth kinetics of kiPSC during the screening of VTN coated microcarriers. kiPSC were harvested from 8 VTN coated microcarriers 96 h post seeding at  $4 \times 10^4$  cells/cm<sup>2</sup>. Negative control (no microcarrier) were ULA wells seeded with kiPSC at 0 h, followed by the removal of suspended cells at 24 h. No cells were detected attached onto the ULA. The positive control (VTN coated TCP) were cultures of kiPSCs on TCP multi-well plates coated with VTN and harvested after 96 h in incubation. VCN were obtained at harvest and the SPGR (A), DT (B) and FI (C) were calculated. Cytodex microcarriers generally performed poorer in terms of permitting kiPSC growth compared to others. Overall, all microcarriers performed poorly compared to the positive control. Data is shown as mean  $\pm$  SD. N = 3, biological repeats. \*p  $\leq$  0.05, \*\*p < 0.01, \*\*\*p < 0.001 and \*\*\*\*p < 0.0001, one-way ANOVA, Tukey's multiple t-test.

#### **4.2.2.3. Glucose and lactate profiles of kiPSCs cultured on VTN coated microcarriers in static conditions**

The metabolic profiles during the screening of VTN coated microcarriers were measured and used as indicators of growth activity. Medium samples from each condition were taken before and after medium exchanges, then analysed for glucose and lactate concentrations throughout the 96 h culture period.

Generally, for all conditions of the screening except the negative control, a similar glucose and lactate profile was observed to that in Chapter 3 (Figure 13D; conditions of the positive control) for the expansion of kiPSCs on planar platform was observed: glucose concentrations are replenished after medium exchanges (indicated by a sudden spike upwards) whilst lactate concentrations sharply decreases (indicated by a sudden spike downwards), as seen in and Figure 4.8 and 4.9 Figure 4.9. , respectively.

Stock mTeSR<sup>TM</sup>-Plus medium was measured to contain ~13 mmol/L of glucose. The lactate concentration of the stock medium was 0 mM (below the limits of detection). Control wells containing no microcarriers showed a decrease in glucose and corresponding small increase in lactate concentrations after 24 h. This accounts for the glucose consumption of cells that survived in suspension. Their subsequent removal after a 100% medium exchange was confirmed with no further metabolic activity within the negative control wells for the duration of the screening period. However, it was realised that for the microcarrier conditions, glucose concentration do not fully replenish to the stock glucose concentration following medium exchange since only 50 % of the medium are exchange, thus diluting the glucose concentrations. Similarly, lactate concentrations are not depleted to 0 mM after each medium exchange due to residual lactate molecules in the 50 % medium which are not removed.

For kiPSC cultures on VTN coated Collagen, Cytodex 3, Hillex, Plastic, Plastic Plus and Pronectin microcarriers, the glucose and lactate concentration trends were similar (Figure 4.8 and 4.9). The glucose and lactate profiles of cultures with VTN coated Cytodex 1 remained comparable to the profiles of cultures on other microcarriers throughout the first 48 h of the culture. After 48 h, the glucose consumption of cultures with VTN coated Cytodex 1, were noticeably less in comparison to cultures with other microcarriers. This differentiation is also true for the lactate profile of cultures in VTN coated Cytodex 1, whereby lactate production by 96 h in culture was recorded lowest amongst other conditions.

The calculated lactate yield for each microcarrier condition from 1 mol of glucose ranged from ~1.5 – ~2.4 mol throughout the duration of the screening.

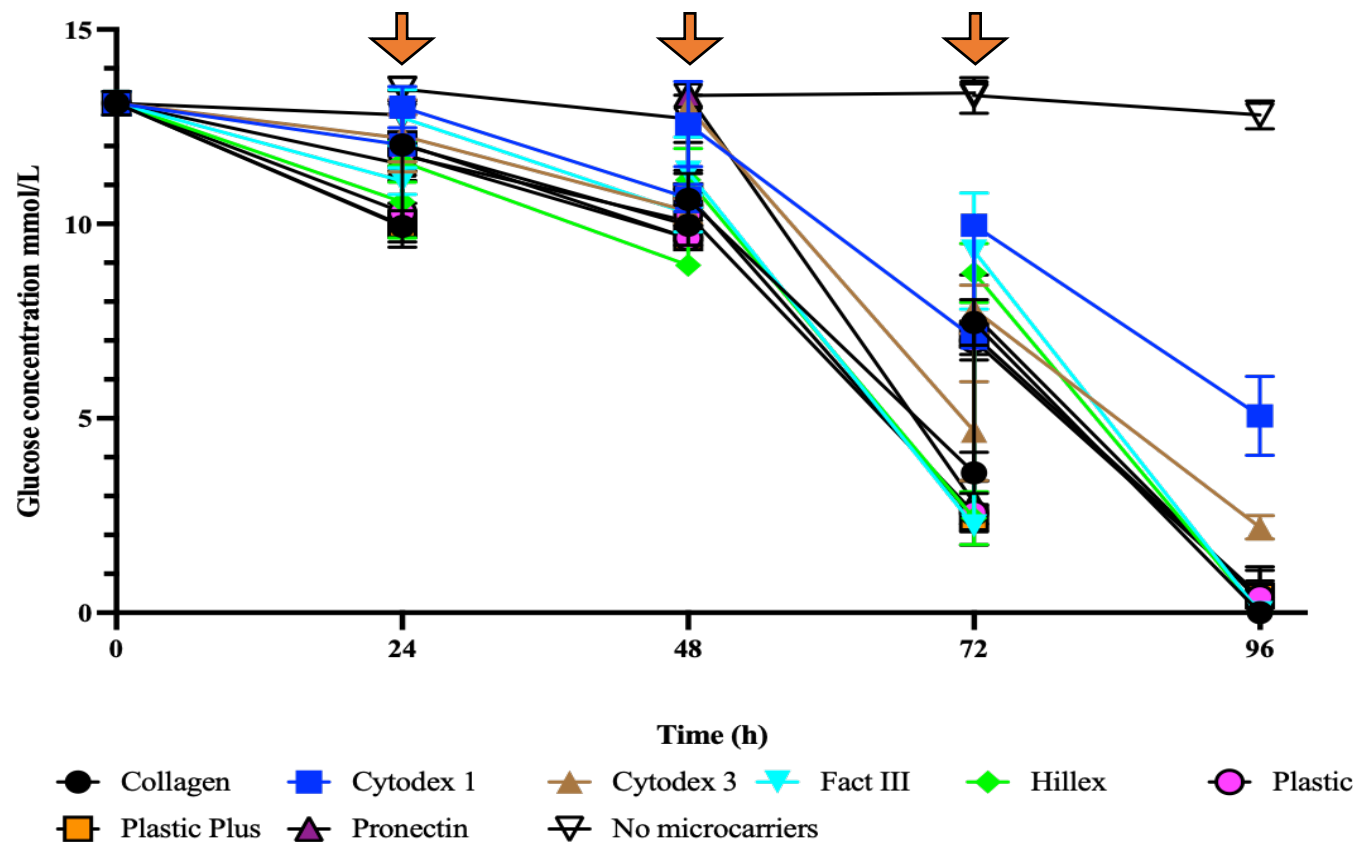


Figure 4.8. Glucose concentrations of kiPSCs cultures during the screening of different VTN coated microcarriers. 8 different microcarriers (shown in the key) were coated with VTN and seeded with kiPSCs at  $4 \times 10^4$  cells/cm<sup>2</sup> in static cultures on ULA well plates. Glucose concentrations were recorded at the start of the culture (0 h) then before and after each medium exchanges performed every 24 h (indicated by the arrows). The data here shows an overall decreasing trend of glucose as cultures progresses in all cases except for the negative control which contained no microcarriers and no cells attached onto the ULA. Data is presented as the mean  $\pm$  SD. N = 3, biological repeat.

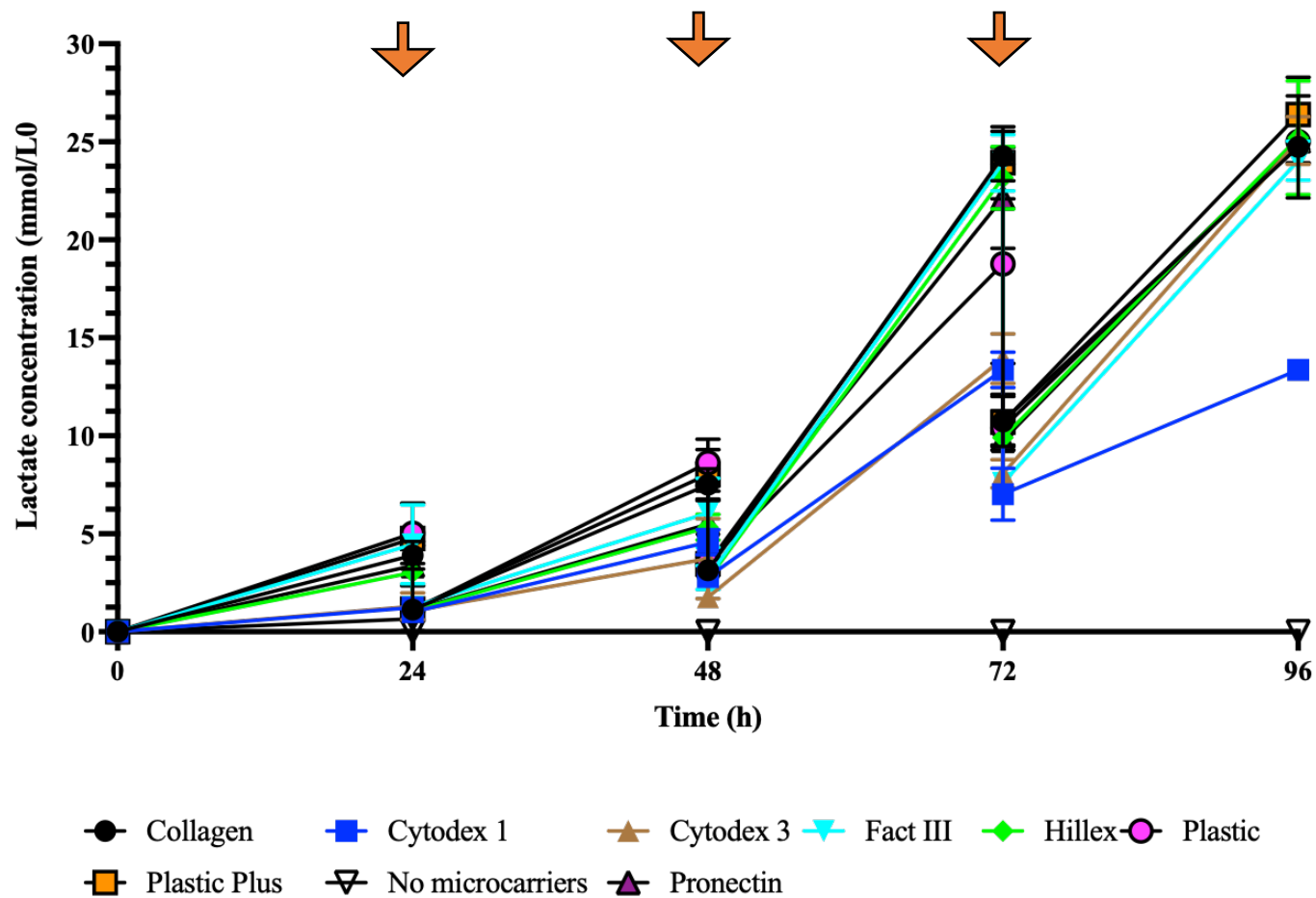


Figure 4.9. Lactate concentrations of kiPSCs cultures during the screening of different VTN coated microcarriers. 8 different microcarriers (shown in the key) were coated with VTN and seeded with kiPSCS at  $4 \times 10^4$  cells/cm<sup>2</sup> in static cultures on ULA well plates. Lactate concentrations were recorded at the start of the culture (0 h) and then before and after each medium exchanges performed every 24 h (indicated by the arrows). The data here shows an overall increasing trend of lactate as the cultures progresses in all conditions except for the negative control which contained no microcarriers and no cells attached onto the ULA. Control lactate concentrations remained low throughout. Data is presented as the mean  $\pm$  SD. N = 3, biological repeats.

### **4.2.3. Determining the efficiency of the harvest process of kiPSCs from VTN-coated microcarriers in static conditions**

After observing low VCN obtained from the VTN coated microcarrier compared to cultures on VTN coated TCP planar platforms, it was questioned whether the obtainable cells could be limited by the harvest process. To determine whether the harvest process from VTN microcarriers was efficient at detaching the cells from microcarriers, it was decided to compare the cell counts before and after the harvest process. Thus, direct cell counting method on microcarriers was used and such procedures are described in section 2.7.1. This method of cell counting only provides TCC (i.e., counts both viable and dead cells), hence, it was compared to the TCC data of each respective microcarrier condition obtained from section 4.2.2. Briefly, an identical experimental setup of the screening assay in section 4.2.2 was prepared. However, instead of harvesting after 96 h in culture, the cell-laden microcarriers were analysed for TCC directly on microcarriers using the method. This was considered the expected TCC yield, whilst the harvest yield was the obtainable TCC following the harvest procedure. The passage number of the kiPSC used in these experiments were passaged 12 to 14.

#### **4.2.3.1. Comparison of the total cell count before and after the harvest process**

When comparing the actual harvested TCC yield to the expected TCC yield, significantly lower TCC were obtained for all conditions following the harvest process (Figure 4.10A). kiPSC cultures on VTN coated Collagen were the most significantly affected ( $p < 0.0001$ ) by the harvest process with only  $61.84 \pm 9.42\%$  of the TCC recovered. Similarly, the TCC recovered from the harvest process of VTN coated Cytodex 1 cultures were only  $57.20 \pm 18.92\%$ . Interestingly the TCC obtained directly on the VTN coated Cytodex 1 microcarriers was relatively lower ( $1.09 \pm 0.11 \times 10^6$  TCC) compared to that of other microcarrier conditions (e.g., FACT III,  $1.54 \pm 0.95 \times 10^6$ ; Hillex,  $1.44 \pm 0.95 \times 10^6$ ; Plastic Plus  $1.61 \pm 0.59 \times 10^6$ ).

VTN coated Plastic microcarrier cultures were least significantly impacted by the harvest process ( $p=0.017$ ), yet, when comparing the harvest efficiency of VTN coated microcarriers to the most significantly affect (Collagen), it was comparable ( $61.84 \pm 9.42$  vs  $77.53 \pm 6.92$  %, respectively). In fact, the harvest efficiency was not significantly different between all microcarrier conditions (Figure 4.10B)

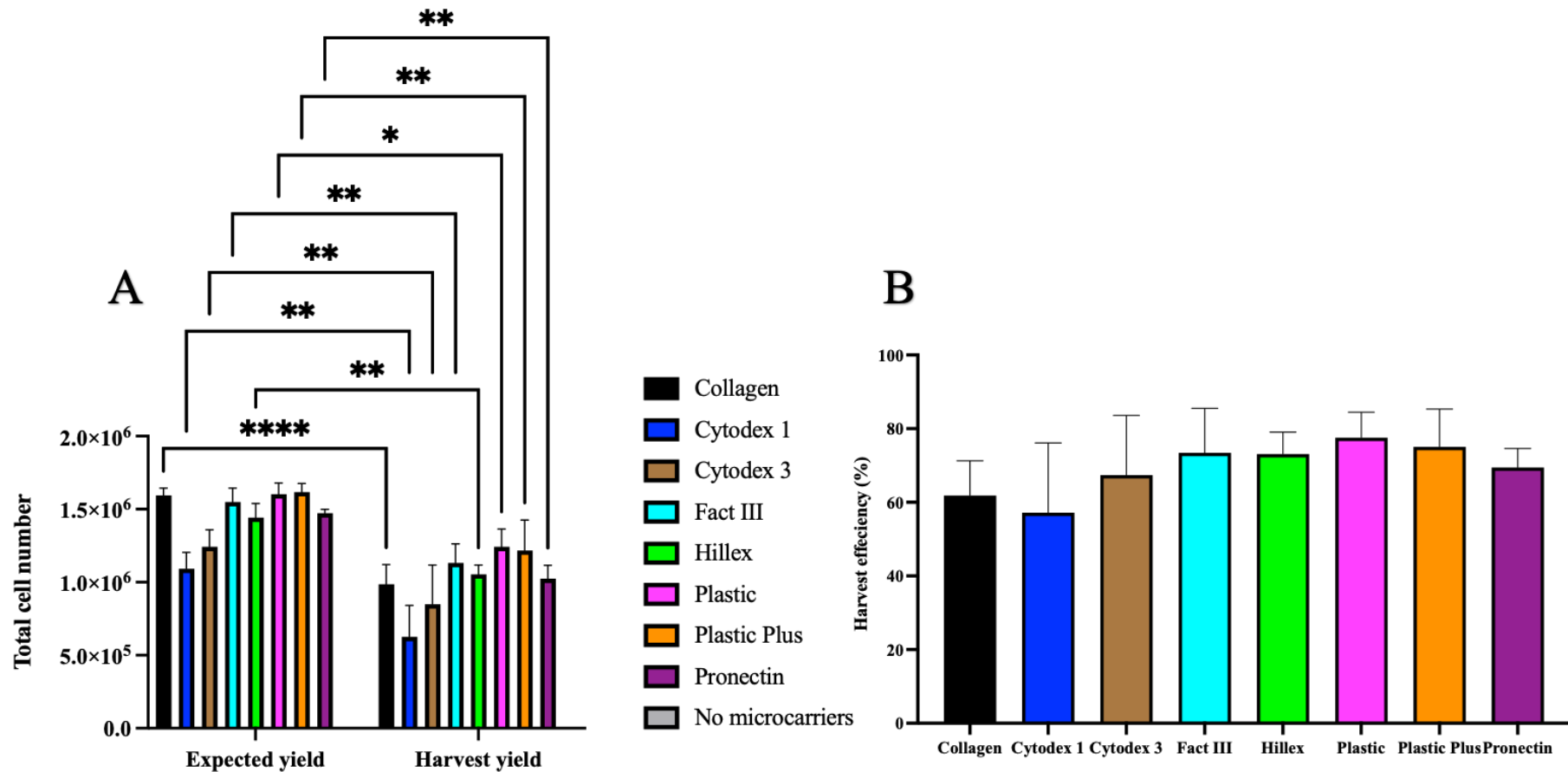


Figure 4.10. Comparison of the expected yield vs the actual yield of the harvesting process from the VTN coated microcarrier screening assay. VTN coated microcarriers seeded with  $4 \times 10^4$  cells/cm<sup>2</sup> were sacrificed for cell counting directly on microcarriers at 96 h in culture. Reagent A100 was used to lyse the cells on the microcarriers, and then reagent B was used to stabilise the solution. The TCC was then obtained on the Nucleocounter 3000 and compared with the TCC from the harvested process. The comparison between expected and harvested yield are shown in (A). The efficiency of the harvest process for each microcarrier are shown in (B). Data is shown as mean  $\pm$  SD. N=3, Biological repeats. \* $p \leq 0.05$ , \*\* $p < 0.01$ . \*\*\* $p < 0.001$  and \*\*\*\* $p < 0.0001$ , two-way ANOVA, Sidaks multiple comparison test.

#### **4.2.4. Screening of VTN coated microcarriers in dynamic conditions**

Previous experiments demonstrated the ability of kiPSCs to attach and adhere onto the 8 screened microcarriers when modified with VTN coating. It was also observed that kiPSCs cultured on VTN coated microcarriers in ULA well plates displayed reduced growth kinetics compared to kiPSC cultures on static 2D planar platforms. Consequently, it was then postulated that kiPSC cultures on microcarriers in static conditions could potentially impede efficient cell growth. Thus, in the next series of experiments it was investigated whether microcarrier cultures of kiPSCs in a dynamic culture environment could promote better cell growth. The kiPSC passage number used in this set of experiments were passage 13 and 14.

The experimental design of the next set of experiments were identical to the microcarrier screening performed in section 4.2.2, but instead of placing the ULA well plates in static conditions within the incubator, they were placed on a rocking platform inside the incubator to provide mechanical agitation to the culture system. To minimise shear stress in dynamic conditions, the rocking platform was set to 30 RPM which was sufficient to gently create hydrodynamic motion across the well.

##### **4.2.4.1. Viability and growth kinetics of kiPSCs on VTN coated microcarriers in dynamic conditions**

After 96 h in culture on VTN coated microcarriers in dynamic conditions, kiPSCs were harvested following the harvest process. For the incubation step of the cells with accutase, the plates were left on the rocking platform in a dynamic environment, to maintain a homogenous distribution of accutase whilst providing agitation for mechanical dissociation from the microcarriers. The rest of the harvesting process proceeded as per the method described in section 2.6.6. The VCN harvested from each microcarrier condition were adjusted to VCN/cm<sup>2</sup>

and compared. Both VCN/cm<sup>2</sup> and cell viability post-harvest are shown in Figures 4.11 A and B, respectively. From the VCN, the SPGR, DT and FI during the culture period were calculated and shown in Figure 4.11 C, D and E, respectively.

The VCN/cm<sup>2</sup> harvested from each VTN coated microcarriers in dynamic conditions were comparable to their respective counterpart from the VTN coated microcarrier screening in static conditions shown in 4.14, and 4.15 (e.g., the VCN/cm<sup>2</sup> from VTN coated Plastic microcarrier were  $3.92 \pm 0.21 \times 10^5$  cells/cm<sup>2</sup> and  $3.78 \pm 0.56 \times 10^5$  cells/cm<sup>2</sup>, for dynamic and static conditions, respectively). The VCN/cm<sup>2</sup> calculated from the harvest of non Cytodex-based microcarriers were relatively similar to each other in dynamic conditions. Since these experiments were performed from only two biological repeats of triplicate wells, no statistical analysis could be conducted.

Nonetheless, similar to the results of the microcarrier screening experiments in static conditions, the lowest VCN/cm<sup>2</sup> calculated for this experiment were from the harvests of VTN coated Cytodex 1 microcarriers ( $1.37 \pm 0.54 \times 10^5$  VCN/cm<sup>2</sup>). The highest average VCN/cm<sup>2</sup> harvested in dynamic conditions was obtained from VTN coated Plastic microcarriers.

Generally, the average cell viability of the harvested kiPSCs after culture on VTN coated microcarriers in dynamic conditions were relatively lower compared to the results obtained in static conditions. This is true for all conditions, except for Cytodex 1. For example, the viability of kiPSC obtained from cultures on VTN coated Hillex microcarriers were  $82.06 \pm 9.35$  % and  $91.93 \pm 3.26$  % in dynamic and static conditions, respectively (Figure 4.15). Similarly, for kiPSC harvested from VTN coated Plastic Plus, the viabilities were  $78.84 \pm 6.36$  % and  $92.40 \pm 2.26$  % in dynamic and static conditions, respectively. For Cytodex 1, the average viability of the cells remained relatively the same at  $67.68 \pm 3.88$  % in dynamic conditions and  $64.80 \pm 19.51$  % in static conditions.

The calculated SPGR of kiPSC after 96 h expansion on the VTN coated microcarriers identified cultures on VTN coated Cytodex 1 to have the poorest SPGR Figure 4.11C. The general trend of the other microcarriers were comparable to those of their counterparts in static conditions.

The DT of kiPSCs for all dynamic conditions were similar to those in static culture. For example, the average DT derived from cultures on VTN coated Cytodex 1 ( $59.37 \pm 20.12$  h) was longer than the average DT in static conditions ( $42.33 \pm 8.09$  h). In both static and dynamic conditions, it was observed that the VCN (also the SPGR, DT and FI) varied largely amongst repeats indicated by large error bars (Figure 11) which is not typically the case for the results obtained from non Cytodex-based microcarriers like FACT III, Hillex and Plastic microcarriers.

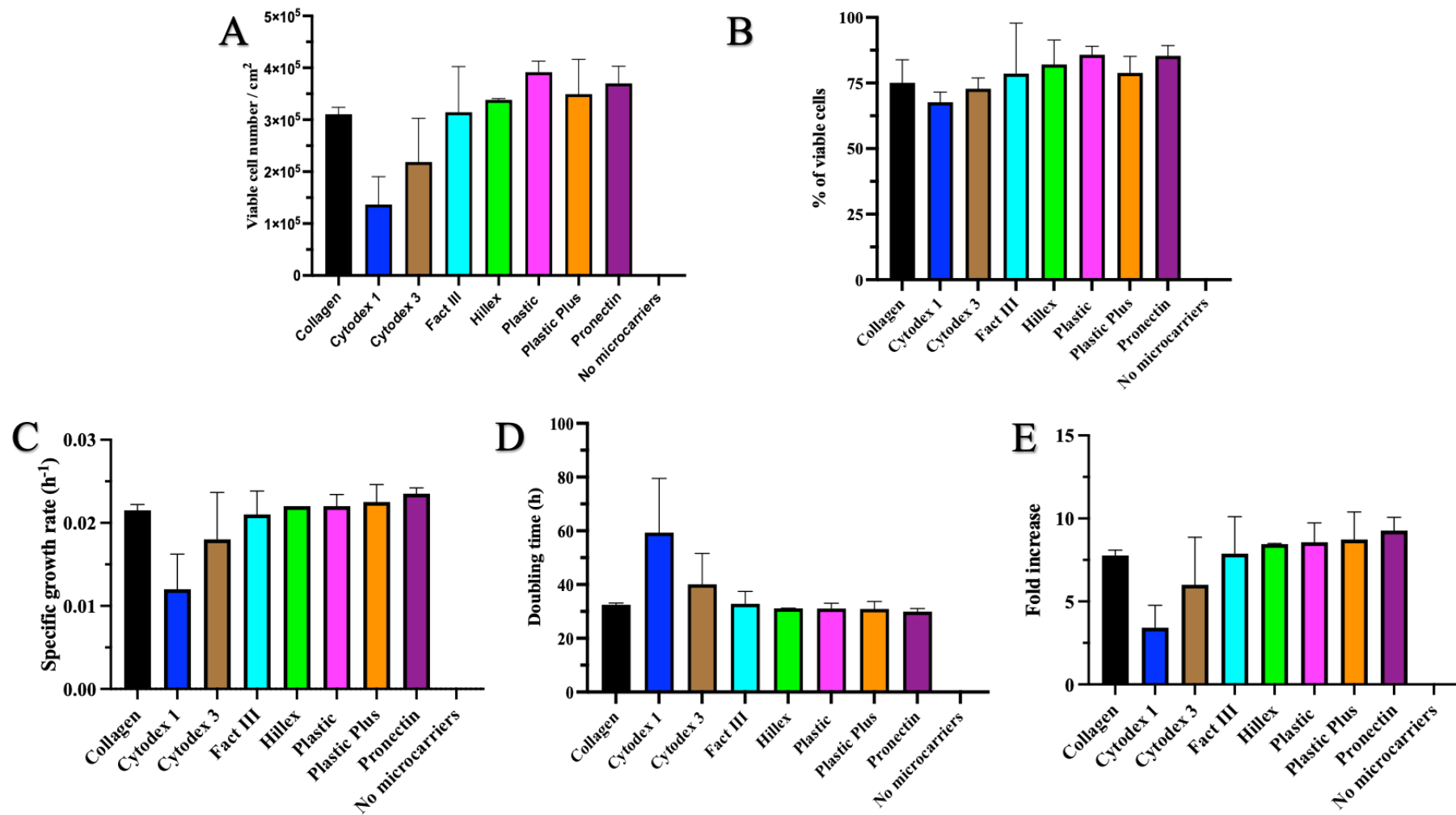


Figure 4.11. Viability and calculated growth kinetics of kiPSC harvested from VTN coated microcarriers, after culturing for 96 h in dynamic conditions. VCN and viability (B) of kiPSCs (passage 13 and 14) were obtained following the harvest process using the Nucleocounter 3000. The measured VCN of the harvested cells from each microcarrier condition was used to derive the VCN/cm<sup>2</sup> (A), SPGR (C), DT (D) and FI (E) after 96 h in culture. Data is presented as mean ± SD. N=2.

#### **4.2.4.2. Glucose and lactate profiles of kiPSCs cultured on VTN coated microcarriers in dynamic conditions**

Since glucose metabolism and lactate production are linked to cellular activity including cell growth and proliferation (Mason and Rathmell, 2011), these parameters were monitored during the cultures of kiPSC on VTN coated microcarriers in dynamic conditions. Samples for glucose and lactate were obtained before and after medium exchanges directly from the wells (indicated in Figures 12 and 13 by arrows). It is important to note that only 50 % medium could be performed to avoid aspirating the suspended microcarriers and cells. Thus, it was recorded that after medium exchange, glucose concentration do not fully recover to the concentrations of the stock medium (~13 mM) as expected when performing 100 % medium exchanges on adherent cultures of kiPSC using planar platforms (see Likewise, residual lactate concentrations are detectable following medium exchange.

As expected, the glucose and lactate concentrations of the negative control wells generally remained similar to the stock solution (~12 - 13 mM) and below the limit of detection (~ 0 mM), respectively, throughout the culture duration.

Over the 96 h culture duration, the glucose and lactate trends of the kiPSC cultures on different VTN coated microcarriers in dynamic conditions, were similar to the glucose and lactate profile trend observed in the microcarrier studies conducted in static conditions. Again, kiPSC cultures on VTN coated Cytodex 1 microcarriers were measured to contain the most glucose concentration and the least lactate concentration at the 96 h timepoint prior to harvest. All other microcarriers followed the same trend.

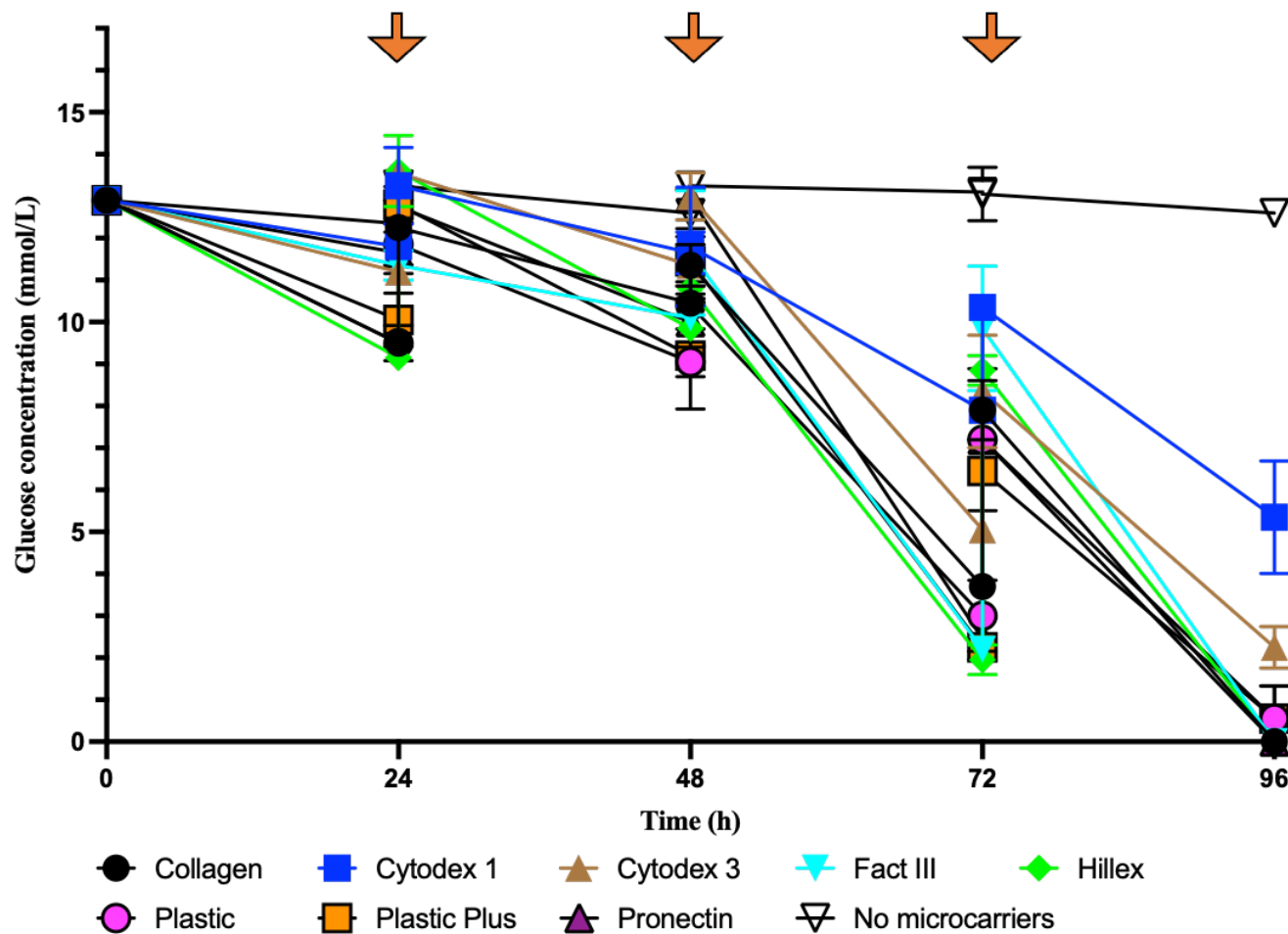


Figure 4.12. Glucose concentration of kiPSC cultured on VTN coated microcarriers in dynamic conditions. Samples were taken directly and carefully from the wells before and after medium exchanges. Samples were then analysed for glucose concentrations. Medium exchanges were performed every 24 h throughout a 96 h culture duration, at which point samples for glucose measurement were taken before proceeding with the harvest process. Data is presented as mean  $\pm$  SD. N=2, biological repeats.

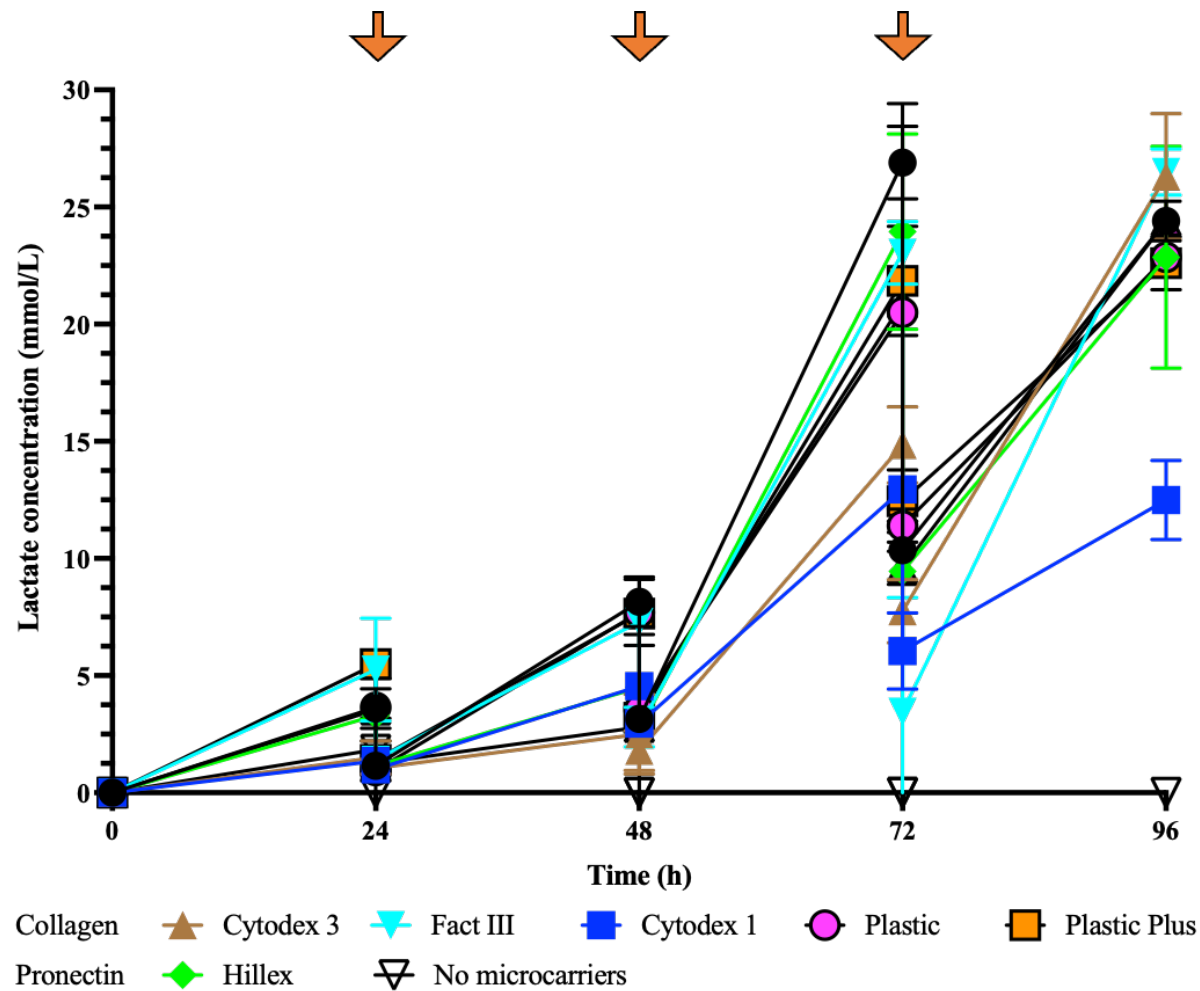


Figure 4.13. Lactate concentrations of kiPSC cultured on VTN coated microcarriers, throughout 96 h of expansion. Samples were taken directly and carefully from the wells before and after medium exchanges. Samples were then analysed for lactate concentrations. Medium exchanges were performed every 24 h throughout a 96 h culture duration, at which point samples for lactate measurement were taken before proceeding with the harvest process. Data is presented as mean  $\pm$  SD. N=2, biological repeats.

#### **4.2.5. Determining the efficiency of the harvest process of kiPSCs from VTN-coated microcarriers in dynamic conditions**

To improve the harvest process from microcarriers in this set of microcarrier screening experiments, the incubation step with accutase was performed on a rocking platform within the incubator. To assess whether this improved the harvest efficiency of kiPSC from the VTN coated microcarriers, the TCC was measured directly on the microcarriers and compared to the TCC measured following the harvest process. This experiment was similar to that conducted in 4.2.3.

However, since the experiments in this section were performed a total of two independent biological repeats, no statistical analysis could be conducted (Figure 4.14 – 4.15).

##### **4.2.5.1. Comparison of the total cell count before and after the harvest process in dynamic conditions**

For all culture conditions with microcarriers, the TCC measured directly on the microcarriers were greater than the actual harvested TCC following the harvest process in dynamic condition.

For example, the average TCC measured directly on VTN coated Cytodex 1 and Cytodex 3 microcarriers were  $1.11 \pm 0.18 \times 10^6$  and  $1.35 \pm 0.03 \times 10^6$ , respectively. In comparison, the TCC after the harvest process in dynamic conditions for Cytodex 1 and Cytodex 3 were  $0.614 \pm 0.27 \times 10^6$  and  $0.89 \pm 0.30 \times 10^6$ . The adjusted values to represent VCN/cm<sup>2</sup> can be found in Figure 4.15. kiPSC cultures on both VTN coated Cytodex 1 and Cytodex 3 microcarriers calculated the lowest average harvest efficiencies of  $53.86 \pm 15.87 \%$  and  $66.27 \pm 23.34 \%$ , respectively. It was noted that the SD from the mean of the measured TCC after harvesting from Cytodex 1 and Cytodex 3 microcarriers are large.

Generally, the average harvest efficiency of the harvest process in dynamic condition were improved compared to the harvest process in static conditions, which were  $75.92 \pm 10.72$  % vs  $61.67 \pm 22.47$  %, respectively (Figure 4.15).

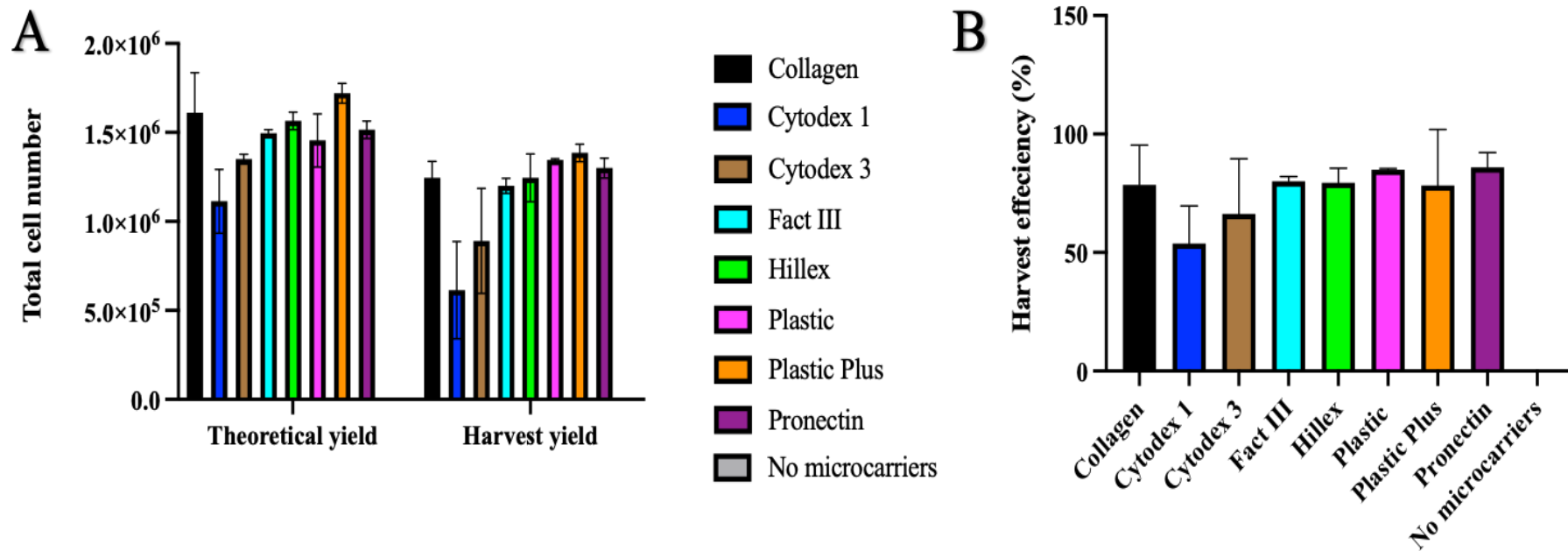


Figure 4.14. Comparison of the expected yield vs the actual yield of the harvesting process of kiPSC from VTN coated microcarriers in dynamic conditions. VTN coated microcarriers seeded with  $4 \times 10^4$  cells/cm<sup>2</sup> kiPSCs at passage 13 or 14 were sacrificed for cell counting directly on microcarriers at 96 h in culture. Reagent A100 was used to lyse the cells on the microcarriers, followed by reagent B to stabilise the solution. The TCC was obtained on the Nucleocounter 3000 and compared with the TCC from the harvest process. The comparison between expected and harvested yield are shown in (A). The efficiency of the harvest process for each microcarrier are shown in (B). Data is shown as mean  $\pm$  SD. N=2, biological repeats.

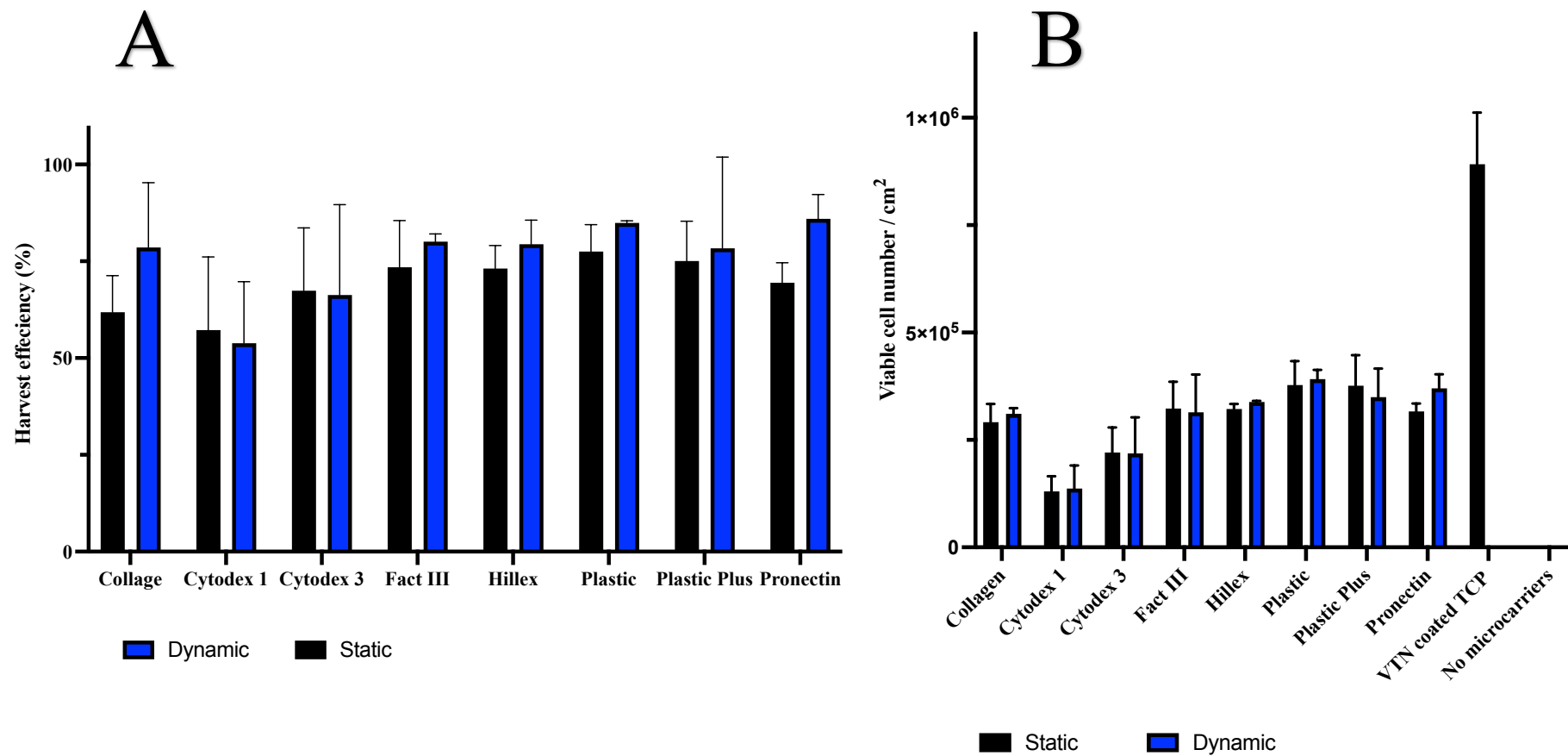


Figure 4.15. Comparison of the (A) harvest efficiency and (B) total VCN/cm<sup>2</sup> on harvest between static and dynamic conditions. Cells were harvested either in static or dynamic conditions. Harvested VCN was then adjusted to yield per available surface area. Data here also shows the yield from VTN coated TCP. Data is shown as mean ± SD. N≥2, biological repeats.

#### **4.2.6. Selection of VTN coated Plastic microcarrier**

Following the results of the microcarrier screening experiments, VTN coated Plastic microcarriers were identified as suitable substrates for hiPSC expansion based on their relative performance to other screened microcarriers. Prior to taking the microcarrier forward, a decision was made to visually assess that VTN was indeed coating the Plastic microcarriers. Therefore, SEM was employed to visually assess the surfaces of native Plastic Microcarriers and VTN coated microcarriers only (Figure 4.16).

Images were taken at different magnifications (Figure 4.16) which revealed that the protocol detailed in section 2.5 for microcarrier coating, indeed caused alterations to the surfaces of Plastic microcarriers. Native Plastic microcarrier surfaces appeared smoother at all magnifications in comparison, whereas Plastic microcarriers treated with VTN solution as per protocol, showed rougher surfaces and mass deposits. It is also shown that the roughness of the surfaces are heterogenous throughout the microcarriers with some surfaces bearing less deposits/layers than others. Thus, it was postulated that VTN deposited onto these surfaces.

However, though no further test were carried out to confirm that the deposits on the microcarrier surface was indeed the protein VTN, the supporting data during microcarrier screening, suggested VTN coated Plastic microcarriers were suitable and hereafter carried forward for further testing.

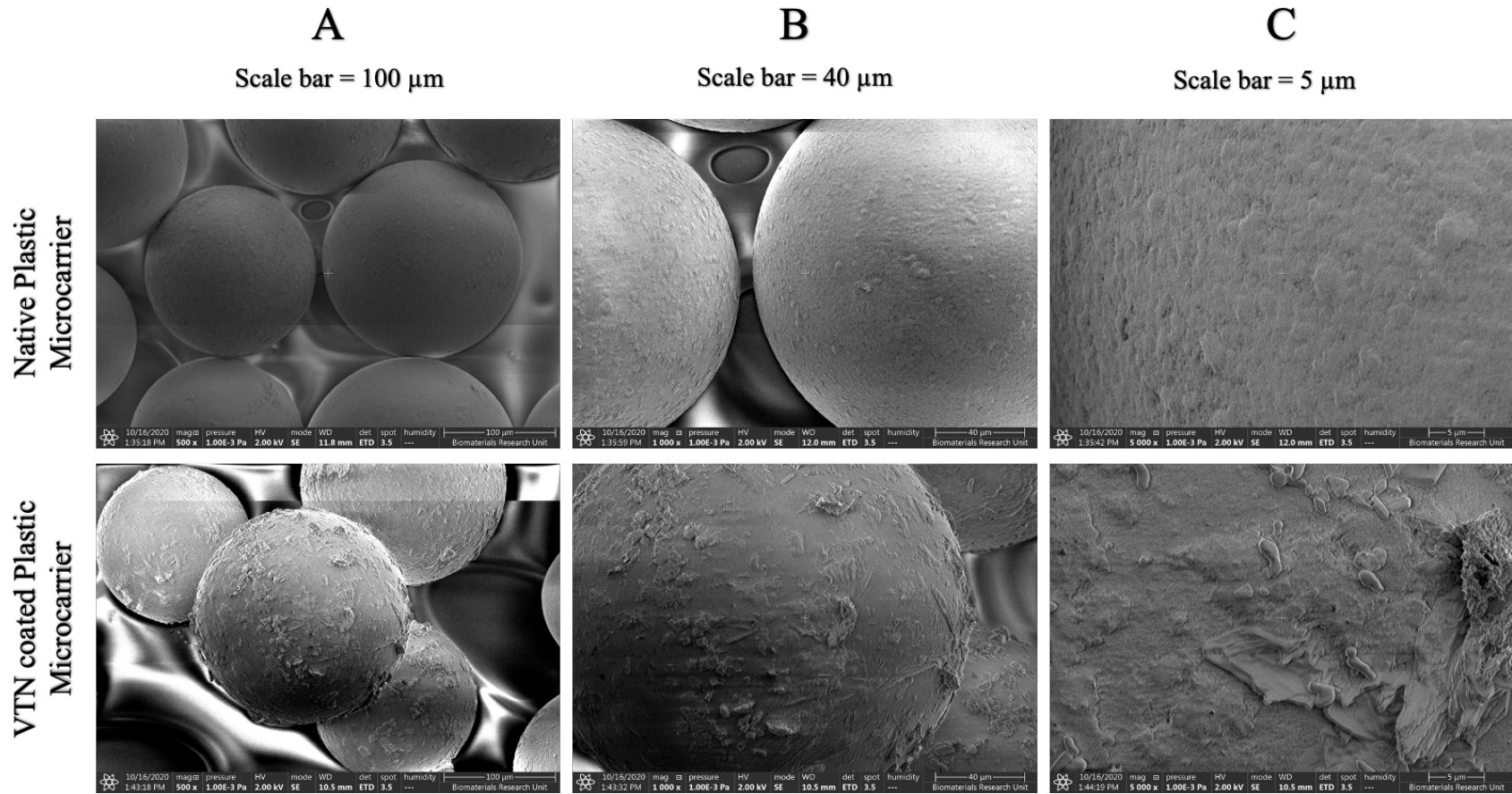


Figure 4.16. Representative SEM images at different magnification of VTN coated and non-modified plastic microcarriers. (A) scale = 100  $\mu\text{m}$ , (B) scale = 40 and (C) scale bar = 5  $\mu\text{m}$   $\mu\text{m}$  N=1, experimental repeat.

#### **4.2.7. Quality assessment of kiPSC on VTN coated Plastic microcarriers**

After performing a series of microcarrier screening assays, the criteria to select a suitable microcarrier was consulted (refer to section 4.1.3 for selection criteria). First, native microcarriers were poor at allowing attachment and adhesion of kiPSC, except for FACT III, Hillex and Pronectin. It was then observed that all VTN coated microcarriers screened supported kiPSC attachment and adhesion. Furthermore, all VTN coated microcarriers could support the expansion of kiPSCs as indicated by the growth kinetics of cells after 96 h of incubation. Nevertheless, kiPSCs cultured on VTN coated Cytodex microcarriers displayed the poorest growth. Thus, these were omitted from further consideration. Additionally, Collagen and FACT III microcarriers were also discarded as options, due to their type 1 porcine collagen coating which are not suitable for xeno-free culture systems.

The growth of kiPSCs on VTN coated Plastic, Plastic Plus, Pronectin and Hillex displayed no significant differences in static screening assays and were all deemed suitable for the expansion of kiPSCs. Note, the harvested cells from cultures using such microcarriers were not assessed for pluripotency, differentiation potential and other CQAs due to time and budget constraints.

Ultimately, Plastic microcarriers were selected as potentially suitable platforms for the expansion of kiPSCs, due to being akin to standard TCP (Polystyrene) which are widely employed both in research and clinical production (i.e., single use bioreactor technology). To confirm the suitability of Plastic microcarriers, it was important to assess the quality of the cells expanded on the microcarrier. In this section, pluripotency was assessed by ICC and the expanded cells were further differentiated towards NPCs to test for their differentiation potential.

#### **4.2.7.1. Morphology and pluripotency assessment of kiPSCs after expansion on VTN coated microcarriers**

Following a 96 h expansion process of kiPSC on VTN coated Plastic microcarriers, cells were harvested and replated onto VTN coated well plates for ICC and morphology assessment.

Figure 4.17A shows a representative phase contrast image of kiPSCs harvested from VTN coated microcarriers 96 h after reseeding onto VTN coated multi-well plates, indicating cells retained their ability to attach, spread and proliferate following culture on VTN coated microcarriers. The cells displayed typical morphologies of hiPSCs and could form cell colonies, similar to those seen in the previous chapter. At this time point, the colonies were starting to merge, which are also similarly observed when culturing kiPSCs using the baseline integrated process.

The results of the assessment for the presence of the nuclear factor of pluripotency, OCT4, in cells harvested from VTN coated Plastic microcarriers are displayed in Figure 4.18B-D. Cells were confirmed positive for OCT4 by ICC. However, it can be clearly noticed that the number OCT4<sup>+</sup> nuclei in comparison to the DAPI stained nuclei, was considerably lower (Figure 4.18B and C).

To quantitate OCT4 expression, OCT4<sup>+</sup> nuclei was counted to provide an indication of the percentage of pluripotent cells within the total cell population which is implied by the count of DAPI<sup>+</sup> nuclei. However, in these set of ICC assays, the OCT4 antibodies used were obtained from R&D systems (part # 967150) since the OCT4 antibodies previously used (ThermoScientific) were not available at the time of these experiments. Because of the indistinctive images obtained from the use of OCT4 (R&D systems) antibodies in combination with the EVOS M5000 for fluorescent imaging, quantitation of the percentage of OCT4<sup>+</sup> cells using the method described in section 2.7.7 could not be accurately performed.

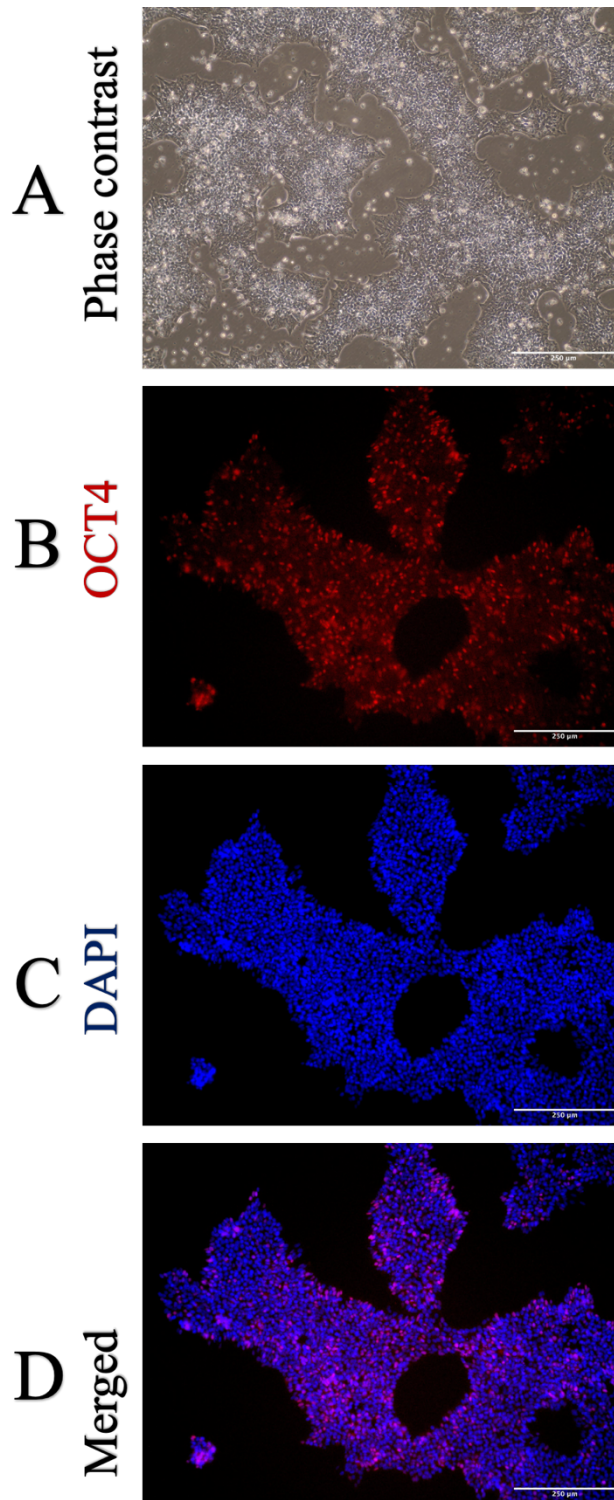


Figure 4.17. Morphology and pluripotency assessment of kiPSC cultured on VTN coated plastic microcarriers. kiPSC were seeded on 3 cm<sup>2</sup> of VTN coated Plastic microcarriers in ULA well plates at a density of 4 x 10<sup>4</sup> cells/cm<sup>2</sup> and expanded for 96 h in static conditions. Cells were harvested from the microcarriers and then seeded onto VTN coated 24 (for morphology assessment) and 48 (for ICC) well plates at 4 x 10<sup>4</sup> cells/cm<sup>2</sup>. (A) shows representative phase contrast at 96 h of culture post seeding. Cells were fixed at 96 h in culture and assessed for the pluripotency marker OCT4 (B;red). Nuclei were stained with DAPI (C;blue). Both red and blue channels were merged in (D). N=3, . Scale bar= 250 μm

#### **4.2.8. Neural induction of kiPSCs on VTN coated Plastic microcarriers**

Finally, before firming the selection of the Plastic microcarrier, the last criteria to appease was demonstrating successful neural commitment of kiPSC following their expansion on the microcarrier.

Figure 4.18 shows a process workflow of the expansion and differentiation of kiPSC on VTN coated microcarriers. This is an integrated bioprocess whereby a single culture vessel (i.e., one well of an ULA well plate) is used for both the expansion and differentiation processes. This process is similar to the baseline integrated bioprocess established in Chapter 3, except the cells are adhered onto suspended VTN coated Plastic microcarrier, instead of the surface of TCP multi-well plate. The process shown in Figure 4.18 is termed in this thesis as the microcarrier integrated bioprocess.

In this experiment, NPCs generated from baseline integrated bioprocess (2D) and microcarrier integrated bioprocess (3D) were compared by assessing for the presence of Nestin, a neural lineage specific intermediate filament marker, using ICC technique. The NP cell line Ax0013 was used as a positive control. The ICC results for the assessment of Nestin in cells obtained from the two bioprocesses are shown in Figure 4.19.

As expected, Ax0013 were positive for Nestin. Cells obtained from both the baseline and microcarrier bioprocesses were also positive for Nestin. Ax0013 Nestin markers could be observed throughout the cell structure, and some cells arranged in a radial fashion indicated by the white circles in Figure 4.19. This arrangement was largely not observed in the cultures of cells harvested from the baseline or microcarrier integrated bioprocess but was observed in the positive control.

Furthermore, the cells harvested from microcarriers were morphologically dissimilar to the cells obtained from the baseline integrated process. For example, representative phase contrast

images shown in 4.18D of the replated harvested cells from microcarriers appear larger and more spread, than the cells shown in the previous chapter follow baseline integrated bioprocessing.

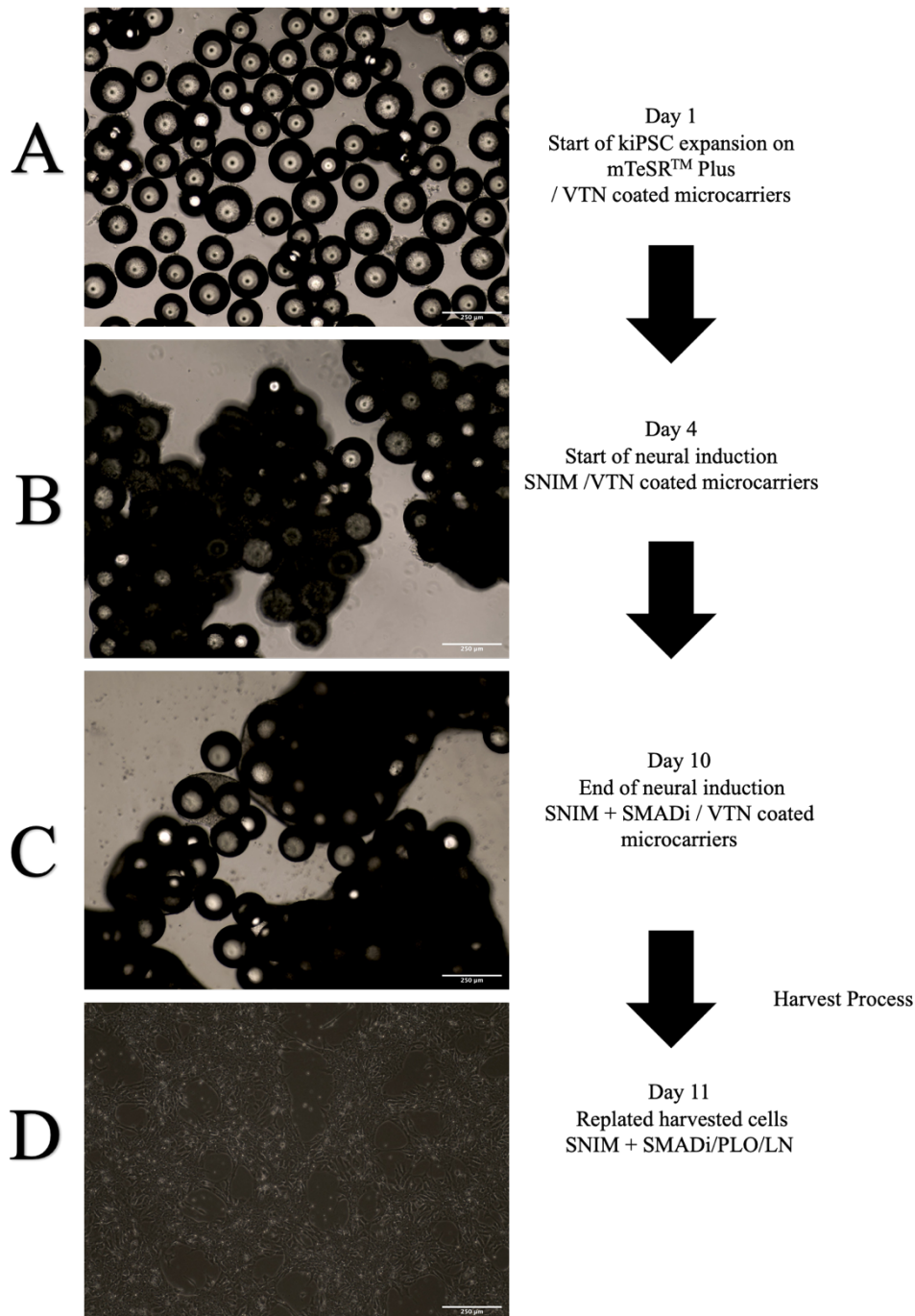


Figure. 4.18. Process workflow of the expansion and neural induction of kiPSC on VTN coated plastic microcarrier. kiPSC are firstly seeded onto VTN coated microcarriers at  $4 \times 10^4$  cells/cm<sup>2</sup> in mTeSR™ Plus + 10  $\mu$ M Y-27632. At day 1 (A) 50% of the medium is exchange with mTeSR™ Plus. Medium exchange is performed every 24 h until day 4. At day 4, as much of the medium is removed from the wells without disturbing the microcarriers, and 100% medium volume of SNIM medium is added. Daily medium exchanges are performed at 80% the well volume until day 10 (a total of 6 days in neural induction medium; C). On day 10, the harvest process in static condition is performed. The harvested cells are replated onto PLO/LN coated well plates in SNIM + SMADi + 10  $\mu$ M Y-27632 for the first 24 h. (D) is acquired 24 h post reseeding (i.e., 11 days after seeding onto the microcarriers). Images are representative of 2 random areas of the centre of the wells. N=3, biological repeats Scale bar = 250  $\mu$ m.

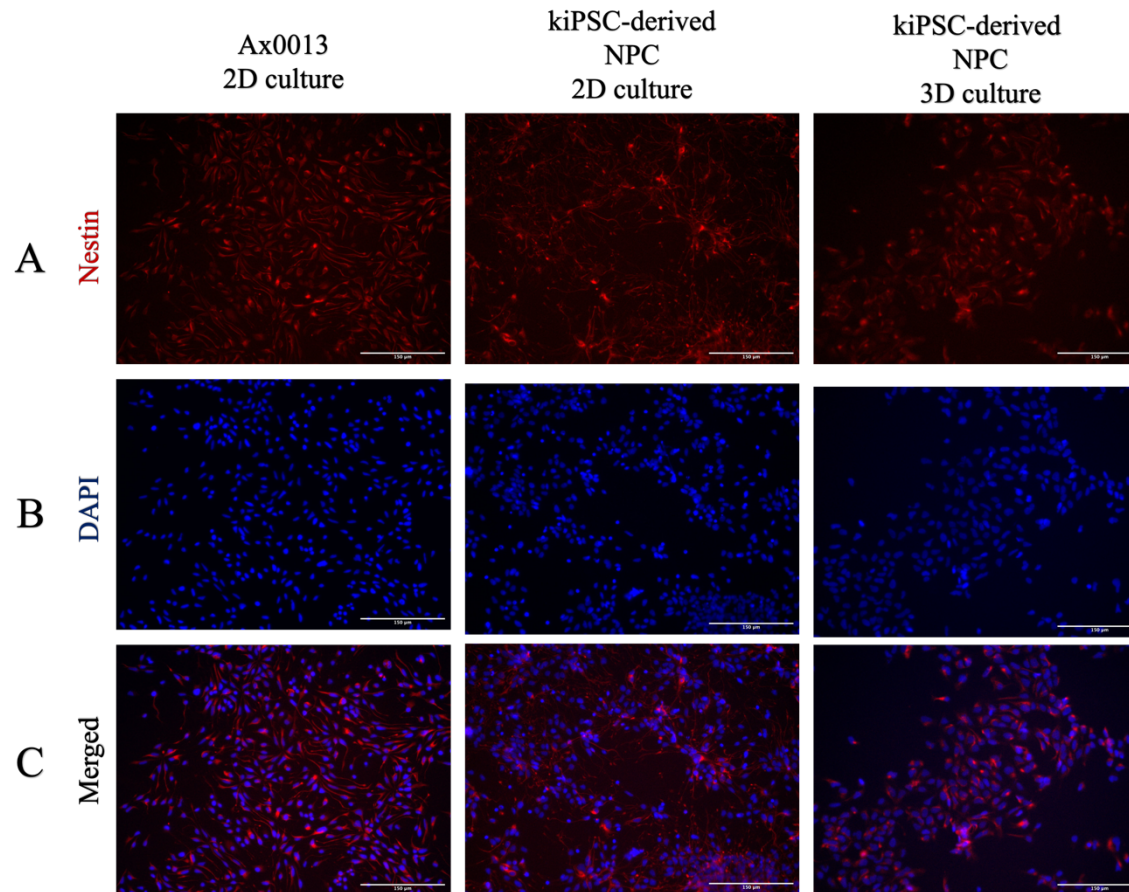


Figure 4.19. Assessment for the presence of Nestin following neural induction of kiPSC on 2D planar and 3D microcarrier platforms. Control Ax0013 were cultured in NP maintenance medium. For kiPSC-derived NPC 2D culture, kiPSCs at passage 12-14 were expanded for 96 h on VTN coated 6 well plate, then differentiated in SNIM + SMADi for a further 6 days. Cells were then dissociated from the culture substrate and prepared for ICC on 48 well plates. For kiPSC-derived NPC 3D culture, kiPSCs were expanded for 96 h on VTN coated Plastic microcarriers, then differentiated in NIM + SMADi for a further 6 days whilst on the microcarriers. Cells were then dissociated from the microcarriers using the harvest process and similarly prepared for ICC on 48 well plates. The presence of neural lineage marker Nestin was assessed by ICC (A;red). The nuclei were stained with DAPI (B;blue). Both red and blue channels were merged (C). N=3, biological repeats. Scale bar = 150 µm.

### **4.3.Discussion**

2D planar platforms can be employed in a scale out approach for the production of hiPSC-derived NPCs at clinically relevant quantities. However, this approach is logistically challenging to implement due to the required handling of multiple individual culture vessel.

The alternative is the culture in 3D platforms using STBs which are proportionally scalable by design allowing for easy scale-up transitions from lab to benchtop to pilot and eventually production scales. However, STBs only support suspended cultures to achieve a homogenous and dynamic culture system.

In this chapter, experimental work was carried out to translate the baseline integrated bioprocess established in Chapter 3, towards suspension culture systems. Considering the adherent culture system of the baseline integrated bioprocess, it was decided to employ microcarriers to enable suspended cultures of substrate adhered iPSCs.

#### **4.3.1.The process of selecting VTN-coated microcarrier**

##### **4.3.1.1.Comparing native commercially available microcarriers**

Although other groups have demonstrated the use of various microcarriers for the culture of PSCs, it is often unclear why particular microcarriers were selected and employed in their studies (Jo'An Bardy *et al.*, 2013; Fan *et al.*, 2014; Gupta *et al.*, 2016; Sara M Badenes *et al.*, 2016; Laco *et al.*, 2020). In some cases, screening of commercially available microcarriers were performed, but the results are not clearly or explicitly presented. Furthermore, Matrigel, MEF feeder layers and Geltrex were typically used as coatings for the screening of microcarriers which pose several limitations when applied in clinical production settings (Phillips *et al.*, 2008; Nie *et al.*, 2010). In addition, contradicting results of microcarrier usage in the literature suggests that their ability to support PSC expansion and differentiation is

heavily dependent on the culture system conditions (e.g., static or dynamic) and the cell line (Phillips *et al.*, 2008; Nie *et al.*, 2010; Laco *et al.*, 2020)

Therefore, to distinguish and select a suitable microcarrier for the expansion and differentiation of kiPSCs, it was necessary to screen several commercially available microcarriers. This included microcarriers with a range of surface chemistries and core materials: Collagen, Cytodex 1, Cytodex 3, FACT III, Hillex, Plastic, Plastic Plus and Pronectin. The potential of these microcarriers in their native, non-modified state was firstly assessed for their ability to support kiPSC attachment and adhesion. The results of this investigation reported in section 4.2.1 demonstrated that the majority of commercially available microcarriers were unable to support the efficient adhesion of kiPSCs. These microcarriers included Cytodex 3, Cytodex 1, Pronectin, Plastic, and Plastic Plus, where cells cultured with such microcarriers formed cell-cell aggregates confirming their partiality to each other rather than the available surfaces of microcarriers. The inability of some of these microcarrier to support PSCs have also been confirmed by Chen *et al.*, (2011) and Nie *et al.*, (2009). In particular, these studies report the inefficiency of Cytodex microcarriers to support PSC expansion (Phillips *et al.*, 2008).

Hillex, Collagen and FACT III microcarriers were shown capable of supporting the attachment and adhesions of kiPSC over 96 h in culture. This was also confirmed by Phillips *et al.*, (2008), by demonstrating the expansion of hESCs on FACT III and Hillex microcarriers in their screening assay. However, to the best of the authors knowledge, FACT III and Collagen microcarriers have not yet been employed in spinner flask or bioreactor platforms for hiPSC expansion, unlike Hillex.

It was also unclear what promoted the successful adhesion of kiPSCs onto native Hillex, Collagen and FACT III microcarriers. First, it was predicted that the surface composition of the microcarriers play a significant role in the adhesion of kiPSCs. However, both FACT III

and Collagen microcarriers from Solohill are coated with type 1 porcine collagen, yet interestingly, Cytodex 3, with similar type 1 porcine collagen coating did not support kiPSCs adhesion. Next it was postulated that the charge of the microcarriers could significantly affect the cells, as the cells are relatively negatively charge. Nonetheless, positively charged microcarriers like Cytodex 1 and Plastic Plus microcarriers, also did not support efficient kiPSC adhesion like the positively charged Hillex and FACT III. Overall, these results suggests that the successful attachment and adhesion of kiPSC may be owed to multiple combinations of microcarrier characteristics beyond surface chemistries and charge, and may be affected by size, porosity, and density . Better understanding of the mechanisms involved in the interaction between hiPSC and microcarriers is needed in order to rationally design microcarriers in the future to specifically support hiPSC.

The employment of non-modified commercially available microcarriers for the expansion of kiPSC at large scale would simplify the overall process by reducing the need of microcarrier coating processes, and ultimately reduce the operation costs. Native Hillex, FACT III and Collagen microcarriers were shown here to support the attachment and spreading of kiSPCs. However, it was not possible to confirm from phase contrast images alone whether the cells retained pluripotency, the ability to differentiate and other CQAs such as normal karyotype following their growth on such microcarriers due to limitations in resource and time. Further future analysis of cell quality and growth kinetics from Hillex, FACT III and Collagen microcarriers would be an interesting avenue to take. However, since Collagen and FACT III microcarriers are coated with porcine derived substrates, their potential application for the production of clinical therapies is reduced due to potential xeno-derived material contamination.

Hillex on the other hand are animal component free and would be more suitable for clinical scale production. The potential of Hillex microcarriers as a suitable substrate was considered

for future work beyond the scope of this thesis. However, the decision was made to not select Hillex due to absorbing phenol red from the media closing posing larger weight when hydrated compared to other microcarriers (Van Beylen *et al.*, 2021). Employment of heavy microcarriers in STBs would not be ideal as they would require greater dynamic forces to suspend (Gupta *et al.*, 2018). In turn, this would expose cells to greater shear stress which can impact their CQAs.

#### **4.3.1.2. Assessment of VTN coated microcarriers to support kiPSC growth**

As no suitable microcarrier was identified during static native microcarrier screening, the next step was to investigate the implications of various VTN-coated microcarriers on kiPSC growth.

Though VTN coated microcarriers have been used for the expansion of PSCs (Fan *et al.*, 2014; Badenes *et al.*, 2016; Fan *et al.*, 2017), to the best of the authors knowledge, the screening of the 8 different microcarriers listed here, with addition of recombinant human VTN for hiPSC expansion in static or rocking conditions have not been reported elsewhere. This is also the first reporting of cGMP employment of mTseR-plus in microcarrier screenings. The findings of the microcarrier screening experiments confirmed that the VTN modification of all tested microcarriers improved the attachment and spreading of cells even on microcarriers like Plastic and Plastic Plus which did not support kiPSC attachment in their native states.

It was postulated that kiPSCs would display similar growth kinetics and attachment mechanisms on VTN coated microcarriers (Plastic microcarrier in particular) compared to culturing on VTN coated TCP in static. Indeed, stages of attachment and spreading were similar which involved initial attachment, adhesion and followed by cell spreading within 24 h of seeding. This can be observed in the morphologies of cells in the phase contrast and live/dead images in microcarrier cultures within section 4.2.2. During static screening the majority of cells were adhered to the microcarriers 1 hr post seeding, but did not exhibit cell spreading

since the cells remained visually rounded. This was expected as this seeding technique generally require some time for cells and microcarriers to deposit to the bottom of the wells. Thus, the seeded cells are dependent on gravity and chance to encounter the settled microcarriers. Due to the lack of CAM activation and resultant hyperactivation of myosin via the Rho/ROCK pathways contraction of the cytoskeleton occurs (Shi and Wei, 2007), hence the rounded morphology shape. After 24 h, cells were shown to spread on the microcarriers and conform flatter morphologies. Flat cell morphologies suggests that the surfaces of the VTN coated microcarriers are capable of engaging with CAMs, which mature over time to form focal adhesions. Focal adhesions are composed of multiple proteins including vinculin, Talins, paxillin, zyxin and clusters of integrin which interact with  $\alpha$ -actin and actin stress fibres, thus facilitating actin cytoskeleton reorganisation (i.e., cell spreading). Spreading of kiPSCs was observed on microcarriers coated with VTN which have also been demonstrated by other groups for various microcarriers including Plastic and collagen microcarriers (G. Chen *et al.*, 2011; Fan *et al.*, 2014; Rivera *et al.*, 2020).

The screening of VTN coated microcarriers in static conditions also highlighted that regardless of the same concentration of VTN coating on the surface of screened microcarriers, differences in growth kinetics of kiPSCs were still observed between different microcarriers, suggesting that interaction of the native microcarrier surface and the extra additional VTN coating influences cell growth.

Relatively poorer cell growth of kiPSCs was recorded for cultures on VTN coated Cytodex 1 and VTN coated Cytodex 3 yet others have demonstrated the successful expansion of PSCs on Cytodex microcarriers, typically coated with Matrigel or Geltrex (Fernandes *et al.*, 2009; Kehoe *et al.*, 2010b; Nie *et al.*, 2010; Kevin G. Chen *et al.*, 2014; Laco *et al.*, 2020). The results here, however, suggests that the combination of VTN with Cytodex microcarriers were not suitable to support the kiPSC line.

All other non-Cytodex VTN coated microcarriers supported similar growth of kiPSCs. VTN coated Plastic and Plastic Plus yielded the highest VCN on average with the advantage of being defined and xeno-free. However, these results were not significantly different compared to Hillex which are also employable for xeno-free culture systems. This was true for both static and dynamic screening processes.

The expansion of PSCs on Plastic microcarriers have been successfully demonstrated in different platforms, and typically coated with a substrate including VTN, Geltrex, Matrigel, LN, and Poly-l-lysine (Wang, *et al.*, 2013; Badenes *et al.*, 2015; Lam *et al.*, 2015; Badenes *et al.*, 2016; Le and Hasegawa, 2019). Here, it was calculated that a FI of ~10 times can be achieved on VTN coated Plastic microcarriers within 4 days, either in static or rocking dynamic conditions in ULA well plates. Others employing VTN coated Plastic microcarriers have reported ~ 16 FI in dynamic culture conditions over 6 days in TeSR™-E8™ (Fan, Zhang and Tzanakakis, 2017). However, no other groups have reported the combination of VTN coated Plastic with the cGMP grade mTeSR™ Plus medium.

There are several possibilities to explain the disparity in cell growth amongst the different microcarriers, and significantly poorer growth on microcarriers when compared to the kiPSC cultures on 2D planar platforms. First, the growth kinetics of kiPSCs could be directly influenced by the microcarriers, regardless of the additional VTN coating. For example, significant differences were found when culturing kiPSCs on VTN coated Cytodex 1 and Plastic microcarriers, with the same surface area for growth and same surface coating.

Second, regardless of applying the same method of VTN coating to each microcarrier type, the different size, porosity, surface chemistry and shape of each microcarrier could lead to varying efficiencies of VTN adsorption, thus leading to different degrees of VTN coating. However, this is just a speculation stemming from a study reporting VTN coating inefficiencies on Plastic

microcarriers (Fan, Zhang and Tzanakakis, 2017). Here, scanning electron microscopy images of the surfaces of native and VTN-coated Plastic microcarriers (appendix suggests that areas of microcarriers may not be fully coated, when using the coating procedure outlined in the methods. Further work is needed to confirm the different efficiencies of VTN on a screen of microcarriers.

Third, the propensity of the microcarriers to promote the formation of cell-microcarrier aggregates and complexes can influence the growth rates of kiPSCs. Cell-microcarrier aggregation limits the available surface area for growth on microcarriers and causes inefficient diffusion of growth factors and nutrients into the centre of the aggregates. Contact inhibition also limits cell growth and can even further cause differentiation. The screening of VTN coated microcarrier in dynamic rocking conditions were designed to try and mitigate the aggregation. However, formation of cell-microcarrier aggregates were still observed by the time of harvest in all microcarrier conditions. In fact, the growth of kiPSCs on microcarriers in their respective static and dynamic screening conditions were comparable. This was also confirmed by similar glucose and lactate profiles of the cultures on microcarriers. The aggregation in dynamic conditions may be attributed to the dimensional limitation of the 24 ULA well; a total surface area of 1.9 cm<sup>2</sup> for microcarriers to distribute. In addition, although the hydrodynamic flows by rocking motion were able to distribute the microcarriers across the x axis of the wells, the conditions did not provide sufficient up lift by hydrodynamic flow for the microcarriers to distribute in a fully suspended manner. Thus, aggregations occur due to cell-microcarrier contact and collision.

Fourth, glucose and lactate concentrations play a significant role in the growth of kiPSCs. From the screening studies in both static and dynamic conditions, the glucose and lactate profiles of kiPSC cultures were suggestive of typical high dependency on glycolysis for energy (Wilmes *et al.*, 2017; Odenwelder, Lu and Harcum, 2021). Lactate yield from 1 mM of glucose was F.D., de la Raga, PhD Thesis, Aston University, 2022

calculated to be  $\sim 2$  mM, although variation was calculated between each microcarrier condition. Due to the logistical limitations of platform design, a full 100% medium exchange could not be performed for microcarrier cultures in ULA well plates especially at early stages of the expansion as the cells and microcarriers were easily disturbed by the aspiration of the media. Thus, the inability to fully replenish the glucose concentration and remove the lactate from cultures can negatively impact the growth of kiPSCs. For example, accumulation of lactate decreases the cell environment pH which can inhibit cell growth and lead to cell death (Horiguchi *et al.*, 2018). As lactate is fully removed in 2D planar platform cultures, this may explain why such significant differences were observed when comparing the VCN obtained from the microcarrier to that of standard well plates.

At later stages of the cultures (72 h to 96 h), where cell-microcarrier aggregates formed, the cell-laden microcarriers and complexes could be visibly sedimented to the corner of the wells when tilted due to their increased size and density. Hence, medium could be exchanged at almost 100% to initiate the neural induction process; it is important to remove pluripotency maintaining factors in the mTeSR<sup>TM</sup> Plus medium before replacing with the neural induction medium, otherwise, components of the mTeSR<sup>TM</sup> Plus such as pluripotency maintenance factors which would disturb the neural induction process and affect the efficiency.

It was also investigated whether cells were lost during the harvest process, leading to inaccurate representation of the actual VCN on the microcarriers. Therefore, a method to count the cells directly on microcarriers were employed. However, this method was limited as it was unable to distinguish viability and instead measured the total number of cells, including dead and viable cells. Nevertheless, this method confirmed higher TCC directly from microcarriers (i.e., without proceeding with the harvest process) compared to the TCC of the harvested cells using the harvest process, which was true for all conditions. This suggested that the harvest process employed was not efficiently collecting the cells from the microcarriers. Even when performing

F.D., de la Raga, PhD Thesis, Aston University, 2022 232

the harvest process in dynamic conditions (i.e., whilst cells were treated with accutase), the harvest efficiency was still on average below 80%.

The process of filtration through a 100 µm cell strainer was decided to isolate the microcarriers and collect the single cell dissociated kiPSC in the flow through. However, the formation of large cell-microcarrier aggregates by the time of harvest presents the challenge of effective proteolytic activity by the accutase enzyme, especially at the core of the aggregates. Consequently, this could lead to inefficient single cell dissociation and leave remnants of undissociated and aggregated cells, in turn being too large to filter through the pores of the filter, thus leading to low VCN post-harvest. This may explain the harvest inefficiencies from microcarriers. Other groups have used different treatment times and dissociation reagents to dislodge the cells into single cell suspension (Phillips *et al.*, 2008; Badenes *et al.*, 2015) but the harvest efficiencies of these processes were not reported. An interesting avenue was explored recently, employing dissolvable microcarriers to avoid the filtration and separation of microcarriers (Rodrigues *et al.*, 2019).

Nevertheless, these studies showed that although cells were lost in the harvest process, the yield of VCN of kiPSC per cm<sup>2</sup> of available surface area for growth from any of the screened VTN coated microcarriers, in either static or dynamic screening, were significantly lower compared to the achievable yield of VCN/cm<sup>2</sup> in static planar platforms. It was then postulated that the dynamic stirred environment offered by STBs could potentially reduce the amount of aggregation and promote the growth of cells as monolayers on the surface of the microcarriers, which will be further investigated in Chapter 5. The decision was then made to proceed with further studies using a suitable microcarrier for the expansion of kiPSCs.

Ultimately, VTN coated Hillex, Plastic and Plastic plus were considered potentially suitable candidates for the next stage of assessment. Other microcarrier candidates displayed poorer

kiPSC growth and/or did not appease the xeno-free criterion. It was decided to proceed with Plastic microcarriers owing to its similarity to TCP.

The next phase involved assessing the ability of kiPSCs to differentiate towards NPC whilst on VTN coated Plastic microcarriers. Here, it was demonstrated that the kiPSC differentiated on microcarriers expressed the neural marker Nestin, confirmed by ICC. However, morphological differences were found between the NPCs derived from kiPSC in 2D planar platforms, compared to 3D microcarrier neural induction processes. It's uncertain what causes these morphological differences, but this could be indicative of This difference may be due to the gradient concentration of neural inducing factors experienced by the aggregates in the 3D microcarrier neural induction process. Though the cells harvested from the microcarrier integrated bioprocess expressed Nestin, further studies are needed to explore this disparity in morphology. It is possible that due to the inhomogeneity of the neural induction process on aggregated cell, the state of the NPCs may be different (e.g., more naïve or differentiated towards a different brain region NP cell). To further confirm this, further work is needed to identify for markers of stage specific markers for NPCs. However, due to time constraints and availability of reagents this was not possible.

#### **4.3.2.VTN coated Plastic microcarriers supported the expansion and neural induction of kiPSCs**

One of the important objectives set in this chapter is to demonstrate the potential of a suitable microcarrier to permit neural induction of kiPSCs. Indeed, VTN coated Plastic microcarriers were confirmed to support the expansion of kiPSCs as well as their differentiation towards Nestin positive NPC cells. Thus, the expansion and differentiation process on VTN coated

plastic microcarrier developed in this chapter was termed the microcarrier integrated bioprocess.

However, the efficiency of the microcarrier integrated bioprocess to generate NPCs was not calculated as the counting of Nestin<sup>+</sup> cells proved difficult with the methods applied for nuclei stained counting. Future repeats of this work could utilise flow cytometry to measure the number of Nestin<sup>+</sup> cells.

## **5.Expansion and neural induction of hiPSC on microcarrier platforms in STBs**

### **5.1.Introduction**

Integrated bioprocesses for the production of hiPSC derived NPCs have been demonstrated so far using adherent culture systems on either 2D planar or 3D microcarrier platforms. However, both processes have been reliant on multi-well plates incubated in static conditions. STB technologies offer a platform to translate these bioprocesses into scalable dynamic bioprocesses.

After establishing the baseline and microcarrier integrated bioprocesses for the generation of NPCs in Chapters 3 and Chapter 4, respectively, the final stage of this thesis was to develop a scalable bioprocess utilising spinner flask technology. The initial design of such bioprocess required the translation of the process parameters established in Chapters 3 and 4.

#### **5.1.1.Designing the baseline scalable bioprocess**

The 50 mL spinner flask (Wheaton) was identified as a suitable representative scale-down model of larger spinner flasks and were utilised in this chapter as the vessel of choice for dynamic culture systems. The design of the starting bioprocess (or baseline scalable bioprocess) in such spinner flasks required the consideration of multiple process parameters which included temperature, CO<sub>2</sub>, O<sub>2</sub>, humidity, stirring speed, surface area (of microcarriers), working volume, seeding density, protein coating concentration and feeding regime. Some of the process parameters established in 2D bioprocessing could be directly implemented for 3D cultures in spinner flasks, which included CO<sub>2</sub> (5% in air), humidity (95%) and temperature (37°C). These were achieved for spinner flask cultures as they required to be placed on a

magnetic stirrer inside a humidified incubator (similar to well plates), thus the same culture environment could be controlled and applied through the incubator.

Similarly, the working volume, surface area and seeding density parameters were also directly translated from the baseline integrated bioprocess to the baseline scalable bioprocess explored in this chapter. The proportion between the working volume and surface area available for cell growth was maintained from the baseline integrated bioprocess and implemented here. The working volume and the microcarrier surface area used for the baseline scalable bioprocess were calculated from the proportions established in the baseline integrated bioprocess. The surface area in 6 well plates were approximately  $9.8 \text{ cm}^2$  with a working volume of 2 mL. Thus, for spinner flasks,  $100 \text{ cm}^2$  per 20 mL of media volume was used, hence, the proportion of available surface area to medium was maintained between the 2D cultures systems and 3D cultures systems at  $\sim 5 \text{ cm}^2/\text{mL}$ . Additionally, the coating was maintained at  $0.105 \text{ mL}/\text{cm}^2$  and the seeding density at 40,000 cells/ $\text{cm}^2$  in spinner flask studies as per the parameters established in for the microcarrier integrated bioprocess.

For the feeding strategy in spinner flasks, it was not possible to perform a 100% medium exchange as performed in well plates, due to the risk of aspirating the cell laden microcarriers. Instead, an 80% medium exchange was performed daily. To implement a similar feeding regime closely representing that of the baseline integrated bioprocess, the spinner flasks were operated at half the working volume (10 mL) for the first 48 h, then increased to full working volume of 20 mL for the rest of the total 96 h culture duration.

However, stirring speed parameters could not obviously be determined in baseline integrated bioprocesses, as this parameter is exclusive to stirred tank bioreactor culture vessels. Thus, in this chapter, the stirring speed implemented for the baseline scalable bioprocess was the minimum speed required to suspend the microcarriers. An experiment was designed to visually

identify the stirring speed to suspend the microcarriers, and mixing studies were conducted to identify whether the mixing flow can create a homogenous environment.

### **5.1.2. Neural induction in scalable bioprocesses**

Ideally, for this chapter, the design of the scalable bioprocess would include a neural induction step following a 96 h expansion step for PSCs. In line with the parameters established in the baseline integrated bioprocess, the initiation of neural induction would then be conducted at 96 h of culture with a subsequent differentiation duration of 144 h.

As these experiments could only be conducted at the later stages of the project, and due to the larger volumes of media required, unfortunately the resources of PSC expansion medium and neural induction medium had been depleted by this time. Resources were reserved to conduct limited studies only. The cost and lead times also proved too costly and too long, respectively, to perform neural induction in spinner flasks.

Instead, working with the limited resources and time, neural induction was performed at smaller scale in well plates. It was then decided that to reflect a “continuous” expansion and differentiation bioprocess, samples containing cell-laden microcarriers from the expansion of kiPSC (at time point 96 h) in spinner flasks, should be transferred into ULA well plates then differentiated in static conditions using less medium. Though this did not reflect a true integrated expansion and differentiation bioprocess contained in spinner flask exclusively, it was performed nonetheless to assess whether PSCs expanded on VTN coated microcarriers in the spinner flasks were capable of differentiating towards NPCs.

### **5.1.3.Chapter aims and objectives**

The overall aim of this chapter is to develop towards a scalable integrated bioprocess in spinner flasks. Considering the remaining available resources and time, 3 objectives were identified:

1. To identify the stirring speed parameter to suspend the microcarriers by performing a visual assessment of the effect of different stirring speeds. This will be used as the initial stirring parameters for the baseline scalable bioprocess.
2. To characterise the growth, quality, and potential to differentiate towards NPCs, of the kiPSCs expanded in the baseline scalable bioprocess.
3. To conduct process optimisation experiments by investigating the effects of process parameters such as stirring speed, on the growth of kiPSCs.

## 5.2.Results

### 5.2.1.Determining the mixing speed required to suspend the microcarriers

First, the parameter of stirring speed for the baseline scalable bioprocess had to be determined. An experiment was designed to explore the effect of a range of stirring speeds on their ability to suspend 100 cm<sup>2</sup> of VTN coated Plastic microcarriers inside the 50 mL spinner flask with a working volume of 20 mL in (DMEM/F12). The range of settings used were between 10 – 70 rotations per minute (RPM) and the magnetic flea of the spinner flask was configured at least 1 cm (high impeller configuration; Figure 5.1 C) and just above the bottom of the vessel (low impeller configuration; Figure 5.1 B).

The effect of the stirring speed on the microcarrier were visually confirmed (data could not be shown). Settings below 30 RPM were not capable of homogenously suspending the microcarriers across the whole volume. This was evident due to all or some of the microcarriers remaining at the bottom of the flasks. At 30 RPM, the turbulence created was able to suspend and distribute the microcarriers homogenously across the working volume of the vessel. This speed setting was considered the just suspended speed ( $N_{JS}$ ). All other speed settings above 30 RPM were also capable of suspending the microcarriers in a homogenous fashion. These effects of different speed settings on the microcarrier distribution were observed regardless of impeller configuration.

Next, the mixing behaviour of different speed settings in combination with the 2 different impeller configurations were tested: one was configured as the high impeller configuration (Figure 5.1 Figure C), and the second sets the stirrer bar as close to the bottom of the vessel whilst leaving a small gap to avoid microcarrier grinding (Figure 5.1 B). On average, low impeller configurations were measured with improved mixing times compared to high impeller

configuration (Figure 5.1 A). No significant difference was found when comparing the two configurations to each other under the same stirring speed conditions.

Increasing the stirring speed also improved the mixing time. Significant differences in mixing times were recorded between the highest mixing speed (50 RPM) and the lowest (30 RPM) regardless of the configuration (all p values were below 0.05; Figure 5.1 A). Interestingly, no significant difference was found with the low impeller configuration when stirred in either 30 RPM and 40 RPM. Significant difference was found between mixing low impeller configuration at 40 RPM and high impeller configuration at 30 RPM ( $p = 0.0011$ ; Figure 5.1 A). All stirring speed settings eventually produced homogenous discolouration of the vessel contents, indicating by homogeneous distribution of reagents within the vessel volume.

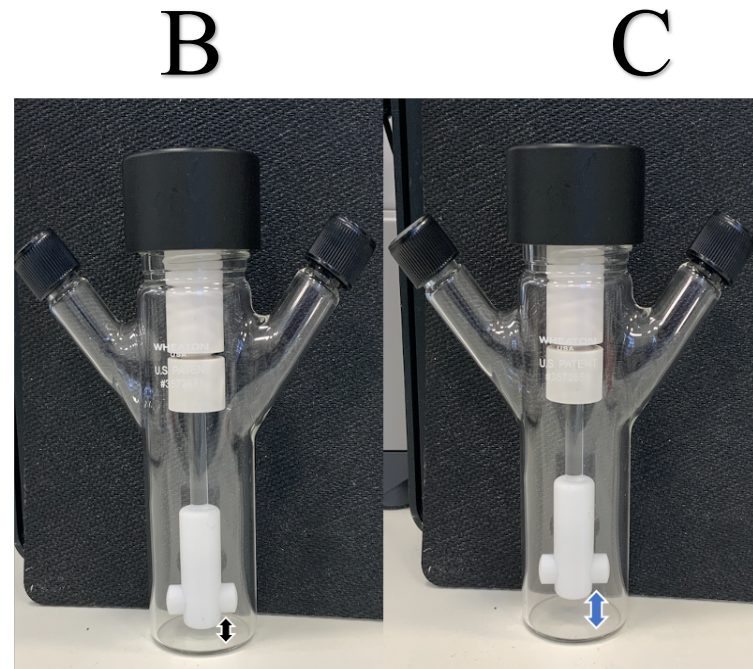
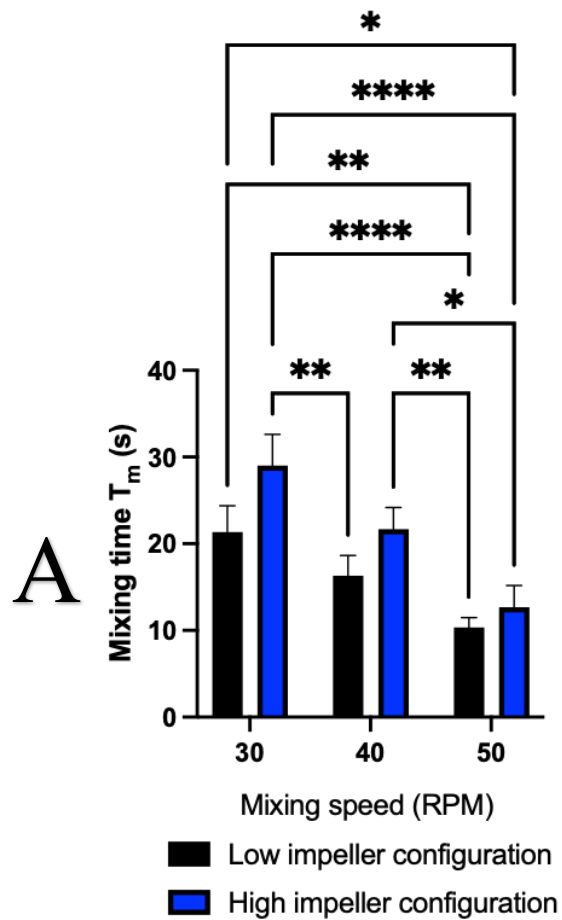


Figure 5.1. Comparing the effect of stirring speed and impeller configuration on the mixing time within the spinner flasks. The mixing times was determined by the speed of the discolouration reaction between sodium thiosulfate and iodine (A). The low impeller configuration of the stirrer bar is shown in (B), where the impeller is placed as close to the bottom as possible and leaving a small gap to reduce the grinding of cells and microcarriers. (C) shows the high impeller configuration where at least 1 cm gap is left from the bottom of the well. Data is shown as mean  $\pm$  SD.  $N=3$  independently prepared reagents. \* $p \leq 0.05$ , \*\* $p < 0.01$ . \*\*\* $p < 0.001$  and \*\*\*\* $p < 0.0001$ , two-way ANOVA, multiple comparison test.

### **5.2.2.Characterising the expansion of kiPSC in the baseline scalable bioprocess**

After identifying the mixing speeds capable of producing a homogenous mixture for the culture of kiPSCs within the bioreactors, the next steps were to assess the designed bioprocess for its potential to expand kiPSCs. For the baseline scalable bioprocess, 30 RPM was chosen as it was the Njs for VTN coated microcarriers, and a homogenous mixture could be obtained. The high impeller configuration (1 cm from the base of the spinner) was chosen to mitigate chances of any microcarrier grinding as no significant difference was seen between the higher and lower impeller configurations at 30 RPM.

#### **5.2.2.1.kiPSC growth kinetics during expansion in baseline scalable bioprocess**

The expansion of the kiPSCs, inoculated at  $4 \times 10^4$  cells/cm<sup>2</sup> in spinner flasks with 100 cm<sup>2</sup> of VTN coated microcarrier (i.e., a total of  $4 \times 10^6$  cells), was measured to generate  $1.20 \pm 0.37 \times 10^7$  viable cells or a  $3.01 \pm 0.91$ -fold increase after 96 h of expansion in dynamic stirred environment (Figure 5.2 A and D). Due to the limited biological repeats of this study (N=2), no statistical analysis could be confirmed to compare the yields of the expansion process from the baseline and microcarrier integrated bioprocesses of the previous results chapters. However, the yield here is notably lower than the yield obtained from the expansion of kiPSC on 2D planar platforms (>20 FI) and VTN coated Plastic microcarrier in well plates under static conditions (>9 FI). kiPSCs cultured in spinner flasks demonstrated long DT ( $64.43 \pm 18.44$  h) and slow SPGR ( $0.011 \pm 0.003$ ). Future repeats of a spinner flask runs using the parameters set for baseline scalable bioprocesses is needed to support these results.

The TCC profile of kiPSC shown in Figure 5.2 A shows a decrease after inoculation. After 24 h, the TCC begin to gradually increase. By 96 h, a large TCC variation is indicated by the SD.

The pH of the culture can impact the quality of the cells. For many other bioprocesses employing mammalian cells at manufacturing scale, the pH parameter is constantly monitored

and adjusted accordingly using base or acids, to ensure the optimal physiological pH for the cells to grow. The pH profile of the culture environment within the spinner flask cultures of kiPSC in the baseline scalable bioprocess remained within a wide range of 6.9 and 7.4 throughout the culture duration Figure 5.2 B.

Metabolites like lactate can also contribute to lowering the pH of the culture environment. In, Figure 5.2 C lactate concentrations remained relatively lower throughout the cultures in spinner flasks, when compared to the lactate profiles of kiPSC in planar or microcarrier platforms (chapters 3 and 4). On the same graph, glucose concentrations were recorded to be higher on average than recorded for planar or microcarrier expansion process (chapters 3 and 4). Both lactate and glucose concentrations were removed and replenished, respectively, after each medium exchange which are indicated by the arrows in Figure 5.2 C.

Live/dead staining at day 2 and day 4 provided means to visually assess the growth of kiPSC (Figure 5.2 E). Day 2 live/dead images revealed the underutilisation of some microcarriers as no live cells were observed attached to their surfaces. Small aggregates of 2 or 3 microcarriers and cells were also observed. At day 4, evident larger cell-microcarrier aggregates and complexes were observed, confirming that kiPSCs did not form monolayers on the microcarriers, and instead formed multilayers of cells indicated by intense Calcein AM stained cells on the surface of microcarriers. Surprisingly, despite the presence of large cell-microcarrier aggregates, the viabilities of the harvested cells were measured at  $90.78 \pm 2.18 \%$ , similar to the viabilities in 2D planar platforms (chapter 3).

#### **5.2.2.2.Pluripotency assessment of the harvested cells**

Following the harvest of the kiPSC after 96 h expansion in the baseline scalable bioprocess, it was important to assess whether the harvested cells maintained their pluripotent quality. To

determine the presence of pluripotent markers OCT4 and SSEA4, harvested cells were replated and cultured on VTN coated multi-well plates for a further 96 h before fixing and preparing for ICC analysis.

Harvested cells were capable of attaching onto the VTN substrate post-harvest, forming typical PSC colonies. Harvested cells also displayed OCT4 and SSEA4 which were detected by ICC staining shown in Figure 5.3. Due to the intense density of the cells within the colonies at the day of fixing (96 h post-harvest), nuclei counting using the method of image analysis was highly unreliable and inaccurate at quantifying the number of OCT4<sup>+</sup> cells. From the qualitative analysis of the images, it is clear that the number of OCT4<sup>+</sup> and SSEA4<sup>+</sup> is relatively less than that of the DAPI<sup>+</sup> population.

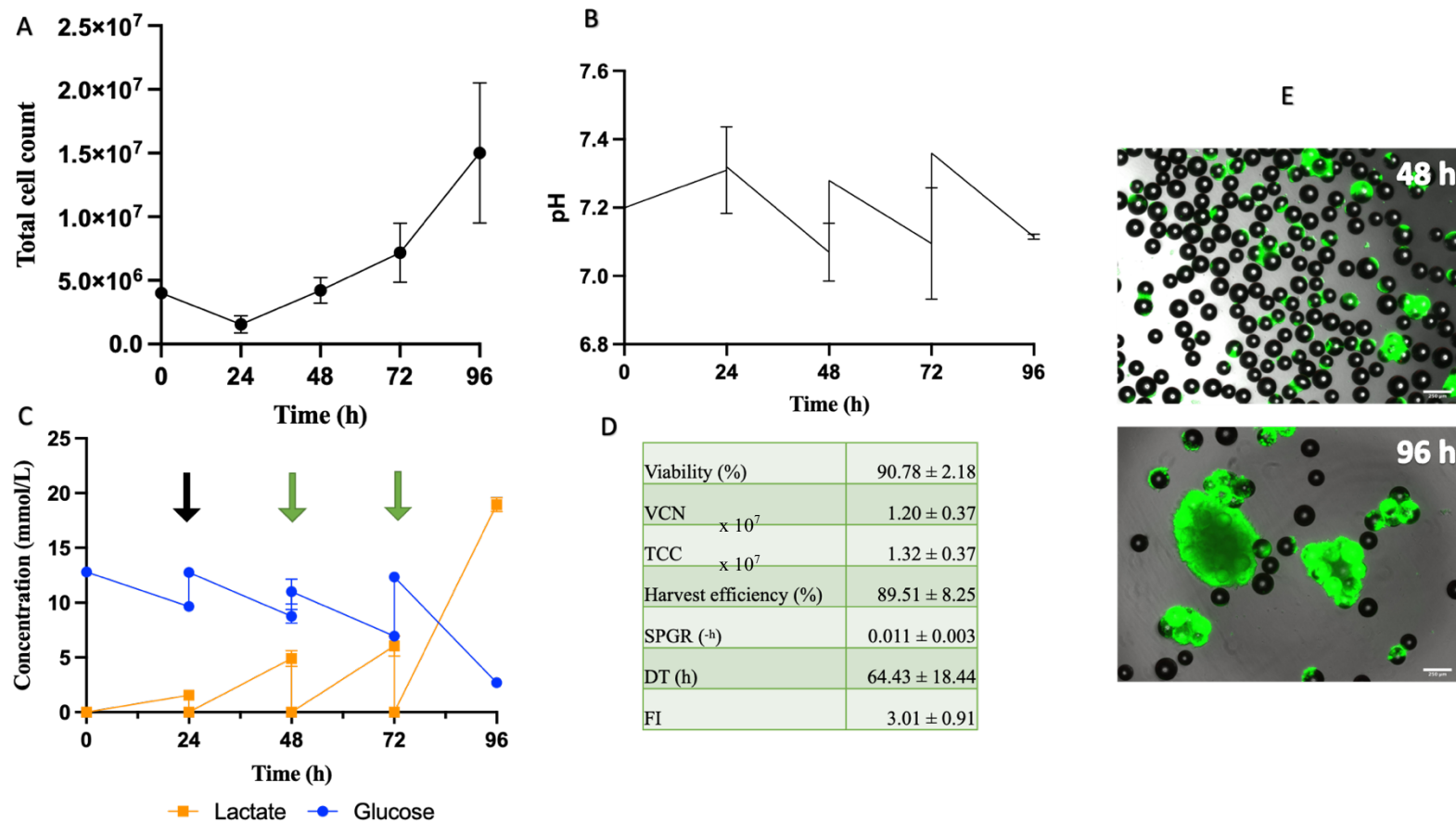


Figure 5.2. Expansion of kiPSC in spinner flasks for 96 h. kiPSCs were seeded at  $4 \times 10^4$  cells/cm<sup>2</sup> onto 100 cm<sup>2</sup> of VTN plastic microcarrier and a maximum 20 mL working volume (mTeSR™ Plus). kiPSC were expanded for 96 h before harvest and the TCC was monitored throughout the expansion process (A). pH of the culture system was taken at the start of the process then before and after each medium exchanges (B). Similarly, the concentration of glucose and lactate were also measured throughout (C); arrows indicate 80% medium exchange (black arrow indicates the culture medium in vessel total of 10 mL, and the green arrows indicate a total culture medium in vessel of 20 mL). The harvest viability, VCN, TCC, efficiency and growth kinetics are shown in table (D) obtained after 96 h of culture. Homogenous samples were taken at 48 h and 96 h of culture and assayed for live/dead staining (E). Images are representative of samples taken from spinner flasks at different timepoints. Data shown here is the mean  $\pm$  SD. N=2, biological repeats. Scale bar = 250  $\mu$ m.

F.D., de la Kaga, PhD thesis, Aston University, 2022

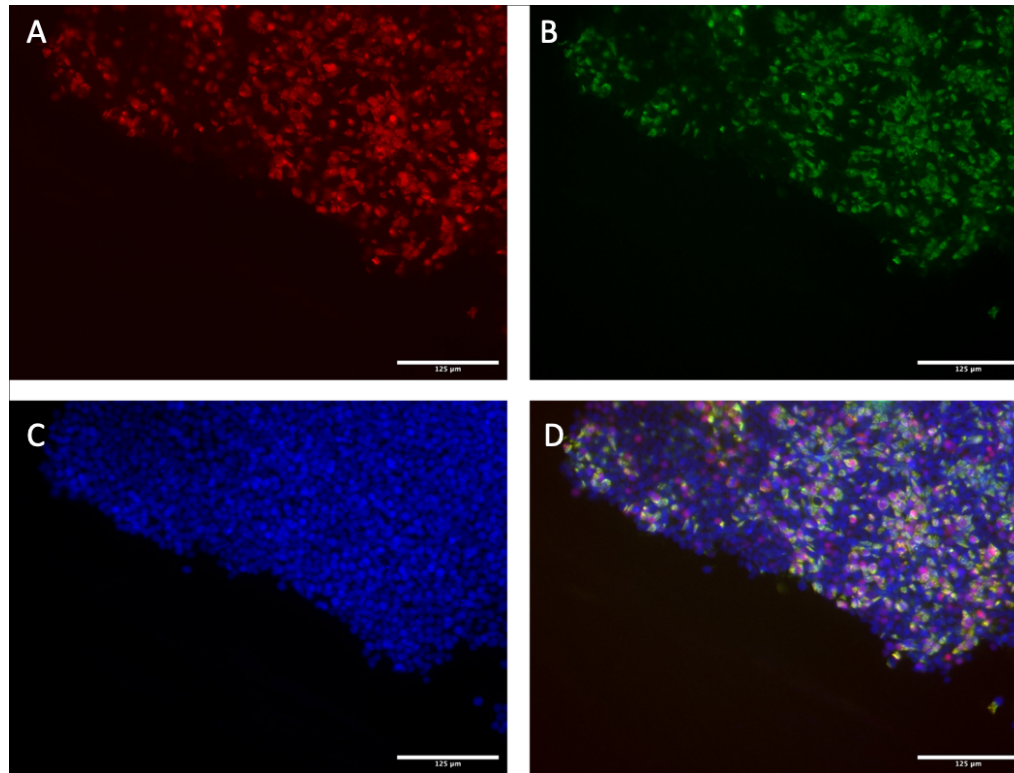


Figure 5.3. Assessment of the harvested cells after expansion of kiPSC in spinner flasks. ICC was used to assess for pluripotency markers after replating the harvested cells. Cells were fixed and stained 4 days post replating. Pluripotency markers OCT4 (A) and SSEA4 (B) were detected by ICC. DAPI staining was used to indicate nuclei (C). (D) shows the merged all channels merged. Representative of N=2, biological repeats. Scale bar = 125 µm

### **5.2.2.3. Neural induction of cell laden microcarriers from the baseline scalable bioprocess**

Before harvesting the cells from cultures in the baseline scalable bioprocess, 1 mL of a homogenous cell sample was taken and transferred into a 24 well plate (~5 cm<sup>2</sup>/mL of microcarrier surface area). The medium was exchanged to SNIM + SMADi and the cells were directed towards the neural lineage by neural induction for 144 h, with daily 50% medium exchanges. The cells were then harvested and re-plated and expanded for 2 days before fixing and staining for the presence of neural lineage marker PAX6 (Figure 5.4).

Cells induced towards the neural lineage on microcarriers from the baseline scalable bioprocess poorly expressed PAX6 and the cells replated displayed a large nucleus. Though some cells can be qualitatively confirmed to express PAX6, the DAPI counter staining of cell nuclei indicate that the majority of cells did not express PAX6 as indicated by the lack of visible stained PAX6 in the merged image (Figure 5.4 C).

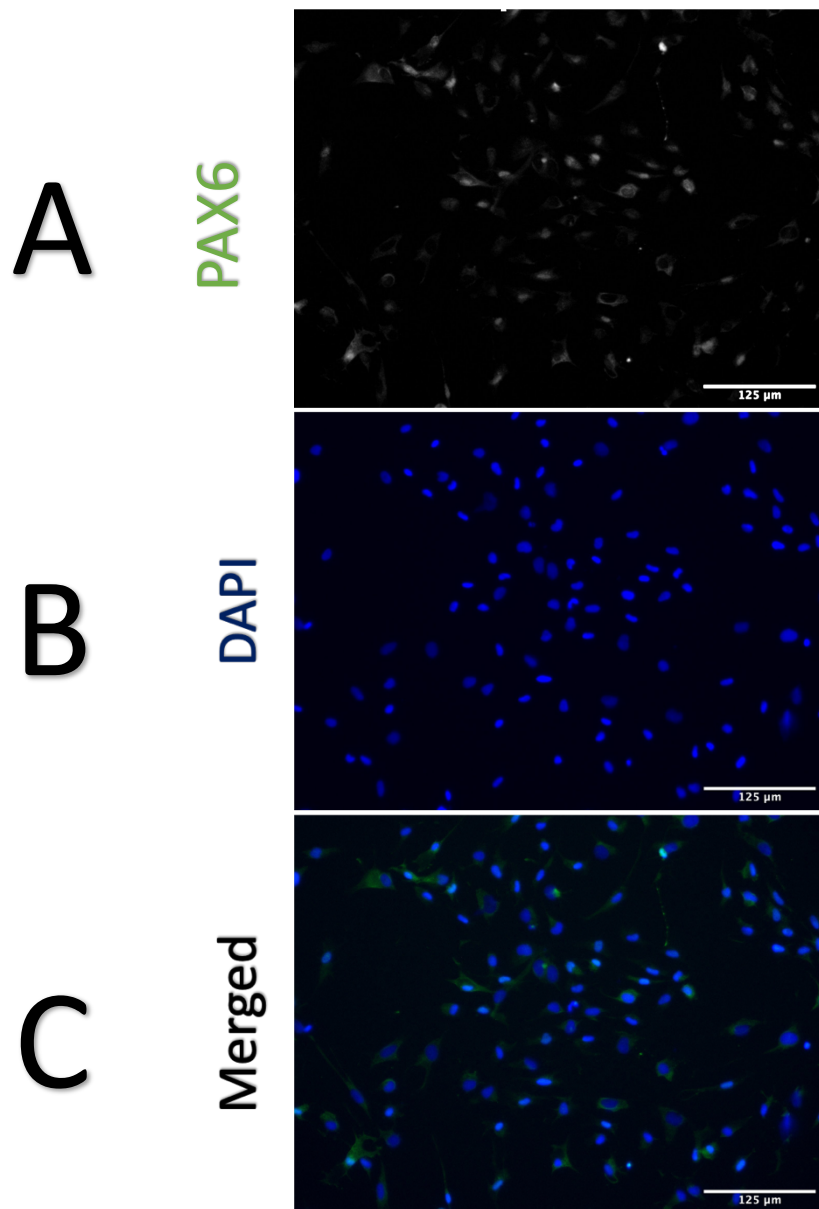


Figure 5.4. Assessing the potential of kiPSC-laden microcarriers from the baseline scalable bioprocess to differentiate towards NPCs. 1 mL sample was taken from spinner flasks prior to proceeding with the spinner flask harvest process. The sample was then transferred into ULA at 500  $\mu$ L per well. The medium was exchange to SNIM + SMADi and differentiated for 6 days. Cells harvested from this neural induction process were fixed for ICC analysis 2 days after replating on PLO/LN. Fixed plates were stained for the presence of PAX6 (A). Nuclei was stained with DAPI (B). (C) is the merged image of the green and blue channels. N=2, biological repeats. Scale bar = 125  $\mu$ m.

### **5.2.3.Optimisation of the baseline scalable bioprocess**

Due to the low fold increase (~3 times) observed from kiPSC expansion in the baseline scalable bioprocess, and the low PAX6 expressing cells of the neurally induced cells harvested, it was clear that the conditions for expansion and differentiation were suboptimal. Hence, the subsequent work detailed in this section (5.2.3) is focused towards the optimisation of the culture conditions in spinner flasks.

#### **5.2.3.1.Assessing the growth kinetics of kiPSCs in spinner flasks using low impeller configuration at different mixing speeds**

Though the Njs (30 RPM) was implemented for the baseline scalable bioprocess to mitigate shear stress exposed to the cells, it was clear, however, that such speed settings in combination with the impeller configuration, was not sufficient to break or prevent large aggregate formations. It was therefore postulated that a lower impeller configuration and/or higher speed settings could potentially mitigate the pooling of cells and microcarriers under the impeller. Therefore, the next set of experiments were to investigate whether the low impeller configuration of the spinner flask, at different stirring speed settings could indeed improve the growth of kiPSC. This is a step towards optimisation of the baseline scalable bioprocess following a one factor at a time approach.

The expansion of kiPSCs in these experiments were performed with identical parameters to those in section 5.2.2 but instead, with the lower impeller configuration. The other parameter explored was stirring speed. kiPSC expansion in spinner flasks with low impeller configuration was also performed in 3 different speed settings to evaluate its effect on kiPSC growth kinetics. Due to equipment and reagent limitations and the time available (being the last series of experiments), it was only possible to perform this set of conditions with two biological repeats

(N=2) whereby repeats were obtained from independently thawed vials of kiPSCs. Unfortunately, with such a limited number of biological repeats, statistical analysis could not be satisfied.

Figure 5.5 shows the measured TCC, viability and growth kinetics of kiPSCs expanded in spinner flask with low impeller configurations, at different mixing speeds. The growth patterns of the kiPSC for all conditions, were similar to the growth profiles observed in Figure 5.2. Expansion of kiPSC in spinner flasks for 96 h. kiPSCs were seeded at  $4 \times 10^4$  cells/cm<sup>2</sup> onto 100 cm<sup>2</sup> of VTN plastic microcarrier and a maximum 20 mL working volume (mTeSR<sup>TM</sup> Plus). kiPSC were expanded for 96 h before harvest and the TCC was monitored throughout the expansion process (A). pH of the culture system was taken at the start of the process then before and after each medium exchanges (B). Similarly, the concentration of glucose and lactate were also measured throughout (C); arrows indicate 80% medium exchange (black arrow indicates the culture medium in vessel total of 10 mL, and the green arrows indicate a total culture medium in vessel of 20 mL). The harvest viability, VCN, TCC, efficiency and growth kinetics are shown in table (D) obtained after 96 h of culture. Homogenous samples were taken at 48 h and 96 h of culture and assayed for live/dead staining (E). Images are representative of samples taken from spinner flasks at different timepoints. Data shown here is the mean  $\pm$  SD. N=2, biological repeats. Scale bar = 250  $\mu$ m. for the baseline scalable bioprocess (Figure 5.2), where the TCC decreases in the first 24 h post inoculation, and cell growth occurs after 24 h in culture as suggested by the increasing of TCC. The viability of the cells following the harvest were comparable across all conditions at  $\sim$ 93% (Figure 5.5 B).

The calculated growth kinetics for kiPSC showed the highest average SPGR ( $0.0137 \pm 0.000$  h), lowest DT ( $50.52 \pm 1.63$  h). and highest FI ( $3.74 \pm 0.16$ -fold) in conditions of 40 RPM compared to the 30 RPM and 50 RPM stirred cultures. For conditions of 30 RPM and 50 RPM, the growth kinetics were not improved compared to the baseline scalable bioprocess, in fact,

the FI reduced to only ~2 fold in both conditions, with DTs increasing up to  $90.49 \pm 12.40$  h in cultures at 50 RPM (Figure 5.5).

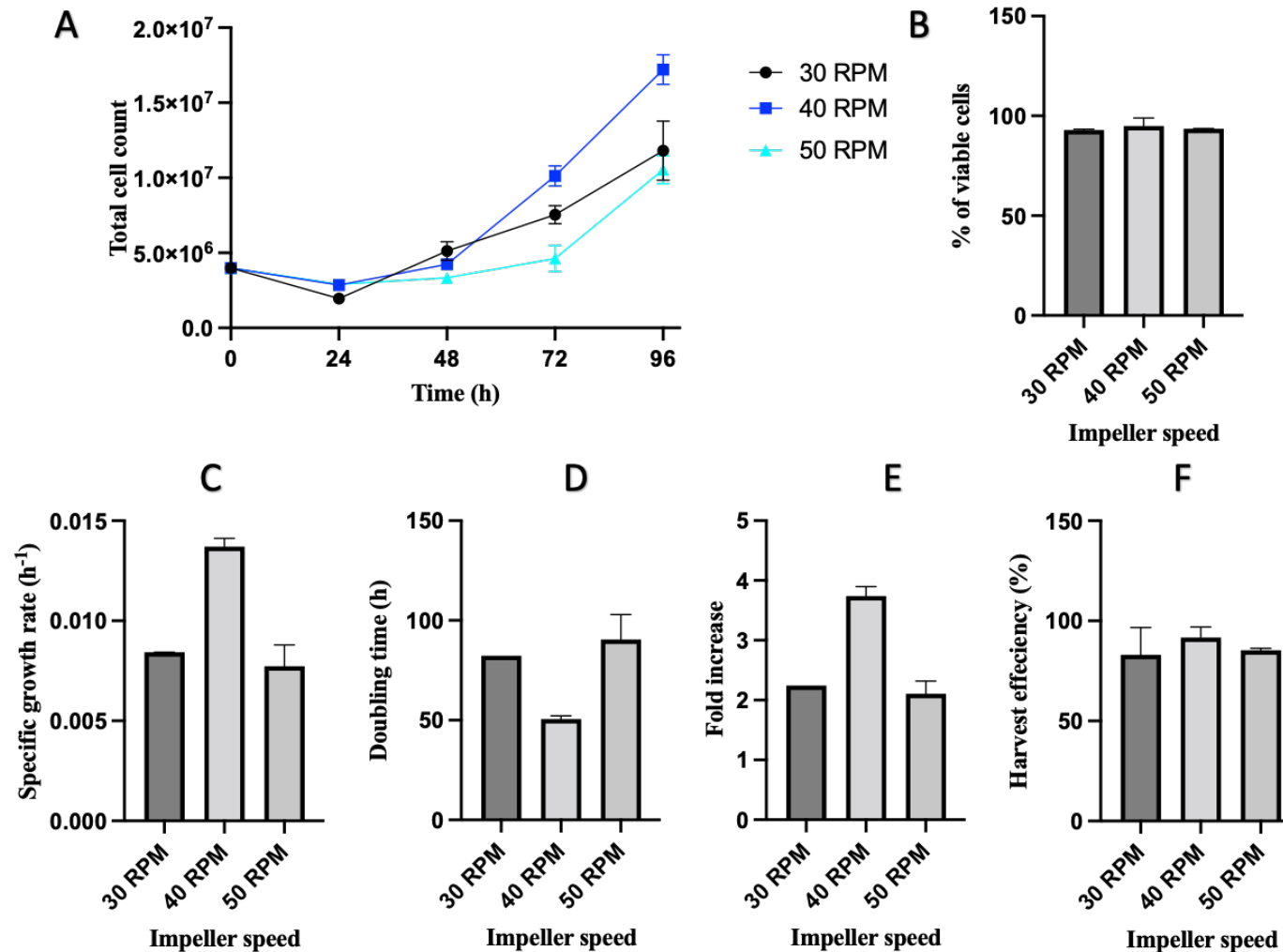


Figure 5.5. Comparison of 3 different impeller stirring speed on the growth of kiPSC with spinner flasks. The impeller speeds compared were 30 , 40 and 50 RPM. TCC through 96 h of expansion was measured (A). Viability was also measured for the harvested cells (B). The SPGR (C), DT (D) and FI (E) were calculated from the VCN at harvest. The harvest efficiency was also calculated (F). Data is shown as mean  $\pm$  SD. N=2, biological repeats.  
 F.D., de la Raga, PhD Thesis, Aston University, 2022

### **5.3.Discussion**

STBs are scalable culture platforms that pave a route for easy process scale-up, hence, streamlining the transitions from lab scale processes to production at commercial scale manufacturing.

In this final results chapter, the bioprocesses established in Chapters 3 and 4 were translated into the design of a scalable bioprocess for expanding kiPSCs and generating NPCs, in a defined culture system using xeno-free microcarriers. This was achieved by utilising spinner flask platforms, cGMP standard mTeSR-Plus and VTN coated Plastic microcarriers. The successfully translated design of the bioprocess in spinner flasks offered a scalable bioprocess for the expansion and differentiation of kiPSCs. However, due to the lack of available resources, it was not possible to demonstrate the neural induction of kiPSCs within spinner flask. Instead, the neural induction was performed on samples from the expansion phase of the baseline scalable bioprocess.

#### **5.3.1.Cell-microcarrier aggregation slows down kiPSC growth in spinner flasks**

For the expansion of kiPSC on microcarriers in spinner flasks platforms, cell growth was expected to, at least, be relatively similar to the growth in microcarrier bioprocessing (chapter 4), or improved due to the dynamic homogenous environment provided by the stirring as seen in other studies (Chen *et al.*, 2011; Wang., *et al.*, 2013; Gupta *et al.*, 2018; Kato *et al.*, 2018). However, this was not observed following the expansion of kiPSCs using the parameters for the baseline scalable bioprocess. kiPSC expanded in baseline scalable bioprocess parameters had poorer growth kinetics in comparison to the kiPSCs expanded in the static baseline (>20 FI) and microcarrier integrated bioprocesses (~10 FI) seen in previous chapters. Here, only a ~3 FI was observed.

Indeed, the reduced cell growth in spinners was interesting. Most of the process parameters were reserved from the baseline and microcarrier integrated bioprocesses in static cultures to spinner flask cultures (e.g., incubator conditions, seeding density, available surface area, coating material etc.). The main difference of spinner flask cultures was the dynamic stirring, therefore, it was postulated that the reduced growth kinetics of iPSCs may be due to suboptimal parameters exclusively for STBs such as impeller design and stirring speed.

Different designs and configurations of the impeller in STBs produces varying fluid flow paths and dynamics which can impact cell growth (Hewitt *et al.*, 2011). To the best of the authors knowledge, no other study has employed the same spinner flask vessel used here to expand PSCs. The impeller designs used by others for the expansion of PSCs typically contain a paddle in addition to the magnetic flea, which is shown to significantly improve mixing (Kehoe *et al.*, 2010b; Hewitt *et al.*, 2011; Jo'An Bardy *et al.*, 2013; Gupta *et al.*, 2016). The paddle in such cases could also act as a physical barrier during collision with suspended cell-microcarrier aggregates, leading to mechanical dissociation of large aggregates, thus reducing the formation of necrotic cores prevalent in such structures (Kempf *et al.*, 2016). The magnetic flea alone without the paddle used here was not sufficient at providing the fluid motions, hydrodynamics and shear at 30 RPM necessary to minimise formation of large aggregates, as such structures were visibly seen particularly at later stages of the culture (Figure 5.2 E at 96 h).

Though live cells were detected by live/dead staining within cell-microcarrier aggregates, the necrotic cores were difficult to capture, potentially due to the limitations of the technique use here to image the cores of aggregates which themselves could measure larger than 500  $\mu\text{m}$  in diameter. Alternatively, the size of the aggregates may not have permitted the delivery of the ethidium homodimer dye to the core of the aggregates. Thus, the lack of aggregate size control throughout the baseline scalable bioprocess may explain why the cell growth kinetics here are

flasks with improved yields compared to 2D static planar expansions, since they report maintenance of aggregate sizes less than 300  $\mu\text{m}$  (Chen *et al.*, 2011; Badenes *et al.*, 2015; Sara M Badenes *et al.*, 2016; Le and Hasegawa, 2019). Further, other techniques could be used to determine the presence of necrotic cores within large aggregates such as confocal or epifluorescence laser scanning microscopy.

Furthermore, the formation of large cell-microcarrier aggregates were exacerbated by the stagnant pool of cell-microcarrier aggregates underneath the impeller, particularly for cultures in the baseline scalable bioprocess conditions (see supplementary Figure A.1). The collection of microcarrier and cells were the result of the combination of suboptimal impeller design, impeller height configuration, and insufficient stirring. First, the impeller design and height configuration caused a central vortex under the impeller, which pulled the cells and microcarriers to collect at the centre. In conjunction, the change in microcarrier density as cells attached and expanded on its surface resulted in the change of the microcarrier buoyancy, hence, the pooling of VTN coated plastic microcarriers alone was not observed during the visual assessment of different mixing speeds or mixing studies (section 5.2.1). Eventually, it became evident that the stirring speed of 30 RPM (Njs) was no longer able to lift and distribute the cell-laden microcarriers homogeneously as the cultures progressed. As a result, the cells and microcarriers collected at the centre and promoted the formation of large cell-microcarrier aggregates.

Cells within this stagnant pool of large aggregates are exposed to a heterogeneous environment due to concentration gradients of growth factors and nutrients across the structures. This was reflected in the poor growth kinetics of kiPSCs and the lack of pluripotency marker expression of harvested cells. To avoid formation of a vortex, the next set of experiments investigated the effect of lowering the impeller height and adjusting the stirring speed. Nevertheless, further characterisation, be it through experimental or computational assessment, of fluidic flow and

hydrodynamic forces in the spinner flask used here is needed, as the lack of understanding in the way cells interact with the spinner flask and its contents leads to unclear routes towards process optimisations.

### **5.3.2. Influence of shear stress on cell growth**

The hydrodynamics in spinner flasks cultures exposes the cells to shear which can lead to physical cell damage and modulation of cell surface membrane molecules. Stimulation of such cell surface membrane molecules or compromise of cell integrity can cause intrinsic pathway activation that leads to reduced growth kinetics or cell death (i.e., apoptosis) (Wolfe *et al.*, 2012; Chen *et al.*, 2013; Fan *et al.*, 2014). Hence, only 30 RPM was firstly applied in the baseline scalable process as this was the lowest speed setting to suspend the microcarriers (Njs), therefore, minimising shear force exposed to cells whilst ensuring the up lift of microcarriers. Yet, there was still a reduction of cell growth in dynamic conditions compared to static (chapter 4) microcarrier cultures. At higher RPM settings of the magnetic platform, where cells were expected to experience greater shear, the results indicated that cell growth may be further thwarted, which is particularly evident when comparing the reduced VCN obtained from 50 RPM cultures to that of 40 RPM cultures.

Other reports have suggested that mechanical stimuli (i.e., from shear force), compressive, and tensile forces can cause PSCs to differentiate towards particular lineages depending on the duration, frequency and magnitude of the applied shear (Wolfe *et al.*, 2012, 2016; Gareau *et al.*, 2014; Lindner *et al.*, 2021). Thus, it may be that PSCs cultured under dynamic conditions have undergone differentiation contributing to the reduced growth and detection of OCT4 positive pluripotent cells. An alternative route to determining the level of differentiation is the

use of flow cytometry and other assays to detect expression of pluripotency/lineage specific genes such as qRT-PCR.

Additionally, others have also reported of shear related dissociation of cells from coated microcarriers (Chen *et al.*, 2011; Fan *et al.*, 2017). Fan *et al.* (2017) also used VTN coated Plastic microcarriers for the expansion of hESCs in spinner flasks and reported cell concentration decline over 5 days in a TeSR<sup>TM</sup>-E8<sup>TM</sup> culture system. Their work suggests that VTN coating alone may be insufficient to support long term PSC expansion on Plastic microcarriers due to cell detachment, which are also echoed here in this study. Additional modifications to the microcarrier such as treatment with HSA or UV for increased protein adsorption or crosslinking, respectively may be necessary to minimise cell detachment. Similarly, addition of Pluronic F68 or Tween 20 to the media could act as a shear protectant agent and an antifoam.

### **5.3.3. Inefficient seeding protocol may lead to reduced cell growth**

Live/dead and phase contrast images of cells and microcarriers during the spinner flask cultures revealed that not all microcarriers were populated with cells from early stages of the culture to the harvest time point, which can be attributed to several potential explanations. First, shear not only affects the cells but could also the coating of microcarriers. Since the VTN coating is reliant on adhesion to the surface of the microcarriers, it is possible that constant shear can cause the detachment of the VTN coating, rendering the surface unsuitable to support kiPSC attachment and adhesion. The instability of VTN on plastic microcarriers have been explored by another group who attempted to stabilise the VTN coating on plastic microcarriers and successfully demonstrated improvement in cell growth following HSA and UV treatment (Fan

*et al.*, 2017). However, the employment of HSA at large scale processes would be an added expensive cost, rendering such processes unsuitable for clinical manufacturing.

In an attempt to improve the stabilisation of the VTN coating, VTN coated microcarriers were conditioned in the mTeSR<sup>TM</sup> Plus medium (which contains BSA and FGF) before inoculating with cells for all spinner flask cultures in this chapter. Regardless, cells did not homogeneously populate and expand on all the microcarriers since unpopulated microcarriers were observed after 24 h by phase contrast microscopy and by the end of the expansion phase of the baseline scalable bioprocess. Under utilisation of microcarrier surfaces may explain the low VCN/cm<sup>2</sup> ( $\sim 1.32 \times 10^5$ ) ratio harvested from the baseline scalable bioprocess.

However, in comparison to kiPSC expanded on VTN coated plastic microcarriers in static conditions, the average yield was  $3.78 \pm 0.56 \times 10^5$  VCN/cm<sup>2</sup>. The disparity between dynamic (in spinner flask) and static VTN coated microcarrier cultures may be explained by potential difference in seeding efficiency. In spinner flasks culture systems, cells are inoculated in a dynamic condition, thus, the formation of initial cell attachment to the microcarrier surface are highly reliant on the chance of collision and exposure time (Eibes *et al.*, 2010). In the case of static microcarrier cultures, cells are deposited on top of the microcarriers which then rely on gravity to deposit onto the surface of the microcarrier, thus, a higher proportion of cells can successfully attach onto the microcarriers. Future work could investigate the seeding efficiency of kiPSCs onto VTN coated microcarriers under dynamic conditions by quantifying the free floating PSCs at 4, 12 or 24 h post seeding (Phillips *et al.*, 2008; Van Beylen *et al.*, 2021).

To improve cell attachment, other inoculation strategies could be employed such as static inoculation whereby cells and microcarriers are allowed to deposit to the bottom of the culture vessel for a certain amount of time until successful cell attachment. Similarly, intermittent spinning following inoculation and during the initial attachment phase could provide time for

cells to settle, interact with microcarriers, and establish attachment whilst intermittently being redistributed to ensure a homogenous population of cells on microcarriers (Correia *et al.*, 2014).

#### **5.3.4. Dynamic cultures negatively affected the differentiation potential of kiPSCs**

Samples of cell-laden microcarriers from spinner flask cultures using the baseline scalable bioprocess, were differentiated in ULA well plates towards NPCs using SNIM + SMADi. The results of the ICC staining showed poor expression of the neural marker PAX6 in the harvested differentiated cells. Cells also appeared to contain larger nuclei compared to the control Ax0013 seen in the previous chapters. This result suggests the inability of kiPSCs to commit towards the neural lineage following expansion in spinner flasks. However, others have successfully reported the differentiation of PSCs on microcarriers towards NPCs (Bardy *et al.*, 2013; Badenes *et al.*, 2016). Bardy *et al.*, (2013), reported a yield of 333 NPCs from 1 hiPSC and characterised the NPCs as PAX6 and Nestin positive cells. Bardy *et al.*, (2013) also determined the relative expression of neural markers PAX6, SOX1, Nestin and MSI by qRT-PCR. They further assessed the potential of the generated NPCs to differentiate towards specific neural cell types by assessing  $\beta$ -tubulin II and GFAP for astrocyte and oligodendrocyte markers respectively. For neuronal potential assessment, they assessed the neuronal activity using Patch-clamp recording, after differentiating the generated NPCs using BDNF, GDNF and NGF containing medium. However, here it was not possible to determine the number of NPCs obtained, as there was not enough resource to differentiate the generated NPCs towards oligodendrocytes, astrocytes and neurons. Future studies and repeats of these experiments could exploit these techniques to further characterise the NPCs generated.

The poor ability of the cells to differentiate towards NPCs following expansion in spinner flasks may be due to multiple factors such as shear stress to the cells causing the loss of differentiation potential. Also, samples for neural induction contained a mixture of microcarriers with minimal or no cells, as well as large cell-microcarrier aggregates. This inhomogeneity sample may have resulted in inconsistent neural induction of the cells, since large cell-microcarrier aggregates could experience concentration gradients of essential neural inducing factors. Differences in morphologies and neural marker expression were observed when comparing the obtained NPCs from different neural induction processes: neural induction of adhere kiPSCs in 2D platforms; neural induction of cell-laden microcarriers in static; and neural induction of cell-laden microcarriers from spinner flask expansion, in static. Quantification of the presence or expression of neural lineage specific markers of products from these different neural induction processes is needed to confirm these differences.

### **5.3.5. Process parameter optimisation**

Preliminary work was conducted to improve the expansion of kiPSC in spinner flask cultures as the impeller configuration and the stirring speed were identified to be suboptimal due to causing the pooling of cell-microcarrier aggregates below the impeller. Although the  $N_{JS}$  speed (30 RPM) was sufficient to suspend the VTN coated plastic microcarriers, when cells populated the microcarriers, it was no longer able to provide enough uplift to suspend the microcarriers. Hence, a mixing study was performed to identify the ideal stirring speed and impeller configuration. These studies suggested that the difference in impeller height had no significance in the mixing times. However, greater significant difference in mixing time is observed when increasing the stirring speed and implementing a low impeller configuration compared to the mixing at speed of 30 RPM with high impeller configuration.

Following these studies, the low impeller configuration was employed for further spinner flask cultures and assessed for its ability to improve kiPSC growth kinetics. The results from these experiments shown in that the expansion of cells was not improved by the lower impeller settings for cultures at speeds of 30 RPM and 50 RPM, since the harvested VCN reduced compared to cultures in the baseline scalable bioprocess. For cultures in 30 RPM settings, some cell-laden microcarriers were not fully suspended, especially aggregates. Nonetheless, the large pool of cells and microcarriers observed with high impeller configuration at the 30 RPM stirring speed was not observed for the lower impeller configuration. For cultures in 50 RPM settings, cell-laden microcarriers were fully suspended and less aggregation was observed. It is possible that at high stirring speeds, cells could be detaching from the microcarrier surfaces due to shear stress which can ultimately cause cell death as a result of anoikis. However, for cultures at speeds of 40 RPM, a slight improvement in growth kinetics were observed. More biological repeats are needed to confirm statistical difference between these conditions.

Overall, the work in this chapter demonstrated the translation of the baseline and microcarrier integrated bioprocesses towards a scalable bioprocess utilising scalable spinner flask (termed here baseline scalable bioprocess). However, considering the time and resource constraints, it was only possible to demonstrate the expansion phase of the designed baseline scalable bioprocess, whilst the neural induction was performed on samples from the expansion runs. Preliminary work was conducted to investigate the expansion of kiPSCs in different stirring conditions towards efforts of optimising the process. However, further work is needed to assess the neural induction of kiPSCs following the expansion phase with spinner flasks and further process development is needed to optimise the expansion of kiPSCs on VTN coated plastic microcarriers.

## **6.Final remarks and Future work**

### **6.1.Future work**

In this thesis, it was demonstrated that it is viable for a 2D expansion processes of hiPSCs to be translated towards a 3D dynamic process using small scale STBs. The studies here also demonstrated the ability of hiPSCs expanded in STBs, to differentiate towards PAX6 positive cells, a key marker for neural lineage commitment. However, an integrated 3D dynamic process was not established due to time constraints and lack of resources. To fully develop a scalable, integrated and optimised bioprocess for the efficient production of NPCs, it is essential to perform further experiments and employ various cell and process characterisation techniques. These will be discussed further in this section.

#### **6.1.1.Future work towards optimising a microcarrier dependent bioprocess**

Given no limitations of time and resources, a thorough and representative microcarrier screening is needed to establish a robust microcarrier dependent bioprocess. Here, 8 different microcarriers were screened, however, this is not exhaustive of the range of commercially available microcarriers. Other commercially available microcarriers include Cultispher G and Cultispher S, Cytopore 1 and Cytopore 2 (VWR), and dissolvable microcarriers (Corning). Similarly, only VTN was used as a coating for the screening in this thesis, however, other surface proteins such as LN, Synthemax II or fibrinogen (Gandhi *et al.*, 2019) could be explored in combination with different microcarriers.

Dissolvable microcarriers are interesting technologies which can significantly impact the downstream process by reducing the need for a separation step via filtration. Although studies have demonstrated ability for Synthemax II coated dissolvable microcarriers to support hiPSC

expansion (Rodrigues *et al.*, 2019), to the authors knowledge, dissolvable microcarriers have not been reported in an integrated bioprocess, in particular for NPC generation.

The screening of microcarriers in well plates on static or rocking platforms is another limitation of this thesis, as these are not representative of the dynamic environments in STBs. Thus, the performance of microcarriers under these conditions are not be translatable/predictable for STB cultures. Systems like the c.bird™ instrument (Cytex) could be utilised to provide a dynamic environment for screening studies in well plates. Simply, the c.bird™ system works by applying continuous cycles of suction and dispensing (up and down) of the well contents (i.e., media, microcarriers and cells), causing turbulence and thus presenting a controllable dynamic environment. Such technologies allow for small scale screening studies to be performed in multi-well plates which maintains low consumable costs and high throughput. The criteria for choosing the ideal microcarrier and coating combination could then be based on best growth curves, high efficiency of differentiation towards NPCs (e.g., conditions with high PAX6<sup>+</sup>, Nestin<sup>+</sup> and SOX2<sup>+</sup> counts, and low OCT4, TRA-1-81 and Nanog expression; determined by flow cytometry and ICC), and highest quality of cell products (e.g., functional differentiation towards specific neuron phenotypes and characterised by optical fluorescent calcium imaging).

Alternatively, multi-vessel mini bioreactors such as the Ambr® systems from Sartorius, offers a high throughput platform for microcarrier screening studies (Rotondi *et al.*, 2021). Although typically requiring larger working volumes (minimum 10 mL working volume per vessel) compared to well plates, microcarrier screening studies performed in such vessels could provide more representative and scalable data as the culture environment within the Ambr® vessels are similar to that of benchtop, pilot and even production scale bioreactors. Advantageously, the Ambr® systems would allow for control of process parameters such as impeller speed which could be used as a variable in investigating the integrity of protein coatings on microcarriers, as this can influence cell attachment and growth (Fan *et al.*, 2017).

To maximise and achieve consistently high productions of hiPSC derived NPCs with a microcarrier dependent bioprocess, optimisation of all process parameters is key. Due to the design and technology limitations of the spinner flasks used in this thesis, process parameters could only be manually monitored. Consequently, the complete optimisation of multiple process parameters such as pH, temperature, stirring speeds, feeding strategy and DO, using spinner flasks would require intense labour and resources. Using the Ambr® systems in conjunction with Design of Experiment (DOE) and MODDE software would allow for efficient experimental designs to optimise such process parameters in a high-throughput fashion.

Once a small-scale integrated bioprocess has been established in STBs, it would then be important to demonstrate process scalability. This is typically achieved by a scaling factor for the process parameters relative to the scaled operating volumes and vessel design (Hanga *et al.*, 2020, 2021). At benchtop bioprocess scales (2L – 10L), future work could explore other popular up and coming technologies to intensify the process and increase output. Indeed, such technologies which simplify the downstream separation of microcarriers include alternating tangential flow (Repligen) or tangential flow filtration (Repligen). The correct filter would need to be large enough to allow single cells to pass yet small enough to retain the microcarriers. These technologies would enable the operation of the bioprocess in a perfusion mode whilst cells are still attached onto the microcarriers. Cells can be collected through across the filter membrane once they have been dissociated from the microcarriers. Although such technologies are promising in the field of biopharmaceuticals (Matanguihan and Wu, 2022), perfusion mode with ATF or TFF bioprocesses are yet to be demonstrated at benchtop or pilot scale for hiPSC derived cell modalities.

Finally, it is well known that the surface topography (e.g., stiffness and substrate) can impact the stem cell behaviour including growth rates, migration pattern, morphology and differentiation potential (Purcell *et al.*, 2012; Li *et al.*, 2014). Here, microcarriers were screened

and assessed solely on their surface substrate. However, recent publications have suggested that surface geometries can also influence stem cell behaviour; for example, MSCs have been shown to migrate faster on concaved pits compared to flat surfaces by forming long cell body extensions covering a larger spanning distance and establishing attachments far from the centre of the cell (Werner *et al.*, 2017). Their migration behaviour on convexed surfaces, however, are similar to typical flat surfaces, whereby first there is a protrusion on the leading edge, then cell body translocation, and retraction of the rear (Werner *et al.*, 2017).

Others have also reported the effects of surface geometries on the gene expression of the cells, particularly those leading to cell differentiation in stem cells (Jimenez-Vergara *et al.*, 2019). The surface geometry is linked to modulate the gene expression by nucleus deformation through a network of complex intracellular pathways, mechanosensitive proteins such as lamins, and focal adhesions. For example, the magnitude of focal adhesions and orientation impacts cytoskeletal networks such as the actin-myosin fibres which in turn can impose tensile or compressive stress forces on the nucleus depending on the surface curvature and stiffness (Delanoë-Ayari *et al.*, 2010). Deformation of the nucleus would trigger alterations to transcriptional activity. If the surface stiffness is more than that of the nucleus, such cytoskeletal configuration would cause deformation of the nucleus. Inversely, if the surface stiffness is less than that of the nucleus, then the surface is deformed (Werner *et al.*, 2017). It would be interesting to investigate effect of the curved surface of microcarriers on kiPSC morphology, gene expression, neural induction potential and migration as this would highlight importance of surface curvature as a parameter to consider during the design of the bioprocess.

### **6.1.2.Future work towards developing a microcarrier independent process**

An alternative route for future work is to abandon the use of microcarriers and develop a microcarrier independent bioprocess. With this avenue of process development, the expansion and differentiation of hiPSCs in STBs is mediated through suspended cell aggregates (Kehoe *et al.*, 2010a; Singh *et al.*, 2010; Abbasalizadeh *et al.*, 2012; Wang, B.-K. Chou, *et al.*, 2013). However, as previously mentioned, the challenge with this approach is the need to re-plate the cells onto a surface since protocols of most commercial differentiation kits are reliant on 2D generation of NPCs (Pauly *et al.*, 2018). However, with the employment of different differentiation technique such as genomic editing of hiPSCs using CRISPR-Cas9 technology, it may be possible to eliminate replating (Liu *et al.*, 2021; McTague *et al.*, 2021). Indeed, companies such as Bit.Bio and Treefrog therapeutics are currently developing process using such strategies for the generation of cell therapies and disease models.

The majority of neural induction kits and protocols, including the kit used in this thesis, typically target neural populations with resemblance to those of human foetal neural cells (Francis *et al.*, 1999; Seri *et al.*, 2004; Stern, 2006; Chambers *et al.*, 2009; Kirkeby *et al.*, 2012; Sugiyama, Osumi and Katsuyama, 2013; Urbán and Guillemot, 2014). However, for the application of neurodegenerative disease modelling and adult cell therapies, foetal like neural cells may not be ideal as they lack morphological and functional relevance (Pas, 2018). Therefore, alternative strategies to obtain physiologically mature neural populations which recapitulate some aspects of late gestational human brain can be achieved through the formation of brain organoids (Pas, 2018; Qian, Song and Ming, 2019). The process of generating cerebral organoids was first described by Lancaster and Knoblich (2014). Generally, the generation of cerebral organoids mediates through the formation of EBs followed by directed differentiation towards the neural lineage. Continuous culture in a 3D format would then eventually lead to form 3D organoids, which was described in spinner flasks (Lancaster F.D., de la Raga, PhD Thesis, Aston University, 2022

and Knoblich, 2014). However, there are limited studies on the optimisation of prolonged cultures of organoids in spinner flasks (Mansour *et al.*, 2018). Further work is needed to optimise process parameters in STBs to ensure efficient mass transfer of oxygen and nutrients to all the cell layers of the organoids. One strategy is to promote the formation of vasculature within the organoids by employing structural scaffolds for cells to use as surfaces for growth (e.g., from decellularised tissues) (Granato *et al.*, 2020). Optimised bioprocesses for would pave a way for accessing functional and physiologically relevant brain tissues for drug discovery, disease modelling, research and therapies.

## **6.2. Experimental improvements**

Due to limitations with resources and time during the stages of experimental design and data collection of this thesis, these have been reflected in this section and several improvements have been suggested.

First, the monitored CQAs of cells were mainly performed by assays determining viability, potency, and characteristics by ICC. However, for clinical applications of hiPSC derived NPCs, the aforementioned tests would not be sufficient for clinical release. Indeed, additional assays are further required to assure identity, microbiological sterility, absence of endotoxins, genetic fidelity and stability, and characterisation by flow cytometry, as outlined in Table 1.2. Thus, to further verify the data obtained in this thesis, the employment of mandatory assays should be implemented at various stages of process development, especially to support the decisions on process parameters such as the microcarrier, feeding regime or stirring speed.

Also, the quantitation of cells positive for pluripotent markers and neural lineage markers should be confirmed by other techniques such as flow cytometry and qRT-PCR (Abujarour *et al.*, 2013; Altieri *et al.*, 2019). One major limitation of this thesis was observed when using

ImageJ analysis software to quantitate the amount of marker specific and DAPI positive cells; particularly challenging to analyse were the ICC images obtained for hiPSC cultures, as cells and colonies were overlapping and compact. The employment of flow cytometry or qRT-PCR would provide more accurate relative quantitation of hiPSCs and NPCs, Compared to the current method. Ideally, throughout the process, cell characterisation should be performed.

For the spinner flask process development work in chapter 5, full identification of cell CQAs at different stages would provide and highlight further effects of different process parameters on cell quality, especially as stem cells are particularly susceptible to stresses (Tower, 2012; Wolfe *et al.*, 2016; Bianchi *et al.*, 2019). To obtain better visibility of the effect of processing on cell quality, ideal timepoints for cell CQA assessment have been suggested by the author of this thesis at the following time points: (1) post thaw of hiPSCs during the early seed train expansion stages in order to check for the batch quality as well as to identify the extent of differentiation early on the process to make a go or no go decision; (2) before inoculation of the spinner flask, to provide a base quality prior to upstream processing; (3) prior to initiating neural induction, to investigate the effect of the expansion stages; (4) after harvest to investigate the effect of the differentiation stages; (5) post filtration to investigate the effect of the downstream process. Note that these time points have been suggested due to cells being exposed to potential stresses.

For the assessment of hiPSC potency, trilineage differentiation was attempted using the StemCell Technologies trilineage differentiation kit. However, it was surprising that both cell lines failed to differentiate effectively towards the endoderm, ectoderm and endoderm lineage, as suggested by the lack of lineage specific markers detected using ICC. Despite several attempts to improve the suggested protocol from StemCell Technologies (i.e., increasing concentration of substrate, using Matrigel, different seeding densities etc.), trilineage specific markers were still poorly detected. Nevertheless, kiPSCs were demonstrated to differentiate

towards NPCs (ectoderm lineage) as shown in Chapter 3, meaning kiPSCs had the potential to differentiate towards ectoderm. This suggested that either the differentiation kit failed to drive lineage commitment, or the ICC kit failed to detect the markers. To confirm this, positive controls should be used to confirm the results as well as comparison with additional hiPSC lines.

The spinner flask employed for these studies were challenging to handle since the arms of the spinners could not accommodate the length of pipettes, thus, any culture manipulations such as medium exchange, sampling and harvest were performed by removing the top lid. To improve, different brands of spinner flasks also with more representative impeller designs such as a paddle or marine impeller should be used.

Finally, the metabolite analysis machine used here to determine glucose and lactate concentrations would be laborious and inefficient at larger scale or high throughput studies, as suggested in the future works. The blood gas analyser machine also displayed wavering glucose concentrations compared to the reported typical TeSR formulation concentration of 15 mM, regardless of being calibrated. This suggested that the accuracy of such device could be improved. To overcome such limitation, automated metabolite analysers such as the Vi-cell Meta-Flex (Beckman Coulter) could improve efficiency of metabolite analysis of large sample quantities and also increase accuracy. Such systems are also capable of analysing other metabolites and gases, osmolality and salt concentrations.

### **6.3. Concluding remarks**

The main aim of this thesis is to develop an integrated scalable bioprocess for the expansion and differentiation of hiPSCs towards NPCs. The process development is initiated by firstly developing the integrated expansion and differentiation processes on standard 2D TCP planar

platforms. Secondly, this process was tested and translated onto 3D microcarrier platforms by employing novel microcarrier screening protocols. Then finally, process parameters established in well plates such as feeding regime and microcarrier were implemented in dynamic 3D spinner flask cultures.

A systematic single factor investigation approach was used to design a scalable bioprocess employing VTN coated plastic microcarriers in 50 mL spinner flasks (maximum working volume 20 mL). The expansion of hiPSCs in STBs were demonstrated for the first time, to the authors knowledge, in cGMP standard mTeSR-Plus media.

Future experiments could utilise high throughput technologies with design of experiment approach in which several experimental parameters could be varied systematically and simultaneously to obtain a better overview of the experimental design.

Although STBs have been successfully employed for the expansion of mammalian cells such as MSC, CHO or HEK cell lines, here surprisingly, it was demonstrated that the expansion of kiPSCs on TCP planar platforms remained superior in terms of maintaining pluripotency, growth kinetics and differentiation potential. This likely due to the complex and sensitive nature of hiPSCs to stresses in dynamic culture environments. However, with further optimisation experiments of the process parameters in spinner flasks cultures, there is potential for hiPSC expansion and differentiation to be improved.

## References

- Cohen, A., Itsykson, P.M., and Reubinoff, B.E., (2007) 'Neural Differentiation of Human ES Cells', *Current Protocols in Cell Biology*, 36(1), pp. 23.7.1-23.7.20. doi: 10.1002/0471143030.cb2307s36.
- Abbasalizadeh, S., Larijani, M. R., (2012) 'Bioprocess development for mass production of size-controlled human pluripotent stem cell aggregates in stirred suspension bioreactor', *Tissue Engineering - Part C: Methods*, 18(11), pp. 831–851. doi: 10.1089/ten.tec.2012.0161.
- Abbott, L. C. and Nigussie, F. (2020) 'Adult neurogenesis in the mammalian dentate gyrus', *Journal of Veterinary Medicine Series C: Anatomia Histologia Embryologia*, 49(1), pp. 3–16. doi: 10.1111/ahe.12496.
- Dayem, A.A., Lee, S., Choi, H.Y., and Cho, S., (2018) 'The Impact of Adhesion Molecules on the In Vitro Culture and Differentiation of Stem Cells', *Biotechnology Journal*, 13(2), pp. 1–10. doi: 10.1002/biot.201700575.
- Abecasis, B. Aguiar, T., Arnault, E., Costa, R., (2017) 'Expansion of 3D human induced pluripotent stem cell aggregates in bioreactors: Bioprocess intensification and scaling-up approaches', *Journal of Biotechnology*, 246, pp. 81–93. doi: 10.1016/j.jbiotec.2017.01.004.
- Abraham, E., Ahmadian, B. B., Holderness, K., Levinson, Y. and McAfee, E., (2018) 'Platforms for manufacturing allogeneic, autologous and iPSC cell therapy products: An industry perspective', *Advances in Biochemical Engineering/Biotechnology*, 165, pp. 323–350. doi: 10.1007/10\_2017\_14.
- Abujarour, R., Valamehr, B., Robinson, M., Rezner, B., Vrance, F. and Flynn, P., (2013) 'Optimized surface markers for the prospective isolation of high-quality hipsacs using flow cytometry selection', *Scientific Reports*, 3. doi: 10.1038/srep01179.
- Aisenbrey, E. A. and Murphy, W. L. (2020) 'Synthetic alternatives to Matrigel', *Nature reviews. Materials*. 2020/05/27, 5(7), pp. 539–551. doi: 10.1038/s41578-020-0199-8.
- Alam, S., Sen, A., Behie, L. A. and Kallos, M. S., (2004) 'Cell cycle kinetics of expanding populations of neural stem and progenitor cells in vitro', *Biotechnology and Bioengineering*, 88(3), pp. 332–347. doi: 10.1002/bit.20246.
- Altieri, F., D'Anzi, A., Martello, F., Tarvido, S., Spasari, I., Ferrari, D., Benadini, L., Lamorte, G., Mazzocoli, G., Valente, E. M., Vescovi, A. L. and Rosati, J., (2019) 'Production and characterization of human induced pluripotent stem cells (iPSC) CSSi007-A (4383) from Joubert Syndrome.', *Stem cell research*, 38, p. 101480. doi: 10.1016/j.scr.2019.101480.
- Andersen, T., Auk-Emblem, P. and Dornish, M. (2015) '3D Cell Culture in Alginate Hydrogels', *Microarrays*, 4(2), pp. 133–161. doi: 10.3390/microarrays4020133.
- Angers, S. and Moon, R. T. (2009) 'Proximal events in Wnt signal transduction.', *Nature reviews. Molecular cell biology*, 10(7), pp. 468–477. doi: 10.1038/nrm2717.
- Badenes, S. M., Fernandes, T. G., Rodrigues, C. A. V., Diogo, M. M. and Cabral, J. M. S., (2015) 'Scalable expansion of human-induced pluripotent stem cells in xeno-free microcarriers', *Methods in Molecular Biology*, 1283(3), pp. 23–29. doi: 10.1007/7651\_2014\_106.

Badenes, S. M., Fernandes, T. G., Cordeiro, C. S. M., Boucher, S., Kuninger, D., Vemuri, M. C., Diogo, M. M. and Cabral, J. M. S., (2016) 'Defined essential 8' medium and vitronectin efficiently support scalable xeno-free expansion of human induced pluripotent stem cells in stirred microcarrier culture systems', *PLoS ONE*, 11(3), pp. 1–19. doi: 10.1371/journal.pone.0151264.

Badenes, S. M., Fernandes, T. G., Rodrigues, C. A., Diogo, M. M. and Cabral, J. M. S., (2016) 'Microcarrier-based platforms for in vitro expansion and differentiation of human pluripotent stem cells in bioreactor culture systems', *Journal of Biotechnology*, 234, pp. 71–82. doi: 10.1016/j.jbiotec.2016.07.023.

Baghbaderani, B. A., Behie, L. A., Sen, A., Mukhida, K., Hong, M. and Mendez, I., (2008) 'Expansion of human neural precursor cells in large-scale bioreactors for the treatment of neurodegenerative disorders', *Biotechnology Progress*, 24(4), pp. 859–870. doi: 10.1021/bp.070324s.

Baghbaderani, B. A., Mukhida, K., Sen, A., Kallos, M. S., Hong, M., Mendez, I. and Behie, L. A., (2010) 'Bioreactor expansion of human neural precursor cells in serum-free media retains neurogenic potential', *Biotechnology and Bioengineering*, 105(4), pp. 823–833. doi: 10.1002/bit.22590.

Baker, K. R. and Rice, L. (2012) 'The amyloidoses: clinical features, diagnosis and treatment.', *Methodist DeBakey cardiovascular journal*, 8(3), pp. 3–7. doi: 10.14797/mdcj-8-3-3.

Balordi, F. and Fishell, G. (2007) 'Hedgehog signaling in the subventricular zone is required for both the maintenance of stem cells and the migration of newborn neurons', *Journal of Neuroscience*, 27(22), pp. 5936–5947. doi: 10.1523/JNEUROSCI.1040-07.2007.

Ban, H., Nishishita, N., Fusaki, N., Tabata, T., Saeki, K., Shikamura, M., Takada, N., Inoue, M., Hasegawa, M., Kawamata, S., and Nishikawa, S. (2011) 'Efficient generation of transgene-free human induced pluripotent stem cells (iPSCs) by temperature-sensitive Sendai virus vectors', *Proceedings of the National Academy of Sciences*, 108(34), pp. 14234 LP – 14239. doi: 10.1073/pnas.1103509108.

Bardy, J., Chen, A. K., Lim, Y. M., Wu, S., Wei, S., Weiping, H., Chan, K., Reuveny, S., & Oh, S. K. (2013). 'Microcarrier Suspension Cultures for High-Density Expansion and Differentiation of Human Pluripotent Stem Cells to Neural Progenitor Cells', *Tissue Engineering Part C: Methods*, 19(2), pp. 166–180. doi: 10.1089/TEN.TEC.2012.0146.

Bartel, R. L. (2014) *Stem Cells and Cell Therapy: Autologous Cell Manufacturing, Translational Regenerative Medicine*. Elsevier Inc. doi: 10.1016/B978-0-12-410396-2.00008-6.

Ben-David, U. and Benvenisty, N. (2011) 'The tumorigenicity of human embryonic and induced pluripotent stem cells', *Nature Reviews Cancer*, 11(4), pp. 268–277. doi: 10.1038/nrc3034.

Berg, D. A., Bond, A. M., Ming, G. L., & Song, H. (2018). 'Radial glial cells in the adult dentate gyrus: what are they and where do they come from?', *F1000Research*, 7.

Van Beylen, K., Papantoniou, I. and Aerts, J. M. (2021) 'Microcarrier Screening and Evaluation for Dynamic Expansion of Human Periosteum-Derived Progenitor Cells in a Xenogeneic Free Medium', *Frontiers in Bioengineering and Biotechnology*, 9(May). doi: 10.3389/fbioe.2021.624890.

Bianchi, F., Pereno, V., George, J. H., Thompson, M. S., & Ye, H. (2019). 'Membrane Mechanical Properties Regulate the Effect of Strain on Spontaneous Electrophysiology in Human iPSC-Derived Neurons', *Neuroscience*, 404, pp. 165–174. doi: 10.1016/j.neuroscience.2019.02.014.

Braam, S. R., Zeinstra, L., Litjens, S., Ward-van Oostwaard, D., van den Brink, S., van Laake, L., Lebrin, F., Kats, P., Hochstenbach, R., Passier, R., Sonnenberg, A., & Mummery, C. L. (2008). 'Recombinant Vitronectin Is a Functionally Defined Substrate That Supports Human Embryonic Stem Cell Self-Renewal via  $\alpha$ V $\beta$ 5 Integrin', *Stem Cells*, 26(9), pp. 2257–2265. doi: 10.1634/stemcells.2008-0291.

Bravery, C. A. (2015) 'Do human leukocyte antigen-typed cellular therapeutics based on induced pluripotent stem cells make commercial sense?', *Stem Cells and Development*, 24(1), pp. 1–10. doi: 10.1089/scd.2014.0136.

Breunig, J. J., Silbereis, J., Vaccarino, F. M., Sestan, N., & Rakic, P. (2007). 'Notch regulates cell fate and dendrite morphology of newborn neurons in the postnatal dentate gyrus', *Proceedings of the National Academy of Sciences of the United States of America*, 104(51), pp. 20558–20563. doi: 10.1073/pnas.0710156104.

Carlén, M., Meletis, K., Göritz, C., Darsalia, V., Evergren, E., Tanigaki, K., Amendola, M., Barnabé-Heider, F., Yeung, M. S., Naldini, L., Honjo, T., Kokaia, Z., Shupliakov, O., Cassidy, R. M., Lindvall, O., & Frisén, J. (2009). 'Forebrain ependymal cells are Notch-dependent and generate neuroblasts and astrocytes after stroke', *Nature neuroscience*, 12(3), pp. 259–267.

Cascione, M., De Matteis, V., Leporatti, S., & Rinaldi, R. (2020). 'The New Frontiers in Neurodegenerative Diseases Treatment: Liposomal-Based Strategies', *Frontiers in bioengineering and biotechnology*, 8, p. 566767. doi: 10.3389/fbioe.2020.566767.

Chambers, S. M., Fasano, C. A., Papapetrou, E. P., Tomishima, M., Sadelain, M., & Studer, L. (2009). 'Highly efficient neural conversion of human ES and iPS cells by dual inhibition of SMAD signaling', *Nature Biotechnology*, 27(3), pp. 275–280. doi: 10.1038/nbt.1529.

Chan, S. W., Rizwan, M. and Yim, E. K. F. (2020) 'Emerging Methods for Enhancing Pluripotent Stem Cell Expansion', *Frontiers in Cell and Developmental Biology*, p. 70. Available at: <https://www.frontiersin.org/article/10.3389/fcell.2020.00070>.

Chan, Y. S., Göke, J., Ng, J. H., Lu, X., Gonzales, K. A., Tan, C. P., Tng, W. Q., Hong, Z. Z., Lim, Y. S., & Ng, H. H. (2013). 'Induction of a human pluripotent state with distinct regulatory circuitry that resembles preimplantation epiblast.', *Cell stem cell*, 13(6), pp. 663–675. doi: 10.1016/j.stem.2013.11.015.

Chandrasekaran, A., Avci, H. X., Ochalek, A., Rösingh, L. N., Molnár, K., László, L., Bellák, T., Téglási, A., Pesti, K., Mike, A., Phanthong, P., Bíró, O., Hall, V., Kitiyanant, N., Krause, K. H., Kobolák, J., & Dinnyés, A. (2017). 'Comparison of 2D and 3D neural induction methods for the generation of neural progenitor cells from human induced pluripotent stem cells', *Stem Cell Research*, 25, pp. 139–151. doi: 10.1016/j.scr.2017.10.010.

Chen, K. G., Mallon, B. S., McKay, R. D., & Robey, P. G. (2014). 'Human Pluripotent Stem Cell Culture: Considerations for Maintenance, Expansion, and Therapeutics', *Cell Stem Cell*, 14(1), pp. 13–26. doi: 10.1016/j.biotechadv.2011.08.021.Secreted.

Chen, A. K., Chen, X., Choo, A. B., Reuveny, S., & Oh, S. K. (2011). 'Critical microcarrier properties affecting the expansion of undifferentiated human embryonic stem cells', *Stem Cell*

*Research*, 7(2), pp. 97–111. doi: 10.1016/j.scr.2011.04.007.

Chen, A. K. L., Reuveny, S. and Oh, S. K. W. (2013) ‘Application of human mesenchymal and pluripotent stem cell microcarrier cultures in cellular therapy: Achievements and future direction’, *Biotechnology Advances*, 31(7), pp. 1032–1046. doi: 10.1016/j.biotechadv.2013.03.006.

Chen, G., Hou, Z., Gulbranson, D. R., & Thomson, J. A. (2010). ‘Actin-myosin contractility is responsible for the reduced viability of dissociated human embryonic stem cells’, *Cell stem cell*, 7(2), pp. 240–248. doi: 10.1016/j.stem.2010.06.017.

Chen, G., Gulbranson, D. R., Hou, Z., Bolin, J. M., Ruotti, V., Probasco, M. D., Smuga-Otto, K., Howden, S. E., Diol, N. R., Propson, N. E., Wagner, R., Lee, G. O., Antosiewicz-Bourget, J., Teng, J. M., & Thomson, J. A. (2011). ‘Chemically defined conditions for human iPSC derivation and culture’, *Nature methods*. 2011/04/10, 8(5), pp. 424–429. doi: 10.1038/nmeth.1593.

Chen, G., Gulbranson, D. R., Yu, P., Hou, Z., & Thomson, J. A. (2012). ‘Thermal stability of fibroblast growth factor protein is a determinant factor in regulating self-renewal, differentiation, and reprogramming in human pluripotent stem cells’, *Stem Cells*, 30(4), pp. 623–630.

Chen, K. G., Mallon, B. S., McKay, R. D., & Robey, P. G. (2014). ‘Human pluripotent stem cell culture: Considerations for maintenance, expansion, and therapeutics’, *Cell Stem Cell*, 14(1), pp. 13–26. doi: 10.1016/j.stem.2013.12.005.

Chen, V. C., Couture, S. M., Ye, J., Lin, Z., Hua, G., Huang, H. I., Wu, J., Hsu, D., Carpenter, M. K., & Couture, L. A. (2012). ‘Scalable GMP compliant suspension culture system for human ES cells’, *Stem Cell Research*, 8(3), pp. 388–402. doi: <https://doi.org/10.1016/j.scr.2012.02.001>.

Chen, W., Jongkamonwiwat, N., Abbas, L., Eshtan, S. J., Johnson, S. L., Kuhn, S., Milo, M., Thurlow, J. K., Andrews, P. W., Marcotti, W., Moore, H. D., & Rivolta, M. N. (2012). ‘Restoration of auditory evoked responses by human ES-cell-derived otic progenitors’, *Nature*, 490(7419), pp. 278–282. doi: 10.1038/nature11415.

Chen, X., Chen, A., Woo, T. L., Choo, A. B., Reuveny, S., & Oh, S. K. (2010). ‘Investigations into the metabolism of two-dimensional colony and suspended microcarrier cultures of human embryonic stem cells in serum-free media’, *Stem Cells and Development*, 19(11), pp. 1781–1792.

Cheng, L., Hammond, H., Ye, Z., Zhan, X., & Dravid, G. (2003). ‘Human adult marrow cells support prolonged expansion of human embryonic stem cells in culture.’, *Stem cells (Dayton, Ohio)*, 21(2), pp. 131–142. doi: 10.1634/stemcells.21-2-131.

Cimler, R., Maresova, P., Kuhnova, J., & Kuca, K. (2019). ‘Predictions of Alzheimer’s disease treatment and care costs in European countries’, *PloS one*, 14(1), pp. e0210958–e0210958. doi: 10.1371/journal.pone.0210958.

Clark, A. T., Bodnar, M. S., Fox, M., Rodriguez, R. T., Abeyta, M. J., Firpo, M. T., & Pera, R. A. (2004). ‘Spontaneous differentiation of germ cells from human embryonic stem cells in vitro’, *Human Molecular Genetics*, 13(7), pp. 727–739. doi: 10.1093/hmg/ddh088.

Corbin, J. G., Gaiano, N., Juliano, S. L., Poluch, S., Stancik, E., & Haydar, T. F. (2008). ‘Regulation of neural progenitor cell development in the nervous system’, *Journal of F.D., de la Raga, PhD Thesis, Aston University, 2022*

*Neurochemistry*, 106(6), pp. 2272–2287. doi: 10.1111/j.1471-4159.2008.05522.x.

Correia, C., Serra, M., Espinha, N., Sousa, M., Brito, C., Burkert, K., Zheng, Y., Hescheler, J., Carrondo, M. J., Sarić, T., & Alves, P. M. (2014). ‘Combining hypoxia and bioreactor hydrodynamics boosts induced pluripotent stem cell differentiation towards cardiomyocytes’, *Stem cell reviews and reports*, 10(6), pp. 786–801. doi: 10.1007/s12015-014-9533-0.

Croft, D. R., Coleman, M. L., Li, S., Robertson, D., Sullivan, T., Stewart, C. L., & Olson, M. F. (2005). ‘Actin-myosin-based contraction is responsible for apoptotic nuclear disintegration.’, *The Journal of cell biology*, 168(2), pp. 245–255. doi: 10.1083/jcb.200409049.

Crompton, L. A., Byrne, M. L., Taylor, H., Kerrigan, T. L., Bru-Mercier, G., Badger, J. L., Barbuti, P. A., Jo, J., Tyler, S. J., Allen, S. J., Kunath, T., Cho, K., & Caldwell, M. A. (2013). ‘Stepwise, non-adherent differentiation of human pluripotent stem cells to generate basal forebrain cholinergic neurons via hedgehog signaling’, *Stem Cell Research*, 11(3), pp. 1206–1221. doi: 10.1016/j.scr.2013.08.002.

Cruvinel, E., Ogusuku, I., Cerioni, R., Rodrigues, S., Gonçalves, J., Góes, M. E., Alvim, J. M., Silva, A. C., Lino, V. S., Boccardo, E., Goulart, E., Pereira, A., Dariolli, R., Valadares, M., & Biagi, D. (2020). ‘Long-term single-cell passaging of human iPSC fully supports pluripotency and high-efficient trilineage differentiation capacity’, *SAGE Open Medicine*, 8, p. 2050312120966456. doi: 10.1177/2050312120966456.

Daniszewski, M., Crombie, D. E., Henderson, R., Liang, H. H., Wong, R. C. B., Hewitt, A. W., & Pébay, A. (2018). ‘Automated Cell Culture Systems and Their Applications to Human Pluripotent Stem Cell Studies’, *SLAS Technology*, 23(4), pp. 315–325. doi: 10.1177/2472630317712220.

Dayem, A. A., Won, J., Goo, H. G., Yang, G. M., Seo, D. S., Jeon, B. M., Choi, H. Y., Park, S. E., Lim, K. M., Jang, S. H., Lee, S. B., Choi, S. B., Kim, K., Kang, G. H., Yeon, G. B., Kim, D. S., & Cho, S. G. (2020). The immobilization of fibronectin- and fibroblast growth factor 2-derived peptides on a culture plate supports the attachment and proliferation of human pluripotent stem cells. *Stem cell research*, 43, 101700. <https://doi.org/10.1016/j.scr.2020.101700>Decimo, I. et al. (2012) ‘Neural Stem Cell Niches in Health and Diseases’, *Current Pharmaceutical Design*, 18(13), pp. 1755–1783. doi: 10.2174/138161212799859611.

Delanoë-Ayari, H., Rieu, J. P., & Sano, M. (2010). 4D traction force microscopy reveals asymmetric cortical forces in migrating Dictyostelium cells. *Physical review letters*, 105(24), 248103. <https://doi.org/10.1103/PhysRevLett.105.248103>Deuschl, G. et al. (2006) ‘A randomized trial of deep-brain stimulation for Parkinson’s disease’, *New England Journal of Medicine*, 355(9), pp. 896–908.

Dibajnia, P. and Morshead, C. M. (2013) ‘Role of neural precursor cells in promoting repair following stroke’, *Acta Pharmacologica Sinica*. 2012/10/15, 34(1), pp. 78–90. doi: 10.1038/aps.2012.107.

Doetsch, F., Caillé, I., Lim, D. A., García-Verdugo, J. M., & Alvarez-Buylla, A. (1999). Subventricular zone astrocytes are neural stem cells in the adult mammalian brain. *Cell*, 97(6), 703–716. [https://doi.org/10.1016/s0092-8674\(00\)80783-7](https://doi.org/10.1016/s0092-8674(00)80783-7)Doetsch, F., Garcia-Verdugo, J. M. and Alvarez-Buylla, A. (1997) ‘Cellular composition and three-dimensional organization of the subventricular germinal zone in the adult mammalian brain’, *Journal of Neuroscience*, 17(13), pp. 5046–5061.

- Drago, J., Murphy, M., Carroll, S. M., Harvey, R. P., & Bartlett, P. F. (1991). Fibroblast growth factor-mediated proliferation of central nervous system precursors depends on endogenous production of insulin-like growth factor I. *Proceedings of the National Academy of Sciences of the United States of America*, 88(6), 2199–2203. <https://doi.org/10.1073/pnas.88.6.2199>
- Dugger, B. N. et al. (2014) ‘Concomitant pathologies among a spectrum of parkinsonian disorders’, *Parkinsonism and Related Disorders*, 20(5), pp. 525–529. doi: 10.1016/j.parkreldis.2014.02.012.
- Dugger, B. N. and Dickson, D. W. (2017) ‘Pathology of Neurodegenerative Diseases’, *Cold Spring Harbor perspectives in biology*, 9(7), p. a028035. doi: 10.1101/cshperspect.a028035.
- Durruthy-Durruthy, J., Briggs, S. F., Awe, J., Ramathal, C. Y., Karumbayaram, S., Lee, P. C., Heidmann, J. D., Clark, A., Karakikes, I., Loh, K. M., Wu, J. C., Hoffman, A. R., Byrne, J., Reijo Pera, R. A., & Sebastiano, V. (2014). Rapid and efficient conversion of integration-free human induced pluripotent stem cells to GMP-grade culture conditions. *PloS one*, 9(4), e94231. <https://doi.org/10.1371/journal.pone.0094231>
- Eibes, G. et al. (2010) ‘Maximizing the ex vivo expansion of human mesenchymal stem cells using a microcarrier-based stirred culture system’, *Journal of Biotechnology*, 146(4), pp. 194–197. doi: 10.1016/j.jbiotec.2010.02.015.
- Eiraku, M., Watanabe, K., Matsuo-Takasaki, M., Kawada, M., Yonemura, S., Matsumura, M., Wataya, T., Nishiyama, A., Muguruma, K., & Sasai, Y. (2008). Self-organized formation of polarized cortical tissues from ESCs and its active manipulation by extrinsic signals. *Cell stem cell*, 3(5), 519–532. <https://doi.org/10.1016/j.stem.2008.09.002>
- El-Kadiry, A. E.-H., Rafei, M. and Shammaa, R. (2021) ‘Cell Therapy: Types, Regulation, and Clinical Benefits’, *Frontiers in Medicine*, 8(November), pp. 1–24. doi: 10.3389/fmed.2021.756029.
- Eliasson, P., & Jönsson, J. I. (2010). The hematopoietic stem cell niche: low in oxygen but a nice place to be. *Journal of cellular physiology*, 222(1), 17–22. <https://doi.org/10.1002/jcp.21908>
- Elkabetz, Y. et al. (2008) ‘Human ES cell-derived neural rosettes reveal a functionally distinct early neural stem cell stage’, *Genes & development*, 22(2), pp. 152–165.
- Eminli, S., Foudi, A., Stadtfeld, M., Maherali, N., Ahfeldt, T., Mostoslavsky, G., Hock, H., & Hochedlinger, K. (2009). Differentiation stage determines potential of hematopoietic cells for reprogramming into induced pluripotent stem cells. *Nature genetics*, 41(9), 968–976. <https://doi.org/10.1038/ng.428>
- Enam, S. (2015) ‘Substrates for clinical applicability of stem cells’, *World Journal of Stem Cells*, 7(2), p. 243. doi: 10.4252/wjsc.v7.i2.243.
- Enam, S. and Jin, S. (2015) ‘Substrates for clinical applicability of stem cells’, *World journal of stem cells*, 7(2), pp. 243–252. doi: 10.4252/wjsc.v7.i2.243.
- Ezashi, T., Das, P. and Roberts, R. M. (2005) ‘Low O<sub>2</sub> tensions and the prevention of differentiation of hES cells’, *Proceedings of the National Academy of Sciences of the United States of America*, 102(13), pp. 4783 LP – 4788. doi: 10.1073/pnas.0501283102.
- Faigle, R. and Song, H. (2013) ‘Signaling mechanisms regulating adult neural stem cells and neurogenesis Roland’, *Biochem Biophys Acta*, 1830(2), pp. 2435–2448. doi: 10.1016/j.earlhumdev.2006.05.022.
- Fan, Y., Hsiung, M., Cheng, C., & Tzanakakis, E. S. (2014). Facile engineering of xeno-free microcarriers for the scalable cultivation of human pluripotent stem cells in stirred suspension. *Tissue engineering. Part A*, 20(3-4), 588–599. <https://doi.org/10.1089/ten.TEA.2013.0219>
- Fan, Y., Zhang, F. and Tzanakakis, E. S. (2017) ‘Engineering Xeno-Free Microcarriers with Recombinant Vitronectin, Albumin and UV F.D., de la Raga, PhD Thesis, Aston University, 2022

Irradiation for Human Pluripotent Stem Cell Bioprocessing', *ACS Biomaterials Science and Engineering*, 3(8), pp. 1510–1518. doi: 10.1021/acsbiomaterials.6b00253.

Fedorova, V., Vanova, T., Elrefae, L., Pospisil, J., Petrasova, M., Kolajova, V., Hudacova, Z., Baniariova, J., Barak, M., Peskova, L., Barta, T., Kaucka, M., Killinger, M., Vecera, J., Bernatik, O., Cajanek, L., Hribkova, H., & Bohaciakova, D. (2019). Differentiation of neural rosettes from human pluripotent stem cells in vitro is sequentially regulated on a molecular level and accomplished by the mechanism reminiscent of secondary neurulation. *Stem cell research*, 40, 101563. <https://doi.org/10.1016/j.scr.2019.101563>

Fernandes, A. M., Marinho, P. A., Sartore, R. C., Paulsen, B. S., Mariante, R. M., Castilho, L. R., & Rehen, S. K. (2009). Successful scale-up of human embryonic stem cell production in a stirred microcarrier culture system. *Brazilian journal of medical and biological research = Revista brasileira de pesquisas medicas e biologicas*, 42(6), 515–522.

Fernandez-Muñoz, B., Garcia-Delgado, A. B., Arribas-Arribas, B., & Sanchez-Pernaute, R. (2021). Human Neural Stem Cells for Cell-Based Medicinal Products. *Cells*, 10(9), 2377. <https://doi.org/10.3390/cells10092377>Flahou, C. et al. (2021) 'Fit-For-All iPSC-Derived Cell Therapies and Their Evaluation in Humanized Mice With NK Cell Immunity', *Frontiers in Immunology*. Available at: <https://www.frontiersin.org/article/10.3389/fimmu.2021.662360>.

Francis, F., Koulakoff, A., Boucher, D., Chafey, P., Schaar, B., Vinet, M. C., Friocourt, G., McDonnell, N., Reiner, O., Kahn, A., McConnell, S. K., Berwald-Netter, Y., Denoulet, P., & Chelly, J. (1999). Doublecortin is a developmentally regulated, microtubule-associated protein expressed in migrating and differentiating neurons. *Neuron*, 23(2), 247–256. [https://doi.org/10.1016/s0896-6273\(00\)80777-1](https://doi.org/10.1016/s0896-6273(00)80777-1)Fridley, K. M., Kinney, M. A. and McDevitt, T. C. (2012) 'Hydrodynamic modulation of pluripotent stem cells', *Stem Cell Research & Therapy*, 3(6), p. 45. doi: 10.1186/scrt136.

Fukumoto, H., Asami-Odaka, A., Suzuki, N., & Iwatsubo, T. (1996). Association of A beta 40-positive senile plaques with microglial cells in the brains of patients with Alzheimer's disease and in non-demented aged individuals. *Neurodegeneration : a journal for neurodegenerative disorders, neuroprotection, and neuroregeneration*, 5(1), 13–17. <https://doi.org/10.1006/neur.1996.0002>

Furue, M. K., Na, J., Jackson, J. P., Okamoto, T., Jones, M., Baker, D., Hata, R., Moore, H. D., Sato, J. D., & Andrews, P. W. (2008). Heparin promotes the growth of human embryonic stem cells in a defined serum-free medium. *Proceedings of the National Academy of Sciences of the United States of America*, 105(36), 13409–13414. <https://doi.org/10.1073/pnas.0806136105>

Gage F. H. (2000). Mammalian neural stem cells. *Science (New York, N.Y.)*, 287(5457), 1433–1438. <https://doi.org/10.1126/science.287.5457.1433>

Galiakberova, A. A. and Dashinimaev, E. B. (2020a) 'Neural Stem Cells and Methods for Their Generation From Induced Pluripotent Stem Cells in vitro', *Frontiers in cell and developmental biology*, 8, p. 815. doi: 10.3389/fcell.2020.00815.

G Gandhi, J. K., Knudsen, T., Hill, M., Roy, B., Bachman, L., Pfannkoch-Andrews, C., Schmidt, K. N., Metko, M. M., Ackerman, M. J., Resch, Z., Pulido, J. S., & Marmorstein, A. D. (2019). Human Fibrinogen for Maintenance and Differentiation of Induced Pluripotent Stem Cells in Two Dimensions and Three Dimensions. *Stem cells translational medicine*, 8(6), 512–521. <https://doi.org/10.1002/sctm.18-0189>

Gareau, T., Lara, G. G., Shepherd, R. D., Krawetz, R., Rancourt, D. E., Rinker, K. D., & Kallos, F.D., de la Raga, PhD Thesis, Aston University, 2022

M. S. (2014). Shear stress influences the pluripotency of murine embryonic stem cells in stirred suspension bioreactors. *Journal of tissue engineering and regenerative medicine*, 8(4), 268–278. <https://doi.org/10.1002/term.1518>.

Garitaonandia, I., Gonzalez, R., Sherman, G., Semechkin, A., Evans, A., & Kern, R. (2018). Novel Approach to Stem Cell Therapy in Parkinson's Disease. *Stem cells and development*, 27(14), 951–957. <https://doi.org/10.1089/scd.2018.0001> Geiger, B. and Yamada, K. M. (2011) 'Molecular architecture and function of matrix adhesions.', *Cold Spring Harbor perspectives in biology*, 3(5). doi: 10.1101/cshperspect.a005033.

Ghasemi-Dehkordi, P., Allahbakhshian-Farsani, M., Abdian, N., Mirzaeian, A., Saffari-Chaleshtori, J., Heybati, F., Mardani, G., Karimi-Taghanaki, A., Doosti, A., Jami, M. S., Abolhasani, M., & Hashemzadeh-Chaleshtori, M. (2015). Comparison between the cultures of human induced pluripotent stem cells (hiPSCs) on feeder-and serum-free system (Matrigel matrix), MEF and HDF feeder cell lines. *Journal of cell communication and signaling*, 9(3), 233–246. <https://doi.org/10.1007/s12079-015-0289-3>

Gilmozzi, V. *et al.* (2021) 'Generation of hiPSC-Derived Functional Dopaminergic Neurons in Alginate-Based 3D Culture ', *Frontiers in Cell and Developmental Biology* . Available at: <https://www.frontiersin.org/article/10.3389/fcell.2021.708389>.

Goetz, C. G., Poewe, W., Rascol, O., & Sampaio, C. (2005). Evidence-based medical review update: pharmacological and surgical treatments of Parkinson's disease: 2001 to 2004. *Movement disorders : official journal of the Movement Disorder Society*, 20(5), 523–539. <https://doi.org/10.1002/mds.20464>

Goldman, O., Feraud, O., Boyer-Di Ponio, J., Driancourt, C., Clay, D., Le Bousse-Kerdiles, M. C., Bennaceur-Griscelli, A., & Uzan, G. (2009). A boost of BMP4 accelerates the commitment of human embryonic stem cells to the endothelial lineage. *Stem cells (Dayton, Ohio)*, 27(8), 1750–1759. <https://doi.org/10.1002/stem.100>

Grainger, A. I., King, M. C., Nagel, D. A., Parri, H. R., Coleman, M. D., & Hill, E. J. (2018). In vitro Models for Seizure-Liability Testing Using Induced Pluripotent Stem Cells. *Frontiers in neuroscience*, 12, 590. <https://doi.org/10.3389/fnins.2018.00590>

Grainger, A. I. and Grainger, A. I. (2020) 'Development of human induced pluripotent stem cell-derived neural cultures for seizure-liability testing'.

Greuel, S., Freyer, N., Hanci, G., Böhme, M., Miki, T., Werner, J., Schubert, F., Sittinger, M., Zeilinger, K., & Mandenius, C. F. (2019). Online measurement of oxygen enables continuous noninvasive evaluation of human-induced pluripotent stem cell (hiPSC) culture in a perfused 3D hollow-fiber bioreactor. *Journal of tissue engineering and regenerative medicine*, 13(7), 1203–1216. <https://doi.org/10.1002/term.2871>

Granato, A. E. C., da Cruz, E. F., Rodrigues-Junior, D. M., Mosini, A. C., Ulrich, H., Rodrigues, B. V. M., Cheffer, A., & Porcionatto, M. (2020). A novel decellularization method to produce brain scaffolds. *Tissue & cell*, 67, 101412. <https://doi.org/10.1016/j.tice.2020.101412>

Gunther, K. (2016) 'Rapid Monolayer Neural Induction of induced Pluripotent Stem Cells Yields Stably Proliferating Neural Stem Cells', *Journal of Stem Cell Research & Therapy*, 06(05), pp. 1–6. doi: 10.4172/2157-7633.1000341.

Guo, C. W., Kawakatsu, M., Idemitsu, M., Urata, Y., Goto, S., Ono, Y., Hamano, K., & Li, T. F.D., de la Raga, PhD Thesis, Aston University, 2022

S. (2013). Culture under low physiological oxygen conditions improves the stemness and quality of induced pluripotent stem cells. *Journal of cellular physiology*, 228(11), 2159–2166. <https://doi.org/10.1002/jcp.24389>

Guo, N. N., Liu, L. P., Zheng, Y. W., & Li, Y. M. (2020). Inducing human induced pluripotent stem cell differentiation through embryoid bodies: A practical and stable approach. *World journal of stem cells*, 12(1), 25–34. <https://doi.org/10.4252/wjsc.v12.i1.25>

Gupta, P., Ismadi, M. Z., Verma, P. J., Fouras, A., Jadhav, S., Bellare, J., & Hourigan, K. (2016). Optimization of agitation speed in spinner flask for microcarrier structural integrity and expansion of induced pluripotent stem cells. *Cytotechnology*, 68(1), 45–59. <https://doi.org/10.1007/s10616-014-9750-z>

Gupta, P., Geris, L., Luyten, F. P., & Papantoniou, I. (2018). An Integrated Bioprocess for the Expansion and Chondrogenic Priming of Human Periosteum-Derived Progenitor Cells in Suspension Bioreactors. *Biotechnology journal*, 13(2), 10.1002/biot.201700087. <https://doi.org/10.1002/biot.201700087>

Gurusamy, N., Alsayari, A., Rajasingh, S., & Rajasingh, J. (2018). Adult Stem Cells for Regenerative Therapy. *Progress in molecular biology and translational science*, 160, 1–22. <https://doi.org/10.1016/bs.pmbts.2018.07.009>

Hadjiev, D., Sabiri, N. E. and Zanati, A. (2006) ‘Mixing time in bioreactors under aerated conditions’, *Biochemical Engineering Journal*, 27(3), pp. 323–330. doi: 10.1016/j.bej.2005.08.009.

Hadjihannas, M. V., Bernkopf, D. B., Brückner, M., & Behrens, J. (2012). Cell cycle control of Wnt/ $\beta$ -catenin signalling by conductin/axin2 through CDC20. *EMBO reports*, 13(4), 347–354. <https://doi.org/10.1038/embor.2012.12>

Hanga, M. P., Ali, J., Moutsatsou, P., de la Raga, F. A., Hewitt, C. J., Nienow, A., & Wall, I. (2020). Bioprocess development for scalable production of cultivated meat. *Biotechnology and bioengineering*, 117(10), 3029–3039. <https://doi.org/10.1002/bit.27469>

Hanga, M. P., de la Raga, F. A., Moutsatsou, P., Hewitt, C. J., Nienow, A. W., & Wall, I. (2021). Scale-up of an intensified bioprocess for the expansion of bovine adipose-derived stem cells (bASCs) in stirred tank bioreactors. *Biotechnology and bioengineering*, 118(8), 3175–3186. <https://doi.org/10.1002/bit.27842>

Haridhasapavalan, K. K., Borgohain, M. P., Dey, C., Saha, B., Narayan, G., Kumar, S., & Thummer, R. P. (2019). An insight into non-integrative gene delivery approaches to generate transgene-free induced pluripotent stem cells. *Gene*, 686, 146–159. <https://doi.org/10.1016/j.gene.2018.11.069>

Harris, V. K., Stark, J., Vyshkina, T., Blackshear, L., Joo, G., Stefanova, V., Sara, G., & Sadiq, S. A. (2018). Phase I Trial of Intrathecal Mesenchymal Stem Cell-derived Neural Progenitors in Progressive Multiple Sclerosis. *EBioMedicine*, 29, 23–30. <https://doi.org/10.1016/j.ebiom.2018.02.002>

Hata, A., & Chen, Y. G. (2016). TGF- $\beta$  Signaling from Receptors to Smads. *Cold Spring Harbor perspectives in biology*, 8(9), a022061. <https://doi.org/10.1101/cshperspect.a022061>

He, X., Cao, Y., Wang, L., Han, Y., Zhong, X., Zhou, G., Cai, Y., Zhang, H., & Gao, P. (2014).

Human fibroblast reprogramming to pluripotent stem cells regulated by the miR19a/b-PTEN axis. *PLoS one*, 9(4), e95213. <https://doi.org/10.1371/journal.pone.0095213>

Heemels, M.-T. (2016) 'Neurodegenerative diseases', *Nature*, 539(7628), p. 179. doi: 10.1038/539179a.

Hegarty, S. V, O'Keeffe, G. W. and Sullivan, A. M. (2013) 'BMP-Smad 1/5/8 signalling in the development of the nervous system', *Progress in Neurobiology*, 109, pp. 28–41.

Hemmings, B. A. and Restuccia, D. F. (2012) 'PI3K-PKB/Akt pathway', *Cold Spring Harbor perspectives in biology*, 4(9), pp. a011189–a011189. doi: 10.1101/cshperspect.a011189.

Hewitt, C. J., Lee, K., Nienow, A. W., Thomas, R. J., Smith, M., & Thomas, C. R. (2011). Expansion of human mesenchymal stem cells on microcarriers. *Biotechnology letters*, 33(11), 2325–2335. <https://doi.org/10.1007/s10529-011-0695-4>

Higuchi, A., Kao, S. H., Ling, Q. D., Chen, Y. M., Li, H. F., Alarfaj, A. A., Munusamy, M. A., Murugan, K., Chang, S. C., Lee, H. C., Hsu, S. T., Kumar, S. S., & Umezawa, A. (2015). Long-term xeno-free culture of human pluripotent stem cells on hydrogels with optimal elasticity. *Scientific reports*, 5, 18136. <https://doi.org/10.1038/srep18136>

Hoffman, L. M., Hall, L., Batten, J. L., Young, H., Pardasani, D., Baetge, E. E., Lawrence, J., & Carpenter, M. K. (2005). X-inactivation status varies in human embryonic stem cell lines. *Stem cells (Dayton, Ohio)*, 23(10), 1468–1478. <https://doi.org/10.1634/stemcells.2004-0371>

Horiguchi, I., Urabe, Y., Kimura, K., & Sakai, Y. (2018). Effects of glucose, lactate and basic FGF as limiting factors on the expansion of human induced pluripotent stem cells. *Journal of bioscience and bioengineering*, 125(1), 111–115. <https://doi.org/10.1016/j.jbiosc.2017.08.004>

Horiguchi, I., & Sakai, Y. (2015). Alginate Encapsulation of Pluripotent Stem Cells Using a Co-axial Nozzle. *Journal of visualized experiments : JoVE*, (101), e52835. <https://doi.org/10.3791/52835>

Hou, Y., Dan, X., Babbar, M., Wei, Y., Hasselbalch, S. G., Croteau, D. L., & Bohr, V. A. (2019). Ageing as a risk factor for neurodegenerative disease. *Nature reviews. Neurology*, 15(10), 565–581. <https://doi.org/10.1038/s41582-019-0244-7>

Huang, H., Nakayama, Y., Qin, K., Yamamoto, K., Ando, J., Yamashita, J., Itoh, H., Kanda, K., Yaku, H., Okamoto, Y., & Nemoto, Y. (2005). Differentiation from embryonic stem cells to vascular wall cells under in vitro pulsatile flow loading. *Journal of artificial organs : the official journal of the Japanese Society for Artificial Organs*, 8(2), 110–118. <https://doi.org/10.1007/s10047-005-0291-2>

Hughes, C. S., Postovit, L. M. and Lajoie, G. A. (2010) 'Matrigel: a complex protein mixture required for optimal growth of cell culture.', *Proteomics*, 10(9), pp. 1886–1890. doi: 10.1002/pmic.200900758.

Iglesias-Lopez, C., Agustí, A., Vallano, A., & Obach, M. (2021). Current landscape of clinical development and approval of advanced therapies. *Molecular therapy. Methods & clinical development*, 23, 606–618. <https://doi.org/10.1016/j.omtm.2021.11.003>

Jamali, F., Aldughmi, M., Khasawneh, M. W., Dahbour, S., Salameh, A. A., & Awidi, A. (2021). A New Tool for Safety Evaluation and a Combination of Measures for Efficacy Assessment of Cotransplanting Human Allogenic Neuronal Stem Cells and Mesenchymal Stem Cells for the Treatment of Parkinson Disease: Protocol for an Interventional Study. *JMIR*

research protocols, 10(10), e29695. <https://doi.org/10.2196/29695>

James, D., Levine, A. J., Besser, D., & Hemmati-Brivanlou, A. (2005). TGFbeta/activin/nodal signaling is necessary for the maintenance of pluripotency in human embryonic stem cells. *Development (Cambridge, England)*, 132(6), 1273–1282. <https://doi.org/10.1242/dev.01706>

Janowski, M., Walczak, P., & Date, I. (2010). Intravenous route of cell delivery for treatment of neurological disorders: a meta-analysis of preclinical results. *Stem cells and development*, 19(1), 5–16. <https://doi.org/10.1089/scd.2009.0271>

Jenkins, M. J., & Farid, S. S. (2015). Human pluripotent stem cell-derived products: advances towards robust, scalable and cost-effective manufacturing strategies. *Biotechnology journal*, 10(1), 83–95. <https://doi.org/10.1002/biot.201400348>

Jensen, J. B. and Parmar, M. (2006) ‘Strengths and limitations of the neurosphere culture system - Jensen and Parmar Mol Neurobiol 2006 (1).pdf’, 34(3), pp. 153–154. Available at: [file:///C:/Users/marrac/Downloads/Jensen and Parmar Mol Neurobiol 2006 \(1\).pdf](file:///C:/Users/marrac/Downloads/Jensen%20and%20Parmar%20Mol%20Neurobiol%202006%20(1).pdf).

Jha, B. S., Farnoodian, M. and Bharti, K. (2021) ‘Regulatory considerations for developing a phase I investigational new drug application for autologous induced pluripotent stem cells-based therapy product’, *Stem Cells Translational Medicine*, 10(2), pp. 198–208. doi: 10.1002/sctm.20-0242.

Jia, F., Wilson, K. D., Sun, N., Gupta, D. M., Huang, M., Li, Z., Panetta, N. J., Chen, Z. Y., Robbins, R. C., Kay, M. A., Longaker, M. T., & Wu, J. C. (2010). A nonviral minicircle vector for deriving human iPS cells. *Nature methods*, 7(3), 197–199. <https://doi.org/10.1038/nmeth.1426>

Jimenez-Vergara, A. C., Zurita, R., Jones, A., Diaz-Rodriguez, P., Qu, X., Kusima, K. L., Hahn, M. S., & Munoz-Pinto, D. J. (2019). Refined assessment of the impact of cell shape on human mesenchymal stem cell differentiation in 3D contexts. *Acta biomaterialia*, 87, 166–176. <https://doi.org/10.1016/j.actbio.2019.01.052>

Jin, K., Sun, Y., Xie, L., Batteur, S., Mao, X. O., Smelick, C., Logvinova, A., & Greenberg, D. A. (2003). Neurogenesis and aging: FGF-2 and HB-EGF restore neurogenesis in hippocampus and subventricular zone of aged mice. *Aging cell*, 2(3), 175–183. <https://doi.org/10.1046/j.1474-9728.2003.00046.x>

Joyce, N., Annett, G., Wirthlin, L., Olson, S., Bauer, G., & Nolte, J. A. (2010). Mesenchymal stem cells for the treatment of neurodegenerative disease. *Regenerative medicine*, 5(6), 933–946. <https://doi.org/10.2217/rme.10.72>

Kardel, M. D., Wong, M. K., Knock, E., Chew, L., Moosa, A., LeBlanc, N., Legree, J., Frohlich, R. J., Wu, C., Hunter, A. L., Thomas, T. E., Eaves, A. C., and Louis, S. A. (no date) ‘Modifications Designed to Stabilize the mTeSR™ 1 Medium Formulation Do Not Impact Downstream Differentiation’, p. 13485.

Kato, R., Matsumoto, M., Sasaki, H., Joto, R., Okada, M., Ikeda, Y., Kanie, K., Suga, M., Kinohara, M., Yanagihara, K., Liu, Y., Uchio-Yamada, K., Fukuda, T., Kii, H., Uozumi, T., Honda, H., Kiyota, Y., & Furue, M. K. (2016). Parametric analysis of colony morphology of non-labelled live human pluripotent stem cells for cell quality control. *Scientific reports*, 6, 34009. <https://doi.org/10.1038/srep34009>

Kato, Y., Kim, M. H., & Kino-Oka, M. (2018). Comparison of growth kinetics between static F.D., de la Raga, PhD Thesis, Aston University, 2022

and dynamic cultures of human induced pluripotent stem cells. *Journal of bioscience and bioengineering*, 125(6), 736–740. <https://doi.org/10.1016/j.jbiosc.2018.01.002>

Kefalopoulou, Z., Politis, M., Piccini, P., Mencacci, N., Bhatia, K., Jahanshahi, M., Widner, H., Rehncrona, S., Brundin, P., Björklund, A., Lindvall, O., Limousin, P., Quinn, N., & Foltynie, T. (2014). Long-term clinical outcome of fetal cell transplantation for Parkinson disease: two case reports. *JAMA neurology*, 71(1), 83–87. <https://doi.org/10.1001/jamaneurol.2013.4749>

Kehoe, D. E., Jing, D., Lock, L. T., & Tzanakakis, E. S. (2010). Scalable stirred-suspension bioreactor culture of human pluripotent stem cells. *Tissue engineering. Part A*, 16(2), 405–421. <https://doi.org/10.1089/ten.tea.2009.0454>

Kempermann, G., Song, H. and Gage, F. H. (2015) ‘Neurogenesis in the Adult Hippocampus’, *Cold Spring Harbor perspectives in biology*, 7(9), p. a018812. doi: 10.1101/cshperspect.a018812.

Kempf, H., Andree, B. and Zweigerdt, R. (2016) ‘Large-scale production of human pluripotent stem cell derived cardiomyocytes’, *Advanced Drug Delivery Reviews*, 96, pp. 18–30. doi: 10.1016/j.addr.2015.11.016.

Khlongkhlaeo, A., Carter, R. L., Parnpai, R., and Chan, A. W. S. (2016) ‘Comparison of methods for deriving neural progenitor cells from nonhuman primate embryonic stem cells’, *Asian Biomedicine*, 10(5), pp. 423–433. doi: 10.5372/1905-7415.1005.505.

Kim, I. (2013) ‘A brief overview of cell therapy and its product’, *Journal of the Korean Association of Oral and Maxillofacial Surgeons*, 39(5), p. 201. doi: 10.5125/jkaoms.2013.39.5.201.

Kim, J. H., Jo, H. Y., Ha, H. Y., & Kim, Y. O. (2021). Korea National Stem Cell Bank. *Stem cell research*, 53, 102270. <https://doi.org/10.1016/j.scr.2021.102270>

Kim, K., Doi, A., Wen, B., Ng, K., Zhao, R., Cahan, P., Kim, J., Aryee, M. J., Ji, H., Ehrlich, L. I., Yabuuchi, A., Takeuchi, A., Cunniff, K. C., Hongguang, H., McKinney-Freeman, S., Naveiras, O., Yoon, T. J., Irizarry, R. A., Jung, N., Seita, J., ... Daley, G. Q. (2010). Epigenetic memory in induced pluripotent stem cells. *Nature*, 467(7313), 285–290. <https://doi.org/10.1038/nature09342>

Kim, M.-H., Takeuchi, K. and Kino-oka, M. (2019) ‘Role of cell-secreted extracellular matrix formation in aggregate formation and stability of human induced pluripotent stem cells in suspension culture’, *Journal of Bioscience and Bioengineering*, 127(3), pp. 372–380. doi: <https://doi.org/10.1016/j.jbiosc.2018.08.010>.

Kim, M., Erickson, I. E., Huang, A. H., Garrity, S. T., Mauck, R. L., & Steinberg, D. R. (2018). Donor Variation and Optimization of Human Mesenchymal Stem Cell Chondrogenesis in Hyaluronic Acid. *Tissue engineering. Part A*, 24(21-22), 1693–1703. <https://doi.org/10.1089/ten.TEA.2017.0520>

Kirkeby, A., Grealish, S., Wolf, D. A., Nelander, J., Wood, J., Lundblad, M., Lindvall, O., & Parmar, M. (2012). Generation of regionally specified neural progenitors and functional neurons from human embryonic stem cells under defined conditions. *Cell reports*, 1(6), 703–714. <https://doi.org/10.1016/j.celrep.2012.04.009>

Kleinman, H. K., McGarvey, M. L., Liotta, L. A., Robey, P. G., Tryggvason, K., & Martin, G. R. (1982). Isolation and characterization of type IV procollagen, laminin, and heparan sulfate F.D., de la Raga, PhD Thesis, Aston University, 2022

proteoglycan from the EHS sarcoma. *Biochemistry*, 21(24), 6188–6193. <https://doi.org/10.1021/bi00267a025>

Kleinman, H. K., & Martin, G. R. (2005). Matrigel: basement membrane matrix with biological activity. *Seminars in cancer biology*, 15(5), 378–386. <https://doi.org/10.1016/j.semcancer.2005.05.004>

Koch, P., Opitz, T., Steinbeck, J. A., Ladewig, J., & Brüstle, O. (2009). A rosette-type, self-renewing human ES cell-derived neural stem cell with potential for in vitro instruction and synaptic integration. *Proceedings of the National Academy of Sciences of the United States of America*, 106(9), 3225–3230. <https://doi.org/10.1073/pnas.0808387106>

Koenig, L., Ramme, A., Faust, D., Lauster, R., and Marx, U. (2018) ‘Production of Human Induced Pluripotent Stem Cell-Derived Cortical Neurospheres in the DASbox® Mini Bioreactor System’, *Application note*, (364), pp. 1–12.

Kolhar, P., Kotamraju, V. R., Hikita, S. T., Clegg, D. O., & Ruoslahti, E. (2010). Synthetic surfaces for human embryonic stem cell culture. *Journal of biotechnology*, 146(3), 143–146. <https://doi.org/10.1016/j.jbiotec.2010.01.016>

Kovacs, G. G. (2018) ‘Chapter 25 - Tauopathies’, in Kovacs, G. G. and Alafuzoff, I. B. T.-H. of C. N. (eds) *Neuropathology*. Elsevier, pp. 355–368. doi: <https://doi.org/10.1016/B978-0-12-802395-2.00025-0>.

Krawetz, R., Taiani, J. T., Liu, S., Meng, G., Li, X., Kallos, M. S., & Rancourt, D. E. (2010). Large-scale expansion of pluripotent human embryonic stem cells in stirred-suspension bioreactors. *Tissue engineering. Part C, Methods*, 16(4), 573–582. <https://doi.org/10.1089/ten.TEC.2009.0228>

Kuijk, E., Jager, M., van der Roest, B., Locati, M. D., Van Hoeck, A., Korzelius, J., Janssen, R., Besselink, N., Boymans, S., van Boxtel, R., & Cuppen, E. (2020). The mutational impact of culturing human pluripotent and adult stem cells. *Nature communications*, 11(1), 2493. <https://doi.org/10.1038/s41467-020-16323-4>

Kumar, M., Bagchi, B., Gupta, S. K., Meena, A. S., Gressens, P., & Mani, S. (2007). Neurospheres derived from human embryoid bodies treated with retinoic Acid show an increase in nestin and ngn2 expression that correlates with the proportion of tyrosine hydroxylase-positive cells. *Stem cells and development*, 16(4), 667–681. <https://doi.org/10.1089/scd.2006.0115>

Kunath, T., Saba-El-Leil, M. K., Almousaillekh, M., Wray, J., Meloche, S., & Smith, A. (2007). FGF stimulation of the Erk1/2 signalling cascade triggers transition of pluripotent embryonic stem cells from self-renewal to lineage commitment. *Development (Cambridge, England)*, 134(16), 2895–2902. <https://doi.org/10.1242/dev.02880>

Laco, F., Lam, A. T., Woo, T. L., Tong, G., Ho, V., Soong, P. L., Grishina, E., Lin, K. H., Reuveny, S., & Oh, S. K. (2020). Selection of human induced pluripotent stem cells lines optimization of cardiomyocytes differentiation in an integrated suspension microcarrier bioreactor. *Stem cell research & therapy*, 11(1), 118. <https://doi.org/10.1186/s13287-020-01618-6>

Lam, A. T., Li, J., Chen, A. K., Birch, W. R., Reuveny, S., & Oh, S. K. (2015). Improved Human Pluripotent Stem Cell Attachment and Spreading on Xeno-Free Laminin-521-Coated Microcarriers Results in Efficient Growth in Agitated Cultures. *BioResearch open access*, 4(1),

242–257. <https://doi.org/10.1089/biores.2015.0010>

Lam, A. T., Chen, A. K., Ting, S. Q., Reuveny, S., & Oh, S. K. (2016). Integrated processes for expansion and differentiation of human pluripotent stem cells in suspended microcarrier cultures. *Biochemical and biophysical research communications*, 473(3), 764–768. <https://doi.org/10.1016/j.bbrc.2015.09.079>

Lam, M. T. and Longaker, M. T. (2012) ‘Comparison of several attachment methods for human iPS, embryonic and adipose-derived stem cells for tissue engineering’, *Journal of Tissue Engineering and Regenerative Medicine*. 2012/05/18, 6(SUPPL. 3), pp. s80–s86. doi: 10.1002/term.1499.

Lambshead, J. W., Meagher, L., O'Brien, C., & Laslett, A. L. (2013). Defining synthetic surfaces for human pluripotent stem cell culture. *Cell regeneration (London, England)*, 2(1), 7. <https://doi.org/10.1186/2045-9769-2-7>

Lampe, K. J., Namba, R. M., Silverman, T. R., Bjugstad, K. B., & Mahoney, M. J. (2009). Impact of lactic acid on cell proliferation and free radical-induced cell death in monolayer cultures of neural precursor cells. *Biotechnology and bioengineering*, 103(6), 1214–1223. <https://doi.org/10.1002/bit.22352>

Lancaster, M. A. and Knoblich, J. A. (2014) ‘Generation of cerebral organoids from human pluripotent stem cells’, *Nature protocols*. 2014/09/04, 9(10), pp. 2329–2340. doi: 10.1038/nprot.2014.158.

Lanier, L. L. (2008) ‘Up on the tightrope: natural killer cell activation and inhibition’, *Nature Immunology*, 9(5), pp. 495–502. doi: 10.1038/ni1581.

Laperle, A., Masters, K. S. and Palecek, S. P. (2015) ‘Influence of substrate composition on human embryonic stem cell differentiation and extracellular matrix production in embryoid bodies’, *Biotechnology Progress*, 31(1), pp. 212–219. doi: <https://doi.org/10.1002/btpr.2001>.

Lavon, N., Zimmerman, M. and Itskovitz-Eldor, J. (2017) ‘Scalable Expansion of Pluripotent Stem Cells’, in: Springer, Cham, pp. 23–37. doi: 10.1007/10\_2017\_26.

Le, M. N. T. and Hasegawa, K. (2019) ‘Expansion culture of human pluripotent stem cells and production of cardiomyocytes’, *Bioengineering*, 6(2). doi: 10.3390/bioengineering6020048.

Leclerc, M., Dudonné, S. and Calon, F. (2021) ‘Can natural products exert neuroprotection without crossing the blood–brain barrier?’, *International Journal of Molecular Sciences*, 22(7). doi: 10.3390/ijms22073356.

Lee, E. H., Kim, S. M., Kim, C. H., Pagire, S. H., Pagire, H. S., Chung, H. Y., Ahn, J. H., & Park, C. H. (2019). Dopamine neuron induction and the neuroprotective effects of thyroid hormone derivatives. *Scientific reports*, 9(1), 13659. <https://doi.org/10.1038/s41598-019-49876-6>

Lee, J. Y. and Hong, S.-H. (2020) ‘Hematopoietic Stem Cells and Their Roles in Tissue Regeneration’, *International journal of stem cells*, 13(1), pp. 1–12. doi: 10.15283/ijsc19127.

Lees, J. G., Gardner, D. K. and Harvey, A. J. (2017) ‘Pluripotent stem cell metabolism and mitochondria: beyond ATP’, *Stem cells international*, 2017.

Leung, H. W., Chen, A., Choo, A. B., Reuveny, S., & Oh, S. K. (2011). Agitation can induce differentiation of human pluripotent stem cells in microcarrier cultures. *Tissue engineering. Part C, Methods*, 17(2), 165–172. <https://doi.org/10.1089/ten.TEC.2010.0320>

F.D., de la Raga, PhD Thesis, Aston University, 2022

- Levenstein, M. E., Ludwig, T. E., Xu, R. H., Llanas, R. A., VanDenHeuvel-Kramer, K., Manning, D., & Thomson, J. A. (2006). Basic fibroblast growth factor support of human embryonic stem cell self-renewal. *Stem cells (Dayton, Ohio)*, 24(3), 568–574. <https://doi.org/10.1634/stemcells.2005-0247>
- Li, Yan, Meimei Liu, Yuanwei Yan, S.-T. Y. (2014) ‘Neural differentiation from pluripotent stem cells: The role of natural and synthetic extracellular matrix’, *World Journal of Stem Cells*, 6(1), p. 11. doi: 10.4252/wjsc.v6.i1.11.
- Li, L., Bennett, S. A. L. and Wang, L. (2012) ‘Role of E-cadherin and other cell adhesion molecules in survival and differentiation of human pluripotent stem cells’, *Cell adhesion & migration*, 6(1), pp. 59–70. doi: 10.4161/cam.19583.
- Lin, W. L., Castanedes-Casey, M. and Dickson, D. W. (2009) ‘Transactivation response DNA-binding protein 43 microvasculopathy in frontotemporal degeneration and familial lewy body disease’, *Journal of Neuropathology and Experimental Neurology*, 68(11), pp. 1167–1176. doi: 10.1097/NEN.0b013e3181baacec.
- Lindner, M., Laporte, A., Block, S., Elomaa, L., & Weinhart, M. (2021). Physiological Shear Stress Enhances Differentiation, Mucus-Formation and Structural 3D Organization of Intestinal Epithelial Cells In Vitro. *Cells*, 10(8), 2062. <https://doi.org/10.3390/cells10082062>
- Liszewska, E., Majchrowicz, L., Krogulec, E., Kotulska, K., Kaczmarek, L., Kalita, K., Dobrzyń, A., & Jaworski, J. (2021). Establishment of two hiPSC lines (IIMCBi001-A and IIMCBi002-A) from dermal fibroblasts of healthy donors and characterization of their cell cycle. *Stem cell research*, 52, 102225. <https://doi.org/10.1016/j.scr.2021.102225>
- Liu, H., Bockhorn, J., Dalton, R., Chang, Y. F., Qian, D., Zitzow, L. A., Clarke, M. F., & Greene, G. L. (2011). Removal of lactate dehydrogenase-elevating virus from human-in-mouse breast tumor xenografts by cell-sorting. *Journal of virological methods*, 173(2), 266–270. <https://doi.org/10.1016/j.jviromet.2011.02.015>
- Liu, S., Striebel, J., Pasquini, G., Ng, A. H. M., Khoshakhlagh, P., Church, G. M., & Busskamp, V. (2021). Neuronal Cell-type Engineering by Transcriptional Activation. *Frontiers in genome editing*, 3, 715697. <https://doi.org/10.3389/fgeed.2021.715697>
- Liu, X.-Y., Yang, L.-P. and Zhao, L. (2020) ‘Stem cell therapy for Alzheimer’s disease’, *World journal of stem cells*, 12(8), pp. 787–802. doi: 10.4252/wjsc.v12.i8.787.
- Liu, X., Huang, J., Chen, T., Wang, Y., Xin, S., Li, J., Pei, G., & Kang, J. (2008). Yamanaka factors critically regulate the developmental signaling network in mouse embryonic stem cells. *Cell research*, 18(12), 1177–1189. <https://doi.org/10.1038/cr.2008.309>
- Lu, J., Hou, R., Booth, C. J., Yang, S. H., & Snyder, M. (2006). Defined culture conditions of human embryonic stem cells. *Proceedings of the National Academy of Sciences of the United States of America*, 103(15), 5688–5693. <https://doi.org/10.1073/pnas.0601383103>
- Ludwig, T. and A. Thomson, J. (2007) ‘Defined, Feeder-Independent Medium for Human Embryonic Stem Cell Culture’, *Current Protocols in Stem Cell Biology*, (September), pp. 1–16. doi: 10.1002/9780470151808.sc01c02s2.
- Ludwig, T. E., Bergendahl, V., Levenstein, M. E., Yu, J., Probasco, M. D., & Thomson, J. A. (2006). Feeder-independent culture of human embryonic stem cells. *Nature methods*, 3(8), 637–646. <https://doi.org/10.1038/nmeth902>

Lukovic, D., Diez Lloret, A., Stojkovic, P., Rodríguez-Martínez, D., Perez Arago, M. A., Rodriguez-Jimenez, F. J., González-Rodríguez, P., López-Barneo, J., Sykova, E., Jendelova, P., Kostic, J., Moreno-Manzano, V., Stojkovic, M., Bhattacharya, S. S., & Erceg, S. (2017). Highly Efficient Neural Conversion of Human Pluripotent Stem Cells in Adherent and Animal-Free Conditions. *Stem cells translational medicine*, 6(4), 1217–1226. <https://doi.org/10.1002/sctm.16-0371>

Macarthur, C. C., Fontes, A., Ravinder, N., Kuninger, D., Kaur, J., Bailey, M., Taliana, A., Vemuri, M. C., & Lieu, P. T. (2012). Generation of human-induced pluripotent stem cells by a nonintegrating RNA Sendai virus vector in feeder-free or xeno-free conditions. *Stem cells international*, 2012, 564612. <https://doi.org/10.1155/2012/564612>

Machold, R., Hayashi, S., Rutlin, M., Muzumdar, M. D., Nery, S., Corbin, J. G., Gritli-Linde, A., Dellovade, T., Porter, J. A., Rubin, L. L., Dudek, H., McMahon, A. P., & Fishell, G. (2003). Sonic hedgehog is required for progenitor cell maintenance in telencephalic stem cell niches. *Neuron*, 39(6), 937–950. [https://doi.org/10.1016/s0896-6273\(03\)00561-0](https://doi.org/10.1016/s0896-6273(03)00561-0)

Madonna, R., Geng, Y. J., Shelat, H., Ferdinandy, P., & De Caterina, R. (2014). High glucose-induced hyperosmolarity impacts proliferation, cytoskeleton remodeling and migration of human induced pluripotent stem cells via aquaporin-1. *Biochimica et biophysica acta*, 1842(11), 2266–2275. <https://doi.org/10.1016/j.bbadis.2014.07.030>

Madrazo, I., Kopyov, O., Ávila-Rodríguez, M. A., Ostrosky, F., Carrasco, H., Kopyov, A., Avendaño-Estrada, A., Jiménez, F., Magallón, E., Zamorano, C., González, G., Valenzuela, T., Carrillo, R., Palma, F., Rivera, R., Franco-Bourland, R. E., & Guízar-Sahagún, G. (2019). Transplantation of Human Neural Progenitor Cells (NPC) into Putamina of Parkinsonian Patients: A Case Series Study, Safety and Efficacy Four Years after Surgery. *Cell transplantation*, 28(3), 269–285. <https://doi.org/10.1177/0963689718820271>

Madrid, M., Sumen, C., Aivio, S., & Saklayen, N. (2021). Autologous Induced Pluripotent Stem Cell-Based Cell Therapies: Promise, Progress, and Challenges. *Current protocols*, 1(3), e88. <https://doi.org/10.1002/cpz1.88> Madrid, M. *et al.* (2021b) ‘Autologous Induced Pluripotent Stem Cell-Based Cell Therapies: Promise, Progress, and Challenges’, *Current Protocols*, 1(3), p. e88. doi: <https://doi.org/10.1002/cpz1.88>.

Mansour, A. A., Gonçalves, J. T., Bloyd, C. W., Li, H., Fernandes, S., Quang, D., Johnston, S., Parylak, S. L., Jin, X., & Gage, F. H. (2018). An in vivo model of functional and vascularized human brain organoids. *Nature biotechnology*, 36(5), 432–441. <https://doi.org/10.1038/nbt.4127>

Marchand, M., Anderson, E. K., Phadnis, S. M., Longaker, M. T., Cooke, J. P., Chen, B., & Reijo Pera, R. A. (2014). Concurrent generation of functional smooth muscle and endothelial cells via a vascular progenitor. *Stem cells translational medicine*, 3(1), 91–97. <https://doi.org/10.5966/sctm.2013-0124>

Martin G. R. (1981). Isolation of a pluripotent cell line from early mouse embryos cultured in medium conditioned by teratocarcinoma stem cells. *Proceedings of the National Academy of Sciences of the United States of America*, 78(12), 7634–7638. <https://doi.org/10.1073/pnas.78.12.7634>

Martínez-Cerdeño, V. and Noctor, S. C. (2018) ‘Neural Progenitor Cell Terminology’, *Frontiers in Neuroanatomy*, 12(December), pp. 1–8. doi: 10.3389/fnana.2018.00104.

Mason, E. F. and Rathmell, J. C. (2011) ‘Cell metabolism: an essential link between cell growth  
F.D., de la Raga, PhD Thesis, Aston University, 2022

and apoptosis', *Biochimica et biophysica acta*. 2010/09/08, 1813(4), pp. 645–654. doi: 10.1016/j.bbamcr.2010.08.011.

Massagué, J. (2012) 'TGF $\beta$  signalling in context', *Nature Reviews Molecular Cell Biology*, 13(10), pp. 616–630. doi: 10.1038/nrm3434.

Matanguihan, C. and Wu, P. (2022) 'Upstream continuous processing: recent advances in production of biopharmaceuticals and challenges in manufacturing', *Current Opinion in Biotechnology*, 78, p. 102828. doi: 10.1016/j.copbio.2022.102828.

Mattapally, S., Pawlik, K. M., Fast, V. G., Zumaquero, E., Lund, F. E., Randall, T. D., Townes, T. M., & Zhang, J. (2018). Human Leukocyte Antigen Class I and II Knockout Human Induced Pluripotent Stem Cell-Derived Cells: Universal Donor for Cell Therapy. *Journal of the American Heart Association*, 7(23), e010239. <https://doi.org/10.1161/JAHA.118.010239>

Mayshar, Y., Ben-David, U., Lavon, N., Biancotti, J. C., Yakir, B., Clark, A. T., Plath, K., Lowry, W. E., & Benvenisty, N. (2010). Identification and classification of chromosomal aberrations in human induced pluripotent stem cells. *Cell stem cell*, 7(4), 521–531. <https://doi.org/10.1016/j.stem.2010.07.017>

Mazzini, L., Gelati, M., Profico, D. C., Sgaravizzi, G., Progetti Pensi, M., Muzi, G., Ricciolini, C., Rota Nodari, L., Carletti, S., Giorgi, C., Spera, C., Domenico, F., Bersano, E., Petruzzelli, F., Cisari, C., Maglione, A., Sarnelli, M. F., Stecco, A., Querin, G., Masiero, S., ... Vescovi, A. L. (2015). Human neural stem cell transplantation in ALS: initial results from a phase I trial. *Journal of translational medicine*, 13, 17. <https://doi.org/10.1186/s12967-014-0371-2>

Mazzini, L., Gelati, M., Profico, D. C., Sgaravizzi, G., Progetti Pensi, M., Muzi, G., Ricciolini, C., Rota Nodari, L., Carletti, S., Giorgi, C., Spera, C., Domenico, F., Bersano, E., Petruzzelli, F., Cisari, C., Maglione, A., Sarnelli, M. F., Stecco, A., Querin, G., Masiero, S., Cantello, R., Ferrari, D., Zalfa, C., Binda, E., Visioli, A., Trombetta, D., Novelli, A., Torres, B., Bernardini, L., Carriero, A., Prandi, P., Servo, S., Cerino, A., Cima, V., Gaiani, A., Nasuelli, N., Massara, M., Glass, J., Sorarù, G., Boullis, Nicholas M., *et al.* (2015) 'Human neural stem cell transplantation in ALS: Initial results from a phase I trial', *Journal of Translational Medicine*, 13(1), pp. 1–16. doi: 10.1186/s12967-014-0371-2.

McCann, H., Stevens, C. H., Cartwright, H., & Halliday, G. M. (2014).  $\alpha$ -Synucleinopathy phenotypes. *Parkinsonism & related disorders*, 20 Suppl 1, S62–S67. [https://doi.org/10.1016/S1353-8020\(13\)70017-8](https://doi.org/10.1016/S1353-8020(13)70017-8)

McTague, A., Rossignoli, G., Ferrini, A., Barral, S., & Kurian, M. A. (2021). Genome Editing in iPSC-Based Neural Systems: From Disease Models to Future Therapeutic Strategies. *Frontiers in genome editing*, 3, 630600. <https://doi.org/10.3389/fgeed.2021.630600>

Meng, G., Liu, S., Krawetz, R., Chan, M., Chernos, J., & Rancourt, D. E. (2008). A novel method for generating xeno-free human feeder cells for human embryonic stem cell culture. *Stem cells and development*, 17(3), 413–422. <https://doi.org/10.1089/scd.2007.0236>

Mingliang, R., Bo, Z. and Zhengguo, W. (2011) 'Stem cells for cardiac repair: Status, mechanisms, and new strategies', *Stem Cells International*, 2011(Figure 1). doi: 10.4061/2011/310928.

Mira, H., Andreu, Z., Suh, H., Lie, D. C., Jessberger, S., Consiglio, A., San Emeterio, J., Hortigüela, R., Marqués-Torrejón, M. A., Nakashima, K., Colak, D., Götz, M., Fariñas, I., & Gage, F. H. (2010). Signaling through BMPR-IA regulates quiescence and long-term activity of neural stem cells in the adult hippocampus. *Cell stem cell*, 7(1), 78–89.

<https://doi.org/10.1016/j.stem.2010.04.016>

Miranda, C. C., Fernandes, T. G., Diogo, M. M., & Cabral, J. M. (2016). Scaling up a chemically-defined aggregate-based suspension culture system for neural commitment of human pluripotent stem cells. *Biotechnology journal*, *11*(12), 1628–1638. <https://doi.org/10.1002/biot.201600446>

Miranda, C. C., Akenhead, M. L., Silva, T. P., Derr, M. A., Vemuri, M. C., Cabral, J. M. S., & Fernandes, T. G. (2022). A Dynamic 3D Aggregate-Based System for the Successful Expansion and Neural Induction of Human Pluripotent Stem Cells. *Frontiers in cellular neuroscience*, *16*, 838217. <https://doi.org/10.3389/fncel.2022.838217>

Modi, G., Pillay, V. and Choonara, Y. E. (2010) ‘Advances in the treatment of neurodegenerative disorders employing nanotechnology’, *Annals of the New York Academy of Sciences*, 1184, pp. 154–172. doi: 10.1111/j.1749-6632.2009.05108.x.

Morante-Redolat, J. M. and Porlan, E. (2019) ‘Neural Stem Cell Regulation by Adhesion Molecules Within the Subependymal Niche ’, *Frontiers in Cell and Developmental Biology* . Available at: <https://www.frontiersin.org/article/10.3389/fcell.2019.00102>.

Morizane, A., Doi, D., Kikuchi, T., Nishimura, K., & Takahashi, J. (2011). Small-molecule inhibitors of bone morphogenic protein and activin/nodal signals promote highly efficient neural induction from human pluripotent stem cells. *Journal of neuroscience research*, *89*(2), 117–126. <https://doi.org/10.1002/jnr.22547>

Morshead, C. M., Reynolds, B. A., Craig, C. G., McBurney, M. W., Staines, W. A., Morassutti, D., Weiss, S., & van der Kooy, D. (1994). Neural stem cells in the adult mammalian forebrain: a relatively quiescent subpopulation of subependymal cells. *Neuron*, *13*(5), 1071–1082. [https://doi.org/10.1016/0896-6273\(94\)90046-9](https://doi.org/10.1016/0896-6273(94)90046-9)

Mount, N. M. *et al.* (2015) ‘Cell-based therapy technology classifications and translational challenges’, *Philosophical Transactions of the Royal Society B: Biological Sciences*, *370*(1680). doi: 10.1098/rstb.2015.0017.

Nagoshi, N. and Okano, H. (2018) ‘iPSC-derived neural precursor cells: potential for cell transplantation therapy in spinal cord injury’, *Cellular and Molecular Life Sciences*, *75*(6), pp. 989–1000. doi: 10.1007/s00018-017-2676-9.

Nakagawa, M., Taniguchi, Y., Senda, S., Takizawa, N., Ichisaka, T., Asano, K., Morizane, A., Doi, D., Takahashi, J., Nishizawa, M., Yoshida, Y., Toyoda, T., Osafune, K., Sekiguchi, K., & Yamanaka, S. (2014). A novel efficient feeder-free culture system for the derivation of human induced pluripotent stem cells. *Scientific reports*, *4*, 3594. <https://doi.org/10.1038/srep03594>

Nakamura, T., Okamoto, I., Sasaki, K., Yabuta, Y., Iwatani, C., Tsuchiya, H., Seita, Y., Nakamura, S., Yamamoto, T., & Saitou, M. (2016). A developmental coordinate of pluripotency among mice, monkeys and humans. *Nature*, *537*(7618), 57–62. <https://doi.org/10.1038/nature19096>

Nakayama, T., Momoki-Soga, T., Yamaguchi, K., & Inoue, N. (2004). Efficient production of neural stem cells and neurons from embryonic stem cells. *Neuroreport*, *15*(3), 487–491. <https://doi.org/10.1097/00001756-200403010-00021>

Narsinh, K. H., Jia, F., Robbins, R. C., Kay, M. A., Longaker, M. T., & Wu, J. C. (2011). Generation of adult human induced pluripotent stem cells using nonviral minicircle DNA vectors. *Nature protocols*, *6*(1), 78–88. <https://doi.org/10.1038/nprot.2010.173>

Nie, Y., Bergendahl, V., Hei, D. J., Jones, J. M., & Palecek, S. P. (2009). Scalable culture and cryopreservation of human embryonic stem cells on microcarriers. *Biotechnology progress*, 25(1), 20–31. <https://doi.org/10.1002/btpr.110>

Nie, Y., Wang, W., Xu, X., Ma, N., and Lendlein, A. (2021) ‘The response of human induced pluripotent stem cells to cyclic temperature changes explored by BIO-AFM’, *MRS Advances*, 6(31), pp. 745–749. doi: 10.1557/s43580-021-00110-4.

Nienow, A. W., Hewitt, C. J., Heathman, T. R. J., Glyn, V. A. M., Fonte, G. N., Hanga, M. P., Coopman, K., Rafiq, Q. A. (2016) ‘Agitation conditions for the culture and detachment of hMSCs from microcarriers in multiple bioreactor platforms’, *Biochemical Engineering Journal*, 108, pp. 24–29. doi: 10.1016/j.bej.2015.08.003.

Nishimura, K., Fukuda, A. and Hisatake, K. (2019) ‘Mechanisms of the Metabolic Shift during Somatic Cell Reprogramming’, *International journal of molecular sciences*, 20(9), p. 2254. doi: 10.3390/ijms20092254.

Nogueira, D. E. S., Rodrigues, C. A. V., Carvalho, M. S., Miranda, C. C., Hashimura, Y., Jung, S., Lee, B., & Cabral, J. M. S. (2019). Strategies for the expansion of human induced pluripotent stem cells as aggregates in single-use Vertical-Wheel™ bioreactors. *Journal of biological engineering*, 13, 74. <https://doi.org/10.1186/s13036-019-0204-1>

Odenwelder, D. C., Lu, X. and Harcum, S. W. (2021) ‘Induced pluripotent stem cells can utilize lactate as a metabolic substrate to support proliferation’, *Biotechnology Progress*, 37(2). doi: 10.1002/btpr.3090.

Oh, S. K., Chen, A. K., Mok, Y., Chen, X., Lim, U. M., Chin, A., Choo, A. B., & Reuveny, S. (2009). Long-term microcarrier suspension cultures of human embryonic stem cells. *Stem cell research*, 2(3), 219–230. <https://doi.org/10.1016/j.scr.2009.02.005>

Okumura, T., Horie, Y., Lai, C. Y., Lin, H. T., Shoda, H., Natsumoto, B., Fujio, K., Kumaki, E., Okano, T., Ono, S., Tanita, K., Morio, T., Kanegane, H., Hasegawa, H., Mizoguchi, F., Kawahata, K., Kohsaka, H., Moritake, H., Nunoi, H., Waki, H., ... Otsu, M. (2019). Robust and highly efficient hiPSC generation from patient non-mobilized peripheral blood-derived CD34<sup>+</sup> cells using the auto-erasable Sendai virus vector. *Stem cell research & therapy*, 10(1), 185. <https://doi.org/10.1186/s13287-019-1273-2>

Olmer, R., Lange, A., Selzer, S., Kasper, C., Haverich, A., Martin, U., & Zweigerdt, R. (2012). Suspension culture of human pluripotent stem cells in controlled, stirred bioreactors. *Tissue engineering. Part C, Methods*, 18(10), 772–784. <https://doi.org/10.1089/ten.TEC.2011.0717>

Osnato, A., Brown, S., Krueger, C., Andrews, S., Collier, A. J., Nakanoh, S., Quiroga Londoño, M., Wesley, B. T., Muraro, D., Brumm, A. S., Niakan, K. K., Vallier, L., Ortmann, D., & Rugg-Gunn, P. J. (2021). TGFβ signalling is required to maintain pluripotency of human naïve pluripotent stem cells. *eLife*, 10, e67259. <https://doi.org/10.7554/eLife.67259>

Ottoboni, L., von Wunster, B. and Martino, G. (2020) ‘Therapeutic Plasticity of Neural Stem Cells’, *Frontiers in Neurology*. Available at: <https://www.frontiersin.org/article/10.3389/fneur.2020.00148>.

Panopoulos, A. D., Yanes, O., Ruiz, S., Kida, Y. S., Diep, D., Tautenhahn, R., Herrerías, A., Batchelder, E. M., Plongthongkum, N., Lutz, M., Berggren, W. T., Zhang, K., Evans, R. M., Siuzdak, G., & Izpisua Belmonte, J. C. (2012). The metabolome of induced pluripotent stem cells reveals metabolic changes occurring in somatic cell reprogramming. *Cell research*, 22(1),

168–177. <https://doi.org/10.1038/cr.2011.177>

Pardridge W. M. (2020). Blood-Brain Barrier and Delivery of Protein and Gene Therapeutics to Brain. *Frontiers in aging neuroscience*, *11*, 373. <https://doi.org/10.3389/fnagi.2019.00373>

Parr, A. M., Walsh, P. J., Truong, V., & Dutton, J. R. (2016). cGMP-Compliant Expansion of Human iPSC Cultures as Adherent Monolayers. *Methods in molecular biology (Clifton, N.J.)*, *1357*, 221–229. [https://doi.org/10.1007/7651\\_2015\\_243](https://doi.org/10.1007/7651_2015_243)

Pas, S. P. (2018) ‘The rise of three-dimensional human brain cultures’, *Nature*, *553*(7689), pp. 437–445. doi: 10.1038/nature25032.

Patten, I. and Placzek, M. (2000) ‘The role of sonic hedgehog in neural tube patterning’, *Cellular and Molecular Life Sciences*, *57*(12), pp. 1695–1708. doi: 10.1007/PL00000652.

Pauly, M. G., Krajka, V., Stengel, F., Seibler, P., Klein, C., & Capetian, P. (2018). Adherent vs. Free-Floating Neural Induction by Dual SMAD Inhibition for Neurosphere Cultures Derived from Human Induced Pluripotent Stem Cells. *Frontiers in cell and developmental biology*, *6*, 3. <https://doi.org/10.3389/fcell.2018.00003>

Pavel, M., Renna, M., Park, S. J., Menzies, F. M., Ricketts, T., Füllgrabe, J., Ashkenazi, A., Frake, R. A., Lombarte, A. C., Bento, C. F., Franze, K., & Rubinsztein, D. C. (2018). Contact inhibition controls cell survival and proliferation via YAP/TAZ-autophagy axis. *Nature communications*, *9*(1), 2961. <https://doi.org/10.1038/s41467-018-05388-x>

Petropoulos, S., Edsgård, D., Reinius, B., Deng, Q., Panula, S. P., Codeluppi, S., Plaza Reyes, A., Linnarsson, S., Sandberg, R., & Lanner, F. (2016). Single-Cell RNA-Seq Reveals Lineage and X Chromosome Dynamics in Human Preimplantation Embryos. *Cell*, *165*(4), 1012–1026. <https://doi.org/10.1016/j.cell.2016.03.023>

Petry, F., Smith, J. R., Leber, J., Salzig, D., Czermak, P., & Weiss, M. L. (2016). Manufacturing of Human Umbilical Cord Mesenchymal Stromal Cells on Microcarriers in a Dynamic System for Clinical Use. *Stem cells international*, *2016*, 4834616. <https://doi.org/10.1155/2016/4834616>

Pettinato, G., Wen, X., & Zhang, N. (2014). Formation of well-defined embryoid bodies from dissociated human induced pluripotent stem cells using microfabricated cell-repellent microwell arrays. *Scientific reports*, *4*, 7402. <https://doi.org/10.1038/srep07402>

Phillips, B. W., Horne, R., Lay, T. S., Rust, W. L., Teck, T. T., & Crook, J. M. (2008). Attachment and growth of human embryonic stem cells on microcarriers. *Journal of biotechnology*, *138*(1-2), 24–32. <https://doi.org/10.1016/j.jbiotec.2008.07.1997>

Philp, A., Macdonald, A. L. and Watt, P. W. (2005) ‘Lactate—a signal coordinating cell and systemic function’, *Journal of Experimental Biology*, *208*(24), pp. 4561–4575.

Piccolo, S., Sasai, Y., Lu, B., & De Robertis, E. M. (1996). Dorsoventral patterning in *Xenopus*: inhibition of ventral signals by direct binding of chordin to BMP-4. *Cell*, *86*(4), 589–598. [https://doi.org/10.1016/s0092-8674\(00\)80132-4](https://doi.org/10.1016/s0092-8674(00)80132-4)

Pittenger, M. F., Discher, D. E., Péault, B. M., Phinney, D. G., Hare, J. M., & Caplan, A. I. (2019). Mesenchymal stem cell perspective: cell biology to clinical progress. *NPJ Regenerative medicine*, *4*, 22. <https://doi.org/10.1038/s41536-019-0083-6>

Porta, C., Paglino, C. and Mosca, A. (2014) ‘Targeting PI3K/Akt/mTOR Signaling in Cancer’, *Frontiers in Oncology*. Available at: F.D., de la Raga, PhD Thesis, Aston University, 2022 291

<https://www.frontiersin.org/article/10.3389/fonc.2014.00064>.

Pownall, M. E. and Isaacs, H. V (2010) *FGF Signalling in Vertebrate Development*. San Rafael (CA): Morgan & Claypool Life Sciences. Available at: <https://www.ncbi.nlm.nih.gov/books/NBK53169/>.

Prochazkova, M., Chavez, M. G., Prochazka, J., Felfy, H., Mushegyan, V., and Klein, O. D. (2015) 'Chapter 18 - Embryonic Versus Adult Stem Cells', in Vishwakarma, A. et al. (eds). Boston: Academic Press, pp. 249–262. doi: <https://doi.org/10.1016/B978-0-12-397157-9.00020-5>.

Prowse, A. B., Chong, F., Gray, P. P., & Munro, T. P. (2011). Stem cell integrins: implications for ex-vivo culture and cellular therapies. *Stem cell research*, 6(1), 1–12. <https://doi.org/10.1016/j.scr.2010.09.005>

Purcell, E. K., Naim, Y., Yang, A., Leach, M. K., Velkey, J. M., Duncan, R. K., & Corey, J. M. (2012). Combining topographical and genetic cues to promote neuronal fate specification in stem cells. *Biomacromolecules*, 13(11), 3427–3438. <https://doi.org/10.1021/bm301220k>

Qian, X., Song, H. and Ming, G.-L. (2019) 'Brain organoids: advances, applications and challenges.', *Development (Cambridge, England)*, 146(8). doi: 10.1242/dev.166074.

Quintanilla, R. H., Jr, Asprer, J. S., Vaz, C., Tanavde, V., & Lakshmipathy, U. (2014). CD44 is a negative cell surface marker for pluripotent stem cell identification during human fibroblast reprogramming. *PLoS one*, 9(1), e85419. <https://doi.org/10.1371/journal.pone.0085419>

Rafiq, Q. A., Brosnan, K. M., Coopman, K., Nienow, A. W., & Hewitt, C. J. (2013). Culture of human mesenchymal stem cells on microcarriers in a 5 l stirred-tank bioreactor. *Biotechnology letters*, 35(8), 1233–1245. <https://doi.org/10.1007/s10529-013-1211-9>

Rafiq, Q. A., Coopman, K., Nienow, A. W., & Hewitt, C. J. (2016). Systematic microcarrier screening and agitated culture conditions improves human mesenchymal stem cell yield in bioreactors. *Biotechnology journal*, 11(4), 473–486. <https://doi.org/10.1002/biot.201400862>

Ratti, A. and Buratti, E. (2016) 'Physiological functions and pathobiology of TDP-43 and FUS/TLS proteins', *Journal of Neurochemistry*, 138, pp. 95–111. doi: 10.1111/jnc.13625.

GBD 2016 Parkinson's Disease Collaborators (2018). Global, regional, and national burden of Parkinson's disease, 1990–2016: a systematic analysis for the Global Burden of Disease Study 2016. *The Lancet. Neurology*, 17(11), 939–953. [https://doi.org/10.1016/S1474-4422\(18\)30295-3](https://doi.org/10.1016/S1474-4422(18)30295-3)

Rehakova, D., Souralova, T. and Koutna, I. (2020) 'Clinical-Grade Human Pluripotent Stem Cells for Cell Therapy: Characterization Strategy', *International journal of molecular sciences*, 21(7), p. 2435. doi: 10.3390/ijms21072435.

Reinhardt, P., Glatza, M., Hemmer, K., Tsytsyura, Y., Thiel, C. S., Höing, S., Moritz, S., Parga, J. A., Wagner, L., Bruder, J. M., Wu, G., Schmid, B., Röpke, A., Klingauf, J., Schwamborn, J. C., Gasser, T., Schöler, H. R., & Sternecker, J. (2013). Derivation and expansion using only small molecules of human neural progenitors for neurodegenerative disease modeling. *PLoS one*, 8(3), e59252. <https://doi.org/10.1371/journal.pone.0059252>

Rigamonti, A., Repetti, G. G., Sun, C., Price, F. D., Reny, D. C., Rapino, F., Weisinger, K., Benkler, C., Peterson, Q. P., Davidow, L. S., Hansson, E. M., & Rubin, L. L. (2016). Large-

Scale Production of Mature Neurons from Human Pluripotent Stem Cells in a Three-Dimensional Suspension Culture System. *Stem cell reports*, 6(6), 993–1008. <https://doi.org/10.1016/j.stemcr.2016.05.010>

Riley, J., Federici, T., Polak, M., Kelly, C., Glass, J., Raore, B., Taub, J., Kesner, V., Feldman, E. L., & Boulis, N. M. (2012). Intraspinal stem cell transplantation in amyotrophic lateral sclerosis: a phase I safety trial, technical note, and lumbar safety outcomes. *Neurosurgery*, 71(2), 405–416. <https://doi.org/10.1227/NEU.0b013e31825ca05f>

Rivera-Ordaz, A., Peli, V., Manzini, P., Barilani, M., & Lazzari, L. (2021). Critical Analysis of cGMP Large-Scale Expansion Process in Bioreactors of Human Induced Pluripotent Stem Cells in the Framework of Quality by Design. *BioDrugs : clinical immunotherapeutics, biopharmaceuticals and gene therapy*, 35(6), 693–714. <https://doi.org/10.1007/s40259-021-00503-9>

Rivera, T., Zhao, Y., Ni, Y., & Wang, J. (2020). Human-Induced Pluripotent Stem Cell Culture Methods Under cGMP Conditions. *Current protocols in stem cell biology*, 54(1), e117. <https://doi.org/10.1002/cpsc.117>

Robinton, D. A. and Daley, G. Q. (2012) ‘The promise of induced pluripotent stem cells in research and therapy’, *Nature*, 481(7381), pp. 295–305. doi: 10.1038/nature10761.

Rodin, S., Antonsson, L., Niaudet, C., Simonson, O. E., Salmela, E., Hansson, E. M., Domogatskaya, A., Xiao, Z., Damdimopoulou, P., Sheikhi, M., Inzunza, J., Nilsson, A. S., Baker, D., Kuiper, R., Sun, Y., Blennow, E., Nordenskjöld, M., Grinnemo, K. H., Kere, J., Betsholtz, C., ... Tryggvason, K. (2014). Clonal culturing of human embryonic stem cells on laminin-521/E-cadherin matrix in defined and xeno-free environment. *Nature communications*, 5, 3195. <https://doi.org/10.1038/ncomms4195>

Rodrigues, A. L., Rodrigues, C. A. V., Gomes, A. R., Vieira, S. F., Badenes, S. M., Diogo, M. M., & Cabral, J. M. S. (2019). Dissolvable Microcarriers Allow Scalable Expansion And Harvesting Of Human Induced Pluripotent Stem Cells Under Xeno-Free Conditions. *Biotechnology journal*, 14(4), e1800461. <https://doi.org/10.1002/biot.201800461>

Rodríguez-Pizà, I., Richaud-Patin, Y., Vassena, R., González, F., Barrero, M. J., Veiga, A., Raya, A., & Izpisua Belmonte, J. C. (2010). Reprogramming of human fibroblasts to induced pluripotent stem cells under xeno-free conditions. *Stem cells (Dayton, Ohio)*, 28(1), 36–44. <https://doi.org/10.1002/stem.248>

Rogers, C. D., Moody, S. A. and Casey, E. S. (2009) ‘Neural induction and factors that stabilize a neural fate’, *Birth Defects Research Part C - Embryo Today: Reviews*, 87(3), pp. 249–262. doi: 10.1002/bdrc.20157.

Romito, A. and Cobellis, G. (2016) ‘Pluripotent stem cells: Current understanding and future directions’, *Stem Cells International*, 2016(Icm). doi: 10.1155/2016/9451492.

Rotondi, M., Grace, N., Betts, J., Bargh, N., Costariol, E., Zoro, B., Hewitt, C. J., Nienow, A. W., & Rafiq, Q. A. (2021). Design and development of a new ambr250® bioreactor vessel for improved cell and gene therapy applications. *Biotechnology letters*, 43(5), 1103–1116. <https://doi.org/10.1007/s10529-021-03076-3>

Rowland, T. J., Miller, L. M., Blaschke, A. J., Doss, E. L., Bonham, A. J., Hikita, S. T., Johnson, L. V., & Clegg, D. O. (2010). Roles of integrins in human induced pluripotent stem cell growth on Matrigel and vitronectin. *Stem cells and development*, 19(8), 1231–1240.

<https://doi.org/10.1089/scd.2009.0328>

S Santoro, R., Perrucci, G. L., Gowran, A., & Pompilio, G. (2019). Unchain My Heart: Integrins at the Basis of iPSC Cardiomyocyte Differentiation. *Stem cells international*, 2019, 8203950. <https://doi.org/10.1155/2019/8203950>

Sart, S., Bejoy, J. and Li, Y. (2017) ‘Characterization of 3D pluripotent stem cell aggregates and the impact of their properties on bioprocessing’, *Process Biochemistry*, 59, pp. 276–288. doi: <https://doi.org/10.1016/j.procbio.2016.05.024>.

Sathananthan, A. H. and Trounson, A. (2005) ‘Human embryonic stem cells and their spontaneous differentiation.’, *Italian journal of anatomy and embryology = Archivio italiano di anatomia ed embriologia*, 110(2 Suppl 1), pp. 151–157.

Schlaeger, T. M., Daheron, L., Brickler, T. R., Entwisle, S., Chan, K., Cianci, A., DeVine, A., Ettenger, A., Fitzgerald, K., Godfrey, M., Gupta, D., McPherson, J., Malwadkar, P., Gupta, M., Bell, B., Doi, A., Jung, N., Li, X., Lynes, M. S., Brookes, E., ... Daley, G. Q. (2015). A comparison of non-integrating reprogramming methods. *Nature biotechnology*, 33(1), 58–63. <https://doi.org/10.1038/nbt.3070>

Schnitzler, A. C., Verma, Anjali, V., Kehoe, D. E., Jing, D., Murrell, J. R., Der, K. A., Aysola, M., Rapiejko, P. J., Punreddy, S., and Rook, M. S. (2016) ‘Bioprocessing of human mesenchymal stem/stromal cells for therapeutic use: Current technologies and challenges’, *Biochemical Engineering Journal*, 108, pp. 3–13. doi: 10.1016/j.bej.2015.08.014.

Schuldiner, M., Itskovitz-Eldor, J. and Benvenisty, N. (2003) ‘Selective Ablation of Human Embryonic Stem Cells Expressing a “Suicide” Gene’, *Stem Cells*, 21(3), pp. 257–265. doi: 10.1634/stemcells.21-3-257.

Schwedhelm, I., Zdzieblo, D., Appelt-Menzel, A., Berger, C., Schmitz, T., Schuldt, B., Franke, A., Müller, F.-J., *et al.* (2019) ‘Automated real-time monitoring of human pluripotent stem cell aggregation in stirred tank reactors’, *Scientific Reports*, 9(1), p. 12297. doi: 10.1038/s41598-019-48814-w.

Seita, J. and Weissman, I. L. (2010) ‘Hematopoietic stem cell: self-renewal versus differentiation’, *Wiley interdisciplinary reviews. Systems biology and medicine*, 2(6), pp. 640–653. doi: 10.1002/wsbm.86.

Seki, T., Yuasa, S., Oda, M., Egashira, T., Yae, K., Kusumoto, D., Nakata, H., Tohyama, S., Hashimoto, H., Kodaira, M., Okada, Y., Seimiya, H., Fusaki, N., Hasegawa, M., & Fukuda, K. (2010). Generation of induced pluripotent stem cells from human terminally differentiated circulating T cells. *Cell stem cell*, 7(1), 11–14. <https://doi.org/10.1016/j.stem.2010.06.003>

Seo, M. W., & Park, T. E. (2021). Recent advances with liposomes as drug carriers for treatment of neurodegenerative diseases. *Biomedical engineering letters*, 11(3), 211–216. <https://doi.org/10.1007/s13534-021-00198-5>

Seri, B., García-Verdugo, J. M., Collado-Morente, L., McEwen, B. S., & Alvarez-Buylla, A. (2004). Cell types, lineage, and architecture of the germinal zone in the adult dentate gyrus. *The Journal of comparative neurology*, 478(4), 359–378. <https://doi.org/10.1002/cne.20288>

Serra, M., Brito, C., Costa, E. M., Sousa, M. F., & Alves, P. M. (2009). Integrating human stem cell expansion and neuronal differentiation in bioreactors. *BMC biotechnology*, 9, 82. <https://doi.org/10.1186/1472-6750-9-82>

Serra, M., Brito, C., Costa, E. M., Sousa, M. F., & Alves, P. M. (2009). Integrating human stem cell expansion and neuronal differentiation in bioreactors. *BMC biotechnology*, *9*, 82. <https://doi.org/10.1186/1472-6750-9-82>

Shi, J. and Wei, L. (2007) 'Rho kinase in the regulation of cell death and survival', *Archivum immunologiae et therapeuticae experimentalis*. 2007/03/09, *55*(2), pp. 61–75. doi: 10.1007/s00005-007-0009-7.

Shi, Y., Kirwan, P., Smith, J., Robinson, H. P., & Livesey, F. J. (2012). Human cerebral cortex development from pluripotent stem cells to functional excitatory synapses. *Nature neuroscience*, *15*(3), 477–S1. <https://doi.org/10.1038/nn.3041>

Shin, S. C. and Robinson-Papp, J. (2012) 'Amyloid neuropathies', *Mount Sinai Journal of Medicine*, *79*(6), pp. 733–748. doi: 10.1002/msj.21352.

Sohur, U. S., Emsley, J. G., Mitchell, B. D., & Macklis, J. D. (2006). Adult neurogenesis and cellular brain repair with neural progenitors, precursors and stem cells. *Philosophical transactions of the Royal Society of London. Series B, Biological sciences*, *361*(1473), 1477–1497. <https://doi.org/10.1098/rstb.2006.1887>

Si-Tayeb, K., Noto, F. K., Sepac, A., Sedlic, F., Bosnjak, Z. J., Lough, J. W., & Duncan, S. A. (2010). Generation of human induced pluripotent stem cells by simple transient transfection of plasmid DNA encoding reprogramming factors. *BMC developmental biology*, *10*, 81. <https://doi.org/10.1186/1471-213X-10-81>

Silva, M. M., Rodrigues, A. F., Correia, C., Sousa, M. F., Brito, C., Coroadinha, A. S., Serra, M., & Alves, P. M. (2015). Robust Expansion of Human Pluripotent Stem Cells: Integration of Bioprocess Design With Transcriptomic and Metabolomic Characterization. *Stem cells translational medicine*, *4*(7), 731–742. <https://doi.org/10.5966/sctm.2014-0270>

Simons, B. D. and Clevers, H. (2011) 'Strategies for homeostatic stem cell self-renewal in adult tissues', *Cell*, *145*(6), pp. 851–862.

Singh, H., Mok, P., Balakrishnan, T., Rahmat, S. N., & Zweigerdt, R. (2010). Up-scaling single cell-inoculated suspension culture of human embryonic stem cells. *Stem cell research*, *4*(3), 165–179. <https://doi.org/10.1016/j.scr.2010.03.001>

Singh, V. K., Saini, A., Kalsan, M., Kumar, N., & Chandra, R. (2016). Describing the Stem Cell Potency: The Various Methods of Functional Assessment and *In silico* Diagnostics. *Frontiers in cell and developmental biology*, *4*, 134. <https://doi.org/10.3389/fcell.2016.00134>

Sivarapatna, A., Ghaedi, M., Le, A. V., Mendez, J. J., Qyang, Y., & Niklason, L. E. (2015). Arterial specification of endothelial cells derived from human induced pluripotent stem cells in a biomimetic flow bioreactor. *Biomaterials*, *53*, 621–633. <https://doi.org/10.1016/j.biomaterials.2015.02.121>

Smith, L. R., Cho, S. and Discher, D. E. (2018) 'Stem Cell Differentiation is Regulated by Extracellular Matrix Mechanics', *Physiology (Bethesda, Md.)*, *33*(1), pp. 16–25. doi: 10.1152/physiol.00026.2017.

Song, K., Jiang, S., Tian, J., Jiao, Z., Wang, Y., Zhao, J., and Liu, T. (2016) 'Design and numerical simulation of an immunoisolation perfusion co-culture bioreactor for expansion of NSCs', (Mmebc 2016), pp. 2021–2026. doi: 10.2991/mmebc-16.2016.406.

- Specht, L. (2020) 'An analysis of culture medium costs and production volumes for cultivated meat', *The Good Food Institute: Washington, DC, USA*, p. 30.
- Stern, C. D. (2006) 'Neural induction: 10 years on since the "default model".', *Current opinion in cell biology*, 18(6), pp. 692–697. doi: 10.1016/j.ceb.2006.09.002.
- Stiles, J. and Jernigan, T. L. (2010) 'The basics of brain development', *Neuropsychology review*. 2010/11/03, 20(4), pp. 327–348. doi: 10.1007/s11065-010-9148-4.
- Stover, A. E. and Schwartz, P. H. (2011) 'The generation of embryoid bodies from feeder-based or feeder-free human pluripotent stem cell cultures', *Methods in molecular biology (Clifton, N.J.)*, 767, pp. 391–398. doi: 10.1007/978-1-61779-201-4\_28.
- Sugimoto, K., Matsuura, T., Nakazono, A., Igawa, K., Yamada, S., & Hayashi, Y. (2018). Effects of hypoxia inducible factors on pluripotency in human iPS cells. *Microscopy research and technique*, 81(7), 749–754. <https://doi.org/10.1002/jemt.23032>
- Sugiyama, T., Osumi, N. and Katsuyama, Y. (2013) 'The germinal matrices in the developing dentate gyrus are composed of neuronal progenitors at distinct differentiation stages', *Developmental Dynamics*, 242(12), pp. 1442–1453.
- Sullivan, S., Stacey, G. N., Akazawa, C., Aoyama, N., Baptista, R., Bedford, P., Bennaceur Griscelli, A., Chandra, A., Elwood, N., Girard, M., Kawamata, S., Hanatani, T., Latsis, T., Lin, S., Ludwig, T. E., Malygina, T., Mack, A., Mountford, J. C., Noggle, S., Pereira, L. V., ... Song, J. (2018). Quality control guidelines for clinical-grade human induced pluripotent stem cell lines. *Regenerative medicine*, 13(7), 859–866. <https://doi.org/10.2217/rme-2018-0095>
- Sulzer, D. (2007) 'Multiple hit hypotheses for dopamine neuron loss in Parkinson's disease.', *Trends in neurosciences*, 30(5), pp. 244–250. doi: 10.1016/j.tins.2007.03.009.
- Tagliavini, F., Giaccone, G., Frangione, B., & Bugiani, O. (1988). Preamyloid deposits in the cerebral cortex of patients with Alzheimer's disease and nondemented individuals. *Neuroscience letters*, 93(2-3), 191–196. [https://doi.org/10.1016/0304-3940\(88\)90080-8](https://doi.org/10.1016/0304-3940(88)90080-8)
- Takahashi, K., Tanabe, K., Ohnuki, M., Narita, M., Ichisaka, T., Tomoda, K., & Yamanaka, S. (2007). Induction of pluripotent stem cells from adult human fibroblasts by defined factors. *Cell*, 131(5), 861–872. <https://doi.org/10.1016/j.cell.2007.11.019>
- Takahashi, K. and Yamanaka, S. (2006) 'Induction of pluripotent stem cells from mouse embryonic and adult fibroblast cultures by defined factors.', *Cell*, 126(4), pp. 663–676. doi: 10.1016/j.cell.2006.07.024.
- Takahashi, K. and Yamanaka, S. (2016) 'A decade of transcription factor-mediated reprogramming to pluripotency.', *Nature reviews. Molecular cell biology*, 17(3), pp. 183–193. doi: 10.1038/nrm.2016.8.
- Tan, H. L., Fong, W. J., Lee, E. H., Yap, M., & Choo, A. (2009). mAb 84, a cytotoxic antibody that kills undifferentiated human embryonic stem cells via oncosis. *Stem cells (Dayton, Ohio)*, 27(8), 1792–1801. <https://doi.org/10.1002/stem.109>
- Tang, C., Wang, M., Wang, P., Wang, L., Wu, Q., & Guo, W. (2019). Neural Stem Cells Behave as a Functional Niche for the Maturation of Newborn Neurons through the Secretion of PTN. *Neuron*, 101(1), 32–44.e6. <https://doi.org/10.1016/j.neuron.2018.10.051>
- Tanosaki, S., Tohyama, S., Kishino, Y., Fujita, J., & Fukuda, K. (2021). Metabolism of human F.D., de la Raga, PhD Thesis, Aston University, 2022

pluripotent stem cells and differentiated cells for regenerative therapy: a focus on cardiomyocytes. *Inflammation and regeneration*, 41(1), 5. <https://doi.org/10.1186/s41232-021-00156-9>

Taylor, C. J., Peacock, S., Chaudhry, A. N., Bradley, J. A., & Bolton, E. M. (2012). Generating an iPSC bank for HLA-matched tissue transplantation based on known donor and recipient HLA types. *Cell stem cell*, 11(2), 147–152. <https://doi.org/10.1016/j.stem.2012.07.014>

Tchieu, J., Kuoy, E., Chin, M. H., Trinh, H., Patterson, M., Sherman, S. P., Aimiwu, O., Lindgren, A., Hakimian, S., Zack, J. A., Clark, A. T., Pyle, A. D., Lowry, W. E., & Plath, K. (2010). Female human iPSCs retain an inactive X chromosome. *Cell stem cell*, 7(3), 329–342. <https://doi.org/10.1016/j.stem.2010.06.024>

Teng, Y. D., Benn, S. C., Kalkanis, S. N., Shefner, J. M., Onario, R. C., Cheng, B., Lachyankar, M. B., Marconi, M., Li, J., Yu, D., Han, I., Maragakis, N. J., Lládo, J., Erkmen, K., Redmond, D. E., Jr, Sidman, R. L., Przedborski, S., Rothstein, J. D., Brown, R. H., Jr, & Snyder, E. Y. (2012). Multimodal actions of neural stem cells in a mouse model of ALS: a meta-analysis. *Science translational medicine*, 4(165), 165ra164. <https://doi.org/10.1126/scitranslmed.3004579>

Terstegge, S., Laufenberg, I., Pochert, J., Schenk, S., Itskovitz-Eldor, J., Endl, E., & Brüstle, O. (2007). Automated maintenance of embryonic stem cell cultures. *Biotechnology and bioengineering*, 96(1), 195–201. <https://doi.org/10.1002/bit.21061>

Teslaa, T. and Teitell, M. A. (2015) ‘Pluripotent stem cell energy metabolism: an update’, *The EMBO journal*. 2014/12/04, 34(2), pp. 138–153. doi: 10.15252/embj.201490446.

Theunissen, T. W., Powell, B. E., Wang, H., Mitalipova, M., Faddah, D. A., Reddy, J., Fan, Z. P., Maetzel, D., Ganz, K., Shi, L., Lungjangwa, T., Imsoonthornruksa, S., Stelzer, Y., Rangarajan, S., D'Alessio, A., Zhang, J., Gao, Q., Dawlaty, M. M., Young, R. A., Gray, N. S., ... Jaenisch, R. (2014). Systematic identification of culture conditions for induction and maintenance of naïve human pluripotency. *Cell stem cell*, 15(4), 471–487. <https://doi.org/10.1016/j.stem.2014.07.002>

Theunissen, T. W., Friedli, M., He, Y., Planet, E., O'Neil, R. C., Markoulaki, S., Pontis, J., Wang, H., Iouranova, A., Imbeault, M., Duc, J., Cohen, M. A., Wert, K. J., Castanon, R., Zhang, Z., Huang, Y., Nery, J. R., Drotar, J., Lungjangwa, T., Trono, D., ... Jaenisch, R. (2016). Molecular Criteria for Defining the Naive Human Pluripotent State. *Cell stem cell*, 19(4), 502–515. <https://doi.org/10.1016/j.stem.2016.06.011>

THOMAS, E. D., LOCHTE, H. L., Jr, LU, W. C., & FERREBEE, J. W. (1957). Intravenous infusion of bone marrow in patients receiving radiation and chemotherapy. *The New England journal of medicine*, 257(11), 491–496. <https://doi.org/10.1056/NEJM195709122571102>

Thomson, J. A., Kalishman, J., Golos, T. G., Durning, M., Harris, C. P., & Hearn, J. P. (1996). Pluripotent cell lines derived from common marmoset (*Callithrix jacchus*) blastocysts. *Biology of reproduction*, 55(2), 254–259. <https://doi.org/10.1095/biolreprod55.2.254>

Thomson, J. A., Itskovitz-Eldor, J., Shapiro, S. S., Waknitz, M. A., Swiergiel, J. J., Marshall, V. S., & Jones, J. M. (1998). Embryonic stem cell lines derived from human blastocysts. *Science (New York, N.Y.)*, 282(5391), 1145–1147. <https://doi.org/10.1126/science.282.5391.1145>

Tohyama, S., Fujita, J., Hishiki, T., Matsuura, T., Hattori, F., Ohno, R., Kanazawa, H., Seki,

T., Nakajima, K., Kishino, Y., Okada, M., Hirano, A., Kuroda, T., Yasuda, S., Sato, Y., Yuasa, S., Sano, M., Suematsu, M., & Fukuda, K. (2016). Glutamine Oxidation Is Indispensable for Survival of Human Pluripotent Stem Cells. *Cell metabolism*, 23(4), 663–674. <https://doi.org/10.1016/j.cmet.2016.03.001>

Tohyama, S., Fujita, J., Fujita, C., Yamaguchi, M., Kanaami, S., Ohno, R., Sakamoto, K., Kodama, M., Kurokawa, J., Kanazawa, H., Seki, T., Kishino, Y., Okada, M., Nakajima, K., Tanosaki, S., Someya, S., Hirano, A., Kawaguchi, S., Kobayashi, E., & Fukuda, K. (2017). Efficient Large-Scale 2D Culture System for Human Induced Pluripotent Stem Cells and Differentiated Cardiomyocytes. *Stem cell reports*, 9(5), 1406–1414. <https://doi.org/10.1016/j.stemcr.2017.08.025>

Tonda-Turo, C., Origlia, N., Mattu, C., Accorroni, A., & Chiono, V. (2018). Current Limitations in the Treatment of Parkinson's and Alzheimer's Diseases: State-of-the-Art and Future Perspective of Polymeric Carriers. *Current medicinal chemistry*, 25(41), 5755–5771. <https://doi.org/10.2174/0929867325666180221125759>

Tower, J. (2012) ‘Stress and stem cells.’, *Wiley interdisciplinary reviews. Developmental biology*, 1(6), pp. 789–802. doi: 10.1002/wdev.56.

Trawczynski, M., Liu, G., David, B. T., & Fessler, R. G. (2019). Restoring Motor Neurons in Spinal Cord Injury With Induced Pluripotent Stem Cells. *Frontiers in cellular neuroscience*, 13, 369. <https://doi.org/10.3389/fncel.2019.00369>

Tsujisaka, Y., Hatani, T., Okubo, C., Ito, R., Kimura, A., Narita, M., Chonabayashi, K., Funakoshi, S., Lucena-Cacace, A., Toyoda, T., Osafune, K., Kimura, T., Saito, H., & Yoshida, Y. (2022). Purification of human iPSC-derived cells at large scale using microRNA switch and magnetic-activated cell sorting. *Stem cell reports*, 17(7), 1772–1785. <https://doi.org/10.1016/j.stemcr.2022.05.003>

Tsutsui, H., Valamehr, B., Hindoyan, A., Qiao, R., Ding, X., Guo, S., Witte, O. N., Liu, X., Ho, C. M., & Wu, H. (2011). An optimized small molecule inhibitor cocktail supports long-term maintenance of human embryonic stem cells. *Nature communications*, 2, 167. <https://doi.org/10.1038/ncomms1165>

Tucker, B. A., Anfinson, K. R., Mullins, R. F., Stone, E. M., & Young, M. J. (2013). Use of a synthetic xeno-free culture substrate for induced pluripotent stem cell induction and retinal differentiation. *Stem cells translational medicine*, 2(1), 16–24. <https://doi.org/10.5966/sctm.2012-0040>

Tutukova, S., Tarabykin, V. and Hernandez-Miranda, L. R. (2021) ‘The Role of NeuroD Genes in Brain Development, Function, and Disease’, *Frontiers in Molecular Neuroscience*. Available at: <https://www.frontiersin.org/article/10.3389/fnmol.2021.662774>.

Urbán, N. and Guillemot, F. (2014) ‘Neurogenesis in the embryonic and adult brain: same regulators, different roles’, *Frontiers in cellular neuroscience*, 8, p. 396.

Varum, S., Rodrigues, A. S., Moura, M. B., Momcilovic, O., Easley, C. A., 4th, Ramalho-Santos, J., Van Houten, B., & Schatten, G. (2011). Energy metabolism in human pluripotent stem cells and their differentiated counterparts. *PloS one*, 6(6), e20914. <https://doi.org/10.1371/journal.pone.0020914>

Vitillo, L. and Kimber, S. J. (2017) ‘Integrin and FAK Regulation of Human Pluripotent Stem Cells’, *Current Stem Cell Reports*, 3(4), pp. 358–365. doi: 10.1007/s40778-017-0100-x.

Vlahos, K., Sourris, K., Mayberry, R., McDonald, P., Bruveris, F. F., Schiesser, J. V., Bozaoglu, K., Lockhart, P. J., Stanley, E. G., & Elefanty, A. G. (2019). Generation of iPSC lines from peripheral blood mononuclear cells from 5 healthy adults. *Stem cell research*, *34*, 101380. <https://doi.org/10.1016/j.scr.2018.101380>

Vukicevic, S., Kleinman, H. K., Luyten, F. P., Roberts, A. B., Roche, N. S., & Reddi, A. H. (1992). Identification of multiple active growth factors in basement membrane Matrigel suggests caution in interpretation of cellular activity related to extracellular matrix components. *Experimental cell research*, *202*(1), 1–8. [https://doi.org/10.1016/0014-4827\(92\)90397-q](https://doi.org/10.1016/0014-4827(92)90397-q)

Wakui, T., Matsumoto, T., Matsubara, K., Kawasaki, T., Yamaguchi, H., & Akutsu, H. (2017). Method for evaluation of human induced pluripotent stem cell quality using image analysis based on the biological morphology of cells. *Journal of medical imaging (Bellingham, Wash.)*, *4*(4), 044003. <https://doi.org/10.1117/1.JMI.4.4.044003>

GBD 2016 Multiple Sclerosis Collaborators (2019). Global, regional, and national burden of multiple sclerosis 1990-2016: a systematic analysis for the Global Burden of Disease Study 2016. *The Lancet. Neurology*, *18*(3), 269–285. [https://doi.org/10.1016/S1474-4422\(18\)30443-5](https://doi.org/10.1016/S1474-4422(18)30443-5)

Wang, L., Schulz, T. C., Sherrer, E. S., Dauphin, D. S., Shin, S., Nelson, A. M., Ware, C. B., Zhan, M., Song, C. Z., Chen, X., Brimble, S. N., McLean, A., Galeano, M. J., Uhl, E. W., D'Amour, K. A., Chesnut, J. D., Rao, M. S., Blau, C. A., & Robins, A. J. (2007). Self-renewal of human embryonic stem cells requires insulin-like growth factor-1 receptor and ERBB2 receptor signaling. *Blood*, *110*(12), 4111–4119. <https://doi.org/10.1182/blood-2007-03-082586>

Wang, Y. K., Zhu, W. W., Wu, M. H., Wu, Y. H., Liu, Z. X., Liang, L. M., Sheng, C., Hao, J., Wang, L., Li, W., Zhou, Q., & Hu, B. Y. (2018). Human Clinical-Grade Parthenogenetic ESC-Derived Dopaminergic Neurons Recover Locomotive Defects of Nonhuman Primate Models of Parkinson's Disease. *Stem cell reports*, *11*(1), 171–182. <https://doi.org/10.1016/j.stemcr.2018.05.010>

Wang, Y., Chou, B. K., Dowey, S., He, C., Gerecht, S., & Cheng, L. (2013). Scalable expansion of human induced pluripotent stem cells in the defined xeno-free E8 medium under adherent and suspension culture conditions. *Stem cell research*, *11*(3), 1103–1116. <https://doi.org/10.1016/j.scr.2013.07.011>

Warburg, O. (1956) 'On the origin of cancer cells', *Science*, *123*(3191), pp. 309–314.

Ware, C. B., Nelson, A. M., Meham, B., Hesson, J., Zhou, W., Jonlin, E. C., Jimenez-Caliani, A. J., Deng, X., Cavanaugh, C., Cook, S., Tesar, P. J., Okada, J., Margaretha, L., Sperber, H., Choi, M., Blau, C. A., Treuting, P. M., Hawkins, R. D., Cirulli, V., & Ruohola-Baker, H. (2014). Derivation of naive human embryonic stem cells. *Proceedings of the National Academy of Sciences of the United States of America*, *111*(12), 4484–4489. <https://doi.org/10.1073/pnas.1319738111>

Warren, L., Ni, Y., Wang, J., & Guo, X. (2012). Feeder-free derivation of human induced pluripotent stem cells with messenger RNA. *Scientific reports*, *2*, 657. <https://doi.org/10.1038/srep00657>

Watanabe, K., Ueno, M., Kamiya, D., Nishiyama, A., Matsumura, M., Wataya, T., Takahashi, J. B., Nishikawa, S., Nishikawa, S., Muguruma, K., & Sasai, Y. (2007). A ROCK inhibitor F.D., de la Raga, PhD Thesis, Aston University, 2022

permits survival of dissociated human embryonic stem cells. *Nature biotechnology*, 25(6), 681–686. <https://doi.org/10.1038/nbt1310>

Werner, M., Blanquer, S. B., Haimi, S. P., Korus, G., Dunlop, J. W., Duda, G. N., Grijpma, D. W., & Petersen, A. (2016). Surface Curvature Differentially Regulates Stem Cell Migration and Differentiation via Altered Attachment Morphology and Nuclear Deformation. *Advanced science* (Weinheim, Baden-Wurttemberg, Germany), 4(2), 1600347. <https://doi.org/10.1002/advs.201600347>

Wilmes, A., Rauch, C., Carta, G., Kern, G., Meier, F., Posch, W., Wilflingseder, D., Armstrong, L., Lako, M., Beilmann, M., Gstraunthaler, G., & Jennings, P. (2017). Towards optimisation of induced pluripotent cell culture: Extracellular acidification results in growth arrest of iPSC prior to nutrient exhaustion. *Toxicology in vitro : an international journal published in association with BIBRA*, 45(Pt 3), 445–454. <https://doi.org/10.1016/j.tiv.2017.07.023>

Wilson, S. I. and Edlund, T. (2001) ‘Neural induction: Toward a unifying mechanism’, *Nature Neuroscience*, 4(11s), pp. 1161–1168. doi: 10.1038/nn747.

Van Winkle, A. P., Gates, I. D. and Kallos, M. S. (2012) ‘Mass transfer limitations in embryoid bodies during human embryonic stem cell differentiation.’, *Cells, tissues, organs*, 196(1), pp. 34–47. doi: 10.1159/000330691.

Wolfe, R. P., Leleux, J., Nerem, R. M., & Ahsan, T. (2012). Effects of shear stress on germ lineage specification of embryonic stem cells. *Integrative biology : quantitative biosciences from nano to macro*, 4(10), 1263–1273. <https://doi.org/10.1039/c2ib20040f>

Wolfe, R. P., Guidry, J. B., Messina, S. L., & Ahsan, T. (2016). Applying Shear Stress to Pluripotent Stem Cells. *Methods in molecular biology* (Clifton, N.J.), 1341, 377–389. [https://doi.org/10.1007/7651\\_2015\\_210](https://doi.org/10.1007/7651_2015_210)

Wu, J., Fan, Y. and Tzanakakis, E. S. (2015) ‘Increased culture density is linked to decelerated proliferation, prolonged G1 phase, and enhanced propensity for differentiation of self-renewing human pluripotent stem cells’, *Stem cells and development*. 2014/12/22, 24(7), pp. 892–903. doi: 10.1089/scd.2014.0384.

Xie, A. W., Binder, B. Y. K., Khalil, A. S., Schmitt, S. K., Johnson, H. J., Zacharias, N. A., & Murphy, W. L. (2017). Controlled Self-assembly of Stem Cell Aggregates Instructs Pluripotency and Lineage Bias. *Scientific reports*, 7(1), 14070. <https://doi.org/10.1038/s41598-017-14325-9>

Xu, R. H., Chen, X., Li, D. S., Li, R., Addicks, G. C., Glennon, C., Zwaka, T. P., & Thomson, J. A. (2002). BMP4 initiates human embryonic stem cell differentiation to trophoblast. *Nature biotechnology*, 20(12), 1261–1264. <https://doi.org/10.1038/nbt761>

Xu, R. H., Peck, R. M., Li, D. S., Feng, X., Ludwig, T., & Thomson, J. A. (2005). Basic FGF and suppression of BMP signaling sustain undifferentiated proliferation of human ES cells. *Nature methods*, 2(3), 185–190. <https://doi.org/10.1038/nmeth744>

Xu, Y., Zhu, X., Hahm, H. S., Wei, W., Hao, E., Hayek, A., & Ding, S. (2010). Revealing a core signaling regulatory mechanism for pluripotent stem cell survival and self-renewal by small molecules. *Proceedings of the National Academy of Sciences of the United States of America*, 107(18), 8129–8134. <https://doi.org/10.1073/pnas.1002024107>

Yao, S., Chen, S., Clark, J., Hao, E., Beattie, G. M., Hayek, A., & Ding, S. (2006). Long-term F.D., de la Raga, PhD Thesis, Aston University, 2022 300

self-renewal and directed differentiation of human embryonic stem cells in chemically defined conditions. *Proceedings of the National Academy of Sciences of the United States of America*, 103(18), 6907–6912. <https://doi.org/10.1073/pnas.0602280103>

Yap, M. S., Nathan, K. R., Yeo, Y., Lim, L. W., Poh, C. L., Richards, M., Lim, W. L., Othman, I., & Heng, B. C. (2015). Neural Differentiation of Human Pluripotent Stem Cells for Nontherapeutic Applications: Toxicology, Pharmacology, and In Vitro Disease Modeling. *Stem cells international*, 2015, 105172. <https://doi.org/10.1155/2015/105172>

Yasuda, S. Y., Ikeda, T., Shahsavarani, H., Yoshida, N., Nayer, B., Hino, M., Vartak-Sharma, N., Suemori, H., & Hasegawa, K. (2018). Chemically defined and growth-factor-free culture system for the expansion and derivation of human pluripotent stem cells. *Nature biomedical engineering*, 2(3), 173–182. <https://doi.org/10.1038/s41551-018-0200-7>

YekrangSafakar, A., Acun, A., Choi, J. W., Song, E., Zorlutuna, P., & Park, K. (2018). Hollow microcarriers for large-scale expansion of anchorage-dependent cells in a stirred bioreactor. *Biotechnology and bioengineering*, 115(7), 1717–1728. <https://doi.org/10.1002/bit.26601>

Yin, X., Li, L., Zhang, X., Yang, Y., Chai, Y., Han, X., & Feng, Z. (2013). Development of neural stem cells at different sites of fetus brain of different gestational age. *International journal of clinical and experimental pathology*, 6(12), 2757–2764.

Ying, Q. L., Wray, J., Nichols, J., Batlle-Morera, L., Doble, B., Woodgett, J., Cohen, P., & Smith, A. (2008). The ground state of embryonic stem cell self-renewal. *Nature*, 453(7194), 519–523. <https://doi.org/10.1038/nature06968>

Yoshida, Y., Takahashi, K., Okita, K., Ichisaka, T., & Yamanaka, S. (2009). Hypoxia enhances the generation of induced pluripotent stem cells. *Cell stem cell*, 5(3), 237–241. <https://doi.org/10.1016/j.stem.2009.08.001>

Yuan, X., Tsai, A. C., Farrance, I., Rowley, J., & Ma, T. (2018). Aggregation of Culture Expanded Human Mesenchymal Stem Cells in Microcarrier-based Bioreactor. *Biochemical engineering journal*, 131, 39–46. <https://doi.org/10.1016/j.bej.2017.12.011>

Zaveri, L. and Dhawan, J. (2018) ‘Cycling to Meet Fate: Connecting Pluripotency to the Cell Cycle’, *Frontiers in Cell and Developmental Biology*, p. 57. Available at: <https://www.frontiersin.org/article/10.3389/fcell.2018.00057>.

Zhang, C., Zhou, L., Wang, Z., Gao, W., Chen, W., Zhang, H., Jing, B., Zhu, X., Chen, L., Zheng, C., Shi, K., Wu, L., Cheng, L., Zhang, K., & Sun, Y. E. (2021). Eradication of specific donor-dependent variations of mesenchymal stem cells in immunomodulation to enhance therapeutic values. *Cell death & disease*, 12(4), 357. <https://doi.org/10.1038/s41419-021-03644-5>

Zhang, J., Nuebel, E., Daley, G. Q., Koehler, C. M., & Teitell, M. A. (2012). Metabolic regulation in pluripotent stem cells during reprogramming and self-renewal. *Cell stem cell*, 11(5), 589–595. <https://doi.org/10.1016/j.stem.2012.10.005>

Zhang, S. C., Wernig, M., Duncan, I. D., Brüstle, O., & Thomson, J. A. (2001). In vitro differentiation of transplantable neural precursors from human embryonic stem cells. *Nature biotechnology*, 19(12), 1129–1133. <https://doi.org/10.1038/nbt1201-1129>

Zhang, S., Liu, L., Hu, Y., Lv, Z., Li, Q., Gong, W., Sha, H., & Wu, H. (2017). Derivation of human induced pluripotent stem cell (iPSC) line from a 79year old sporadic male Parkinson's F.D., de la Raga, PhD Thesis, Aston University, 2022

disease patient. *Stem cell research*, 19, 43–45. <https://doi.org/10.1016/j.scr.2016.12.025>

Zhang, W. and Liu, H. T. (2002) ‘MAPK signal pathways in the regulation of cell proliferation in mammalian cells’, *Cell Research*, 12(1), pp. 9–18. doi: 10.1038/sj.cr.7290105.

Zhang, X., Peterson, K. A., Liu, X. S., McMahon, A. P., & Ohba, S. (2013). Gene regulatory networks mediating canonical Wnt signal-directed control of pluripotency and differentiation in embryo stem cells. *Stem cells (Dayton, Ohio)*, 31(12), 2667–2679. <https://doi.org/10.1002/stem.1371>

Zhao, X. and Guan, J.-L. (2011) ‘Focal adhesion kinase and its signaling pathways in cell migration and angiogenesis’, *Advanced drug delivery reviews*. 2010/11/29, 63(8), pp. 610–615. doi: 10.1016/j.addr.2010.11.001.

Zhong, T. P., Childs, S., Leu, J. P., & Fishman, M. C. (2001). Gridlock signalling pathway fashions the first embryonic artery. *Nature*, 414(6860), 216–220. <https://doi.org/10.1038/35102599>

Zimmerman, L. B., De Jesús-Escobar, J. M. and Harland, R. M. (1996) ‘The Spemann organizer signal noggin binds and inactivates bone morphogenetic protein 4’, *Cell*, 86(4), pp. 599–606. doi: 10.1016/S0092-8674(00)80133-6.

## Appendix

### List of equipment utilised

- Class II Biosafety Cabinet (Herasafe KS, Thermofisher Scientific)
- Incubator (Heracell 150i, Thermofisher Scientific)
- Phase contrast microscope (EVOS, Thermofisher Scientific)
- Centrifuge (Rotanta 460, Hettich)
- Microcentrifuge (1-14, Sigma)
- Analytical balance (Practum, Sartorius, 120 g)
- Water bath (Sub Aqua Pro, Grant Instruments)
- Automated cell counter (Nucleocounter NC3000, Chemometec)
- 5-positions magnetic stirrer platform (Bellco)
- 25 mL and 50 mL capacity spinner flasks (Wheaton)
- Fluorescence microscope (EVOS FL, Thermofisher Scientific)
- Handheld, point-of-care device (AccuTrend Plus, Roche Diagnostics)
- Vacuum pump for aspiration system (Fisherbrand)
- Micro-pipettes (mLINE, Sartorius)
- pH meter (FE20 FiveEasy, Mettler Toledo)
- Roller mixer (SRT6, Stuart)
- Rocker (Stuart)

## Supplementary data

This Appendix contains supplementary figures and graphs which are referred to in the main text.

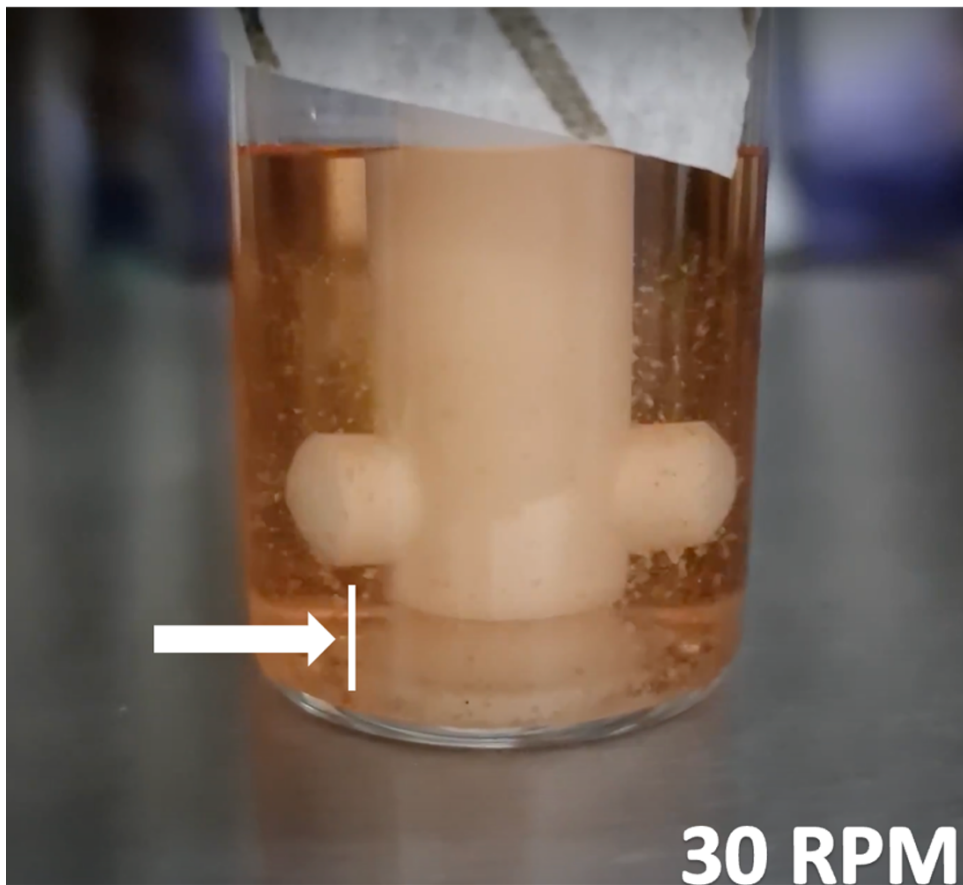


Figure A.1. Example image of microcarrier and cell pooling below the impeller. N=2 biological repeat.

